Universidad de Concepción
Dirección de Postgrado
Facultad de Ciencias Naturales y Oceanográficas
Programa de Doctorado en Sistemática y Biodiversidad

PATRONES DE DIVERSIFICACIÓN Y BIOGEOGRAFÍA HISTÓRICA DE PRIMNOIDES (CNIDARIA: OCTOCORALLIA: PRIMNOIDAE) EN EL OCÉANO AUSTRAL

(Diversification patterns and historical biogeography of primnoids (Cnidaria: Octocorallia: Primnoidae) in the Southern Ocean)

Tesis para optar al grado de Doctor en Sistemática y Biodiversidad

Mónica Coromoto Núñez Flores
CONCEPCIÓN-CHILE
2022

Directores
Dr. Daniel Gómez Uchida Universidad de Concepción-Chile
Dr. Pablo J. López González Universidad de Sevilla-España
Dr. Jorge Avaria Llautureo Centro de Estudios Avanzados en Zonas Áridas, Chile; University of Reading, Reading-UK.

A mis padres

AGRADECIMIENTOS

En primer lugar, a mis padres Coromoto y Saúl, por su confianza, por su apoyo incalculable y sobre todo por creer siempre en mí, por nunca haber perdido la fé, y la esperanza de que cada cosa que me propongo la logro. No hay palabras para agradecerles lo que han hecho por mí. A mi sister Adriana, con su psicología loca siempre me convence, y no hay nadie que me conozca también como tu, somos tan jóvenes, y lo mejor de todo es que cada día estamos mejor, como el vino… aunque yo soy mas joven que tú, de eso no hay duda. Gracias por ese ahijado bello, mi manolo, ha sido el primero en escuchar los resultados de mi tesis doctoral, y vaya preguntas que me ha hecho el niño… A la distancia he tratado de ser la mejor tia-madrina del mundo. No puedo dejar de agradecer a alguien muy especial, el primero, el primero en mi corazón, mi amor, mi compañero de vida, mi cómplice, mi amigo, mi colega de trabajo, Andrés, por ser siempre incondicional conmigo. Me apoyastes desde el inicio, desde que se me ocurrió hacer un doctorado, sabiendo que en algún momento saltaría de continente, y estaríamos a miles de kilometros de distancia. Siempre creyendo en mi, y en mi capacidad para lograrlo. No hay palabras para agradecerte todo lo que has tenido que soportar, mis malas caras, mis quejas por el pasaporte que no llega, mis ganas de entender miles de cosas que no tienen explicaciones, pero que me empeño en buscarlas, mi indecisión para todo. Me has ayudado a sobrellevar cada dificultad que se me ha presentado, siempre con una palabra de aliento, con buena cara y sobretodo con mucho amor. Sin duda sin ti no lo hubiese logrado, así que este titulo también es tuyo.

A mis profesores guias, Daniel Gomez-Uchida por recibirme, apoyarme y aceptar el reto que implica salir de las poblaciones, de los salmones, y expandirse como guía en nuevas áreas. Por darme la oportunidad de ser parte de su grupo de trabajo, aunque yo solo pueda aceptar a los salmones como parte de mi dieta. A Jorge Avaria-Llautureo por guiarme durante los meses más duros de la elaboración de esta tesis; y finalmente a Pablo López-González, por su confianza. Son once años ya de conocernos, de haber comenzado este gran viaje de conocimientos, por darme la oportunidad de trabajar con esta fauna de gorgonias tan interesante, por abrirme las

puertas de su laboratorio y poner a mi disposición cientos de colonias para ser estudidas. Por las innumerables horas de trabajo compartidas, de conocimiento, dedicación y consejos que me ha brindado. No hay nadie mejor que usted para describir y evaluar como ha sido mi evolución durante estos largos años. A los profesores del Doctorado en Sistemática y Biodiversidad de la UdeC, por todos los conocimientos impartidos a lo largo de estos años. A los colegas del laborario de Biología y Ecología Acuatica (BECA) de la Universidad de Sevilla, durante mi estancia de un año, que se alargo a dos, y es que quien va a Sevilla, se queda en Sevilla. Esperanza, Cesar, Badia, por los mometos de charlas y los cafecitos a media mañana para desconectar del trabajo. Todos me han aportado algo durante estos años, me han aconsejado, me han animado, me han apoyado. Agradezco a Josep Maria Gili por facilitar algunos materiales examinados, y al curador de Museu de Zoologia de Barcelona Francesc Uribe, por su amabilidad en acceder a recibir el material estudiado en dicha colección. A Jose Garrido Galan, gracias por tu gran compromiso con el trabajo, por los miles de horas extras en el laboratorio, por las decenas de secuencias generadas, sin duda alguna fuiste un elemento clave para el desarrollo de esta tesis doctoral.

A mis compañeras de doctorado Kateryn, Dania y Heydi, desde el inicio juntas, con distintos acentos, pero con un objetivo en común, superarnos, ser mejores científicas y dejar el nombre de nuestros países (aunque mal paguen) en alto. Cada una con nuestro propio estilo, a nuestros propios tiempos y con nuestras limitaciones. Nadie mejor que nosotras sabemos lo que es alejarnos de nuestra familia, amigos, paisajes, comidas, momentos y seguir adelante, levantándonos una y otra vez a pesar de las adversidades, siempre con la mirada en alto, somos unas luchadoras y hoy puedo decir que lo logramos. A mis amigos y colegas Pablo Savaria y Selim Musleh por su continua compañía, hospitalidad y por lo divertidos momentos compartidos en el GEECLAB. A una amiga, y compañera española muy especial, Lucía, Gracias por las pláticas, los cafecitos, las comidas juntas, por recibirme en tu humilde hogar y por hacerme parte de tu familia. A todas aquellas personas que en este momento se escapan de mi memoria, y que de una u otra forma contribuyeron durante el desarrollo de esta tesis doctoral muchas gracias...

A la Universidad de Concepción (UdeC), a la Universidad de Sevilla, España (US) por el apoyo académico, logístico y financiero.

Finalmente, a la Agencia Nacional de Investigación y Desarrollo (ANID) (ANID/Doctorado Nacional/2017–21170438), al Instituto Antártico Chileno INACH (INACH grant DG_04_19) y al Ministerio de Economía, Industria y Competitividad de España (CTM2017–83920-P DIVERSICORAL), por financiar el desarrollo esta tesis doctoral.

RESUMEN

Los patrones de diversidad global son el resultado de procesos de especiación, extinción y dispersión, que operan a lo largo del espacio geográfico y tiempo. Identificar cómo las condiciones ambientales han históricamente dado forma a tales procesos puede proporcionar un marco de trabajo para predecir la persistencia de las especies ante un escenario de cambio climático global. Las profundidades del Océano (> 200 m) y el Océano Austral (SO) se encuentran entre los ecosistemas más extensos y menos explorados de la Tierra. Tales regiones muestran vacíos de conocimiento significativos para la diversidad de sus especies (déficit "linneano") y distribución (déficit "wallaceano"), pero también se desconoce cómo se originó y diversificó su biodiversidad y cómo su riqueza de especies respondió ante los cambios ambientales del pasado a lo largo del espacio-tiempo (déficit "darwiniano").

La presente tesis doctoral estudió una de las familias de octocorales más diversas que habitan los ambientes bentónicos de aguas profundas en todo el mundo, Primnoidae (Cnidaria: Anthozoa: Octocorallia) o "primnoides". Esta familia tiene significativos vacíos de conocimiento linneano y darwiniano. Para reducir el déficit linneano de la familia, primero evaluamos la riqueza de especies potencialmente no descritas de una colección inédita de colonias del género *Thouarella* Gray, 1870 recuperadas en el SO, utilizando filogenias moleculares y métodos de delimitación basados en marcadores mitocondriales y nucleares, así como estudios morfológicos detallados. En segundo lugar, para reducir el déficit darwiniano, construimos la filogenia calibrada más completa hasta la fecha, para estudiar la biogeografía histórica (e.g., paleolocalizaciones ancestrales y tasas de dispersión) y la dinámica de diversificación y sus impulsores en los primnoides. Evaluamos explícitamente: 1) si su dinámica de diversificación global y regional (SO) estuvo mediada por factores abióticos continuos en el tiempo (e.g., cambios en el CO_2 o la geoquímica oceánica); y 2) si, a escala global y regional (SO), mostraron cambios en las tasas de especiación y extinción en intervalos discretos de tiempo, afectando a todos los linajes, como se propuso previamente para los antozoos.

Usando un enfoque taxonómico integrador por primera vez para la familia, reconocimos y describimos seis nuevas especies dentro del género *Thouarella* (*T. islai, T. weddellensis, T. polarsterni, T. amundseni, T. dolichoespinosa* y *T. pseudoislai*), proporcionando nuevos pasos para revelar la diversidad oculta de la macrofauna bentónica en el SO. Nuestros resultados también arrojan luz sobre varios patrones biogeográficos y evolutivos previamente desconocidos para los primnoides. La familia probablemente se originó en el suroeste del Océano Pacífico durante el Albiense (~ 112 Ma), dispersándose posteriormente a otras regiones. Su dispersion geográfica se caracterizó por movimientos de corta distancia intercalados con unos pocos eventos de dispersión de larga distancia los cuales probablemente se limitaron a primnoides con tipo de reproducción *broadcast spawners*. La colonización del SO por los primnoides inició en el Campaniense (~74 Ma) por el TMRCA del clado de primnoides antárticos y subantárticos, lo que respalda que el grupo tiene una historia evolutiva relativamente larga y próspera en el SO. Desde el Cretácico, el SO actuó como fuente y sumidero de la diversidad de primnoides, pero la dispersión hacia y desde el SO no ocurrió de forma simultánea. Los primnoides migrantes alcanzaron el SO solo durante los últimos 5,3 Ma, mientras que los primnoides emigrantes se dispersaron en diferentes momentos a lo largo del Cenozoico, incluidos los eventos de dispersión posteriores al inicio e intensificación de la ACC. Por otro lado, la muestra seleccionada de factores bióticos y abióticos continuos en el tiempo no se correlacionaron significativamente con la dinámica de diversificación de los primnoides a nivel mundial, mientras que la química del océano (proporción Mg/Ca en el agua de mar) se correlacionó positivamente con la diversificación de los primnoides del SO. Finalmente, nuestros resultados mostraron que el máximo térmico del Paleoceno-Eoceno (~56 Ma), una perturbación climática abrupta a escala planetaria de calor global extremo y acidificación de los océanos marca un periodo de cambio en la diversificación de los primnoides a escala global y regional (SO) probablemente al generar nuevas oportunidades ecológicas.

ABSTRACT

Current global diversity patterns result from processes that include speciation, extinction, and dispersal operating over space and time. Identifying how past environmental conditions shaped such processes could provide a framework for predicting their persistence under global change. The deep-sea and Southern Ocean (SO) are among the Earth's most extensive and yet least-explored ecosystems, and they have experienced dramatic changes in physical and chemical variables in the geological past. As a result, such regions show significant knowledge gaps for species taxonomy (Linnean shortfall) and distribution (Wallacean shortfall), and it remains poorly understood how their biodiversity originated and diversified and how species richness responds to such abiotic changes over time and space (Darwinian shortfall).

This doctoral thesis studied one of the most diverse octocorallian families that inhabit the deep-sea benthonic environments worldwide, Primnoidae (Cnidaria: Octocorallia: Anthozoa) or "primnoids". This family has significant Linnean and Darwinian shortfalls. To reduce the family's Linnean shortfall, we first assessed the undescribed species richness of an unpublished collection of bottlebrush colonies of the *Thouarella* Gray, 1870, genus recovered from the Weddell Sea and Antarctic Peninsula (SO), employing molecular phylogenies and species delimitation methods based on mitochondrial and nuclear DNA markers and detailed morphological studies. Second, to reduce the Darwinian shortfall, we built a new dated species-level phylogeny to study the historical biogeography (e.g., ancestral geographic locations and dispersal rates) and diversification dynamics (and its drivers) of primnoids. Finally, we explicitly tested whether: 1) global and regional (SO) diversification dynamics among primnoids were mediated by abiotic drivers such as changes in CO_2 or ocean geochemistry; and 2) changes in speciation and extinction affecting all primnoid lineages, as previously proposed for anthozoans, occurred at discrete time points at global and regional (SO) scales.

The main results of this Ph.D. thesis can be summarized as follows. Using an integrative taxonomic approach (for the first time for the family), we recognized and described six new species within the genus *Thouarella* (*T. islai, T. weddellensis, T.*

polarsterni, T. amundseni, T. dolichoespinosa, and *T. pseudoislai*), providing new steps for uncovering the benthonic macrofauna's hidden diversity in the SO. Our novel results also shed light on several biogeographic and evolutive patterns previously unrecognized for primnoids. They likely originated in the southwestern Pacific Ocean during the Albian (~112 Ma), further dispersing to other regions. Its geographic dispersal is characterized by short-distance movements interspersed with a few events of more considerable distances. The few instances of long-distance dispersal were likely restricted to lineages of broadcast spawners. The SO colonization of primnoids begins as early as the Campanian (~74 Ma) by the TMRCA of the Antarctic and sub-Antarctic primnoids clade and supports that the group has a relatively long and prosperous *in situ* evolutionary history in the SO. Since the Cretaceous, the SO potentially acted as source and sink of primnoid diversity, but dispersal toward and outward the SO failed to co-occur. Immigrant primnoids reached the SO only during the last 5.3 Ma, while emigrant primnoids disperse outside in different moments along the Cenozoic, including dispersal events after the ACC onset and intensification.

On the other hand, the selected sample of time-continuous biotic and abiotic factors were uncorrelated with the diversification dynamics of primnoids globally, while the ocean chemistry (ratios Mg/Ca on seawater) correlated positively with the diversification of SO primnoids. Finally, our results showed that the Paleocene-Eocene thermal maximum (~56 Ma), an abrupt planetary-scale climatic perturbation of extreme global warmth and ocean acidification, changed the long-term diversification dynamics of primnoids on a global and regional (SO) scale, likely by providing novel ecological opportunities.

ÍNDICE DE CONTENIDOS

INDICE DE FIGURAS

INTRODUCCIÓN GENERAL

La riqueza de especies (diversidad, de aquí en adelante) varía ampliamente entre regiones, hábitats, y grupos taxonómicos. Por ejemplo, muchos grupos de organismos exhiben un gradiente latitudinal con mayor diversidad en las regiones tropicales, que decrece hacia las regiones polares (Willig *et al.* 2003; Hillebrand 2004; Mittelbach *et al.* 2007). Además, linajes cercanamente relacionados pueden mostrar amplias variaciones en su riqueza de especies. (e.g., dentro del Phylum Cnidaria, la Clase Cubozoa incluye sólo 36 especies, respecto a más de 7500 especies descritas en la Clase Anthoza (Daly *et al.* 2007).

Aunque numerosas hipótesis han sido propuestas para explicar estos patrones de diversidad, el número de especies de un determinado linaje y en una determinada región está explicado, en última instancia, por tres procesos que actúan a lo largo del espacio y tiempo: especiación, extinción y dispersión (Futuyma 2005; Jablonski *et al.* 2006; Lomolino *et al.* 2006; Roy and Goldberg 2007; Mittelbach *et al.* 2007; Wiens 2011; Morlon 2014). En primer lugar, la especiación es el proceso por el cual una especie da origen a dos o más especies con el paso del tiempo debido a la aparición de barreras reproductivas (Futuyma 2005). Aunque existen diferentes modos de especiación, la especiación alopátrica asociada a la aparición de una barrera geográfica dentro del rango de distribución de la especie es considerada como la más común en poblaciones naturales (Turelli *et al.* 2001; Futuyma 2005). En segundo lugar, la extinción o desaparición de una o un grupo de especies puede ser estocástica a selectiva (e.g., afectando a aquellas que no pueden adaptarse a nuevas condiciones), y ocurrir a distintas escalas (e.g., locales, regionales y extinciones en masa como la extinción del límite Cretácico-Paleoceno) (Futuyma 2005). Adicionalmente, la extinción puede producir espacio geográfico y nichos ecológicos disponibles para la colonización de nuevos linajes, favoreciendo la

especiación o facilitando el reemplazo funcional de una especie por otra (Futuyma 2005; Reznick y Ricklefs 2009). La diferencia o resta entre especiación y extinción definen el concepto de diversificación, que en su conjunto son los procesos principales que explican los patrones de diversidad de un determinado linaje y en una determinada región (Ricklefs 2007; Morlon 2014), aunque no son los únicos.

Para explicar los patrones de diversidad de una forma teóricamente satisfactoria, es necesario aludir, adicionalmente, al proceso de dispersión. La dispersión es un proceso biogeográfico que implica el movimiento físico de especies fuera de su rango de distribución ancestral (Brown y Lomolino 1998; Futuyma 2005). La dispersión incluye la emigración y la inmigración, pero también la expansión, contracción, y fragmentación del rango de distribución geográfica de especies. Además, la dispersión a larga distancia, un caso especial de dispersión que está en el origen de patrones biogeográficos disyuntos, puede ser directo, mediante la dispersión de propágulos activos, o indirecto mediante rafting pasivo adherido a sustratos flotantes (Lomolino *et al.* 2006; Rogers 2007; Clarke 2008; Pearse *et al.* 2009; Clarke y Crame 2010). La dispersión puede modificar directamente los patrones espaciales de riqueza de especies al incrementar la diversidad sobre escalas locales o regionales sin necesidad de que ocurra especiación (Wiens 2011). Por otra parte, la distancia de dispersión influye en la escala en la que es probable que ocurra la diversificación (Kisel yTimothy 2010), y se ha sugerido que las tasas de dispersión y especiación pueden estar correlacionadas (O'Donovan *et al.* 2018; Avaria-Llautureo *et al.* 2021). De tal forma, altas tasas de dispersión puede dar lugar altas tasas de especiación durante la historia temprana de un grupo, principalmente vía especiación alopátrica, mientras que bajas tasas de dispersión puede asociarse a tasas más bajas de especiación, principalmente vía especiación simpátrica cuando el espacio ecológico esta más saturado (O'Donovan *et al.* 2018). De tal forma, comprender los patrones y mecanismos

asociados a la dispersión de las especies es crítico para determinar cómo ha evolucionado la diversidad en el espacio y tiempo.

Las especies entonces se originan, dispersan y extinguen a lo largo del espacio y tiempo. Sin embargo, se han propuesto dos hipótesis clásicas para agrupar los mecanismos que actúan sobre los procesos macroevolutivos (i.e., especiación y extinción) que generan los patrones de diversidad de especies. La hipótesis “Reina Roja” (*Red Queen Hypothesis*, RQH) sugiere que la diversificación es iniciada y dirigida por factores bióticos intrínsecos a la especie (e.g., historias de vida, morfología, capacidad de dispersión) y por interacciones con otras especies (e.g., competencia) (Van Valen 1973; Benton 2009; Condamine *et al.* 2018b). La interpretación original de la hipótesis RQH sugiere que sin importar cuanto tiempo una especie “corra” una carrera adaptativa ante un ambiente en cambio constante, ésta siempre tendrá el mismo fitness comparado con otras especies, es decir, puede “correr” pero siempre se mantiene en el mismo lugar (tal como dice la Reina Roja a Alicia en el libro “*Through the Looking-Glass*” (Van Valen 1973). La idea es que una especie debe continuamente evolucionar para lidear con las cambiantes condiciones ambientales, pero no solo porque las condiciones abióticas cambian, sino porque todas las otras especies están evolucionando, alterando la disponibilidad de recursos y los patrones de interacciones bióticas (Brown y Lomolino 1998). La RQH predice tasas constantes de especiación y extinción en grupos homogéneos (Van Valen 1973; Venditti *et al.* 2010). Sin embargo, no todos los grupos naturales son homogéneos respecto a su biología y se ha demostrado que las tasas de especiación y extinción varían ampliamente a lo largo del tiempo, espacio y el árbol de la vida. Otros autores, sugieren que en la RQH las especies no "corren en un mismo lugar" sino que simplemente “esperan” a que ocurra la siguiente causa suficiente de especiación (i.e., eventos estocásticos raros que causan aislamiento reproductivo), ocasionada por el efecto gradual de la selección natural (Venditti *et al.* 2010). Se han

propuesto diferentes tipos de factores bióticos ligados a la variación en tasas de especiación y extinción. La evolución de algún rasgo en un linaje (e.g., caracteres morfológicos, o capacidad de dispersión), por ejemplo, tiene el potencial de ofrecer nuevas oportunidades ecológicas, incrementando así los eventos de especiación por unidad de tiempo, o disminuyendo el riesgo de extinción (FitzJohn *et al.* 2009; Ng y Smith 2014).

Alternativamente, la hipótesis “Bufón de Corte” (*Court Jester Hypothesis*, CJH) propone que la dinámica de diversificación es iniciada y dirigida por factores abióticos históricos, tales como cambios abruptos en el clima, o eventos tectónicos (Vrba 1993; Barnosky 2001; Benton 2009; Condamine *et al.* 2018b). El nombre "Bufón de Corte” alude al comportamiento caprichoso e inesperado del “tonto” de la época medieval (Benton 2009). En este contexto, los movimientos tectónicos pueden actuar inesperadamente y cambiar la dinámica “constante” esperada bajo la RQH, al generar cambios en el ambiente físico y fragmentar poblaciones (Hoorn *et al.* 2010; Leprieur *et al.* 2016; Zaffos *et al.* 2017). Asimismo, los cambios globales de temperatura (Zachos *et al.* 2001) son usualmente considerados un factor abiótico importante, ya que pueden actuar sobre las dinámicas de diversificación al afectar factores intrínsecos de las especies como la tasa metabólica, o las interacciones ecológicas (e.g., “la Reina Roja corre más rápido cuando está caliente”) (Erwin 2009; Brown 2014). Esto último apunta a que RQH y CJH podrían estar estrechamente relacionadas.

Cambios climáticos y ambientales bruscos también pueden modificar la dinámica de la especiación y extinción ya que, por ejemplo, si éstos cambios son muy rápidos para permitir que las especies se adapten pueden dar lugar a un incremento en la tasa de extinción (Vrba 1993). Es importante señalar que si factores abióticos, tales como cambios climáticos abruptos, actúan directamente sobre las dinámicas de diversificación, entonces dentro de un clado o en una región determinada, los cambios en las tasas de éstos procesos

serian sincrónicos y ocurrirían en “pulsos” (e.g., *turnover-pulse hypothesis*; Vrba 1993). Aunque se ha sugerido que las hipótesis RQH y CJH operan a distintas escalas, con los factores abióticos influenciando los patrones de diversificación a escalas espaciales y temporales amplias, y los factores bióticos operando en escalas geográficas locales y en tiempos cortos (Barnosky 2001; Benton 2009), diferentes estudios empíricos sugieren que ambos mecanismos pueden actuar en conjunto para generar y mantener la diversidad (Alroy 2010; Lehtonen *et al.* 2017; Condamine *et al.* 2018b; Solórzano *et al.* 2020).

Comprender cómo y por qué los procesos de especiación, extinción y dispersión varían a lo largo del tiempo, espacio geográfico y entre linajes, es clave para entender como se ha generado y mantenido la diversidad (Brandt *et al.* 2007b; Ricklefs 2007; Wiens 2011; Condamine *et al.* 2013; Morlon 2014). Avances recientes en el modelado mecanicista de la macroevolución han permitido, además, estimar los efectos relativos de las interacciones bióticas intrínsecas (o rasgos) y los factores abióticos extrínsecos sobre la diversificación mediante el modelado de las tasas de diversificación en función del tiempo, la diversidad y los cambios ambientales utilizando filogenias calibradas temporalmente (Stadler 2011; Condamine *et al.* 2013; Morlon *et al.* 2016; Condamine *et al.* 2018a). Sin embargo, tales métodos se han empleado principalmente para desentrañar las historias evolutivas de taxones continentales, y con menos intensidad para taxones que viven en ambientes marinos. Esto es especialmente llamativo, considerando que los oceanos cubren ~70% de la superficie del planeta (Tittensor *et al.* 2010), y que los organismos continentales y marinos probablemente han diversificado en formas diferentes (Benton 1997).

Los océanos sustentan un sistema dinámico en el que los organismos experimentan movimientos constantes, y aunque algunos parezcan estacionarios, todos son capaces de invadir nuevos territorios en alguna etapa

de su ciclo de vida (Briggs 2003). De tal forma, los océanos con su relativa estabilidad y gran área geográfica pueden albergar una gran riqueza de especies (Grassle 1989). Se estima que una sexta parte de las especies modernas descritas son marinas, aunque estudios recientes sugieren que alrededor del 91% de las especies que habitan los ecosistemas marinos aún no han sido descritas (Bouchet 2006; Mora *et al.* 2011). Sin embargo, aunque los océanos ocupan aproximadamente tres cuartas partes de la superficie de la tierra (Tyler 2003; Brandt *et al.* 2004), el conocimiento de sus patrones globales de riqueza de especies, así como de los procesos y mecanismos que la generan es mucho más limitado.

Esta escasez de conocimiento se acentúa aún más hacia las zonas oceánicas profundas ("*deep-sea*"; >200 m de profundidad), que representan el 65% de los fondos marinos del planeta, así como las regiones polares (Tittensor *et al.* 2010). Esto puede deberse, entre otras cosas, a las dificultades (logísticas y económicas) de muestrear en tales ambientes remotos. A pesar de esta situación, es claro que los fondos oceánicos profundos y las regiones polares han experimentado dramáticos cambios ambientales (incluyendo variaciones geoquímicas, climáticas, oceanográficas) en el pasado geológico (Zachos *et al.* 2001; Yasuhara *et al.* 2008; Yasuhara y Danovaro 2016; Sweetman *et al.* 2017). Ya que los ecosistemas marinos de aguas profundas y regiones polares están entre los menos explorado del planeta (Tittensor *et al.* 2010), sigue sin comprenderse bien cómo se originaron y diversificaron las especies que allí habitan, y cómo su diversidad respondió a los diferentes cambios ambientales (abióticos) en escalas temporales y espaciales extendidas (Costello y Chaudhary 2017; Sweetman *et al.* 2017; Condamine y Kergoat 2021).

La presente tesis doctoral realizó un aporte en dos temáticas principales: 1) incrementó nuestro entendimiento de la diversidad moderna en ambientes bentónicos profundos del Océano Austral, reduciendo el déficit linneano y wallaceano, utilizando un enfoque taxonómico integrativo, y 2) contribuyó a

comprender el papel desempeñado por los factores abióticos sobre los procesos macroevolutivos que han dado origen a la fauna moderna del Océano Austral. Dado que la presente tesis doctoral se enfocó geográficamente en el Océano Austral, en la siguiente sección se provee información geográfica, geológica y oceanográfica relevante sobre esta región, así como los patrones evolutivos que exhiben sus faunas. Adicionalmente, en las secciones subsiguientes, se proveen más detalles del modelo de estudio abordado: una familia de octocorales (Cnidaria: Anthozoa: Octocorallia: Primnoidae) típicos de aguas profundas con una amplia distribución (Ártico hasta la Antártica), particularmente diversa en el Océano Austral.

El Océano Austral: generalidades

El Océano Austral (en adelante SO) comprende todas las aguas ubicadas al sur de los 60°de latitud sur y que rodean el continente Antártico (Figura 0.1). Desde un punto de vista oceanográfico, el SO comprende todas aquellas aguas limitadas al norte por el Frente Subantártico (ASF) y al sur por el Continente Antártico. En la frontera norte se forma la corriente Circumpolar Antártica (ACC) limitado al norte por el ASF y al sur por el Frente Polar Antártico (APF) (Figura 0.1). La formación del APF coincide con la formación del ASF y el establecimiento de la Corriente Circumpolar Antártica (ACC). Ambos frentes están marcados por la diferencia de varios grados en la temperatura del agua en una corta distancia geográfica. Con el tiempo y dependiendo de las condiciones climáticas, la intensidad de estos gradientes térmicos puede variar significativamente y, como resultado, probablemente impacte el flujo de genes dentro y fuera del Océano Austral.

La ACC, característica fundamental del SO, también conocida como la corriente de deriva del viento del Oeste, es una corriente impulsada por el viento que fluye de oeste a este alrededor de la Antártica y conecta los océanos Atlántico, Pacífico e Índico, sirviendo como principal vía de

comunicación entre ellos (Lagabrielle *et al.* 2009). La ACC está asociada con otras dos características oceanográficas importantes. La primera es una serie de contracorrientes (conocidas como corriente de deriva del viento del este) que se mueven junto a la masa continental antártica (Figura 0.1). En la literatura antártica, a menudo se dice que los patrones de movimiento del hielo y la dispersión pasiva de organismos se deben a la deriva del viento del oeste o del este. Además, como ocurre con cualquier otra corriente oceanográfica importante, la ACC genera remolinos de mesoescala (decenas de kilómetros cuadrados de superficie) que mueven el agua a través de corrientes y frentes.

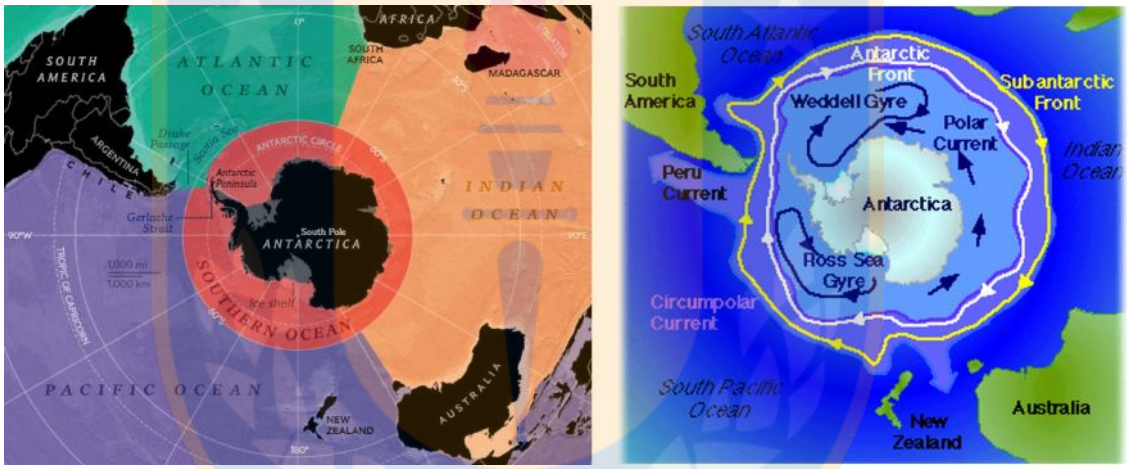

Figura 0.1. Mapa de las masas continentales y océanos en el hemisferio sur (izquierda), y principales corrientes y frentes oceánicos del Océano Austral (derecha). Nótese que el Océano Austral se ubica geográficamente hacia el sur de los 60°S,

El Frente Polar Antártico (APF) es un importante límite biogeográfico en el Hemisferio Sur, ya que limita las aguas frías y baja en salinidad al Sur, de las aguas más templadas al norte, a su vez esta limita al SO en dos regiones: la Región Subantártica al norte y la Región Antártica al sur (Clarke 2008; Convey *et al.* 2014). La región Antártica se extiende desde el continente Antártico hasta el APF, e incluye a las islas del arco de Escocia, Georgia del Sur, islas Bouvet y la meseta de las Kerguelen. La región Subantártica se encuentra limitada al

Sur por el APF, y al norte por el frente subtropical, excediendo el norte del ASF, incluyendo así, el sur de la Patagonia, las islas Malvinas y las aguas al sur de Tasmania y Nueva Zelanda (Griffiths *et al.* 2009) (Figura 0.2).

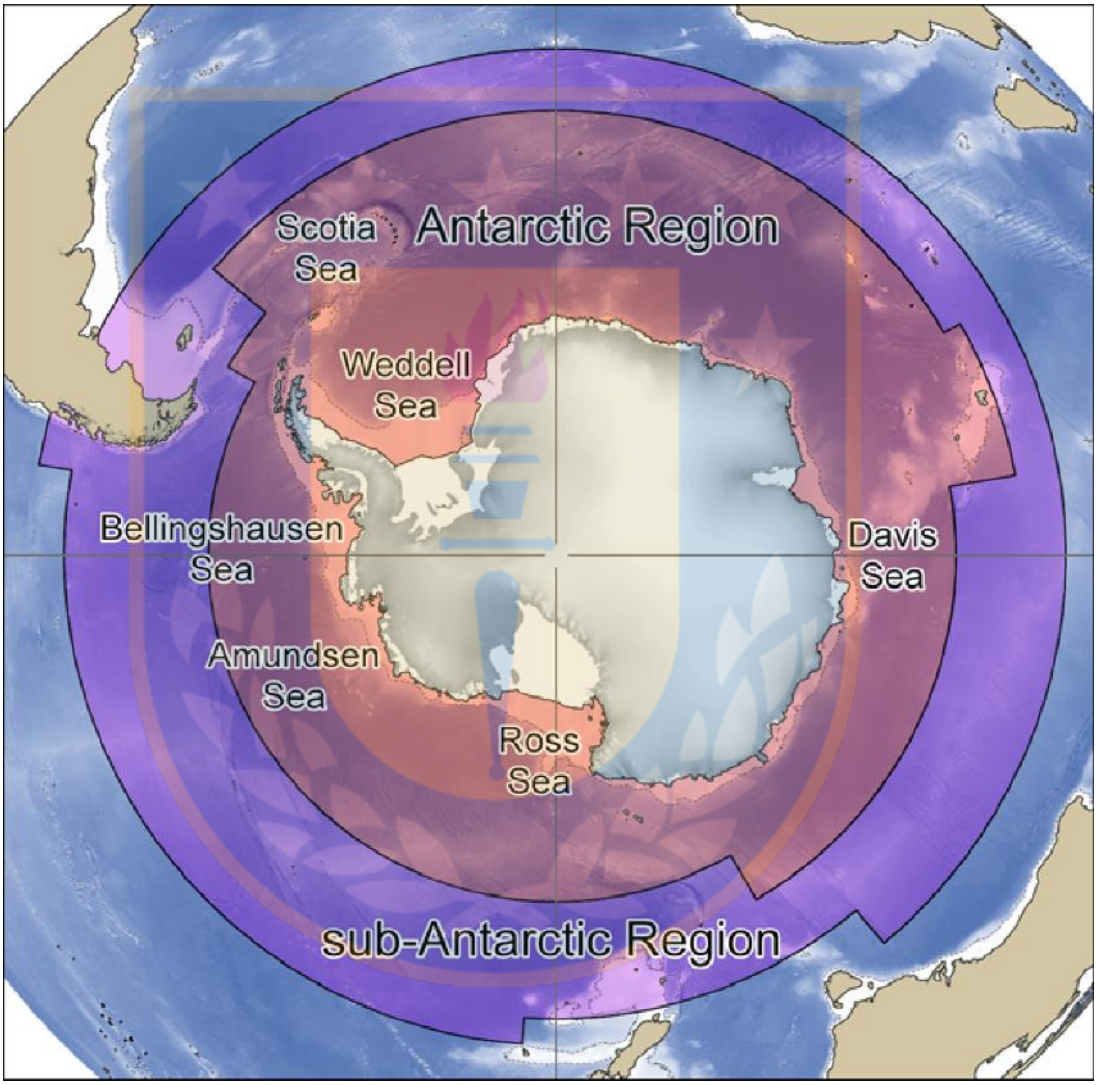

Figura 0.2. Mapa de las dos grandes Regiones del Océano Austral, región Antártica y región Subantártica (Griffiths *et al.* 2009).

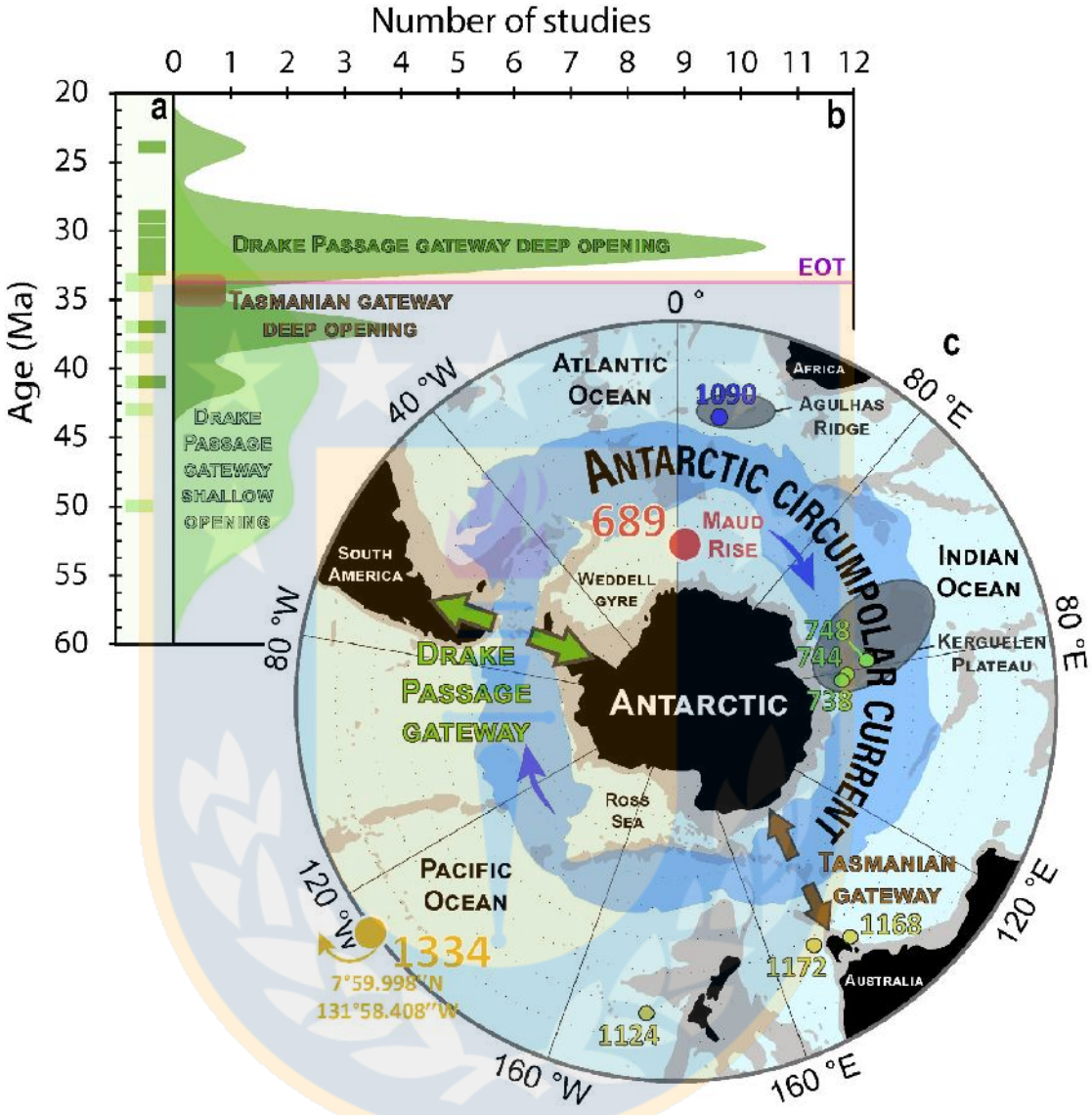

Figura 0.3. Recopilación de las edades de apertura del Pasaje de Drake reportadas en la literatura. El paso de Tasmania se abrió a la circulación oceánica profunda entre 35,5-33,5 Ma, mientras que la apertura y profundización del Paso Drake, y consiguiente inicio de la ACC, ocurrió entre 31-26 Ma (Hodel *et al.* 2021).

El SO presenta una geomorfología compleja, así como una historia tectónica y climática única. Geomorfológicamente se caracteriza por presentar una plataforma continental inusualmente profunda (450 m en promedio, aunque

supera los 1000 m en algunas zonas) como resultado de la erosión y carga isostática asociada a las grandes masas de hielo que alberga (Clarke y Johnston 2003). Además, la progresiva fragmentación de Gondwana durante los últimos 165 millones de años ocasionó la sucesiva separación física del continente Antártico y las masas de tierra que hoy conforman Australia, África y Suramérica (Torsvik *et al.* 2007). Sin embargo, el aislamiento total del continente Antártico es considerado efectivo a partir de la apertura de pasaje Drake (~31-26 Ma) (Hodel *et al.* 2021), que separa la península Antárctica del extremo sur de la Patagonia y Tierra del Fuego.

Es durante el Eoceno (~42 Ma) que se produce el inicio del cese de la conexión terrestre entre el continente Antártico y Suramérica, marcando los estadios iniciales de la apertura del Paso Drake (Cristini *et al.* 2012; Halanych y Mahon 2018), mientras que su completo aislamiento geográfico se produce a partir del Oligoceno (~31 Ma) con el establecimiento de la Corriente Circumpolar Antártica (ACC) (Lawver y Gahagan 2003; Chown *et al.* 2015; Hodel *et al.* 2021) (Figura 0.3).

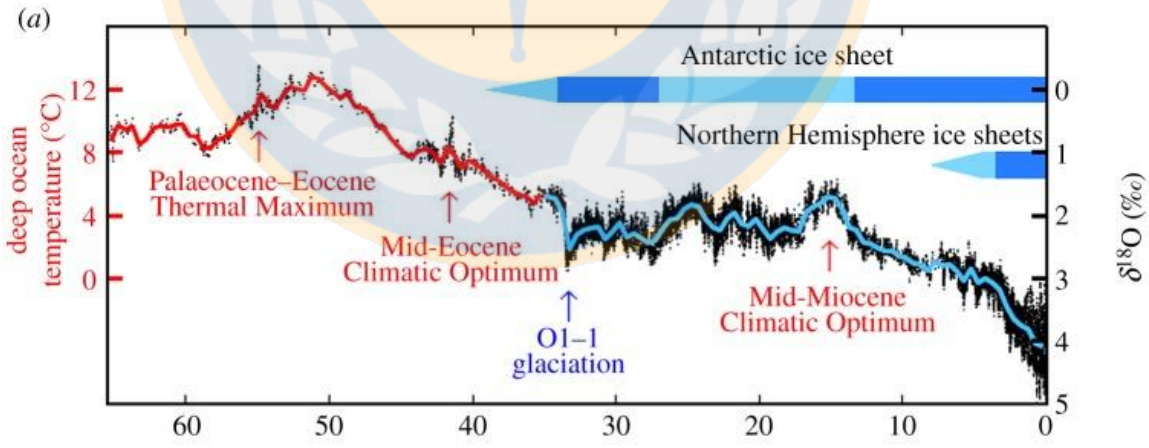

Figura 0.4. Cambios climáticos globales del Cenozoico basados en la composición isotópica del oxígeno 18 ($\delta^{18}O$) de foraminíferos de aguas profundas. Nótese, además, los episodios más importantes en la fluctuación del clima global (e.g., Máximo termal del

Paleoceno-Eoceno), así como el inicio de la acumulación de capas de hielo en la Antártica. Tomado de Zachos *et al.* (2001).

La historia geológica de la Antártica esta intrínsicamente relacionada a los cambios climáticos globales del Cenozoico (Zachos *et al.* 2001; Cristini *et al.* 2012) (Figura 0.4). El clima global se caracterizó por condiciones cálidas durante el Cretácico-Eoceno (*greenhouse*), y condiciones más frías (*icehouse*) a partir del límite Eoceno-Oligoceno (38 Ma) (Tripati *et al.* 2005; Liebrand *et al.* 2017). Durante el Eoceno temprano ocurrió un episodio caracterizado por un fuerte calentamiento, conocido como el Óptimo Climático del Eoceno (Zachos *et al.* 2001), mientras que el Oligoceno fue un período dominado por un enfriamiento gradual (glaciaciones), así como por fluctuaciones en el volumen de la capa de hielo, que culminaron en el Mioceno temprano (Roberts *et al.* 2003; Pekar y DeConto 2006), y los cuales parecen estar asociados a una considerable reducción de fauna. Este período de bajas temperaturas fue seguido por un período cálido prolongado, denominado "Óptimo Climático del Mioceno Medio" (MMCO) hacia los 17–15 Ma (Lagabrielle *et al.* 2009; Hauptvogel y Passchier 2012). El MMCO fue seguido de un largo periodo de enfriamiento conocido como la “Transición Climática del Mioceno Medio” (TMMC), de 14.2 -13.8 Ma, la cual estuvo marcada por un crecimiento rápido de la capa de hielo en la Antártica (Davies *et al.* 2012). La TMMC coincide con una nueva ampliación y profundización del Paso de Drake y un posible reforzamiento de la ACC hacia los 14-15 Ma (Lagabrielle *et al.* 2009). Finalmente, numerosos eventos glaciales (alternancia de ciclos glaciares e interglaciares) han ocurrido en los últimos cinco millones de años en la Antártica (Zachos *et al.* 2001; Davies *et al.* 2012).

Origen, patrones y procesos evolutivos de la fauna marina Antárctica

En el Océano Austral existe una importante diversidad, especialmente de invertebrados marinos (Clarke y Crame 2010), aunque diferentes estimaciones sugieren que solo conocemos entre el 40-60 % de su diversidad total (Gutt *et al.* 2004; Costello *et al.* 2010). Este océano alberga uno de los ecosistemas marinos de altas latitudes más interesantes, con faunas adaptadas a condiciones extremas de baja temperatura (Clarke y Johnston 2003; Clarke 2008; Convey *et al.* 2014). Se han descrito más de 8000 especies de invertebrados del Océano Austral, con un número total estimado de 20000 (Gutt *et al.* 2004). Asimismo dependiendo del grupo taxonómico examinado, entre el 50% y 97% de la fauna bentónica antártica se caracteriza por presentar altos niveles de endemismo (Griffiths *et al.* 2009; Kaiser *et al.* 2013; Broyer *et al.* 2014). Además, muchos linajes en el SO (e.g., isópodos, anfípodos, peces óseos) exhiben patrones de diversidad y disparidad eco-morfológica similares a los encontrados en regiones tropicales o templadas (Clarke y Johnston 2003; Brandt *et al.* 2007a; Clarke y Crame 2010; Kaiser *et al.* 2013; Chown *et al.* 2015). Sin embargo, y a pesar de los avances conseguidos en los últimos años, muchos de los especímenes colectados a lo largo de diferentes expediciones aún no han sido estudiados, sugiriendo que muchas especies marinas antárticas que pueden ser esenciales para mejorar nuestra comprensión de los procesos macroevolutivos que dieron origen a la fauna moderna del SO permanecen aún sin describir (Kaiser *et al.* 2013).

Aunque la fauna marina del SO ha sido generada y mantenida durante el progresivo aislamiento y enfriamiento a la que ha sido sometida durante los últimos 40 Ma (Norris *et al.* 2013), el origen de sus comunidades faunísticas modernas es extremadamente complejo, ya que consiste de elementos endémicos diversificando *in situ* (incluso desde el Mesozoico). El origen de muchos linajes se remonta al Eoceno, y algunos de ellos se remontan al Cretácico Superior. También se ha invocado una larga evolución y diversificación *in situ* que se remonta al Cretácico tardío-Cenozoico temprano

para explicar el alto nivel de diversidad de la fauna de aguas profundas del Océano Austral (Thatje *et al.* 2005). Una segunda fuente de taxones se considera de aquellos que han migrado desde Sudamérica a través del Arco de Escocia y/o de cuencas profundas adyacentes en diferentes pulsos durante el Cenozoico (Crame 2018; Halanych y Mahon 2018). Clarke (2008) señaló que algunos taxones originados en el SO también podrían haber migrado a lo largo del Arco de Scotia en la dirección contraria hacia el norte, fuera de la Antártica. Sin embargo, la dirección y magnitud de la dispersión de taxones hacia o desde el SO, así como sus dinámicas de diversificación, parece ser linaje dependiente. De tal forma, el SO puede ser considerado, a nivel macroevolutivo, tanto fuente como sumidero (esencialmente refugios para taxa que han sido desplazados progresivamente a lo largo de los gradientes de competencia meridionales) de fauna marina (Briggs 2003; Rogers 2007; Clarke 2008). El SO es considerado, junto con el norte del Pacífico y las Indias orientales (Filipinas, Malasia y Nueva Guinea) como un “centro de origen” de taxones marinos (Briggs 2003). Adicionalmente, ya que el SO contribuye con aguas frías y profundas a la circulación oceánica global esta región tiene el potencial de ser una “fuente” de diversidad de organismos de aguas profundas que pueden dispersarse globalmente (Strugnell *et al.* 2008).

Estudios biogeográficos (Brandt *et al.* 2007a; Griffiths *et al.* 2009; Broyer *et al.* 2014) sugieren la existencia de tres grandes regiones biogeográficas en el SO y sus alrededores: Nueva Zelanda, el sur de América del Sur y las islas subantárticas, y la Antártica. Además resaltan, entre otras cosas que: 1) el Océano Austral representa una "unidad funcional única" sin evidencia de una división biogeográfica entre el este y el oeste; 2) existe poca evidencia de una relación biogeográfica entre las faunas de la Antártida o América del Sur con aquellas de Nueva Zelanda/Tasmania; 3) existen fuertes vínculos faunisticos entre la Antártida y Sudamérica; 4) las afinidades faunísticas entre conjuntos magallánicos y subantárticos, esta probablemente impulsadas por la ACC que

fluye hacia el oeste, lo que permite la dispersión de propágulos a larga distancia (Griffiths *et al.* 2009). Sin embargo, las relaciones biogeográficas y la conectividad en el SO y regiones adyacentes difieren entre grupos taxonómicos y tipos de estrategias reproductivas (i.e., *brooding* vs. *broadcasting*) (Griffiths *et al.* 2009; Moreau *et al.* 2017).

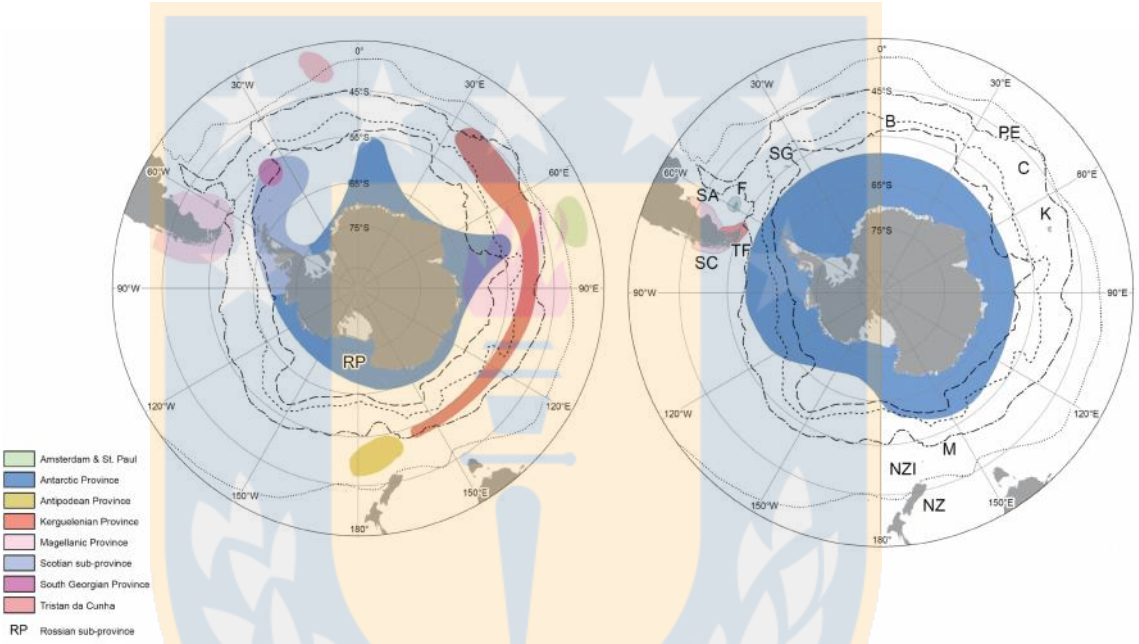

Figura 0.5. Izquierda: División biogeográfica de la zona litoral de las aguas temperadas del sur y de la Antártica sensu Knox (1960). Derecha: Las regiones biogeográficas antárticas y subantárticas según Briggs and Bowen (2012). **Provincias Sudamericanas**: SC, Sur de Chile; TF, Tierra del Fuego; SA, Sur de Argentina; F, Islas Malvinas. **Provincias subantárticas**: SG, Georgia del Sur; B, Isla Bouvet; PE, Islas Príncipe Eduardo; C, Islas Crozet; K, Islas Kerguelen; M, Isla Macquarie. **Provincia de las Antípodas**: NZI, Auckland, Antípodas, Islas Campbell y Bounty; NZ, Provincia de Nueva Zelanda. El área azul indica la Región Antártica fría (Broyer *et al.* 2014).

Es importante señalar que el reconocimiento de distintas provincias biogeográficas en el SO y sus alrededores (e.g., Knox 1960; Briggs y Bowen 2012) ha estado basado principalmente en análisis de listados de presencia de especies (Figura 0.5). Sin embargo, esta metodología no está exenta de

posibles limitaciones, especialmente por la reconocida existencia de especies cripticas en el SO (De Broyer *et al.* 2011; Baird *et al.* 2011; Allcock *et al.* 2011; Halanych y Mahon 2018). De tal forma, especies consideradas alguna vez como circumpolares (especies ampliamente distribuidas en todo el SO) de hecho pueden representar complejos de especies cripticas (Held 2003; Linse *et al.* 2007; Allcock *et al.* 2011), y recientes análisis biogeográficos de invertebrados bentónicos marinos (e.g., moluscos,) basados en datos moleculares están mostrando que los patrones de distribución de linajes son más complejos de lo que se pensaba anteriormente y no pueden generalizarse (González-Wevar *et al.* 2010; González-Wevar *et al.* 2017).

Se pueden reconocer tres períodos donde ocurrieron los cambios climáticos/oceanográficos Cenozoicos más dramáticos en el SO los cuales pueden haber impactado sobre los procesos biogeográficos y macroevolutivos que han dado origen a la fauna marina moderna en el SO:

1. **el límite Eoceno/Oligoceno (34-28 Ma),** cuando ocurre la formación del Pasaje Drake, y el establecimiento de la ACC modificando la circulación oceánica global por primera vez, lo cual coincide a su vez con la formación del Frente Polar Antártico y el Frente Subantártico, y ocasionó un completo aislamiento térmico y geográfico de la biota marina antártica (Lawver y Gahagan 2003; Mackensen 2004; Chown *et al.* 2015). A partir del establecimiento de la ACC las especies con baja capacidad de dispersión (*brooding*) pudieron ser transportadas (por la ACC) a nuevos hábitats favoreciendo la especiación alopátrica, o creando una barrera marina natural para el intercambio genético con poblaciones aisladas al norte y sur del APF impulsando así la especiación alopátrica (Pearse *et al.* 2009; Chenuil *et al.* 2018).

2. **el Mioceno medio a tardío (14-12 Ma),** cuando se produce una intensificación de la ACC probablemente debido a la profundización del paso Drake (Mackensen 2004). El establecimiento de la ACC y de los Frentes

Polares (APF, SAF), y particularmente la intensificación de una ACC profunda hacia los 14-12 Ma puede representar un mecanismo que favoreció el aislamiento geográfico e incremento la diversificación de diferentes linajes dentro de la fauna marina del SO (González-Wevar *et al.* 2010; Near *et al.* 2012; Poulin *et al.* 2014; Colombo *et al.* 2015).

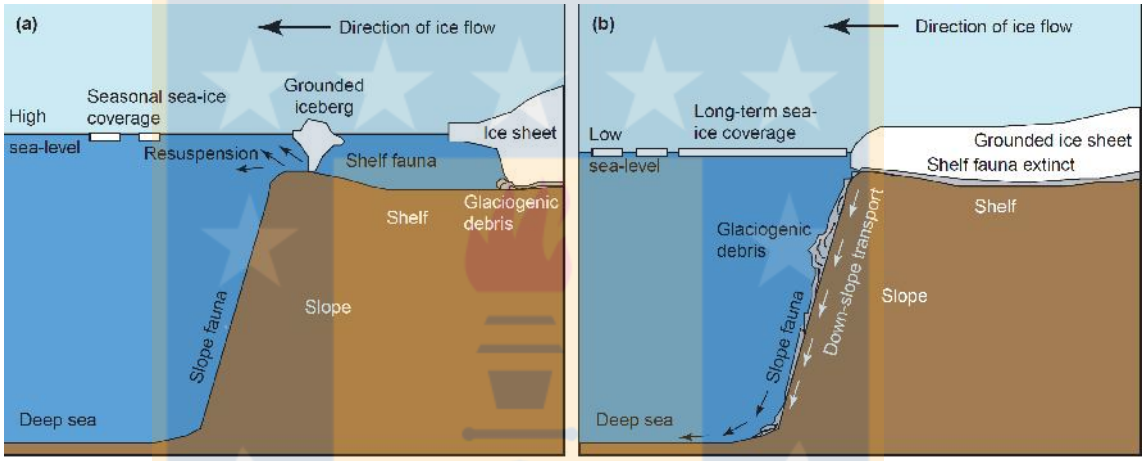

Figura 0.6. Condiciones ambientales en el margen continental antártico durante un ciclo glacial-interglaciar del Cuaternario tardío (Thatje *et al.* 2005).

3) el Cuaternario (2.5-0.01 Ma), caracterizado por pronunciados cambios en temperatura asociados a periodos glaciares e interglaciares que afectaron la estacionalidad e intensidad de la formación de capas de hielo sobre el SO (Mackensen 2004; Chown *et al.* 2015). Dichos ciclos glaciales pudieron generar refugios y/o extinciones locales de la fauna bentónica (Clarke y Crame 1992; Krug *et al.* 2010), pero también estimulando eventos de especiación (Near *et al.* 2012) por fragmentación poblacional en áreas aisladas de la plataforma (durante épocas glaciales) o desplazamiento poblacional en refugios alrededor de islas subantárticas (González-Wevar *et al.* 2013) o en las profundidades marinas (Figura 0.6) (Thatje *et al.* 2005; Clarke y Crame 2010).

Considerando lo anteriormente expuesto, si alguno de estos tres períodos desencadenó cambios macroevolutivos en el SO, entonces deberíamos

detectar una correlación entre las dinámicas de diversificación de la fauna marina antártica coincidentes temporalmente con alguno de ellos (34-28 Ma; 14-12 Ma; 2.5-0.01 Ma) (Clarke y Crame 1992; Thatje *et al.* 2005; Pearse *et al.* 2009; Clarke y Crame 2010; Chenuil *et al.* 2018). Sin embargo, cuál de estos episodios climático/oceanográfico discreto ejerció un mayor impacto sobre los procesos macroevolutivos en el SO, parece ser taxón dependiente. Y es por ello que se hacen necesarios nuevos estudios, en grupos taxonómicos hasta el momento no estudiados pero diversos en la región (e.g., octocorales), para poder realizar "generalizaciones" sobre los impulsores evolutivos de la fauna marina del SO (Saucède *et al.* 2014).

Modelo de Estudio: Familia Primnoidae (Cnidaria: Anthozoa: Octocorallia)

Los octocorales (Octocorallia) exhiben una gran abundancia en las comunidades bentónicas marinas alrededor del planeta, con más de 3100 especies habitando desde ambientes someros hasta abisales (Daly *et al.* 2007; Pérez *et al.* 2016). Los octocorales representan uno de los principales contribuyentes a la diversidad y biomasa en las comunidades bentónicas (Gutt y Starmans 1998; Clarke y Arntz 2006), siendo las gorgonias las más características y ecológicamente importantes al proporcionar un hábitat para el asentamiento de otras especies (Buhl-Mortensen y Buhl-Mortensen 2006).

La familia Primnoidae, representa una de las 50 familias más diversas dentro de la subclase Octocorallia (López-González *et al.* 2002; Cairns 2016; Pérez *et al.* 2016). Miembros de esta familia habitan los fondos marinos desde el Ártico hasta la Antártica, y el 96% de las especies tienen rangos batimétricos que se extienden por debajo de 200 m, aunque la mayoría viven mucho más profundo (hasta 6400 metros) (Cairns 2016). Morfológicamente se caracterizan por presentar un eje altamente calcificado y pólipos no retráctiles que están fuertemente blindados con escamas calcáreas (Daly *et al.* 2007; Cairns y Bayer 2009), ausencia de escleritos tentaculares, pólipos a menudo dispuestos en

verticilios y escamas operculares a menudo con quillas (Cairns y Bayer 2009). Primnoidae está conformada por 43 géneros y más de 280 especies (Cairns y Wirshing 2018) con tres géneros, *Narella* Gray, 1870, *Plumarella* Gray, 1870, y *Thouarella* Gray, 1870, con una distribución cosmopolita (Cairns 2006; Taylor *et al.* 2013; Taylor y Rogers 2017; Cordeiro *et al.* 2018).

Durante las últimas décadas se han intensificado los estudios taxonómicos en primnoides, permitiendo reconocer numerosas especies nuevas (López-González *et al.* 2002; López-González 2006; Zapata-Guardiola y López-González 2010b; Zapata-Guardiola y López-González 2010e; Zapata-Guardiola y López-González 2010d; Zapata-Guardiola y López-González 2012; Zapata-Guardiola *et al.* 2013). En estos trabajos las descripciones de especies nuevas se basan exclusivamente en características macro y microscópicas de las colonias y el escleroma. Sin embargo, tales aproximaciones presentan desafíos y limitaciones debido a que: 1) la variabilidad de los caracteres macro y microscópicos empleados generalmente en la taxonomía de primnoides es difícil de describir con caracteres discretos (Taylor *et al.* 2013); 2) se ha propuesto que muchos de los caracteres utilizados para las delineaciones taxonómicas de la familia (y en octocorales en general) pueden ser homoplásicos lo que limita su utilidad para estudios filogenéticos basados en caracteres morfológicos (Dueñas y Sánchez 2009; Cairns y Wirshing 2018); y 3) hay evidencias de plasticidad fenotípica en ciertos caracteres diagnósticos en octocorales como respuesta a fluctuaciones ambientales (Prada *et al.* 2008).

Es por ello que los taxónomos pueden diferir en la forma en que interpretan la variabilidad de los caracteres de las colonias y escleroma. Como consecuencia, no son raras las opiniones contradictorias sobre las delimitaciones de especies en la literatura, y existen casos bien ejemplificados sobre la inestabilidad en la asignación de especies y géneros en la familia Primnoidae (Cairns 2006; Zapata-Guardiola y López-González 2010b; Taylor *et al.* 2013; Cairns y Wirshing 2018). Por esta razón, cuando sea posible, los

caracteres morfológicos no deberían ser la única base para definir los límites de las especies en los octocorales (McFadden *et al.* 2010; McFadden *et al.* 2011; Xu *et al.* 2020).

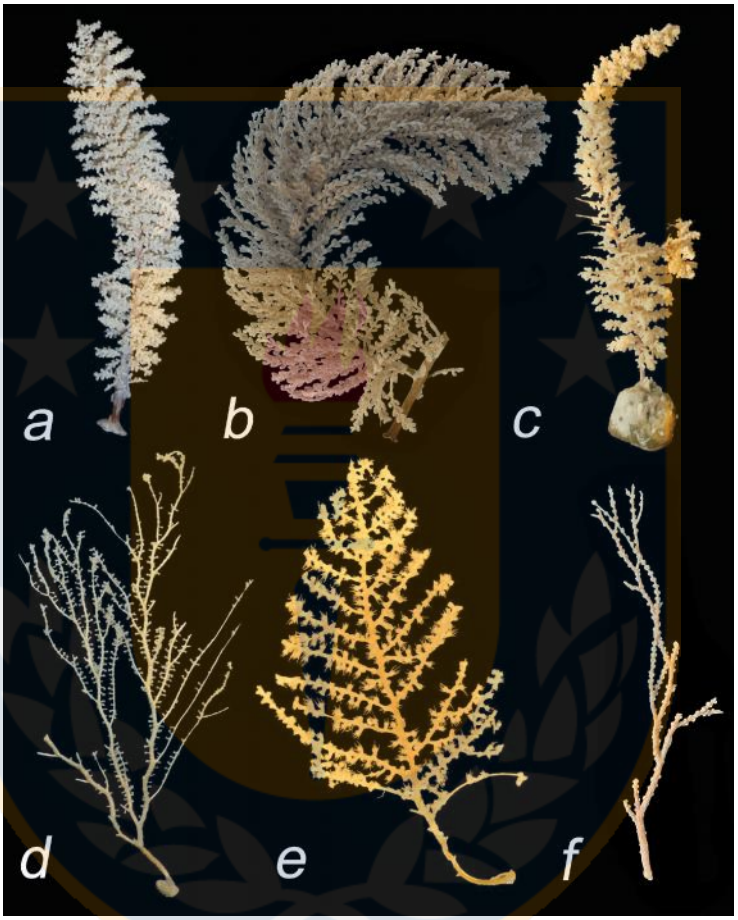

Figura 0.7. Tipo de ramificación de colonias del género *Thouarella.* a) *Thouarella chilensis* (bottlebrush), b) *Thouarella brucei* (bottlebrush), c) *Thouarella antarctica* (bottlebrush), d) *Thouarella coronata*, e) *Thouarella diadema*, f) *Thouarella porcupinensis* (Taylor *et al.* 2013).

La utilidad de caracteres moleculares en la taxonomía de primnoides ha sido recientemente sugerida por el descubrimiento de potenciales nuevas especies dentro de uno de los géneros con más especies descritas en esta familia, *Thouarella* (Bogantes *et al.* 2020). *Thouarella* Gray, 1870 es un género de octocorales primnoides dentro de la clase Anthozoa. Este género se

caracteriza por presentar, entre otros caracteres, colonias arquitectónicamente delicadas comúnmente con forma de escobillón (*bottlebrush;* Figura 0.7), pólipos de 6-8 filas de escamas en la pared del cuerpo, y escamas de la fila axial (adaxiales) que a menudo se reducen en tamaño y número (Taylor *et al.* 2013), así como por presentar ejes de gorgonina calcificados, continuos y sólidos (Cairns y Bayer 2009).

Por otra parte, trabajos recientes han incrementado la diversidad de especies de la familia Primnoidae en el SO (Zapata-Guardiola y López-González 2010b; Zapata-Guardiola y López-González 2010e; Zapata-Guardiola y López-González 2010d). Estos trabajos han demostrado que la endemicidad de géneros en esta región (~60%) es mayor al conseguido en otros océanos (e.g., (López-González *et al.* 2002)). A nivel de especies, la mayor diversidad específica de la familia se registra en el Océano Pacífico (117 sp.), mientras que en el SO solo encontramos un cuarto del número total de especies (Cairns y Bayer 2009).

Existen al menos tres hipótesis filogenéticas para la familia, basadas tanto en datos morfológicos (Cairns y Bayer 2009) como datos moleculares (Taylor y Rogers 2015; Cairns y Wirshing 2018). Taylor y Rogers (2015) realizan la primera filogenia molecular de la familia que incluyó una importante cantidad de taxones (64 spp. y 25 géneros), utilizando genes nucleares (*28S*, *18S*) y mitocondriales (*MutS*, *Cox1*, *16S*) (Figura 0.8). Estos autores sugieren que: 1) Primnoidae es una familia monofilética, siendo Chrysogorgiidae su grupo hermano, ambos divergirían hace 150-90 Ma; y 2) la presencia de un clado que incluye a la mayoría de primnoides comunes o geográficamente restringidos a las regiones antártica y subantártica.

Aunque el aislamiento geográfico y las condiciones extremas podrían explicar el alto nivel de endemismo a nivel de géneros de esta familia en el SO (Briggs 2003), nuestro entendimiento de la historia biogeográfica de esta familia es incompleto. Por ejemplo, ¿cuál es el área ancestral de la familia?

permanece como una pregunta abierta. En su árbol consenso, basado en parsimonia y caracteres morfológicos, Cairns y Bayer (2009) encuentran que varios de los géneros más basales dentro de la familia (e.g., *Ainigmaptilon*) están restringidos al SO, sugiriendo que el origen de la familia pudo haberse dado en la región Antártica. Por otra parte, los taxones más basales dentro de la filogenia molecular de Taylor y Rogers (2015; Figura 0.8) (e.g., *Narella*, *Parastenella*) provienen del Océano Pacífico, lo que lleva a los autores a hipotetizar que esta zona representa el área ancestral de la familia. Además, proponen que la diversidad subantártica probablemente se deba a una radiación secundaria, producida antes de la apertura del Paso Drake y la formación de la ACC (Taylor y Rogers 2015).

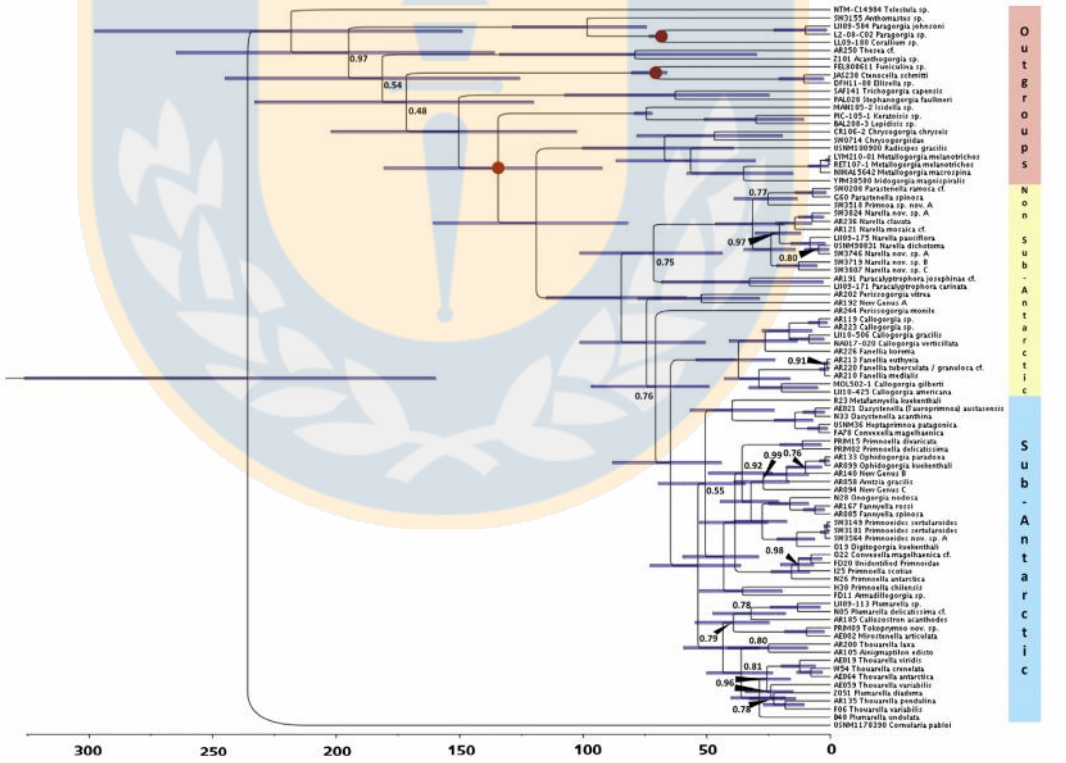

Figura 0.8. Filogenia molecular calibrada de la familia Primnoidae (Taylor and Rogers 2015). Nótese que la misma solo incluye 64 especies de primnoides.

Por otra parte, la dinámica de diversificación de los antozoos (Cnidaria: Anthozoa), un grupo que incluye corales formadores de arrecife (Hexacorallia) y octocorales (Octocorallia), parece estar afectada significativamente por eventos de extinción en masa y grandes crisis arrecifales desencadenadas por la acidificación de los océanos y/o el calentamiento global (e.g., máximo termal del Paleoceno-Eoceno), y además la geoquímica oceánica (i.e., proporción Mg/Ca en el agua de mar) parece influir en la evolución de sus esqueletos (Quattrini *et al.* 2020). Por lo tanto, los eventos históricos de acidificación abrupta del océano, el calentamiento global y los cambios en las condiciones químicas oceánicas del pasado podrían ser hipotetizados como los principales factores abióticos que podrían impulsar la dinámica de diversificación de los primnoides. Adicionalmente, eventos históricos de vicarianza (e.g., asociados al establecimiento e intensificación de la ACC) y gradientes ambientales, también se han considerado como esenciales para la evolución de los primnoides (Quattrini *et al.* 2013; Dueñas *et al.* 2016).

Resumen del problema de tesis

El estado actual del conocimiento muestra que gran parte de los trabajos que han abordado el estudio de la familia Primnoidae se han enfocado en definir nuevos taxones basados principalmente en caracteres morfológicos (López-González *et al.* 2002; López-González 2006; Cairns y Baco 2007; Zapata-Guardiola y López-González 2010d; Zapata-Guardiola y López-González 2010b; Zapata-Guardiola y López-González 2010e; Altuna y López-González 2019), revisar su estatus taxonómico (Cairns y Bayer 2009; Zapata-Guardiola *et al.* 2013; Taylor *et al.* 2013), y esclarecer sus relaciones filogenéticas (Taylor y Rogers 2015; Cairns y Wirshing 2018). Sin embargo, nuestra comprensión de cómo, cuándo y dónde han evolucionado los primnoides es limitada (Taylor y Rogers 2017; Quattrini *et al.* 2020), y preguntas como: ¿la tasa de diversificación de los primnoides fue homogénea o

heterogénea a través del tiempo?, ¿Cuáles fueron los impulsores de la diversificación de los primnoides?, ¿Cuáles son los patrones biogeográficos históricos de los primnoides?, ¿cuál es el área ancestral de la familia?, permanecen sin una respuesta clara. Es por ello que detectamos un vacío de conocimiento que existe respecto al origen, historia biogeográfica, y patrones de diversificación (y potenciales drivers) de este grupo de organismos ecológicamente importantes y diversos en los fondos profundos del SO y del planeta.

Considerando su larga historia de aislamiento geográfico y compleja evolución geológica y climática hacen del SO un escenario ideal para investigar el impacto de los factores abióticos (CJH) sobre los procesos macroevolutivos que han generado la diversidad de organismos marinos en ambientes de altas latitudes. Adicionalmente, las gorgonias de la familia Primnoidae son un buen modelo de estudio para investigar tales temáticas, porque presentan una amplia distribución geográfica, tienen una larga historia evolutiva, y son lo suficientemente antiguos en el SO (presentes en el SO desde hace 50 Ma *sensu* Taylor y Rogers 2015) como para haber experimentado los dramáticos cambios climáticos pasados ocurridos en el SO (Mackensen 2004). Por ejemplo, trabajos previos sugieren que las fluctuaciones en el posicionamiento latitudinal del ACC durante el Mioceno medio (14-12 Ma) contribuyeron a la diversificación de un género de primnoides con forma de escobillón (*bottlebrush*) en el SO (Dueñas *et al.* 2016), sin embargo, esta hipótesis aún debe ser puesta a prueba con una muestra más significativa de primnoides antárticos.

Por otra parte, la diversidad del SO esta probablemente subestimada (Gutt *et al.* 2004; Costello *et al.* 2010). Es por ello por lo que para lograr un mejor entendimiento sobre los factores que generan y mantienen su biodiversidad es necesario reducir el déficit linneano. Durante los últimos 20 años se han colectado numerosas colonias de primnoides en el SO, que están

actualmente depositadas en la colección Biodiversidad y Ecología Acuática (BECA) de la Universidad de Sevilla (España). El estudio de esta colección nos brindó la oportunidad para investigar la diversidad de primnoides del SO. En particular, durante el desarrollo de la presente tesis doctoral, me centré en el estudio de la diversidad del género *Thouarella* en el SO. Las especies de este género suelen ser muy similares macro y microscópicamente, por lo que su identificación morfológica es compleja, y su taxonomía inestable (Taylor *et al.* 2013; Cairns y Wirshing 2018). Considerando las potenciales limitaciones de los caracteres morfológicos como las fuentes únicas de información para delimitar y definir especies (e.g., caracteres homoplásicos), las colonias de *Thouarella* se deberían estudiar utilizando aproximaciones integrativas a fin de poder delimitar posibles especies nuevas desde perspectivas múltiples y complementarias (Dayrat 2005; De Queiroz 2005; Pante *et al.* 2015; Kapli *et al.* 2017; Xu *et al.* 2020).

Hipótesis de Investigación

***Hipótesis*.** La diversidad moderna de los primnoides antárticos fue generada por la acción de factores abióticos actuando sobre los procesos macroevolutivos a lo largo del tiempo geológico. Estos factores comenzaron a actuar posterior a la colonización temprana del Océano Austral por pocos linajes de primnoides.

> ***Predicción*.** La tasa de diversificación de los primnoides antárticos es variable a lo largo del tiempo. Los cambios de tasa se dieron en pulsos, durante alguno de los siguientes intervalos temporales: 2.58–0.01 Ma, 34–28 Ma, 14–12 Ma y/o se relacionan con factores abióticos que varían de forma continua a lo largo del tiempo (e.g., temperatura, geoquímica de los océanos).

Objetivos

Objetivo general. Determinar el papel desempeñado por los factores abióticos sobre los procesos macroevolutivos que han dado origen a la fauna moderna de primnoides en el Océano Austral.

Objetivos específicos

1. Reconocer y describir especies de primnoides antárticos con morfotipos *bottlebrush*, con especial énfasis en aquellas incluidas dentro del género *Thouarella*, a partir de materiales inéditos, utilizando un enfoque integrativo.
2. Refinar la sistemática molecular de la familia Primnoidae, a partir de la adición de datos moleculares de potenciales nuevas especies, así como de especies ya descritas, pero sin datos moleculares disponibles.
3. Estimar el área geográfica ancestral de la familia Primnoidae.
4. Determinar la influencia de diversos factores abióticos episódicos y continuos en el tiempo (e.g., temperatura global, concentraciones de dióxido de carbono, nivel del mar, geoquímica oceánica, fragmentación continental) sobre la dinámica de diversificación de los primnoides antárticos.

Metodología

Para el logro de los objetivos planteados, se realizaron distintas actividades (consistentes con los objetivos específicos) que se describen brevemente a continuación. Para mayores detalles sobre los métodos empleados durante el desarrollo de la presente tesis doctoral revise la sección "*material and methods*" de los Capítulos I–III.

Diversidad y sistemática molecular de primnoides

El SO es una zona con un alto potencial de albergar especies no descritas (Gutt *et al.* 2004; Costello *et al.* 2010). Para estudiar la historia evolutiva de un clado es necesario, en primer lugar, tratar de reducir tanto el déficit linneano como el wallaceano al abordar el estudio de su diversidad no descrita. En este sentido, la presente tesis doctoral se centró, inicialmente, en el estudio de una muestra de ejemplares de gorgonias de la familia Primnoidae colectados principalmente cerca de la Península Antártica y el Mar de Weddell durante expediciones realizadas entre los años 1998-2018 en el marco de distintas campañas (e.g., ANT, EASIZ-II, LAMPOS, ANDEEP-I, ANDEEP-II, CAML-CLIMANT, y CAML-ECOWED; Figura 0.9). Estos ejemplares están depositados en la colección del grupo de investigación Biodiversidad y Ecología Acuática (BECA) del Departamento de Zoología de la Universidad de Sevilla, España, y comprenden más de 3000 lotes.

El estudio de estos materiales inéditos requirió, inicialmente, reconocer especies (la unidad fundamental en biología), así mismo como dilucidar sus relaciones de parentesco evolutivo. Para ello primero se investigó la existencia de linajes evolutivos independientes (De Queiroz 2005; De Queiroz 2007) a partir del análisis de marcadores moleculares mitocondriales y nucleares, caracteres morfológicas de las colonias examinadas y métodos de delimitación de especies; ya sea proponiendo nuevas especies o reconociendo algunas ya descritas en la literatura. Esta aproximación “integrativa” que incluye la taxonomía clásica (técnicas morfológicas tradicionales para el reconocimiento de morfoespecies), y el uso de herramientas moleculares, se centró específicamente en morfoespecies de *Thouarella* que exhiben una ramificación tipo *bottlebrush*.

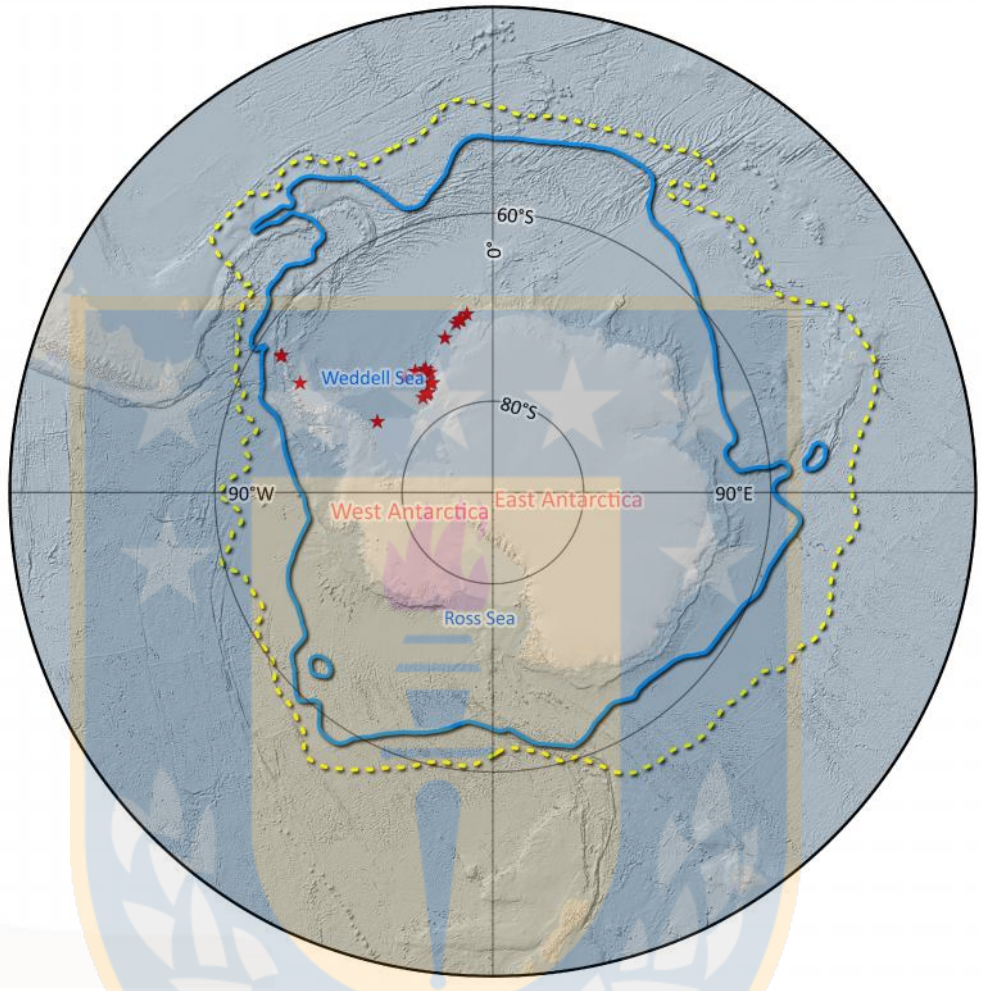

Figura 0.9. Área de muestreo. Estrellas rojas indican la proveniencia geográfica de las colonias estudiadas, durante el desarrollo de la presente tesis doctoral. Línea azul indica la ubicación de la Corriente Circumpolar Antárctica (ACC). Línea amarilla indica la ubicación del Frente Polar Antárctico APF).

Para llevar a cabo las identificaciones de los ejemplares nos enfocamos en la anatomía externa e interna de las colonias, utilizando la nomenclatura anatómica actualizada (ver detalles en el capítulo correspondiente). Dado que el número de escamas por fila longitudinal sobre los pólipos, su tamaño y su forma, así como los del cenénquima son uno de los caracteres taxonómicos más importantes en primnoides (Cairns y Bayer 2009; Taylor *et al.* 2013), éstos fueron medidos y fotografiados utilizando microscopia electrónica de barrido

(SEM) en el Centro de Investigación, Tecnología e Innovación de la Universidad de Sevilla (CITIUS), España. Se realizaron, además, comparaciones con las descripciones de especies descritas en la literatura (e.g., Taylor *et al.* 2013). Asimismo, los holotipos a partir de los cuales se describieron nuevas especies fueron depositados en el Museo de Zoología de Barcelona (MZB), España.

Para los análisis moleculares se emplearon segmentos de genes mitocondriales (*MutS, Cox1*) y nucleares (*28S*), los cuales han sido utilizados como *barcode* a nivel de especies, lográndose obtener hasta un 70% de morfoespecies de octocorales distinguidas genéticamente (McFadden *et al.* 2006; McFadden *et al.* 2010; Mcfadden *et al.* 2011; McFadden y van Ofwegen 2013b). Para más detalles de la metodología empleada, ver detalles en el capítulo correspondiente. Adicionalmente, para delimitar especies candidatas u OTUS se utilizaron los marcadores moleculares antes mencionados, y métodos de delimitación de especies como el ABGD (Puillandre *et al.* 2012) y el bPTP (Zhang *et al.* 2013), así como los resultados de los análisis morfológicos obtenidos en etapas previas (ver Capítulos I y II para más detalles sobre estos métodos de delimitación).

La reconstrucción de las relaciones filogenéticas de la familia Primnoidae (y algunos subgrupos) se llevó a cabo utilizando aproximaciones moleculares de acuerdo con el siguiente protocolo general. La edición y alineamiento de las secuencias se realizaron con los Software Mega 7 (Kumar *et al.* 2016) y MAFFT. Se evaluó la saturación de los genes (Xia *et al.* 2002) en el software DAMBE (Xia y Xie 2001). Esta prueba permite evaluar si los genes han alcanzado la saturación total, lo cual, de ser cierto indicaría que ya no son informativos sobre los procesos evolutivos subyacentes. En ninguno de los loci evaluados en la presente tesis doctoral se encontró evidencia de saturación.

Adicionalmente a las secuencias inéditas obtenidas durante el desarrollo del proyecto doctoral, se usaron secuencias de las diferentes especies que conforman el resto de la familia Primnoidae disponibles en el Genbank (Ver

apéndices). En general, se utilizó un método de inferencia bayesiana (BI), para un set de datos de genes mitocondriales y nucleares (analizados de forma individual y concatenada), utilizando diferentes softwares (e.g., Mr. Bayes). Con el fin de considerar explícitamente en el análisis la heterogeneidad en las tasas y los patrones de evolución, se utilizaron modelos mixtos según lo descrito por Pagel & Meade, (2004) basados en el modelo General de Tiempo Reversible (GTR). Los modelos mixtos permiten detectar diferentes patrones de evolución en las secuencias, sin el conocimiento a priori de esos patrones, ni necesidad de particionar los datos. Esta aproximación permite explorar diferentes modelos de evolución (en este caso número de matrices GTR) y sus respectivos parámetros, convergiendo en el modelo que mejor se ajusta a los datos en la muestra de árboles (Pagel y Meade 2008).

Análisis de tiempos de divergencia

Se realizó una calibración de la filogenia molecular de los Primnoidae utilizando una aproximación bayesiana mediante Cadenas de Markov y Monte Carlo, la cual permite incorporar la incertidumbre en la topología del árbol y la longitud de ramas. Las relaciones filogenéticas y el tiempo de divergencia se infirieron en BEAST 2.6.6, empleando el modelo *Fossilized Birth-Dead* (FBD) con el paquete *Sampled Ancestors* (Gavryushkina *et al.* 2014; Heath *et al.* 2014). Ya que los primnoides carecen de representantes fósiles, se utilizaron octocorales extintos estrechamente relacionados a los primnoides (Taylor y Rogers 2015; Quattrini *et al.* 2020; McFadden *et al.* 2021), para calibrar el árbol. En el Capítulo III se proveen mayores detalles de la metodología aplicada.

Biogeografía histórica de primnoides

Para evaluar dónde ocurrió la diversificación, reconstruimos ubicaciones geográficas en espacio continuo y tres dimensiones (O'Donovan *et al.* 2018) a partir de las ubicaciones geográficas (latitud, longitud) de los primnoides

incluidos en nuestra filogenia obtenidas a partir de la literatura y bases de datos (e.g., GBIF). Las ubicaciones ancestrales se estimaron para cada nodo filogenético utilizando el modelo geográfico de BayesTraits 3.0 (O'Donovan *et al.* 2018), que utiliza datos continuos (coordenadas geográficas), en lugar de regiones codificadas discretamente, para estimar tendencias de dispersión en resoluciones más finas sin necesidad de definir áreas geográficas *a priori* (O'Donovan *et al.* 2018). Junto con las ubicaciones ancestrales, estimamos simultáneamente las tasas de dispersión a través de la filogenia utilizando el modelo de tasa variable. La tasa de dispersión geográfica, es decir, la distancia que se mueve una especie en un intervalo de 1 Myr, se puede considerar como la velocidad de movimiento de la especie (O'Donovan *et al.* 2018; Avaria-Llautureo *et al.* 2021). Utilizando los resultados de este modelo fue posible estimar posibles rutas de dispersión, la tasa de dispersión, así como la ubicación geográfica de los nodos ancestrales de la filogenia en un marco de trabajo bayesiano.

Patrones de diversificación de primnoides y sus impulsores

Inicialmente, se investigó si la tasa de diversificación es constante, o no, a través del tiempo y las ramas del árbol utilizando el modelo *speciation-extinction* en el programa *Bayesian Analysis of Macroevolutionary Mixtures* (BAMM v.2.5.0) (Rabosky 2014).

Posteriormente, ajustamos modelos para detectar posibles cambios en la especiación y extinción que ocurrieron en periodos temporales discretos y que afectan simultáneamente a todos los clados (*episodic birth-death diversification* (Stadler 2011)), utilizando el paquete *TREEPAR* en R. Diferentes modelos episódicos fueron ajustados inicialmente en el árbol de primnoides global, y posteriormente en un árbol únicamente constituido por primnoides cuya distribución geográfica se ha descrito en las regiones antárticas y subantárticas (>55°S). Dichos cambios de diversificación episódicos, si los hubiera, podrían

estar potencialmente relacionados con eventos históricos abruptos que podrían tener graves consecuencias para los ecosistemas antiguos, incluyendo aquellos episodios geológicos, oceanográficos, y climáticos Cenozoicos considerados importantes en la evolución de la fauna marina del SO (Mackensen 2004).

Los cambios abruptos no son los únicos que pueden afectar las dinámicas de diversificación, los cambios continuos en el tiempo también tienen el potencial de hacerlo. Es por ello que se ajustaron modelos adicionales para evaluar la contribución relativa de factores bióticos y abióticos que varían a través del tiempo en la dinámica de diversificación de la familia Primnoidae a nivel global y los primnoides antárticos-sub-antárcticos. Para ello se implementaron una serie de modelos macroevolutivos en la filogenia calibrada utilizando un marco de comparación de hipótesis de máxima verosimilitud (Condamine *et al.* 2013; Morlon *et al.* 2016). Se seleccionaron cinco factores abióticos que potencialmente pueden haber afectado la diversificación de los primnoides, la temperatura global (Prokoph *et al.* 2008), la fragmentación continental (Zaffos *et al.* 2017), el nivel del mar (Miller *et al.* 2005), la química de los océanos (Ries 2010), y la concentración de CO_2 como proxy de acidificación de los océanos (Royer *et al.* 2004). También se consideró un potencial factor biótico afectando las dinámicas de diversificación de primnoides, la tasa de dispersión. Además, se consideraron modelos nulos, que incluyen modelos de diversificación constante y dependiente del tiempo. Los diferentes modelos fueron ajustados utilizando máxima verosimilitud usando el paquete RPANDA 1.9 en R (Morlon *et al.* 2016).

Los análisis realizados en TREEPAR y RPANDA fueron realizados utilizando una muestra de 250 árboles aleatorios tomados de la distribución a posteriori de los análisis de calibración. Esto permite considerar las incertezas en la topología de los árboles y tiempo de divergencia entre los linajes analizados. Para cada uno de los análisis realizados (*episodic diversification* vs *time-continuous diversification*) los distintos modelos fueron comparados

utilizando el criterio de información Akaike corregido, y el modelo con el mayor AICω fue considerado como el que tiene mejor ajuste a los datos.

Organización de los resultados

En los Capítulos I y II se utilizó una aproximación "integrativa", que incluyó el uso de marcadores moleculares mitocondriales (*MutS*, *Cox1*) y nucleares (*28S*), caracterización morfológica macro y microscópica y métodos de delimitación de especies, para el estudio de colonias con ramificaciones tipo *bottlebrush* pertenecientes al género *Thouarella* colectados cerca de la Península Antártica y el Mar de Weddell. La integración de datos moleculares y morfológicos nos permitió describir formalmente seis especies nuevas para la ciencia dentro del género *Thouarella*. Finalmente, se determinaron las relaciones filogenéticas del género *Thouarella* utilizando análisis de genes tanto separados como concatenados de los genes disponibles que incluyeron secuencias inéditas de primnoides identificados a partir de la colección BECA, en conjunto con datos del GenBank.

En el Capítulo III se determinaron las relaciones filogenéticas y tiempo de divergencia de la familia Primnoidae utilizando un análisis concatenado de los genes disponibles que incluyeron secuencias inéditas de todas las especies de primnoides identificados a partir de la colección BECA, junto con datos del GenBank. Posteriormente, se utilizó la filogenia calibrada y el modelo geográfico (geo-model) para reconstruir su historia biogeográfica. Primero inferimos las paleo-localizaciones ancestrales más probable, segundo se estimó la tasa de dispersión geográfica y se determinó si la tasa de dispersión de este grupo fue constante, o no, a través del tiempo. Además, se evaluó si la tasa de diversificación de los primnoides a nivel global, y solo los primnoides antárticos y subantárticos estuvo impulsada por potenciales mecanismos actuando de forma abrupta (e.g., glaciaciones cuaternarias, establecimiento del

ACC) o continua en el tiempo (e.g., variación temporal de la temperatura) utilizando un marco comparativo de modelos.

CHAPTER I. Molecular and morphological data reveal three new species of *Thouarella* (Anthozoa: Octocorallia: Primnoidae) from the Southern Ocean[1]

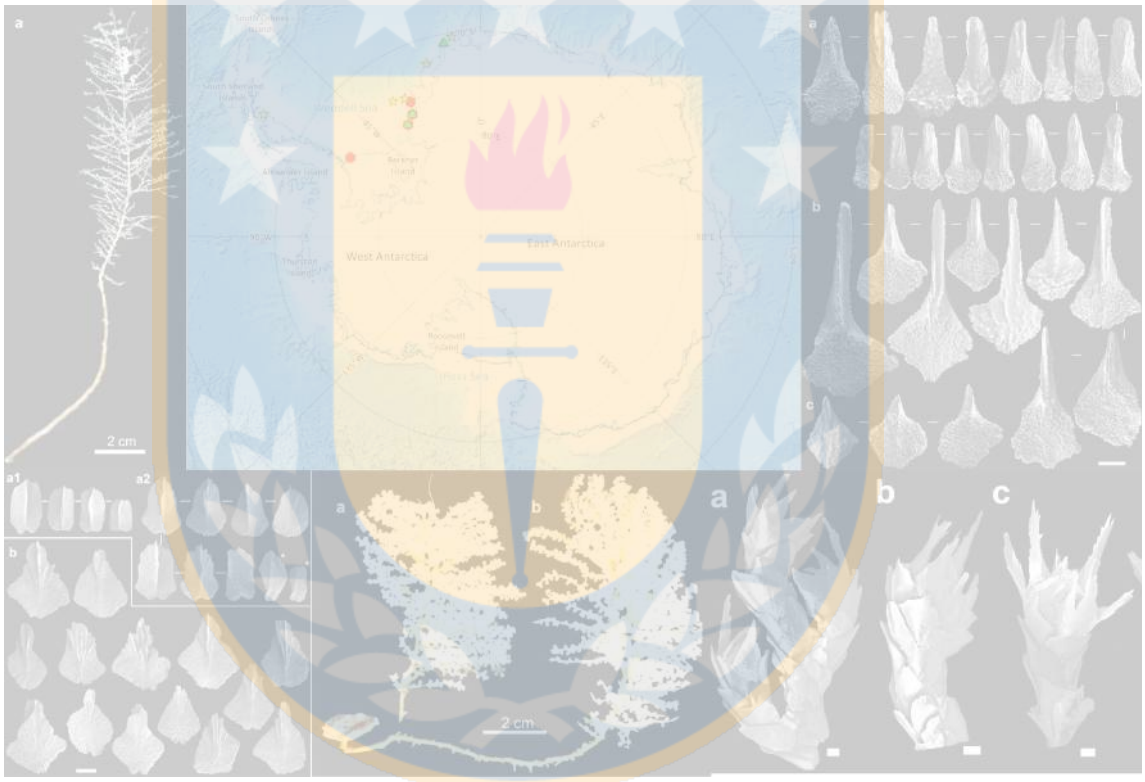

[1]**Artículo publicado.** Núñez-Flores, M., Gomez-Uchida, D. & López-González, P.J. (2020). Molecular and morphological data reveal three new species of *Thouarella* Gray, 1870 (Anthozoa: Octocorallia: Primnoidae) from the Southern Ocean. *Marine Biodiversity* 50, 30. https://doi.org/10.1007/s12526-020-01053-z

Molecular and morphological data reveal three new species of *Thouarella* (Anthozoa: Octocorallia: Primnoidae) from the Southern Ocean

Mónica Núñez-Flores[1,2,3,*], Daniel Gomez-Uchida[2], Pablo J. López-González[3]

[1]Programa de Doctorado en Sistemática y Biodiversidad, Facultad de Ciencias Naturales y Oceanográficas, Universidad de Concepción, Chile.

[2]Genomics in Ecology, Evolution and Conservation Lab (GEECLAB), Department of Zoology, Facultad de Ciencias Naturales y Oceanográficas & Núcleo Milenio INVASAL, Universidad de Concepción, Chile.

[3]Biodiversidad y Ecología Acuática, Departamento de Zoología, Facultad de Biología, Universidad de Sevilla, Reina Mercedes 6, 41012-Sevilla, España.

*Correspondence to nuez.monica@gmail.com

Abstract.

Thouarella Gray, 1870 is one of the most speciose genera among primnoid gorgonians. It has a worldwide distribution that includes Antarctic and sub-Antarctic regions. Based on a combination of detailed morphological studies and analyses using mitochondrial and nuclear DNA markers, we describe and illustrate three new species of bottlebrush-shaped *Thouarella* from the Weddell Sea, Southern Ocean: *T. islai* sp. nov., *T. weddellensis* sp. nov., and *T. polarsterni* sp. nov. For the morphological description we used macro-structural characters, such as branching pattern and polyp arrangement, along with axis and micro-structural characters, such as architecture and shapes of scales and their arrangement in polyps. Additionally, we amplified two mitochondrial (*mtMutS* and *Cox1*), and one nuclear loci (*28S* rDNA) obtaining optimal topologies under a Bayesian approach. Resulting molecular phylogenies corroborated the status of the new taxa and elucidated their relationships to closely related species. With the three new species here described, the global diversity of *Thouarella* has increased to 38 species, 12 of which are endemic to

Antarctic and sub-Antarctic waters. The high number of species from higher latitudes of the Southern Hemisphere, the high grade of endemism in this biogeographic area, and recent phylogenetic analyses support the idea that the Southern Ocean was likely a centre for *Thouarella* species radiation.

Keywords: Antarctic, Cnidaria, marine biodiversity, octocorals, benthos, Weddell Sea.

This article is registered in ZooBank under http://zoobank.org/507D9CC7-5673-4BCC-B5C7-C0F01C304313

1.1. Introduction

The Southern Ocean seafloor harbors one of the richest communities on the planet in terms of species number, being only comparable to ecosystems such as coral reefs or tropical forests (Clarke and Crame 1992; Brandt *et al.* 2007a). Benthic suspension-feeders are among the major contributors to the diversity and biomass of the continental shelf communities here(Starmans *et al.* 1999). Primnoid gorgonians are key components of deep (> 400 m depth) Antarctic benthic communities, playing an important role in structuring these habitats (López-González *et al.* 2002; Brandt *et al.* 2007a; Cairns and Bayer 2009; Taylor *et al.* 2013). The family Primnoidae is one of the most diversified, monophyletic gorgonian lineages, represented by 43 genera and around 279 species that occur in all ocean basins (Cairns and Bayer 2009; Taylor and Rogers 2015; Cairns and Wirshing 2018). Around 25% of primnoid gorgonian species have been sampled only in the Antarctic and sub-Antarctic regions (Taylor and Rogers 2015), which suggests that there is muchendemicity in the region among these species (Zapata-Guardiola and López-González 2012). In fact, Antarctica has been proposed as the centre of origin for primnoid

gorgonians (Cairns and Bayer 2009), although alternative scenarios have also been advocated (Taylor and Rogers 2015).

Thouarella Gray, 1870 is one of the most speciose genera among primnoids, having worldwide distribution but it is most common in Antarctic and sub-Antarctic regions (Cairns and Bayer 2009; Zapata-Guardiola and López-González 2010b; Taylor *et al.* 2013). According to the last revision of the genus (Taylor *et al.* 2013) and subsequent species descriptions (Cairns *et al.* 2018; Cairns and Wirshing 2018; Altuna and López-González 2019), there are at least 35 valid *Thouarella* species. However, taxonomic identification of primnoids to species level can be problematic as many of them may be macroscopically similar, and only are morphologically distinguished from one another throughout a detailed examination of the branching pattern of colonies, polyps distribution, and scanning electron microscopic (SEM) analysis of scales (Hourigan *et al.* 2017; Altuna and López-González 2019). That is why the main characters used for the species recognition are related to the sclerome (i.e., shape and ornamentation of scales) (see Cairns and Bayer 2009; Zapata-Guardiola and López-González 2010a; Taylor et al. 2013). However, when possible, morphological characters should not be the sole basis for defining species boundaries in octocorals, having in mind their possible adaptive phenotypic plasticity in response to different environmental fluctuations (e.g. Prada et al. 2008).

The recovering of molecular information of the most variable mitochondrial genes in octocorals [*mtMutS* (=*msh1*), and *Cox1*] have contributed to increasing our knowledge about the systematics of primnoids (Taylor and Rogers 2015; Taylor and Rogers 2017; Cairns and Wirshing 2018). However, several works have recognized the difficulty to distinguish octocoral species only with mitochondrial information (McFadden *et al.* 2010; McFadden *et al.* 2011; Baco and Cairns 2012; McFadden *et al.* 2014b; Soler-Hurtado *et al.* 2017) since octocoral mitochondria have a unique DNA repair mechanism responsible for

the slow evolution of their genes (Bilewitch and Degnan 2011). In this sense, the description of new taxa can benefit by additional phylogenetically informative nuclear genes (e.g. *28S* rDNA) (France and Hoover 2001; McFadden *et al.* 2011).

During several Antarctic surveys aboard the RV German icebreaker *Polarstern* important collections of primnoid colonies were acquired along the Antarctic Peninsula and the Weddell Sea. After detailed examination and analyses, we present here the description of three new species of the genus *Thouarella,* based on morphological and molecular data.

1.2. Materials and methods

1.2.1 Sample collection

The octocoral colonies here studied were collected on the RV *Polarstern* cruises ANT XII/3 (1995), ANT XXIII/8 (2007), ANT XXIV/2 (2008), ANT XXVII/3 (2011), ANT-XXIX (2014), and ANT-XXXI/2 (2016), along different localities in the Southern Ocean (see Fig. 2.1) mainly using bottom trawls, and exceptionally found adhered to submerged scientific equipment. Colonies were fixed in 10% buffered formalin in seawater and then transferred to 70% ethanol on board, frozen on board and then transferred to absolute ethanol, or were fixed directly in absolute ethanol for future molecular analyses. Permanent mounts were made for light microscopy observation and fragments from different parts of the colonies were prepared for study by SEM employing the usual methodology described in the literature (Bayer and Stefani 1988). The colony and scale terminology herein employed mainly follows Bayer et al. (1983) and Taylor et al. (2013). Scale size measurements and illustrations are from the holotypes.

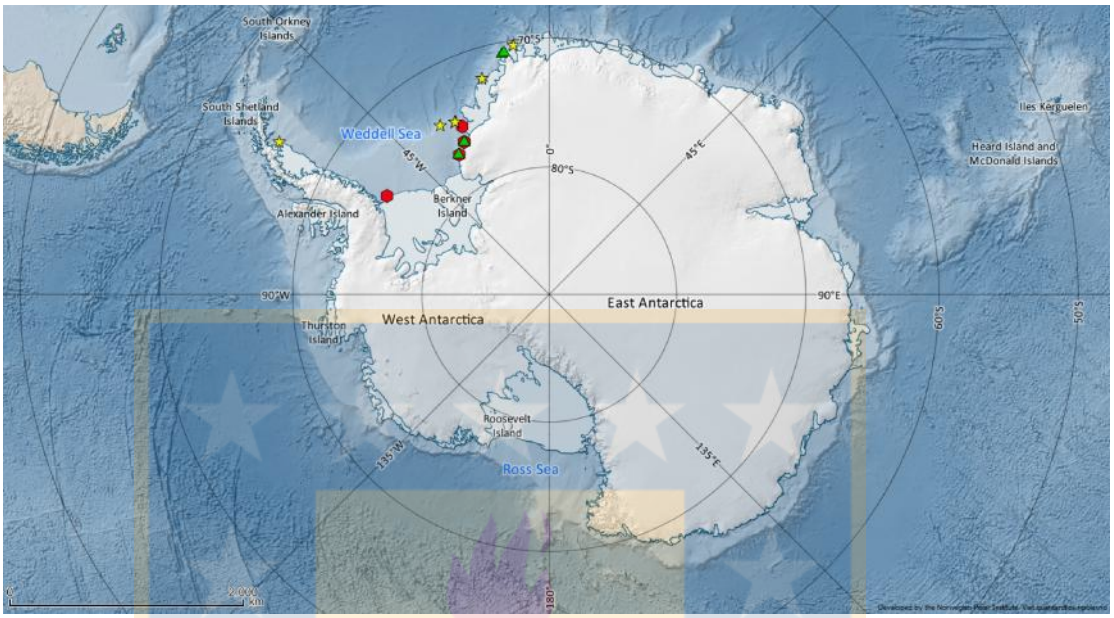

Figure 1.1 Map of the Southern Ocean, showing the sampling localities where each of the new taxa here described as found: *Thouarella islai* sp. nov. (red hexagon), *T. weddellensis* sp. nov. (yellow star), *T. polarsterni* sp. nov. (green triangle). Cartographic base from Matsuoka *et al.* (2018).

1.2.2 DNA extraction, amplification, and sequencing

DNA was extracted from both absolute ethanol or from fixed frozen colonies, using the E.Z.N.A. DNA kit (Omega Biotech) following the manufacturer's instructions. Two mitochondrial regions (*Cox1*, and *mtMutS*) and a nuclear region (*28S* rDNA) were amplified by PCR. Amplifications were performed using 1 U of MyTaq Red DNA Polymerase (Bioline), 10 µl (10 µM) of each primer, approximately 30 ng of genomic DNA, and was brought to a final volume of 20 µl with H_2O. PCR conditions are described in Supplementary File 1. PCR products were purified using ExoSAP–IT™ PCR Product Cleanup Reagent (ThermoFisher Scientific) following the manufacturer's instructions, before strong amplifications were sent to Macrogen Europe for sequencing in both directions. All chromatograms were visualised and sequence pairs matched and edited using Sequencher v4.0.

1.2.3 Phylogeny reconstructions

The new sequences were compared with homologous sequences from primnoid species obtained from GenBank. GenBank sequence accession numbers are listed in the Supplementary File 2. The final dataset contained 98 ingroup taxa (21 genera and 51 species) and one outgroup taxon, the chrysogorgiid *Chrysogorgia averta* Pante and Watling, 2011. This outgroup was chosen because the family Chrysogorgiidae has been shown to be the sister group of Primnoidae (Taylor and Rogers 2015). The set of new sequences obtained in this study (*mtMutS*, *Cox1* and *28S*) and those from GenBank were aligned using MUSCLE, implemented in MEGA7 (Kumar *et al.* 2016). The alignments for the *mtMutS*, *Cox1* and *28S* and concatenated datasets include 98, 99 and 89 specimens, respectively. Only specimens that yielded at least two sequences were used for the concatenated phylogenetic analysis. The concatenated analysis of these three molecular markers has been considered an octocoral barcode (McFadden *et al.* 2014b).

After the alignment, for single genes the best nucleotide substitution model was selected using Criterion (BIC), with jModelTest v.2.0 (Darriba *et al.* 2012). For the concatenated datasets a phylogenetic inference was obtained applying Bayesian inference (BI) methods, carried out in MrBayes 3.2.7 program (Ronquist and Huelsenbeck 2003). For the latter, analyses were performed under the GTR + I + G model of evolution. Bayesian inference posterior probabilities were estimated using the Metropolis coupled Markov chain Monte Carlo algorithm (MCMC), running four chains for 10×10^6 generations were performed, with trees sampled every 10,000 generations, and verifying their convergence in Tracer v1.5 (Rambaut *et al.* 2018). Convergence was obtained when effective sample sizes (ESS) was >200. The initial 10% of sampled trees were discarded as the burn-in and the support values determined by posterior probabilities (PP). The results from four different runs were combined with the

LogCombiner tool, and a Maximum Clade Credibility Tree (MCCT) was reconstructed with TreeAnnotator (Rambaut and Drummond 2010) collapsing nodes with PP < 50.

The type and additional material examined have been deposited in the Museu de Zoologia de Barcelona (MZB) and the collection of the research group Biodiversidad y Ecología Acuática of the University of Seville (BECA). The cartographic base used for the location map is from the *Quantarctica* package (Matsuoka *et al.* 2018).

1.2.4 Abbreviations

BECA: Biodiversidad y Ecología Acuática; H: height; H:W, ratio height/width of a scale; IL: inner lateral scales; L: length of a polyp; M: marginal scale; MZB: Museu de Zoologia de Barcelona; O: opercular scale; OL: outer lateral scales; SEM: Scanning Electron Microscopy; SM: submarginal; W: width.

1.3. Results

Order Alcyonacea Lamouroux, 1812

Suborder Calcaxonia Grasshoff, 1999

Family Primnoidae Milne-Edward, 1857

Genus *Thouarella* Gray, 1870

Species included *Thouarella antarctica* (Valenciennes, 1846) (type species), *T. hilgendorfi* (Studer, 1878), *T. variabilis* Wright & Studer, 1889, *T. brevispinosa* Wright & Studer, 1889, *T. affinis* Wright & Studer, 1889, *T. koellikeri* Wright & Studer, 1889, *T. moseleyi* Wright & Studer, 1889, *T. regularis* (Wright & Studer, 1889), *T. laxa* Versluys, 1906, *T. tydemani* Versluys, 1906, *T. brucei* Thomson & Richie, 1906, *T. striata* Kükenthal, 1907, *T. crenelata* Kükenthal, 1907, *T. clavata* Kükenthal, 1908, *T. pendulina* (Roule, 1908), *T. chilensis* Kükenthal, 1908, *T. coronata* Kinoshita, 1908, *T. parva* Kinoshita, 1908, *T. biserialis*

(Nutting, 1908), *T. hicksoni* Thomson, 1911, *T. dispersa* Kükenthal, 1912, *T. grandiflora* Kükenthal, 1912, *T. bipinnata* Cairns, 2006, *T. grasshoffi* Cairns, 2006, *T. diadema* (Cairns, 2006), *T. viridis* Zapata-Guardiola & López-González, 2010a, *T. minuta* Zapata-Guardiola & López-González, 2010a, *T. andeep* Zapata-Guardiola & López-González, 2010a, *T. undulata* (Zapata-Guardiola & López-González, 2010b), *T. cristata* Cairns, 2011, *T. trilineata* Cairns, 2011, *T. vitjaz* Zapata-Guardiola & López-González, 2012, *T. parachilensis* Taylor, Cairns, Agnew & Rogers, 2013, *T. taylorae* Cairns, Stone, Moon & Lee, 2018, *T. porcupinensis* Altuna & López-González, 2019, *T. islai* sp. nov., *T. weddellensis* sp. nov. and *T. polarsterni* sp. nov.

Remarks The taxonomic status of most *Thouarella* species was reviewed by Taylor et al. (Taylor *et al.* 2013). Several new species have been described since then (Cairns *et al.* 2018; Altuna and López-González 2019). In addition, recent findings (based on molecular information) suggest that some of the species previously considered belonging to *Plumarella* should be included in the genus *Thouarella* (Cairns and Wirshing 2018). Previous to the present work, the genus included 35 valid species.

***Thouarella islai* sp. nov.**

(Figs. 1.2–1.5)

http://zoobank.org/5A2FAD08-855B-4705-9C4F-0FCEBF55131D

Type material MZB 2019-1963, Holotype, whole colony, 17 cm high, *Polarstern* cruise ANT XII/3, stn. 168, 75°10.2’ S, 58° 40.8’ W; Weddell Sea, Antarctica, 601 m depth, 15 February 1995. MZB 2019-1965, Paratype, whole colony, 19 cm high, *Polarstern* cruise ANT-XXIX, stn. 053-1, 76°19.33’ S, 29°8.44’ W, Weddell Sea, Antarctica, 261 m depth, 8 January 2014.

Additional materials examined MZB 2019-1964, fragment of colony, 13 cm high, *Polarstern* cruise ANT-XXIX, Stn. 091-1, 76°58.07’ S, 32°51.48’ W, Weddell Sea, Antarctica, 294 m depth, 14 January 2014. MZB 2019-1966,

fragment of colony, 9 cm high, *Polarstern* cruise ANT-XXIX, stn. 053-1, 76°19.33’ S, 29°8.44’ W, Weddell Sea, Antarctica, 261 m depth, 8 January 2014. BECA-OPRIM-2495, whole colony, 18 cm high, *Polarstern* cruise ANT-XXIX, stn. 018-1, 75°12.03’ S, 27°32.56’ W, Weddell Sea, Antarctica, 391 m depth, 4 January 2014.

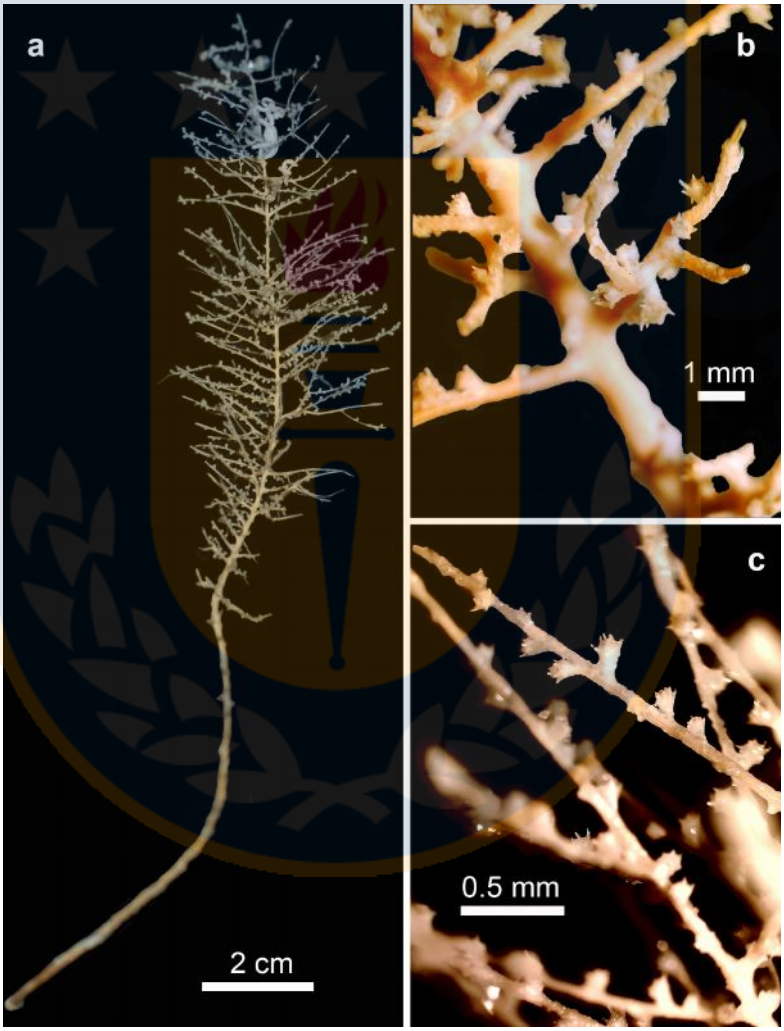

Figure 1.2 *Thouarella islai* sp. nov., holotype MZB 2019-1963. a whole colony; b and c details of polyp distribution.

Etymology The epithet of the new proposed species is named after our friend and colleague, Dr. Enrique Isla Saavedra (Institute of Marine Science, in Barcelona, ICM-CSIC), who promoted the participation of our research team in different Antarctic expeditions.

Diagnosis Colony bottlebrush-shaped with scarce (7–19 polyps/cm), cylindrical, and short (0.78–1.26 mm) isolated polyps; with 2–3 body wall scales in each abaxial row, 2–3 in outer lateral rows, 2–3 inner lateral rows, and 1–2 in adaxial rows; opercular scales of isosceles-triangle shape; marginal scales with a well-developed distal spinose projection, which can be reduced in adaxial scales.

Holotype description Colony bottlebrush-shaped, 17 cm high and 3 cm wide (Fig. 1.2a). Holdfast reduced, circular, 3.3 mm in diameter. Main stem simple, 1.6 mm in diameter proximally, flexible and golden in colour. Basal-most main stem without branchlets. First-order branch arises 9 cm above holdfast, in 3 different directions (Fig. 1.2a). Branchlets (second-order branches) separation ranges between 0.4–2.9 cm, 0.5–1.5 cm in length (n=20), flexible, and in some cases subdivided (up to a third-order ramification).

Polyps relatively scarce (7–14 polyps/cm), isolated on branches and branchlets, with bare intervals of 0.48–3.47 mm (n=30); rarely with polyps on main stem (Figs. 1.2b, c). Polyps short and cylindrical, 0.78–1.26 mm tall (average 0.95 mm, including long marginal spines; n=20), and inclined 43°–66° (average 55°; n=26) with respect to the branches/branchlets (Fig. 1.3). Body wall scales covered by 8 longitudinal rows decreasing in number to 5 at the polyp base, with 2–3 scales (excluding opercular scales) in abaxial rows (Fig. 1.3a), 2–3 scales in outer lateral rows (Fig. 1.3b), 2–3 scales in inner lateral rows, and 1–2 scales in adaxial rows; opercular scales 8; marginal scales 8.

Operculum low (Fig. 1.4a), mainly with isosceles-triangle-shaped scales with dented to rounded proximal edges and rounded distal ends; less commonly tongue-shaped (wide distally) scales with pointed and serrate proximal edges; up to 0.42 x 0.16 mm H x W (average 0.29x0.15 mm H x W; H:W of 1.91–2.82,

average 2.27; Fig. 1.4a). Adaxial scales reduced in size, up to 0.25 x 0.1 mm H x W. The 30–50% of inner proximal surface with complex tubercles, with simple keel distally, rarely with channelled-keels (Fig. 1.4a). Some opercular scales longitudinally concave along the outer surface, with scarce tubercles on proximal area (Fig. 1.4a).

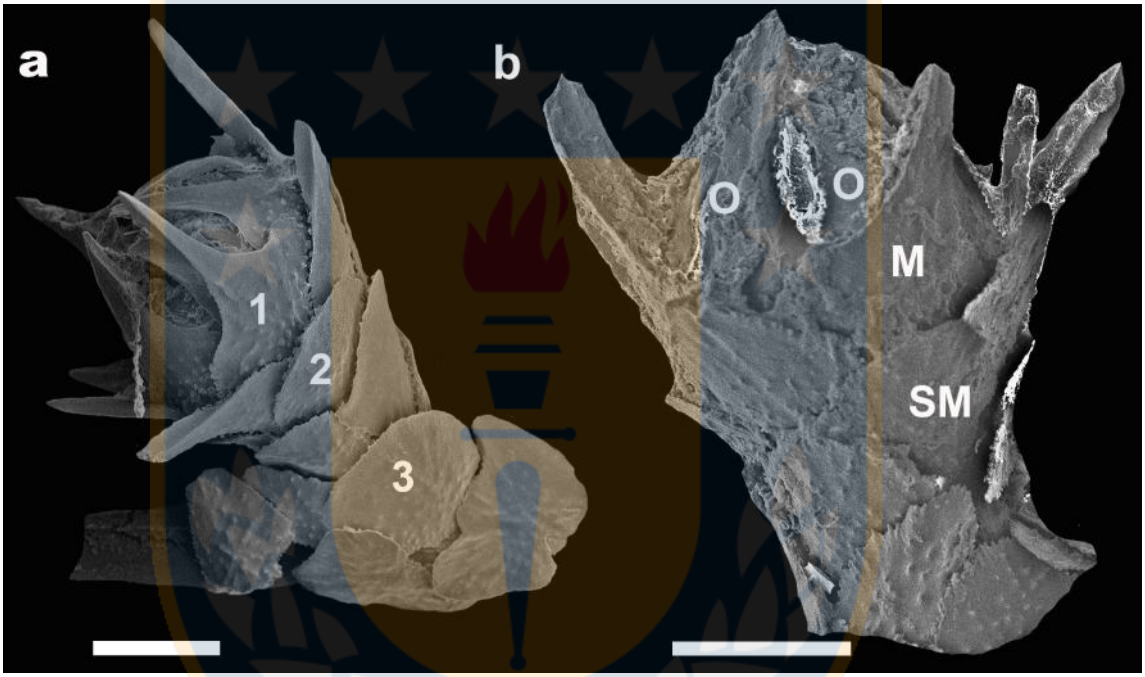

Figure 1.3 *Thouarella islai* sp. nov., holotype MZB 2019-1963. a polyps in outer lateral view; b polyps in adaxial view. Scale bar = 0.2 mm.

Marginal scales predominantly diamond-shaped, with an elongated distal spine and channelled-keels along distal inner surface, up to 0.89 x 0.36 mm H x W (average 0.51 x 0.28 mm H x W; H:W of 1.2–2.6, average 1.8; Fig. 1.4b). Distal spine well-developed, up to 60% of scale height. Proximal area of marginal scales mainly rhomboid in shape, with distinct “V” shaped proximal edges; few scales with widely asymmetric circular to oval edges (Fig. 1.4b). Adaxial marginal smaller than laterals or abaxials, up to 0.29 x 0.24 mm H x W, diamond-shape, with pointed distal edges and short spine (Fig. 1.4c). All the

marginal scales have proximal inner surface with complex tubercles. Basal part range 40–60% of scales height (depending on distal spine length). Lateral edges mostly finely serrated (Fig. 1.4b). Outer surface of medium to large size scales with scarce tubercles on the proximal basal part, more or less radial from proximal area. Outer surface of adaxial scales with faint radial ridges (Fig. 1.4c).

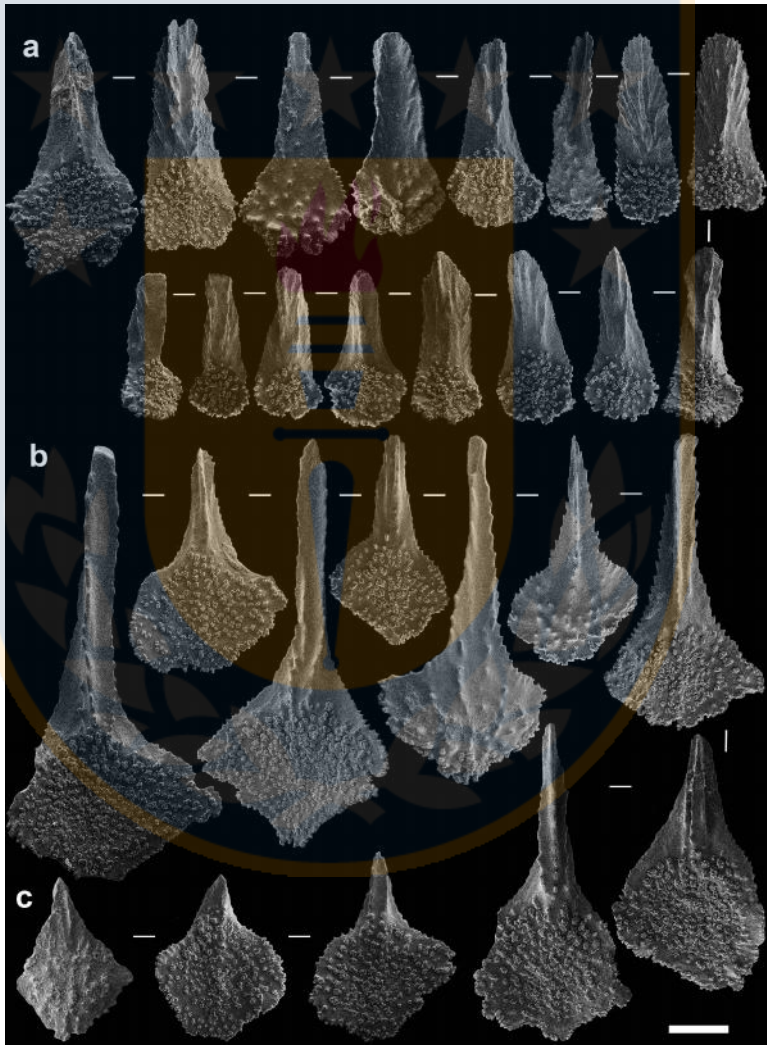

Figure 1.4 *Thouarella islai* sp. nov., holotype MZB 2019-1963. A, opercular scales; b marginal scales; c adaxial marginal scales showing reduced spine. Scale bar = 0.1 mm.

Body wall scales in a variety of sub-circular shapes (also fan-shaped), occasionally with rather acute edges (Fig. 1.5a), up to 0.31 x 0.28 mm H x W (average 0.27 x 0.26 mm H x W; H:W of 0.7–1.5, average 1.1), with tuberculate inner surface, and a sparse granular outer surface (Figs. 1.5a, 3b). Some portions of the lateral edges finely serrated. Coenenchymal scales irregularly oval to elliptic in shape, similar in size to those of the body wall, up to 0.30 x 0.27 mm H x W (average 0.26 x 0.19 mm H x W; H:W of 0.8–1.9, average 1.5). All inner surface with complex tubercles; outer surface with radial short crests and isolated pointed granules (Fig. 1.5b). Lateral edges fine to coarse serrated.

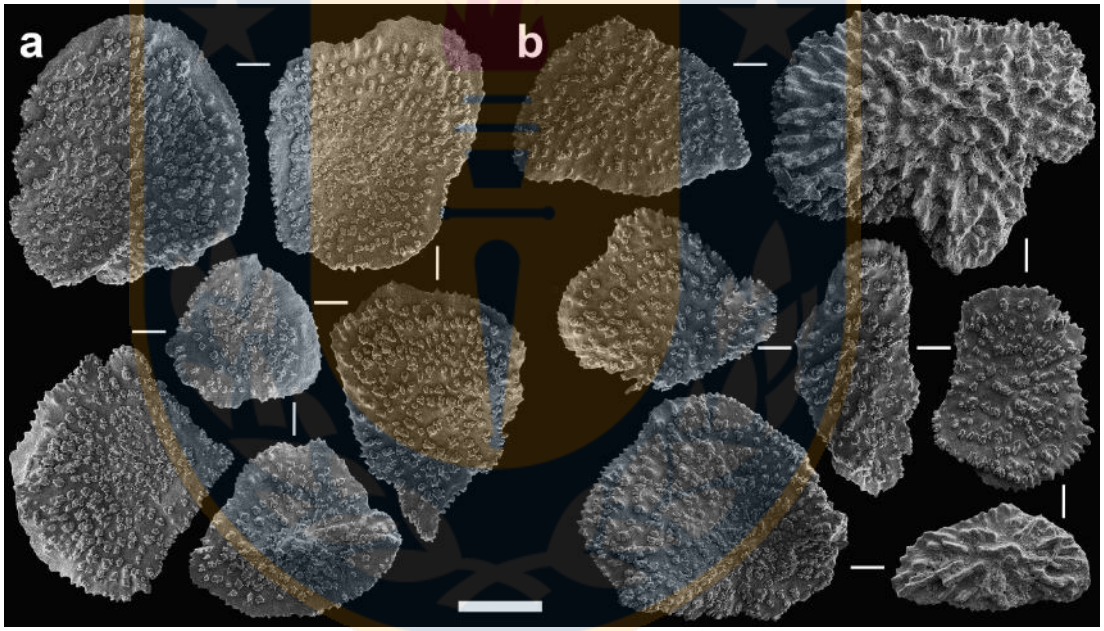

Figure 1.5 *Thouarella islai* sp. nov., holotype MZB 2019-1963. a body scales; b coenenchymal scales. Scale bar = 0.1 mm.

Morphological variation Paratypes and additional material examined generally agree in the distribution, shape and size of the sclerites from polyps and coenenchyme. In the additional examined material up 10–19 polyps/cm have been observed. A complete colony was 19 cm high.

Geographic and bathymetric distribution The species is currently known from four localities in the Weddell Sea, Antarctica (see Fig. 1.1), all of them at latitudes higher than 75ºS, between 261 and 600 m depth.

Remarks According to the key to species in Taylor et al. (2013), *T. islai* falls within “group one” by having isolated polyps. The new species also falls in the subgenus *Thouarella* (*Thouarella*) according to Cairns and Wirshing (2018). The presence of fewer than five abaxial scales, as well as a short polyp length (less than 1.5 mm) indicates close morphological similarities of the new proposed species to *T. pendulina*, *T. hicksoni*, and *T. minuta* (see Taylor et al. 2013: p. 66).

Thouarella islai reaches the lower density of polyps per cm (7–19) when compared to *T. minuta* (11-18), *T. hicksoni* (16–22), and *T. pendulina* (27–41). In reference to the angle between the polyp and its branchlet in the three comparable species (*T. pendulina, T. hicksoni* and *T. minuta*), it varies from 30˚ to nearly appressed, while in *T. islai* this angle varies from 43–66º (average 55°, n=26). The newly proposed species has a lower number of abaxial scales (2–3) than its congeners *T. pendulina, T. hicksoni* and *T. minuta* (which range from 3 to 5) (Zapata-Guardiola and López-González 2010e; Taylor *et al.* 2013).

The sclerome of *Thouarella islai* shows also a unique combination of features that allows us to differentiate it from the three previously mentioned species. Opercular scales of *T. islai* are narrow isosceles-shaped (H:W of 2.27) to tongue-shaped, clearly different from the wide diamond- to isosceles-shaped scales (H:W of 1.5) of *T. pendulina* (see Taylor et al. 2013: fig. 23, p. 58), the wide predominantly lanceolate to tongue-shaped scales of *T. hicksoni* (see Taylor et al. 2013: fig. 27, p. 66), or the isosceles to spoon-shaped scales, with a distinctive distal spine, of *T. minuta* (see Zapata-Guardiola and López-González 2010a: fig. 13, p. 178). Furthermore, opercular scales of *T. islai* are slightly more tuberculate (in their inner surface) than those of *T. pendulina* (see Taylor et al. 2013: fig. 23, p. 58). Finally, *T. islai* has marginal scales with a conspicuous

well-developed and narrow distal spine, which might constitute up 60% of the scale height, unlike the pointed or short spines of *T. pendulina,* and *T. minuta,* or the wide pointed scales of *T. hicksoni* (Zapata-Guardiola and López-González 2010e; Taylor *et al.* 2013).

***Thouarella weddellensis* sp. nov.**

(Figs. 1.6–1.10)

http://zoobank.org/8B6A0856-793A-4EAF-A867-32A79999B32B

Type material MZB 2019-1967, Holotype, fragment of colony, 6 cm high, *Polarstern* cruise ANT XXIII/8, stn. 721-2, 65º55.41'S, 60º34.01'W, 295–299 m depth, Weddell Sea, Antarctica, 20 January 2007. MZB 2019-1969, Paratype, whole colony, 17 cm high, *Polarstern* cruise ANT XXIV/2, stn. 48-1, 70°23.94'S, 8°19.14'W, 600 m depth, Weddell Sea, Antarctica, 12 January 2007. MZB 2019-1971, Paratype, whole colony, 12 cm high; MZB 2019-1975, Paratype, whole colony, 9.5 cm high; MZB 2019-1977, Paratype, whole colony, 9 cm high; MZB 2019-1979, Paratype, whole colony, 7 cm high, *Polarstern* cruise ANT-XXIX, stn. 316-1, 74°39.57' S, 28°45.77' W, 769 m depth, Weddell Sea, Antarctica, 10 February 2014.

Additional material examined MZB 2019-1968, fragment of colony, 6 cm high, *Polarstern* cruise ANT XXIV/2, stn. 48-1, 70°23.94'S, 8°19.14'W, 600 m depth, Weddell Sea, Antarctica, 12 January 2007. MZB 2019-1970, fragment of colony, 4 cm high, *Polarstern* cruise ANT-XXIX, stn. 266-1, 74°18.39' S, 32°50.05' W, 718 m depth, Weddell Sea, Antarctica, 05 January 2014. MZB 2019-1976, fragment of colony, 4.5 cm high, *Polarstern* cruise ANT-XXXI/2, stn. 090-1, 72°22.11'S, 17°18.61' W, 1097 m depth, Weddell Sea, Antarctica, 28 January 2016. MZB 2019-1972, fragment of colony, 5 cm high; MZB 2019-1973, fragment of colony, 12 cm high; MZB 2019-1974, fragment of colony, 9 cm high; MZB 2019-1978, fragment of colony 4.5 cm high; MZB 2019-1980, fragment of

colony, 9 cm high; BECA-OPRIM-2400, whole colony, 5 cm high, *Polarstern* cruise ANT-XXIX, stn. 316-1, 74°39.57’ S, 28°45.77’ W, 769 m depth, Weddell Sea, Antarctica, 10 February 2014.

Etymology The species name is derived from the Weddell Sea, the area where the colonies studied were recovered.

Diagnosis Colony bottlebrush-shaped with isolated, flared and short (1.5 mm) polyps; 3–4 scales in abaxial rows, 3 in outer lateral rows, 3 in inner lateral rows, and 2–3 in adaxial rows; opercular scales broad with simple keels, and serrated distal edges; marginal scales without distal spine; marginal and opercular scales aligned, and with small tubercules on their inner surface.

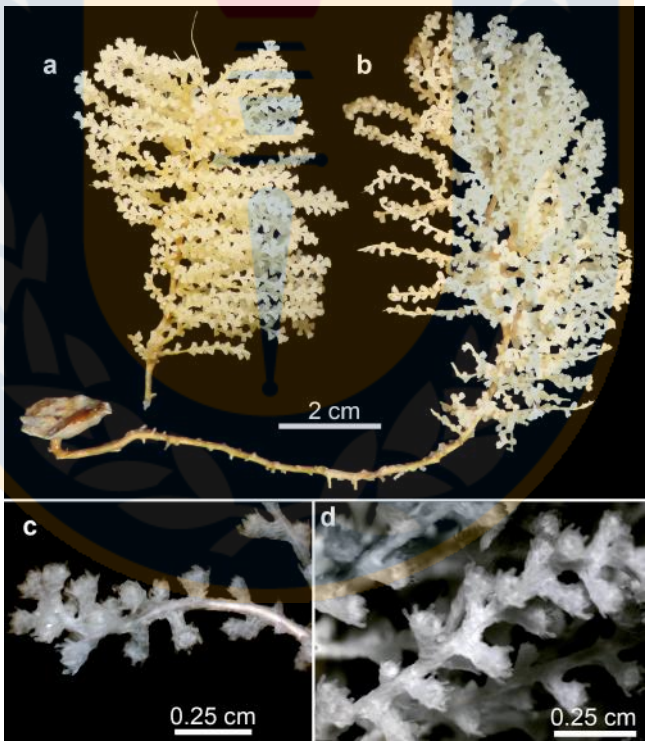

Figure 1.6 *Thouarella weddellensis* sp. nov., holotype MZB 2019-1967. a colony; b additional exanimated colony MZB 2019-1969. c–d details of the general polyp arrangement of the holotype.

Holotype description Colony bottlebrush-shaped, 6 cm high and 5 cm wide, without holdfast (Fig. 1.6a). Main stem simple, 1.6 mm in diameter proximally, and light golden in colour. Basal-most main stem without branchlets. First-order branches arise in three different directions, forming angle of 60–63° with main stem (Fig. 1.6b–d). Branchlets (second-order branch) separation ranges between 0.9–1.5 mm intervals, 1.2–2.8 cm in length (n=20), flexible, and in some cases subdivided (up to a third-order ramification; Fig. 1.6c,d).

Figure 1.7 *Thouarella weddellensis* sp. nov., holotype MZB 2019-1967. a Polyp arrangement on a branches; b polyp in abaxial view; c–d polyp in adaxial view; e polyp in inner lateral view. Scale bar = 0.2 mm.

Polyps relatively scarce (13–19 polyps/cm), isolated on branches and branchlets, distally flared, separated at intervals of 0.2–1.4 mm (average 0.75 mm; n=23); occasionally with polyps on main stem (Fig. 1.7a). Polyps short, distally flared, 1.4–1.7 mm tall (average 1.5 mm; n=32), and inclined 42°–69° (average 55°; n=26) with respect to branches/branchlets. Body scales covered by 8 longitudinal rows, with 3–4 scales (excluding opercular scales) in abaxial rows, 2–3 scales in outer lateral rows, 2–3 scales in inner lateral rows, and 2–3 scales in adaxial rows (Fig. 1.7b–e); opercular scales 8; marginal scales 8.

Operculum diameter up to 0.85mm (Fig. 1.8). Opercular scales do not form a perfect opercular cone (Fig. 1.8), generally having a broad tongue-shaped scales, with variable subparallel to concave lateral edges, serrate and broad distal edges, and W- shaped to irregular and straight proximal edges (Fig. 1.9a1), up to 0.69 x 0.38 mm H x W (average 0.52 x 0.22 mm H x W; H:W of 1.1–3, average 1.95). OL and IL broad lanceolate to subtriangular opercular scales with broadly pointed distal edges, up to 0.70 x 0.43 mm H x W (average 0.57 x 0.35 mm H x W; H:W of 1.3–1.9, average 1.51), are also present (Fig. 1.9a2). The 30–40% of inner proximal surface with small tubercles and simple keels, finely serrated distal edges (Fig. 1.9a1–a2). Outer surfaces strongly longitudinally concave (Fig. 1.9*), with sparse granules in the central proximal area, and striations spreading radially from the centre towards the distal edge.

Marginal scales larger than operculars, predominantly rhomboidal shaped, up to 0.82 x 0.60 mm H x W (average 0.72 x 0.55 mm H x W; H:W of 1–1.7, average 1.4; Fig. 1.9b). Distal inner surface with complex multi-keels, lateral projections adjacent to the main keel, and serrate distal edges. Proximal edges variable from W-shaped, V-shaped, straight, and irregularly rounded (Fig. 1.9b). The 40–70% of inner proximal surface with small tubercles. Outer surface flat, with densely sparsely distributed granules radiating along the middle scale area (Fig. 1.9b). Some of the marginal scales with concave lateral edges. Opercular and marginal scales aligned (Fig. 1.8).

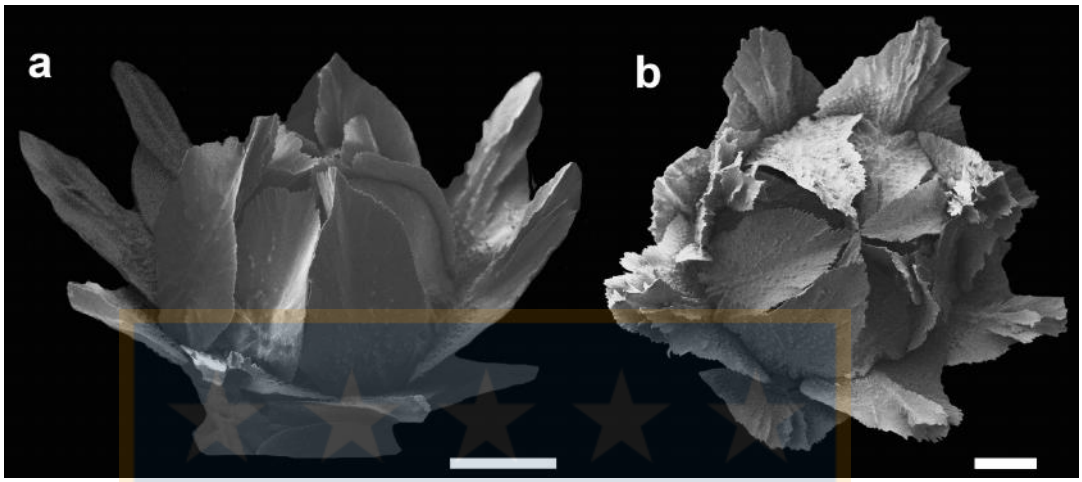

Figure 1.8. *Thouarella weddellensis* sp. nov., holotype MZB 2019-1967. a detail of the alignment of marginal and opercular scales; b details of the operculum. Scale bar = 0.2 mm.

Body-wall formed by two types of scales: fan-shaped submarginals with pointed distal edges (bearing simple or double keels) or distal radial ridges on their inner surface, and irregular to V-shaped proximal edges, up 0.65 x 0.68 mm H x W (average 0.55 x 0.51mm H x W; H:W of 0.69–1.32, average 1; Fig. 1.10a); and body-wall scales rather oval in shape, up to 0.55 x 0.55mm H x W(average 0.40 x 0.40mm H x W; H:W of 0.75–1.3, average 1; Fig. 1.10a), occasionally with small radial ridges in their distal area (Fig. 1.10a). Outer surface with granules and ridges more densely packed along the proximal edge; 90-95% of the inner surfaces with small tubercules. Coenenchymal scales irregularly oval to pentagonal shaped, up to 0.43 x 0.70 mm H x W (average 0.30 x 0.46 mm H x W; H:W of 0.3–1.4, average 0.7; Fig. 1.10b). Inner surface almost completely covered with small tubercles closely arranged (Fig. 1.10b). Outer surface with radial granules, and in a few cases radial ridges.

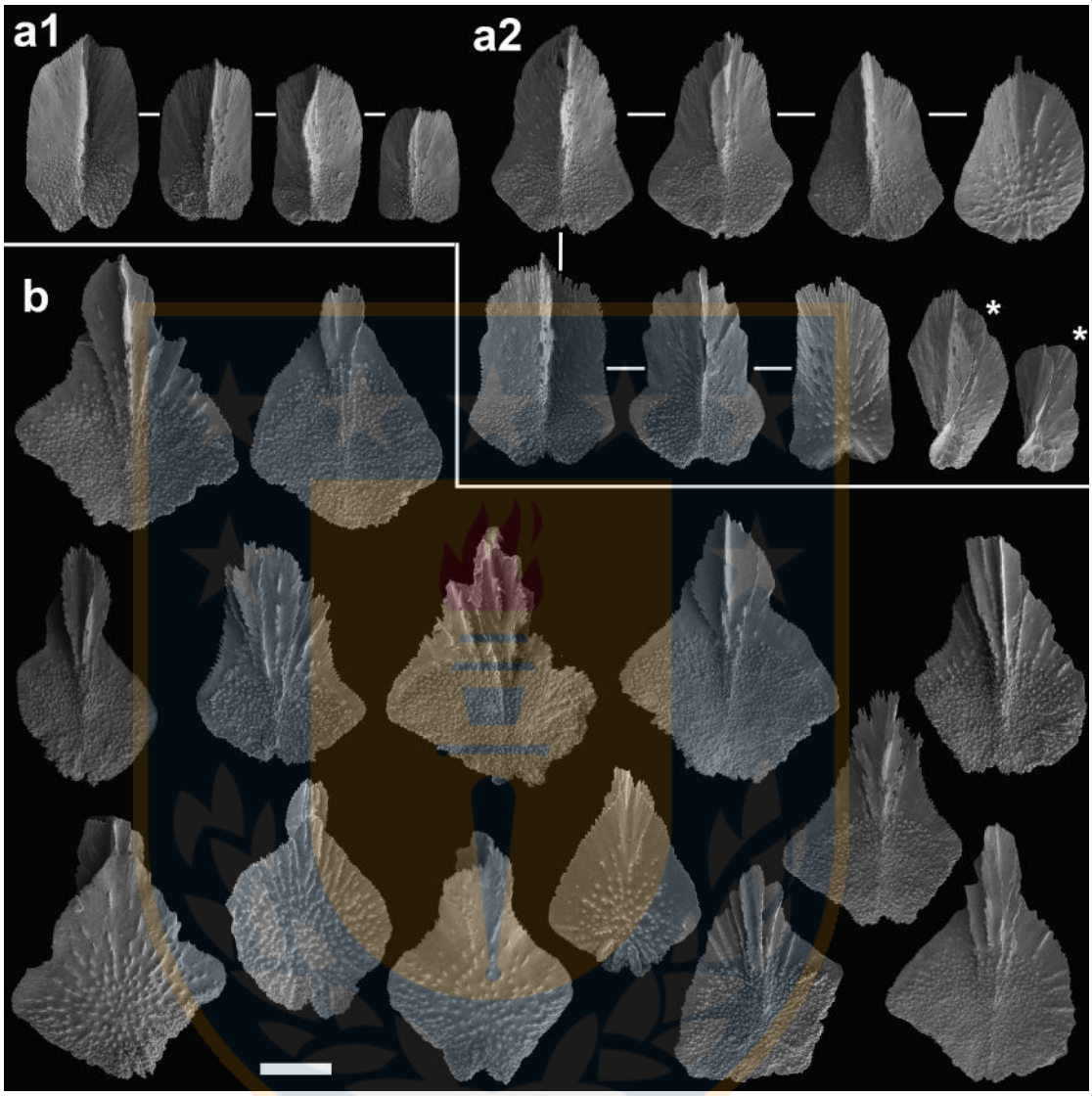

Figure 1.9. *Thouarella weddellensis* sp. nov., holotype MZB 2019-1967. a opercular scales (a1 broad tongue-shaped scales; a2 lanceolate to subtriangular scales with broadly pointed distal edges; * indicate details of the concave (in the outer face) shape of the opercular scales); b marginal scales. Scale bar = 0.2 mm.

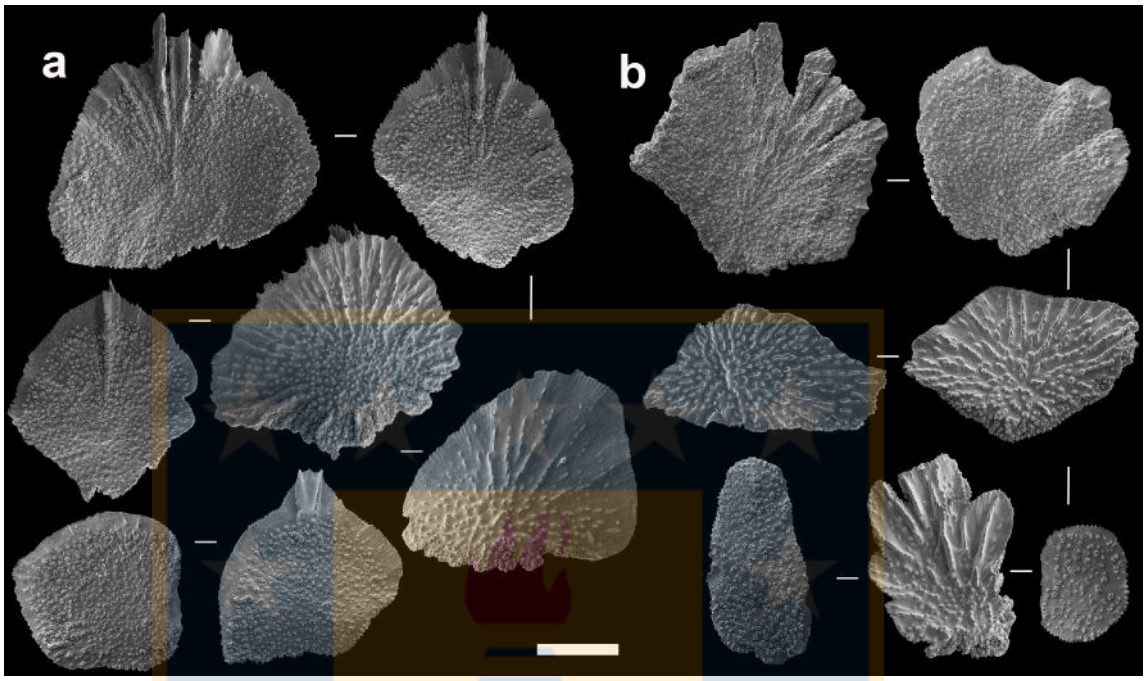

Figure 1.10. *Thouarella weddellensis* sp. nov., holotype MZB 2019-1967. a body scales; b coenenchymal scales. Scale bar = 0.2 mm.

Morphological variation Paratypes and additional material examined generally agree in the distribution, shape and size of the sclerites from polyps and coenenchyme. The larger colony reaches 17 x 6 cm H x W, up to third-order ramification, and branches up to 2.9 cm long. Some colonies show a polyp density of 15–23 polyps/cm. Tongue-shaped opercular scales with rather subparallel to concave lateral edges are consistently present in all the examined colonies, the presence of subtriangular opercular scales are not so constantly observed in the examined material. The number of abaxial scales consistently ranges between 3 and 4.

Geographic and bathymetric distribution The species is currently known from five localities in the Weddell Sea, Antarctica (Fig. 1.1), all of them at latitudes higher than 65ºS, at 295–1097 m depth.

Remarks *Thouarella weddellensis* falls also within the “group one” (Taylor *et al.* 2013) and the subgenus *Thouarella* (*Thouarella*) (*sensu* Cairns and Wirshing

2018) that have isolated polyps. Within this group, *T. weddellensis* is characterized by the lack of a spine on the marginal scales. These features have been considered attributes of the subgenus "*Epithouarella"* Kükenthal, 1915, which included *T. regularis*, *T. dispersa*, *T. grandiflora*, *T. crenelata*, *T. affinis*, *T. chilensis* and *T. viridis* (Cairns and Bayer 2009; Zapata-Guardiola and López-González 2012). However, it is necessary to note that this grouping is not recognized by Taylor et al. (2013) or Cairns and Wirshing (2018). In any case, the seven previously mentioned species have polyps with a higher number of scales in the longitudinal abaxial rows, ranging from 5–10 (Zapata-Guardiola and López-González 2012; Taylor *et al.* 2013), compared to those of *T. weddellensis* (3–4). Considering the reduced number of scales in the longitudinal abaxial rows, the low polyp height and the presence of tongue-shaped opercular scales, *T. weddellensis* broadly resembles *T. hicksoni*. However, the last has marginal scales with distal spinose projections (see Taylor et al. 2013: fig. 27, p. 66), unlike those of *T. weddellensis.* Finally, the alignment between marginal and opercular scales observed in this new taxon has not been previously mentioned for any other *Thouarella* species.

***Thouarella polarsterni* sp. nov.**

(Figs. 1.11–1.14)

http://zoobank.org/75DD303B-36F2-4FFD-80D6-AFDDAE98AE68

Type material MZB 2019-1984, Holotype, whole colony, 18 cm high; MZB 2019-1987, Paratype, whole colony, 35 cm high; MZB 2019-1989 Paratype, whole colony, 60 cm high; MZB 2019-1992, Paratype, whole colony, 31 cm high; MZB 2019-1993, Paratype, whole colony, 31 cm high; MZB 2019-1986, Paratype, whole colony, 44 cm high, *Polarstern* cruise ANT-XXIX, stn. 053-1, 76°19.33'S, 29°08.44'W, 261 m depth, Weddell Sea, Antarctica, 08 January 2014. MZB 2019-1981, Paratype, whole colony, 33 cm high, *Polarstern* cruise

ANT-XXIX, stn. 88-1, 76°57.98'S, 32°56.67'W, 265 m depth, Weddell Sea, Antarctica, 14 January 2014. MZB 2019-1982, Paratype, whole colony, 9.5 cm high, *Polarstern* cruise ANT-XXXI/2, stn. 001-9, 70°53.45'S, 11°08.2'W, 314 m depth, Weddell Sea, Antarctica, 24 December 2015.

Additional examined materials MZB 2019-1983, fragment of colony, 10 cm high; MZB 2019-1990, fragment of colony; MZB 2019-1991, whole colony, 30 cm high; BECA-OPRIM-2211, whole colony 30 cm high; MZB 2019-1985, fragment of colony, 42 cm high, *Polarstern* cruise ANT-XXIX, stn. 053-1, 76°19.33'S, 29°08.44'W, 261 m depth, Weddell Sea, Antarctica, 08 January 2014. MZB 2019-1988, fragment of colony, 9 cm high, *Polarstern* cruise ANT-XXVII-3, stn. 292-2, 70°49.41'S, 10°33.8'W, 281 m depth, Weddell Sea, Antarctica, 31 March 2011.

Etymology The species name is derived after the RV *Polarstern*, a German research vessel of the Alfred Wegener Institute for Polar and Marine Research, for its significant support in increasing knowledge about marine biodiversity in the Southern Ocean.

Diagnosis Colony bottlebrush in shape with isolated, short (~1.3 mm) and nearly appressed (22–47°) polyps; 3–5 scales in abaxial row, 3–4 in outer lateral rows, 3 in inner lateral rows, and 2–3 adaxials. Apical portion of colony with a higher density of polyps (>25 polyps / cm), than the rest of colony (average 19 polyps / cm). Opercular and marginal scales of similar isosceles-triangular shape, both type of scales with channelled keels; adaxial opercular scales reduced in size, lacking keels and with few tubercles on inner and outer surface.

Holotype description Colony bottlebrush-shaped, 18 cm high and 3.8 cm wide (Fig. 1.11a), without holdfast. Main stem simple and flexible, 1.5 mm in diameter proximally, and bronze in colour. Basal-most main stem without branchlets. Colony distally pointed (Fig. 1.11a). Basal-most main stem without branchlets. First-order branches arise in 3 different directions, forming angle of 30–75° with main stem (the lowest angle are found towards the apical region of the colony).

Branchlets (second-order branches) separation ranges between 0.7–3.7 mm (average 2 mm; n=20), 2.3 cm in length (average 1.8 cm; n=20), flexible, and generally simple (but up to a second-order ramification) (Fig. 1.11a–d).

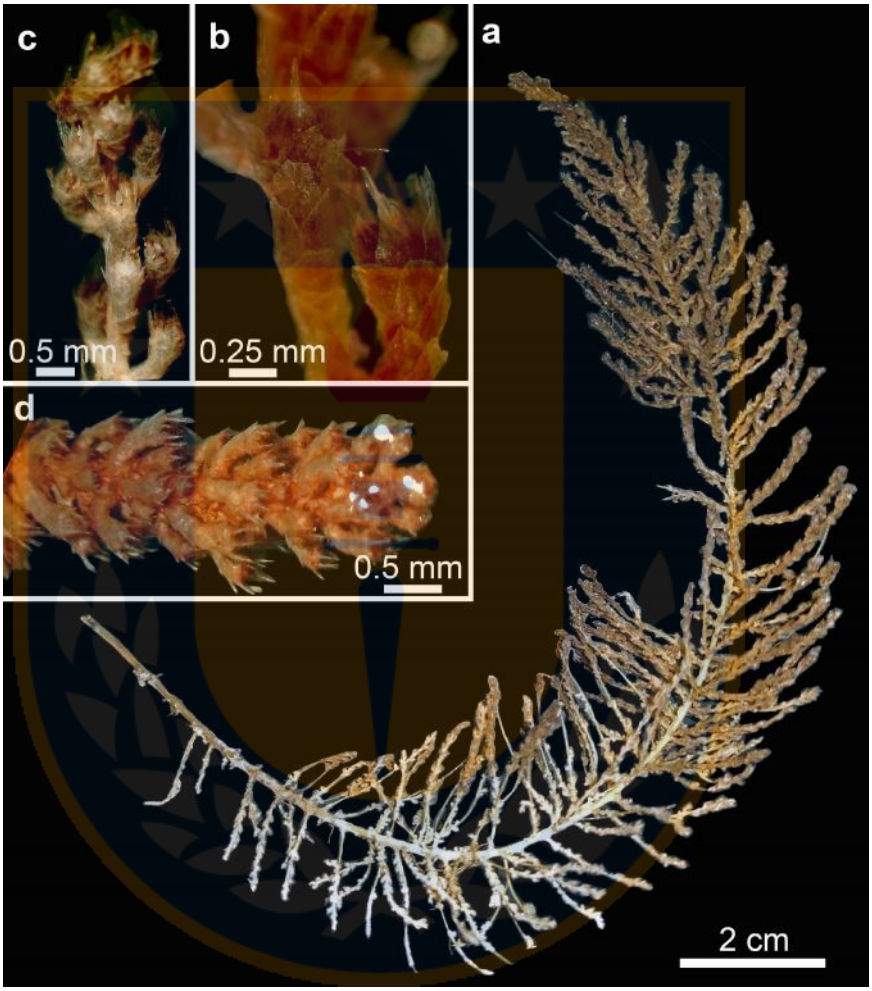

Figure 1.11. *Thouarella polarsterni* sp. nov., holotype MZB 2019-1984. a whole colony; b–c details of the general polyp arrangement; d details of the densely packed polyps at the apical portion of the colony (>25 polyps per cm).

Polyps cylindrical and moderately abundant, 14–25 polyps/cm (average 19 polyps/ cm; n=23), usually clustered in apical section; occasionally with polyps on main stem. Polyps short, 0.9–1.9 mm tall (average 1.3 mm including

the longest marginal spines; n=33; Figs. 1.11, 1.12), cylindrical, and inclined 22°–47° respect to the branchlets (average 30°; n=24; Fig. 2.11, 2.12). Apical-most portion of colony with an unusual higher density of polyps (approx. 40 polyps per cm; Fig. 11d), respect to relative abundance of polyps in the rest of the colony (Fig. 1.11b, c). Body scales covered by 8 longitudinal rows reducing to 5 at the polyp base, with 3–5 scales (excluding opercular scales) in the abaxial row, 3–4 scales in the outer lateral rows, 3 scales in the inner lateral rows, and 2–3scales in the adaxial rows (Fig. 1.12); opercular scales 8; marginal scales 8.

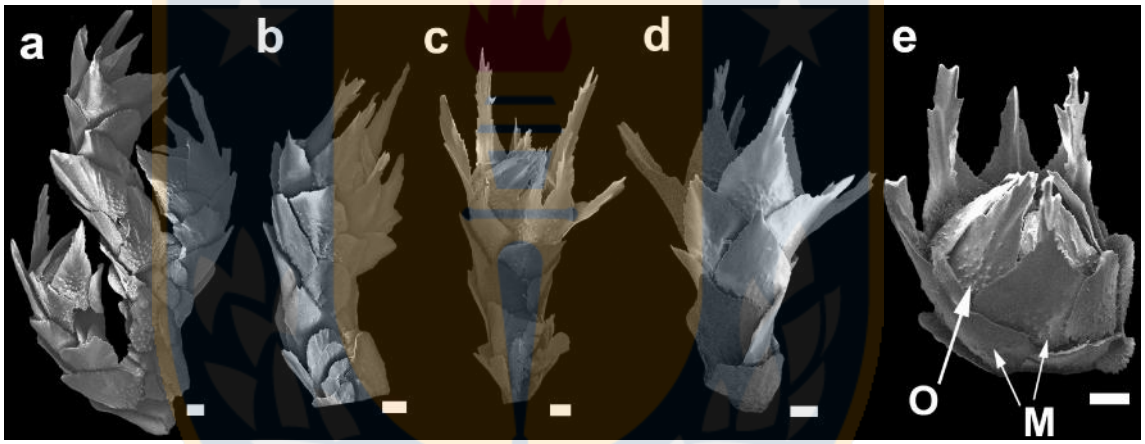

Figure 1.12. *Thouarella polarsterni* sp. nov., holotype MZB 2019-1984. a general polyp arrangement; b polyps in outer lateral view; c polyps in adaxial view; d polyps in abaxial view; e details of the operculum. Scale bar = 0.1 mm.

Opercular scales triangular isosceles-shaped with acute distal edges, and rounded proximal areas, distal edges irregular to indented, up to 0.47 x 0.24 mm H x W (average 0.29 x 0.16 mm; H:W of 0.75–3.5, average 1.96; Fig. 1.13a). Two smaller adaxial scales, triangular isosceles in shape but with broadly rounded distal edges (although no tongue-shaped), up to 0.23 x 0.131 mm H x W (average 0.16 x 0.10 mm H x W; H:W of 1.2–1.8, average 1.6; Fig. 1.13a*). The 35–60% of the inner proximal surface of large opercular scales with

complex tubercles, mostly with channelled keels (simple keel rarely present), finely serrated distal edges (Fig. 1.9a1–a2) and a smooth area towards their lateral (in some cases even toward the proximal) edges. Adaxial scales without keels, and scarce tubercles and granules on the inner and outer surface, respectively (Fig. 1.13a*).

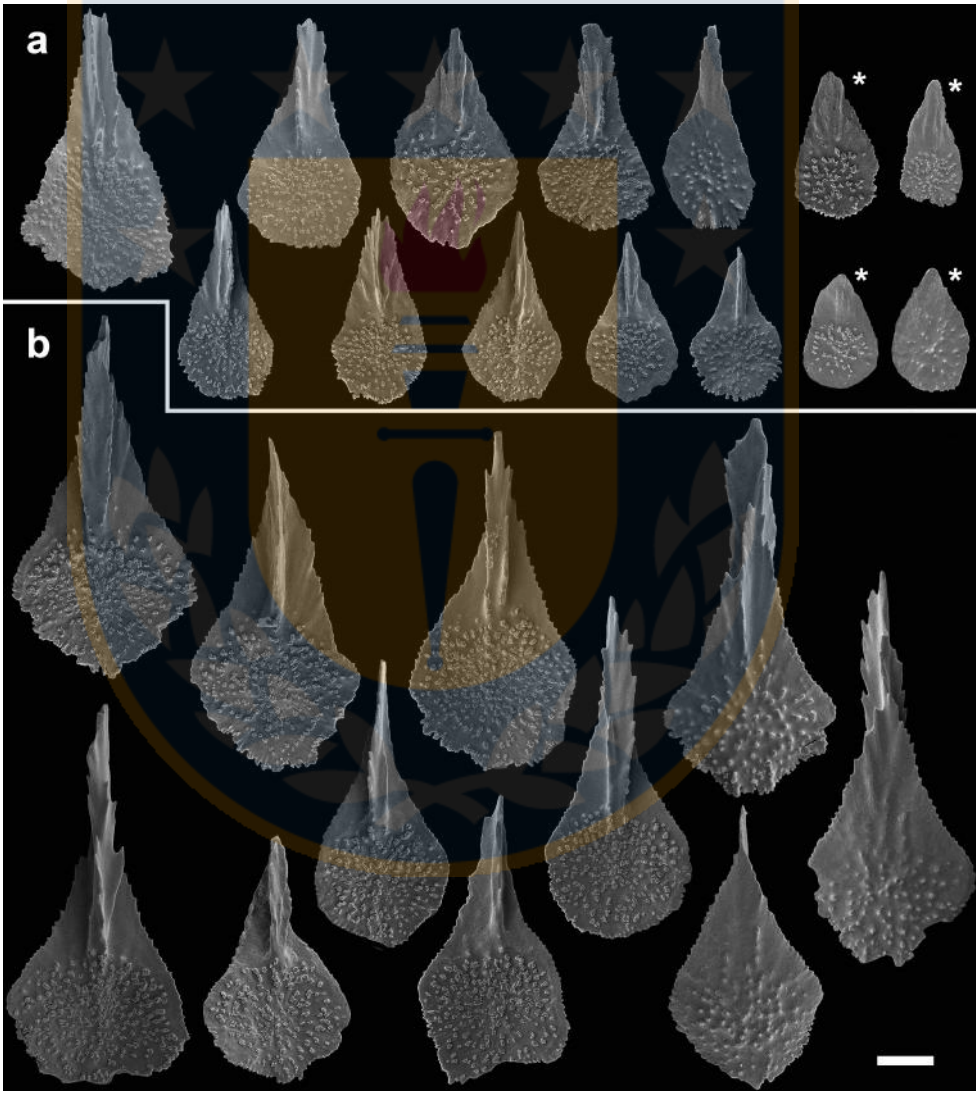

Figure 1.13. *Thouarella polarsterni* sp. nov., holotype MZB 2019-1984. a opercular scales (asterisk indicates the adaxial scales); b marginal scales. Scale bar = 0.1 mm

Marginal scales similar in shape to operculars; triangular isosceles-shaped with a slightly narrow distal area, rhombohedral to pentagonal proximal area, irregular to dentate proximal edges, up to 0.78 x 0.4 mm W x H (average 0.50 x 0.27 mm W x H; H:W of 0.9–2.8, average 1.9; Fig. 1.13b). Inner 40–60% of proximal surface with small tubercles and smooth towards the lateral (in some cases even toward the proximal) edges, finely serrated lateral edges, moderate spine and generally channelled-keels, distinct smooth triangular areas from proximal keel towards lateral scale edges, keels usually serrated (especially toward its distal-most portion). Outer surface with small and relatively sparse granules in the proximal area, channelled keels visible on the distal area.

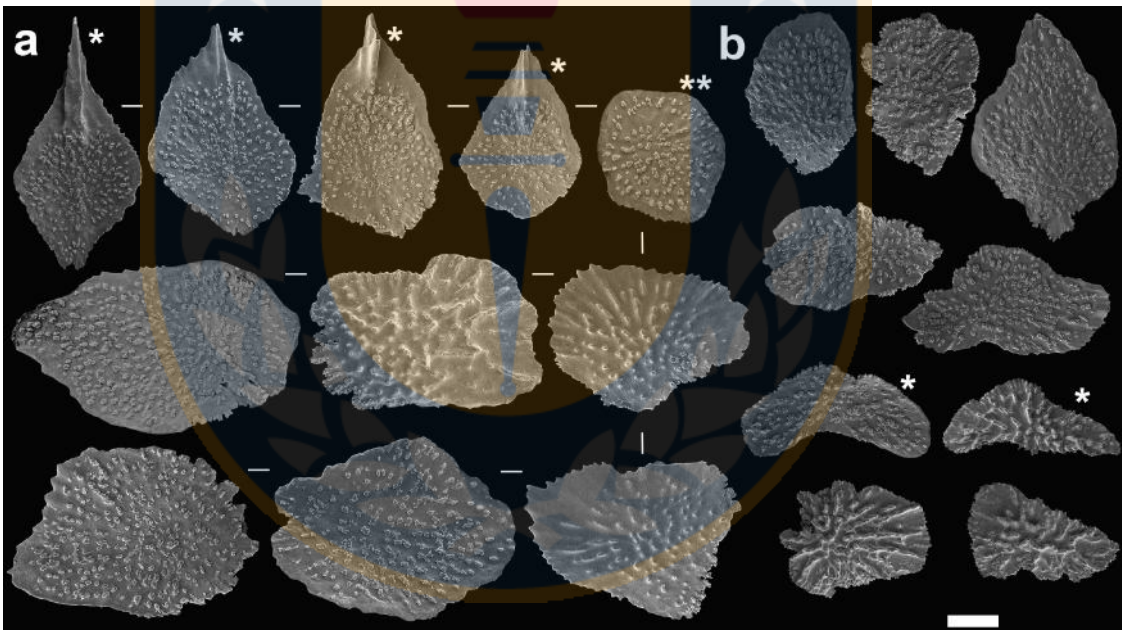

Figure 1.14. *Thouarella polarsterni* sp. nov., holotype MZB 2019-1984. a body scales (asterisks indicate the pointed sub-marginal scales; stars indicate the rounded adaxial body-wall scales); b coenenchymal scales (asterisks indicate boomerang-shaped coenenchymal scales). Scale bar = 0.1 mm.

Submarginal scales smaller than marginal, diamond-like shaped, generally pointed, with a reduced keel distally on inner surface, proximal inner

surface with complex tubercles, lateral edges serrated to smooth, up to 0.56 x 0.37 mm H x W (average 0.43 x 0.29 mm H x W; H:W of 1.2–1.9, average 1.5; Fig. 1.14a*). Remaining body wall scales in a variety of shapes from circular to rectangular, with finely serrated edges up to 0.51x 0.39 mm H x W (average 0.31x 0.27 mm H x W; H:W of 0.5–2.5, average 1.2; Fig. 1.14a). The 60–95% of the inner surface densely covered with complex tubercles; outer surface strongly curved, covered with granules and ridges, without pointed edges, and generally serrated. Adaxial body-wall scales slightly smaller than others and rounded (Fig. 1.14a**). Coenenchymal scales with irregular forms, predominantly elliptical (Fig. 1.14b), but boomerang-like scales are also present (Fig. 1.14b*), up to 0.44 x 0.27 mm H x W (average 0.31 x 0.18 mm H x W; H:W of 0.9–2.3, average 1.6). Inner surface with tubercles; radial-like broad ridges arrangement in the outer surface. Some portions of lateral edges finely serrated.

Morphological variation Paratypes and additional material examined generally agree in the distribution, shape, and size of the sclerites from polyps and coenenchyme. Larger colonies of 60 x 7 cm H x W, branches up to 3.5 cm long and up to fourth ramification order. Colonies of up to 44 x 5.5 cm H x W, with branches up to 3 cm long. Polyp density ranges among 15–21 per cm, except in the apical region. In the paratypes and additional examined materials bearing its apical region (n=6) the polyp density always unusually high (>25 polyps/cm).

Geographic and bathymetric distribution The species is currently known from four localities in the Weddell Sea, Antarctica (see Fig. 1.1), all of them from latitudes higher than 70ºS, at 261–314 m depth.

Remarks *Thouarella polarsterni* also falls within the “group one” and the subgenus *Thouarella* (*Thouarella*) (*sensu* Cairns and Wirshing 2018) by having isolated polyps (Taylor *et al.* 2013). The presence of less than five abaxial scales, as well as a short polyp length (less than 1.5 mm). indicate close morphological similarities of the newly proposed species to *T. pendulina*, *T.*

hicksoni, *T. minuta* and *T. islai* sp. nov. (see Taylor et al. 2013: p. 66). *Thouarella polarsterni* and *T. hicksoni* have a similar density of polyps per cm (14–25 and 16–22, respectively), lower than *T. pendulina* (27–41), and higher than *T. islai* and *T. minuta* (7–19 and 11–18, respectively). *Thouarella polarsterni*, shares with *T. pendulina, T. hicksoni* and *T. minuta* a low number of abaxial scales (3–5) (Zapata-Guardiola and López-González 2010e; Taylor *et al.* 2013). It is important to mention the observed polyp density dissimilarity between the apical-most part and the rest of the colony observed in *T. polarsterni*, although this fact has not been reported in any of the previously mentioned species (Zapata-Guardiola and López-González 2010e; Taylor *et al.* 2013).

The sclerome of *T. polarsterni* shows a unique combination of features that allow us to differentiate it from the previously mentioned *Thouarella* species. The opercular scales of *T. polarsterni* are isosceles-shaped but taller than wide (H:W= 1.96), clearly different from the diamond-shaped sclerites of *T. pedulina* (see Taylor et al., 2013: fig. 23, p. 58), the wide and predominantly lanceolate to tongue-shaped scales of *T. hicksoni* (see Taylor et al., 2013: fig. 27, p. 66), the isosceles- to spoon-shaped spinose scales of *T. minuta* (see Zapata-Guardiola and López-González 2010b: fig. 13, p. 178), and the isosceles-triangle (with rounded distal ends) to tongue-shaped scales of *T. islai* (Fig. 4). The marginal scales of *T. polarsterni* are triangular isosceles-shaped with slightly narrow distally, spines and channelled keels (Fig. 1.13), unlike those round to rhomboidal shape of *T. minuta* and *T. pedulina* (see Taylor et al. 2013: fig. 23, p. 58; Zapata-Guardiola and López-González, 2010b: fig. 13, p. 178), or the conspicuously well-developed distal spine of *T. islai* (Fig. 1.4). Marginal scales of the new taxon here discussed broadly resembles those of *T. hicksoni* (see Taylor et al. 2013: fig. 27, p. 66) in their isosceles triangular shape. However, *T. polarsterni* has long and narrow marginal scales (H:W=1.96) than *T. hicksoni* (H:W=1.4; Taylor et al. 2013).

1.3.1 Phylogenetic results

New sequences from *mtMutS* (10 sequences), *Cox1* (10 sequences), and *28S* (5 sequences) loci were obtained for the taxa here described and analysed with additional primnoid sequences obtained from GenBank (see Supplementary File 2). We retained only specimens with sequences from two genes or more in the analyses. This resulted in 99 specimens in final phylogenetic analyses. The *28S* rDNA marker nuclear was obtained for three specimens of *T. weddellensis*, one *T. islai*, and one *T. polarsterni*. The *mtMutS*, *Cox1* and *28S* rDNA sequences had a length of 799, 800 and 851 bp, respectively, while the concatenated dataset *mtMutS+Cox1+28S*, contains a total of 2450 characters. Although our preliminary phylogenetic analysis includes 98 primnoids species, henceforth we will focus on species of *Thouarella* as all sequenced specimens fall among other available sequences of this genus.

The phylogenetic analysis of the concatenated matrix contains 514 parsimony informative sites (138 for *mtMutS*, 64 for *Cox1* and 312 for *28S*) and provides relatively well-supported nodes. A portion of the tree resulting in the BI of the concatenated dataset, which includes *Thouarella* and closely related taxa, is shown in Fig. 1.15 (see Supplementary File 3 for the complete tree). In this analysis, all specimens identified as *T. weddellensis* and *T. polarsterni* form single clades with high support values (PP=1; Fig. 1.15). However, the three specimens belonging to *T. islai* appear to be indistinguishable from those of *T. pendulina* AR135 recovered from the GenBank (Fig. 1.15), although the two taxa form a well-supported clade (PP=1). However, *T. islai* differs from *T. pendulina* AR135 in 8 bp on the *28S* locus, while both have identical *mtMutS* and *Cox1* loci.

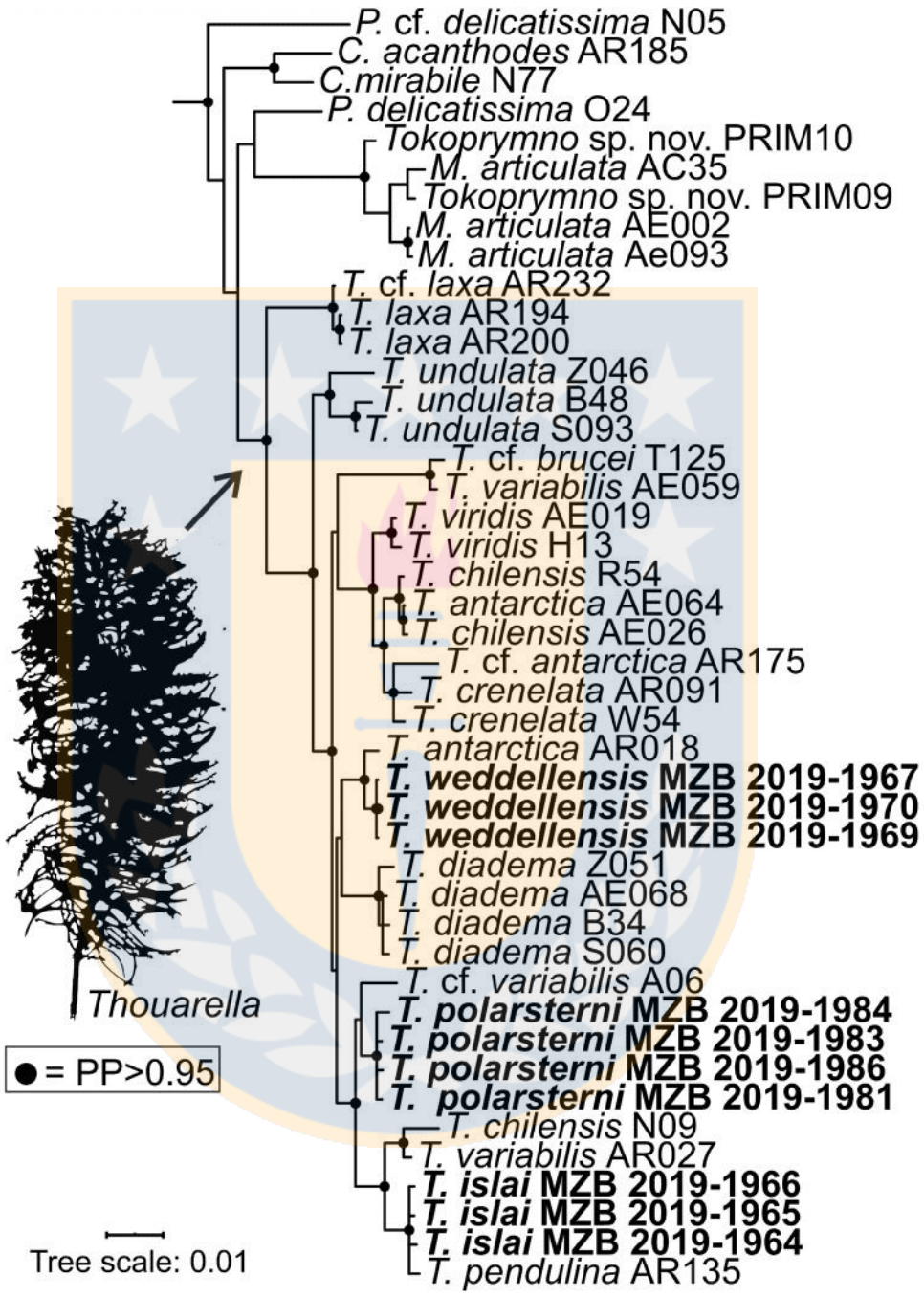

Figure 1.15. Bayesian inference based on a concatenated molecular dataset of mitochondrial (mtMutS+Cox1) and nuclear (28S) loci with emphasis in the *Thouarella* genus and closed allies (nodes with PP<50 were removed). Black circles denote nodes with high support (PP>0.95). The new taxa here described are in bold.

1.4. Discussion

In the present work, we looked for the existence of independently evolving lineages within primnoids combining mitochondrial and nuclear DNA markers and detailed morphological analysis (De Queiroz 2005; De Queiroz 2007). Our integrative approach allowed us to find distinctive properties or lines of evidence supporting the existence of three new species within the primnoid genus *Thouarella*, which are described herein.

Octocorals have unusually slow rates of mitochondrial gene evolution (Bilewitch and Degnan 2011). Nonetheless, several recent studies have identified multilocus barcodes (including the *mtMutS*, *Cox*, and *28S*) capable of distinguishing morphospecies of octocorals with a relatively high (70–83%) success (McFadden *et al.* 2011; Baco and Cairns 2012; McFadden *et al.* 2014b). The combined phylogenetic analyses of mitochondrial and nuclear loci indicated that all specimens identified as *T. weddellensis* and *T. polarsterni* represent well-supported clades (Fig. 1.15). These two taxa are also morphological diagnosable (see details above), thus molecular and morphological evidence strongly supports their distinction as new species.

However, the Bayesian analysis based on mitochondrial and nuclear loci did not recover the monophyly of *T. islai*, because the last taxa and the specimen identified as *T. pendulina* AR135 form a single linage (Fig. 1.15). On the other hand, the *28S* locus indicated that *T. islai* and *T. pendulina* AR135 must represent different lineages because both differ in 8 bp (See Supplementary File 4). In agreement with the data from the *28S* locus, the type and additional materials of *T. islai* and the type material of *T. pendulina* show clear morphological differentiation. Both species are easily differentiated by the lower polyp density and the conspicuously large and narrow distal spine on the marginal scales of the *T. islai* (Taylor et al. 2013; but see more details above). Previous works have suggested that given their low evolution rate in octocorals, and its uniparental inheritance, species delimitation relying solely on mtDNA

could not detect boundaries between closely related octocoral species (e.g. Vargas et al. 2014; Soler-Hurtado et al. 2017), and this appears to be the case for *T. islai* and *T. pendulina* (although additional sequenced materials attributable to the latter taxa are desirable). Despite this situation, the presence of several morphologically distinctive characters traditionally used for primnoid taxonomy (e.g. Taylor et al. 2013), as well as the evolutionary history provided by the *28S* locus (Supplementary File 4), support the formal description of *T. islai* as a new species. Therefore, our findings increase the large body of literature demonstrating the utility of combining morphological and molecular evidences for supporting the proposal and even the delimitation of new taxa (De Queiroz 2007; Padial *et al.* 2010; Dueñas *et al.* 2014; Pante *et al.* 2015; Soler-Hurtado *et al.* 2017).

Finally, although it is beyond the scope of this contribution, some results in our phylogenetic analysis (Fig. 1.15), also observable in Cairns and Wirshing (2018) and Taylor and Rogers (2015), deserve brief comments. On one hand, some *Thouarella* species represented by more than one specimen in the concatenated dataset (e.g. *T. diadema*, *T. laxa*, and *T. undulata*) form distinct clades, although the intraclade genetic variability can be more important than that observed between two other morphologically well identifiable species. However, so far, we have not observed that range of molecular variability in any of the new species here proposed (Fig. 15). On the other hand, the presence of the same given identified species at different placements along the tree (e.g. *T. chilensis*, *T. antarctica,* and *T. variabilis*), resulted in an undesirable polyphyletic status for these species, and thus, an uncertain resolution about their possible phylogenetic relationships. This apparent wide genetic variability attributed to the former taxa could be explained by: 1) the existence of cryptic species (i.e., taxa with unreliable or difficult morphological identification, but recognizable as independent linages by molecular markers) (Bickford *et al.* 2007; McFadden and van Ofwegen 2013a; Tu *et al.* 2015); 2) disseminations in public databases (e.g.

GenBank) of sequences with undetected erroneous sequencher readings; or 3) incorrect specimens' identifications. Perhaps both of these possible cases could be present in *Thouarella* sequences already deposited in these public databases (Leray *et al.* 2019). Therefore, we cannot (in these cases) conclude which of the different sequences identified as to given species is the closest one to the carrier of the species name, and then truly attributable to that species.

Taxonomic works during the last decade have increased our knowledge of the diversity of primnoid gorgonians in Antarctic and sub-Antarctic waters with the discovery of several new species (Zapata-Guardiola and López-González 2010e; Zapata-Guardiola and López-González 2010b; Zapata-Guardiola and López-González 2012; Taylor *et al.* 2013), especially within the genus *Thouarella*. Previous to the present work, the global diversity of this genus reached 35 species, 21 of which were from the Southern Ocean and the Southern Atlantic, nine of them endemic to the Antarctic and sub-Antarctic regions (Zapata-Guardiola and López-González 2010e; Zapata-Guardiola and López-González 2010b; Zapata-Guardiola and López-González 2012; Taylor *et al.* 2013). With the three new species proposed here, the diversity of the genus increased to 38 species, 12 of which are endemic to Antarctica. The high endemicity of this genus in the Southern Ocean is consistent with recognized high levels of endemism for the Antarctic benthic fauna, which varies between 50% and 97% according to the studied group (Griffiths *et al.* 2009; Kaiser *et al.* 2013; Broyer *et al.* 2014). The high number of species from higher latitudes of the Southern Hemisphere (Taylor *et al.* 2013), the high endemicity in the Southern Ocean (12 spp.), as well as recent phylogenetic analyses (Taylor and Rogers 2015) reinforce the idea that the Southern Ocean was likely a diversification centre for *Thouarella* (Taylor *et al.* 2013). Extreme climatic, oceanographic and tectonic changes that the Antarctic region has undergone throughout most of the Cenozoic (Griffiths *et al.* 2009; Cristini *et al.* 2012; Chown *et al.* 2015) must have played an important role in their evolutionary

history as proposed for other groups (Rogers 2007; Chenuil *et al.* 2018). However, a much-expanded taxon sampling is necessary to effectively assess the evolutionary relationships, as well as to elucidate the timing and drivers of *Thouarella* diversification.

Despite the relatively high diversity of *Thouarella*, our understanding of this clade of organisms is likely still incomplete given that most of the deep-sea environments and habitats are poorly sampled, especially in the Southern Ocean (Zapata-Guardiola and López-González 2010b). Given the great extension of the Southern Ocean benthic habitats, and its likely role as centre of *Thouarella* diversification, the discovery of additional new species is expected after increasing sampling efforts, as well as after the detailed study of a large number of materials already deposited in several museums around the world, as the result of many international and collaborative sampling effort in these remote locations.

Acknowledgments The authors wish to acknowledge the valuable assistance of the officers and crew of the RV *Polarstern* and many colleagues on board during the ANT XII/3 (1995), ANT XXIII/8 (2007), ANT XXIV/2 (2008), ANT XXVII-3 (2011), ANT-XXIX (2014), and ANT-XXXI/2 (2016) cruises. We extend our thanks to the cruise leaders and steering committee of the cruises especially Wolf E. Arntz and Julian Gutt (Alfred Wegener Institut, Bremerhaven), who kindly facilitated the work onboard and for the opportunity to collaborate in these Antarctic programs. Special thanks to Josep Maria Gili, Rebeca Zapata-Guardiola and Stefano Ambroso for helping in the collection of octocoral specimens during *Polarstern* cruises. We also acknowledge José Garrido for their help with the DNA extraction and amplification, and Norwegian Polar Institute's for the make available the *Quantarctica* package. Finally, we thank to the editor Bert W. Hoeksema and the two anonymous reviewers for their comments and suggestions that improved the final version of this manuscript.

Funding information This research is supported by the project CTM2017-83920-P (DIVERSICORAL), Spanish Ministry of Economy, Industry and Competitiveness. Different funds for the participation on these *Polarstern* cruises were provided by the Spanish CICYT projects – CLIMANT – POL2006-06399/CGL (ANT XXIII/8). M.N.F. acknowledges partial support from CONICYT-PCHA/Doctorado Nacional/2017-21170438, and Instituto Antártico Chileno (INACH) grant number DG_04_19. D.G.U. acknowledges partial support from Nucleo Milenio INVASAL funded through Chile's Iniciativa Científica Milenio at Ministerio de Economía, Fomento & Turismo, Chile.

Conflict of Interest The authors declare that they have no conflict of interest.

Ethical approval All applicable international, national, and/or institutional guidelines for animal testing, animal care and use of animals were followed by the authors.

Sampling and field studies All necessary permits for sampling and observational field studies have been obtained by the authors from the competent authorities and are mentioned in the acknowledgments, if applicable.

Data availability Additional data, including primers used to amplify the regions of *Cox1*, *mtMutS* and *28S*, GenBank accession numbers of the primnoids specimens used in the molecular analysis, and additional phylogenetic results are in the Supplementary Files.

Author contribution M.N.F., P.L.G. and D.G.U. conceived and designed the study. M.N.F. performed scanning electron microscopy (SEM), conducted morphological examinations and phylogenetic analysis. M.N.F. wrote the first draft of the manuscript that was improved in subsequent revisions by P.L.G and D.G.U. All authors gave final approval for publication.

CHAPTER II. Molecular systematics of *Thouarella* (Octocorallia: Primnoidae) with the description of three new species from the Southern Ocean based on combined molecular and morphological evidence[2]

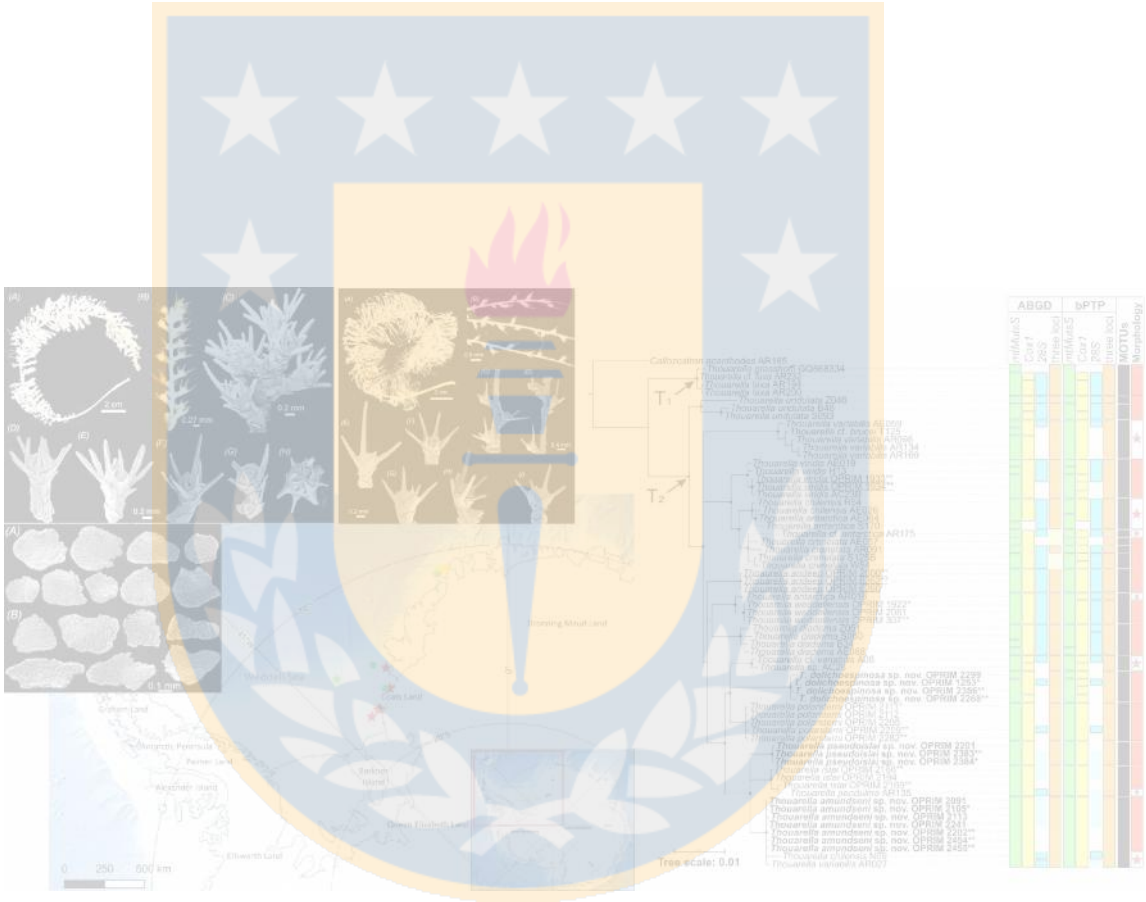

[2]**Artículo publicado.** Núñez-Flores Mónica, Gomez-Uchida Daniel, López-González Pablo J. (2021) Molecular systematics of *Thouarella* (Octocorallia:Primnoidae) with the description of three new species from the Southern Ocean based on combined molecular and morphological evidence. *Invertebrate Systematics* 35, 655-674. https://doi.org/10.1071/IS20078

Molecular systematics of *Thouarella* (Octocorallia: Primnoidae) with the description of three new species from the Southern Ocean based on combined molecular and morphological evidence

Mónica Núñez-Flores[A,B,C,D], Daniel Gomez-Uchida[B], Pablo J. López-González[C]

[A]Programa de Doctorado en Sistemática y Biodiversidad, Facultad de Ciencias Naturales y Oceanográficas, Universidad de Concepción, Concepcion, Chile

[B]Genomics in Ecology, Evolution and Conservation Lab (GEECLAB), Department of Zoology, Facultad de Ciencias Naturales y Oceanográficas & Núcleo Milenio INVASAL, Universidad de Concepción, Concepcion, Chile

[C]Biodiversidad y Ecología Acuática (BECA), Departamento de Zoología, Facultad de Biología, Universidad de Sevilla, Seville, Spain

[D]Corresponding author. Email: nuez.monica@gmail.com

Abstract.

Thouarella Gray, 1870, is one of the most speciose genera among gorgonians of the family Primnoidae (Cnidaria: Octocorallia: Anthozoa) being remarkably diverse in the Antarctic and sub-Antarctic seafloor. However, their diversity in the Southern Ocean is likely underestimated. Phylogenetic analyses of mitochondrial and nuclear DNA markers were integrated with species delimitation approaches as well as morphological colonial/polyps features and skeletal SEM examinations to describe and illustrate three new species within the genus *Thouarella*, from the Weddell Sea, Southern Ocean: *T. amundseni* sp. nov., *T. dolichoespinosa* sp. nov. and *T. pseudoislai* sp. nov. Our species delimitation results suggest, for the first time, the potential presence of Antarctic and sub-Antarctic cryptic species of primnoids, based on the likely presence of sibling species within *T. undulata* and *T. crenelata*. With the three new species here described, the global diversity of *Thouarella* has increased to 41 species, 15 of which are endemic to the Antarctic and sub-Antarctic waters. Consequently, our results provided new steps for uncovering the shelf benthonic

macrofauna's hidden diversity in the Southern Ocean. Finally, we recommend using an integrative taxonomy framework in this group of organisms and species delimitations approaches because the distinction among some *Thouarella* species based only on a superficial examination of their macro and micro-morphological features is in many cases limited.

Keywords: Antarctic marine biodiversity, Integrative Taxonomy, Species Delimitation, Weddell Sea.

2.1. Introduction

Thouarella Gray, 1870 is one of the most speciose genera among primnoids (Octocorallia: Anthozoa: Primnoidae), having a worldwide distribution. But this genus is most common in Antarctic and sub-Antarctic regions (Cairns and Bayer 2009; Zapata-Guardiola and López-González 2010b; Taylor *et al.* 2013). According to the last revision of the genus (Taylor *et al.* 2013) and subsequent species descriptions, there are at least 38 valid *Thouarella* species (Cairns and Wirshing 2018; Cairns *et al.* 2018; Altuna and López-González 2019; Núñez-Flores *et al.* 2020). However, taxonomic identification of *Thouarella* and closely allied taxa to species level can be problematic (Dueñas *et al.* 2016; Bogantes *et al.* 2020) as many of them may be macroscopically similar and only are morphologically distinguished from one another throughout a detailed examination of the branching pattern of colonies, polyps distribution, and specially scanning electron microscopic (SEM) analysis of scales (Taylor *et al.* 2013; Hourigan *et al.* 2017; Altuna and López-González 2019). Indeed, the main characters used for the species recognition in *Thouarella*, as in other octocorals, are related to the sclerome (i.e., shape and ornamentation of scales) (Cairns and Bayer 2009; Zapata-Guardiola and López-González 2010c; Taylor *et al.* 2013). However, when possible, morphological characters should not be the sole basis for defining species boundaries in octocorals, considering their potential adaptive phenotypic plasticity in response to different environmental fluctuations (Prada *et al.* 2008).

The recovery of molecular information of mitochondrial genes in octocorals [*mtMutS* (=*msh1*), and *Cox1*] have contributed to increasing our knowledge about the systematics of primnoids (Taylor and Rogers 2015; Taylor and Rogers 2017; Cairns and Wirshing 2018). Nevertheless, several works have recognized the difficulty of distinguishing species of some octocoral groups only with mitochondrial information (McFadden *et al.* 2010; McFadden *et al.* 2011; Baco and Cairns 2012; McFadden *et al.* 2014b; Soler-Hurtado *et al.* 2017; Quattrini *et al.* 2019; Bogantes *et al.* 2020) since octocoral mitochondria have a unique DNA repair mechanism responsible for the slow evolution of their genes (Bilewitch and Degnan 2011). In this sense, the description of new octocorals can benefit by additional phylogenetically informative nuclear genes such as *28S* ribosomal DNA (France and Hoover 2001; McFadden *et al.* 2011), as well as the complementary use of molecular and morphological evidence (Dueñas *et al.* 2014; Soler-Hurtado *et al.* 2017; Xu *et al.* 2020; Núñez-Flores *et al.* 2020).

During the last decade, and after several Antarctic surveys aboard the German icebreaker RV *Polarstern* important collections of primnoid colonies were acquired along the Weddell Sea (Fig. 1). After detailed skeletal SEM examinations as well as phylogenetic analyses integrated based on mitochondrial (*mtMutS* and *Cox1*) and nuclear (*28S*) loci, and species delimitation approaches (including the Automatic Barcoding Gap Discovery (ABGD) (Puillandre *et al.* 2012), and the Poisson-Tree processes (PTP) (Zhang *et al.* 2013)), we present here the description of three new species of the genus *Thouarella* from the Southern Ocean. Moreover, we provide new molecular sequences from the type materials of two *Thouarella* species already described in the literature, *T. andeep* Zapata-Guardiola and López-González 2010b and *T. viridis* Zapata-Guardiola and López-González 2010b, to explore the broad phylogenetic relationships within this speciose genus based on multi-locus evidence.

2.2 Materials and methods

2.2.1 Sample collections, DNA extraction, amplification, and sequencing

The octocoral colonies here studied were collected on the RV *Polarstern* cruises ANT XVII/3 (2000), ANT XXIX/9 (2014), and ANT XXXI/2 (2016) along with different localities in the Weddell Sea, Southern Ocean (Fig. 2.1) mainly using bottom trawls. Colonies were fixed in 10% buffered formalin in seawater and then transferred to 70% ethanol on board, frozen on board and then moved to absolute ethanol, or were directly fixed in absolute ethanol for future molecular analyses.

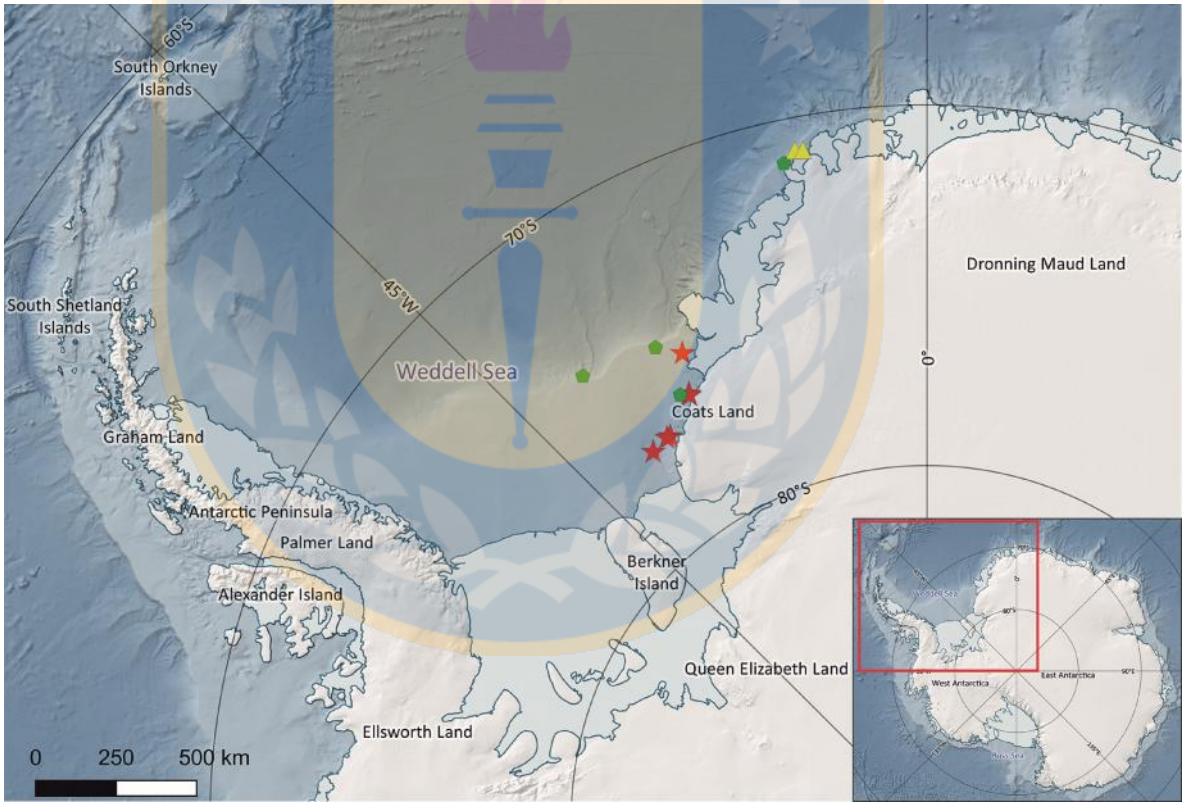

Figure 2.1. Map of the Antarctica and Southern Ocean, showing the sampling localities where the new colonies were recovered. The distinct symbols represent each of the three independent evolutionary lineages recognized and named in the present work, *Thouarella amundseni* sp. nov. (stars), *T. pseduoislai* sp. nov. (triangles) and *T. dolichoespinosa* sp. nov. (pentagons). The

cartographic base used for the location map is from the Quantarctica package (Matsuoka *et al.* 2018).

DNA was extracted from both absolute ethanol fixed or frozen colonies, using the E.Z.N.A. DNA kit (Omega Biotech) following the manufacturer's instructions. PCR amplified two mitochondrial regions (*Cox1* and *MutS*) and a nuclear region (*28S* rDNA). Amplifications were performed using 1 U of MyTaq Red DNA Polymerase (Bioline), 1 µl (10 µM) of each primer, approximately 30 ng of genomic DNA, and was brought to a final volume of 20 µl with H_2O. Primers used to amplify the regions of *Cox1*, *mtMutS* and *28S*, as well as PCR conditions are the same described in Núñez-Flores et al. (Núñez-Flores *et al.* 2020). PCR products were purified using ExoSAP–IT™ PCR Product Cleanup Reagent (ThermoFisher Scientific) following the manufacturer's instructions before robust amplifications were sent to Macrogen Europe for sequencing both directions. All chromatograms were visualized, and sequence pairs matched and edited using Sequencher v4.0. DNA samples from *T. andeep* and *T. viridis* were obtained from type materials, already deposited in the collection of the research group Biodiversidad y Ecología Acuática of the University of Seville (BECA).

2.2.2 Phylogeny reconstructions

The new sequences were compared with homologous sequences from *Thouarella* species obtained from GenBank. The final dataset contained 64 in-group taxa and one outgroup taxon, the primnoid *Callozostron acanthodes* Bayer, 1996. GenBank sequence accession numbers are listed in the Supplementary File (Table S1). The set of new sequences obtained in this study (*MutS*, *Cox1,* and *28S*) and those available from GenBank were aligned using MUSCLE, implemented in MEGA7 (Kumar *et al.* 2016). The alignments for the *MutS*, *Cox1,* and *28S* and a concatenated (*MutS*+*Cox1*+*28S*) datasets include 65, 63, 44, and 65 specimens, respectively. Excepting for *T. grasshoffi* only

samples that yielded information for at least two loci were used for the concatenated phylogenetic analysis. Previous works have shown that a barcode that combines mitochondrial and nuclear genes allows us to distinguish molecular operational taxonomic units, in agreement with 70–83% of morphospecies identifications across a wide taxonomic range of octocorals (McFadden *et al.* 2011; Baco and Cairns 2012; McFadden *et al.* 2014a; McFadden *et al.* 2014b).

For each gene, as well as based on the concatenated dataset, a phylogenetic inference was obtained applying Bayesian inference (BI) methods, carried out in MrBayes 3.2.7 program using the mixed model (lset nst=mixed), which performs Markov chain sampling over the space of all possible reversible substitution models, by grouping the six rates in various combinations (Ronquist and Huelsenbeck 2003). The Bayesian analyses were performed in the CIPRES Science Gateway (Miller *et al.* 2010). Bayesian inference posterior probabilities (PP) were estimated using the Metropolis coupled Markov chain Monte Carlo algorithm (MCMC), running four chains for 20×10^6 generations were performed, with trees sampled every 10,000 generations, and verifying their convergence in Tracer v1.5 (Rambaut *et al.* 2018). Convergence was obtained when effective sample sizes (ESS) was >200. The initial 20% of sampled trees were discarded as the burn-in and the support values determined by posterior probabilities. The results from different runs were combined, and a 50% majority rule consensus was obtained collapsing nodes with PP < 0.5.

2.2.3 Molecular species delimitation

Two independent species delimitation approaches were used to determine putative molecular species (or Molecular Operational Taxonomic Unit) in our dataset: the Automatic Barcoding Gap Discovery (ABGD) (Puillandre *et al.* 2012), and the Poisson-Tree processes (PTP) (Zhang *et al.* 2013). For each approach, we employed the individual markers independently, as well as the concatenated

dataset. Even when the PTP approach is mainly intended for delimiting species in single-locus molecular phylogenies (Zhang *et al.* 2013), we also employed it with the three concatenated loci, because a combination of mitochondrial and nuclear genes has been proposed as a barcode in octocorals (McFadden *et al.* 2011; McFadden *et al.* 2014a; McFadden *et al.* 2014b).

The ABDG automatic procedure sorts the sequences into hypothetical species based on the barcode gap, which can be observed whenever the divergence among organisms belonging to the same species is smaller than divergence among organisms from different species (Puillandre *et al.* 2012). In the present work, the ABDG approach was used to determine groups of putative species based on pairwise genetic distances. Each dataset was imported in MEGA 6.0 (Kumar *et al.* 2016), and matrices of pairwise genetic distances were computed using the p-distance, the Kimura 2-parameter (K2P), and the Jukes-Cantor (JC69) models. These matrices were further used as output files on the ABGD webpage (https://bioinfo.mnhn.fr/abi/public/abgd/abgdweb.html). A range of different settings was tested, showing no major differences in species delimitations hypotheses. Therefore, we set parameters as follows: P_{min} = 0.001, P_{max} = 0.1, Steps = 100, X = 1, and Nb bins = 20.

The PTP method uses the branch lengths to estimate the average expected substitution number per site between two branching events (Zhang *et al.* 2013). The method postulates that the number of substitutions between species is significantly higher than within species, with any individual substitution having a low probability of causing speciation (Zhang *et al.* 2013). The mean numbers of substitutions until speciation events and coalescent events are expected to follow exponential distributions, forming two independent Poisson processes on the tree (Zhang *et al.* 2013). We performed a bayesian PTP (bPTP) analyses on the PTP web server (http://species.h-its.org/ptp/), using the 50% majority-rule consensus topology resulting from BI analysis as an input file. We ran each bPTP analyses for 500,000 MCMC generations, with thinning value = 100, burn-

in = 0.20, and verifying their convergence (Zhang *et al.* 2013). Using independent and concatenated loci, the obtained results from different approaches (ABDG and PTP) were compared to obtain a more robust and conservative inference about species limits within *Thouarella*.

2.2.4 Morphological analyses

Permanent mounts were made for light microscopy observation, and fragments from different parts of the colonies were prepared for study by SEM employing the usual methodology described in the literature (Bayer and Stefani 1988). The colony and scale terminology used mainly follows (Bayer *et al.* 1983) and (Taylor *et al.* 2013). Scale size measurements and illustrations are from the holotypes. The type and additional materials examined for the new species were deposited in the Museu de Zoologia de Barcelona (MZB) and the collection of the research group Biodiversidad y Ecología Acuática of the University of Seville (BECA).

2.2.5 Integrative taxonomy

Here, we assume that species represent 'segments of metapopulation lineages' and that different properties or evidence lines are necessary to recognize them (De Queiroz 2005; De Queiroz 2007). Therefore, we use an integrative taxonomy based on molecular and morphological evidence. In particular, we focus first on the genetic evidence for delineating lineages using phylogenies, and species delimitation approaches based on the new molecular information obtained from several colonies recovered in the SO. After, we carefully look for potential distinctive morphological features on each lineage (see details above) confronted with the described morphology of species in the genus (with or without molecular information available). If presents, we will be able to propose new species.

2.2.6 Nomenclatural acts

This published work and the nomenclatural acts it contains have been registered in ZooBank, the online registration system for the ICZN. The ZooBank Life Science Identifiers (LSID) can be resolved, and the associated information viewed through any standard web browser by appending the LSID to the prefix "http://zoobank.org/". The LSID for this publication is urn:lsid:zoobank.org:pub:AFDA418C-CFD5-47B9-A6A6-FE5CA16FF965.

2.2.7 Abbreviations

BECA: Biodiversidad y Ecología Acuática; H: height; H:W, ratio height/width of a scale; IL: inner lateral scales; M: marginal scale; MZB: Museu de Zoologia de Barcelona; O: opercular scale; OL: outer lateral scales; SEM: Scanning Electron Microscopy; stn: sampling station; SM: submarginal scale; SO: Southern Ocean.

2.3 Results

2.3.1 Phylogenetic analysis and molecular species delimitation

The concatenated alignment was composed of 2447 characters, including 289 variable sites (Svar), of which 215 were parsimony informative (PI). Alignment lengths were 801 bp long for *mtMutS* (Svar = 89, PI = 76), 800 bp for *Cox1* (Svar = 49, PI = 44), and 846 bp for *28S* (Svar = 182, PI = 97). The single-gene trees obtained by BI are shown in Supplementary File; Figs. S1-S3). The gene trees show few local incongruences among the nuclear and the mitochondrial locus (Figs. S1-S3). The clearest example was observed in the sequences identified as *T. islai*, as well as two unnamed lineages. In the mitochondrial locus (*mtMutS* and *Cox1*), each of these three lineages was monophyletic (PP>0.95) and distinguishable from each other, while in the *28S* locus all the specimens are included in a polytomy (PP>0.95). Considering these minor discrepancies

among single gene tree topologies, we focus our results on the tree reconstructed using the concatenated dataset.

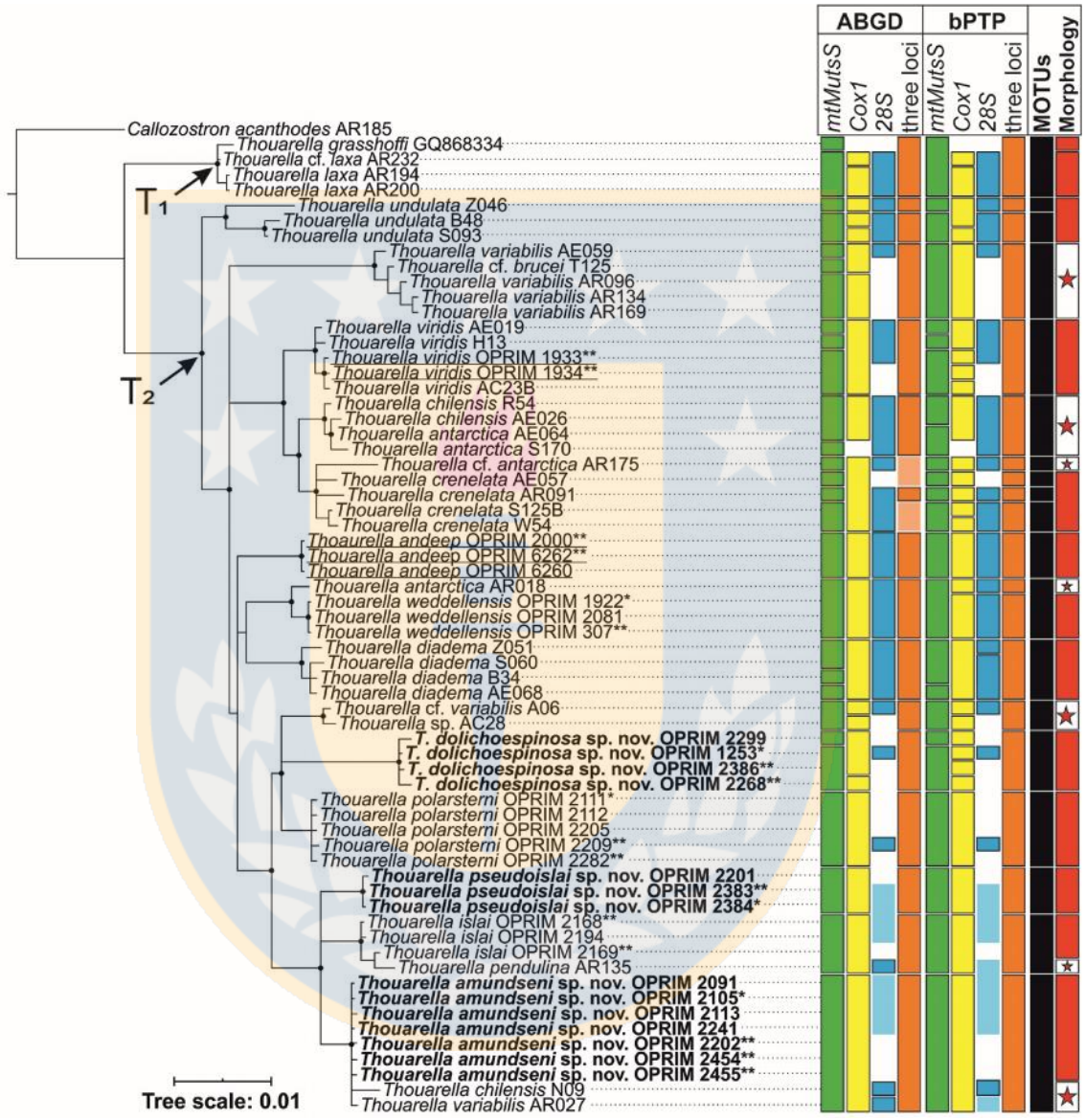

Figure 2.2. Bayesian inference based on a concatenated molecular dataset of mitochondrial (*MutS*+*Cox1*) and nuclear (*28S*) loci of the *Thouarella* genus (nodes with PP<0.5 were removed; black circles denote nodes with high support, PP>0.95). The results of the species delimitation approaches are also showed (toward the left side of the phylogeny), based on single and concatenated loci. The previously unnamed lineages described as new species in the present contribution are in bold. The stars in the column morphology indicate specimens needing to be re-revised to clarify whether they were misidentified or potentially represent cryptic taxa (see

details in the main text). Sequences displaying asterisk were taken from the holotype (*) and paratype (**). New sequences obtained from *T. andeep* and *T. viridis* materials are underlined. The abbreviations T1 and T2 denote the two main clades recovered within the genus *Thouarella* (see details in the main text).

The three-gene genealogy supported two major clades, within a monophyletic genus *Thouarella* (Cairns and Wirshing 2018), the first (informally named T_1) composed by *T. laxa* and *T. grasshoffi*, and the second (informally named T_2) composed by *T. undulata*, *T. andeep*, *T. antarctica*, *T. weddellensis*, *T. diadema*, *T. viridis*, *T. chilensis*, *T. crenelata*, *T. islai*, *T. polarsteni*, *T.* cf. *brucei*, *T. pendulina*, *T. variabilis*, and three lineages of *Thouarella* that cannot be associated with any species described so far (Fig. 2.2). It is also important to highlight that most species from which more than one specimen was sequenced and the three unnamed lineages, are monophyletic (PP>0.95). However, materials attributed to *T. antarctica*, *T. chilensis*, and *T. variabilis* produce polyphyletic results (Fig. 2.2), as already demonstrated by previous authors (Cairns and Wirshing 2018; Núñez-Flores *et al.* 2020). In the previous cases, we cannot conclude which of the different sequences identified as to given species is the closest one to the name-bearer and then truly attributable to that species. Detailed morphologic examination of these materials should be carried out and compared to their respective type materials to search for possible morphological discrepancies, which finally allow us to test whether exist a hidden diversity under similar morphological species.

Among the clade T_2, the most basal taxon is *T. undulata*, which is the sister group of the remaining species in the clade (Fig. 2.2). *Thouarella andeep, T. weddellensis, T. diadema*, *T. viridis, T. crenelata,* and some of the sequences assigned to *T. chilensis* and *T. antarctica*, are included in a poorly resolved group (polytomies; Fig. 2.2). The last clade is sister to a cluster with high nodal support values (PP>0.95), which grouped *T. polarsteni*, *T. islai, T.* cf. *brucei*, *T. pendulina*, some sequences assigned to *T. chilensis,* and *T. variabilis*, as well as

three separate *Thouarella* lineages collected across the Eastern Weddell Sea, which did not resemble any nominal morphological species. Among the three undescribed lineages, one of them appears to be quite divergent compared with the available sequences due to the long branch defining its clade, while the other two are closely allied with *T. islai, T. pendulina,* and some sequences previously assigned to *T. chilensis* and *T. variabilis* (Fig. 2.2).

The single and multi-locus species delimitation results from bPTP and ABGD approaches are summarized in Fig. 2.2 and corresponding output files generated from these analyses are reported in Supplementary File (Figs. S4-S11). These results were somewhat incongruent, but when taken conservatively, were useful to delineate putative species limits. The ABGD method allows for recognizing 28, 21, 18, and 17 putative species based on the *mtMutS*, *Cox1*, *28S,* and concatenated datasets, respectively (Figs. S8-S11). On the other hand, the bPTP approach allows for the recognition of 25, 30, 19, and 20 putative species based on the *mtMutS*, *Cox1*, *28S,* and concatenated datasets, respectively (Figs. S4-S7). The mean support value across bPTP recognized entities, under the concatenated dataset, was moderate (mean of 0.69) ranging from 1 (*Thouarella undulata* Z046) to 0.42 (cluster *Thouarella diadema* AE068*, Thouarella diadema* B34*, Thouarella diadema* S060*, Thouarella diadema* Z051) (Fig. S7). In general, using the concatenated dataset allows detecting a lower number of MOTUs, therefore providing a more conservative species delimitation. Based on the combined results provided by the ABGD and bPTP approaches, we were able to recognize at least 19 MOTUs within *Thouarella* (Fig. 2.2).

The cluster of *T. laxa* and *T. grasshoffi* predominantly indicated a single MOTU. However, it must be noted that the ABGD results on the *mtMutS* locus (the only available from *T. grasshoffi*) both taxa are differentiated (Fig. S8). In the case of *T. undulata*, while the taxon (as currently recognized) is monophyletic, in six of the eight species delimitation analyses (hereafter 6/8

SDA) was suggested it represents two closely allied lineages. Whether these sequences represent two sibling species and not a single species, as currently recognized, deserves further scrutiny, which is out of this contribution's scope. The three sequences of *T. andeep* likely represent a single MOTU, as indicated by the SDA. The three sequences of *T. weddellensis* form a monophyletic clade (Fig. 2.2), which is sister to a single sequence identified as *T. antarctica* (AR018). This cluster (*T. weddellensis* cluster plus *T. antarctica* AR018) was recovered in 5/8 SDA as a single MOTU. *Thouarella antarctica* and *T. weddellensis* are quite different from a morphological perspective (Taylor *et al.* 2013; Núñez-Flores *et al.* 2020). Considering the "polyphyletic" distribution of the sequences assigned to *T. antarctica*, a reevaluation of the colony from which the molecular data (AR018) was obtained will be necessary to clarify whether they should be considered to be *T. weddellensis*, or not. As in 5/8 SDA all the specimens of *T. weddellensis* represents a single MOTU, we thought it as a putative species.

The four sequences of *T. diadema* form a monophyletic and well supported (PP>0.95) clade (Fig. 2.2). In 5/8 SDA, they represent a single MOTU, while finer subdivisions are possible but inconsistent among them. Four sequences from *T. variabilis* (AE059, AR096, AR134, AR169) plus one sequence of *T.* cf. *brucei* represent a well-supported (PP>0.95) monophyletic clade. In 4/8 SDA they represent a single MOTU. However, whether this MOTU represents the species *T. variabilis* or *T.* cf. *brucei* is challenging to assess. The five sequences of *T. viridis* form a well-supported (PP>0.95) monophyletic clade (Fig. 2.2). They appear to represent a single MOTU, as recovered in 5/8 SDA, while finer subdivisions are less likely.

The monophyletic and well-supported (PP>0.95) clade grouping sequences of *T. chilensis* (R54 and AE026) and *T. antarctica* (AE064 and S170B) mainly represent a single MOTU (as recovered in 6/8 SDA). The four sequences of *T. crenelata* plus a single sequence of *T.* cf. *antarctica* (AR175) form a well-

supported (PP>0.95) monophyletic clade. The results of the SDA indicate that the last clade could represent one to five MOTUs. The congruent limits among them allow us to recognize four MOTUs, one representing *T.* cf. *antarctica* (AR175) and three among the sequences attributable to *T. crenelata* (Fig. 2.2).

The four sequences of *T. polarsterni* form a clade with moderate support (PP=0.85), which appears to represent a single MOTU (8/8 SDA). Two sequences regarded as *T.* cf. *variabilis* (A06) and *Thouarella* sp. A (AC28B) form a well-supported clade (PP>0.95), and in most (6/8) of the SDA they represent a single MOTU. As previously mentioned, we cannot clarify whether this MOTU represents *T. variabilis* or a still-unnamed new taxon. The sequences OPRIM-2299, OPRIM-2268, OPRIM-2386, and OPRIM-1253 are included in a clade with high support (PP>0.95). This cluster indicates the existence of one to four MOTUs. However, the limits among these are not congruent, and therefore for the sake of simplicity, we conservatively regarded them as a single MOTU (Fig. 2.2) until more sequences of the *28S* locus from these or additional specimens will be recovered (see also discussion part of this taxon). The latter potentially unnamed lineage from the Southern Ocean is more closely related to *T. polarsterni* and the clade composed by *T.* cf. *variabilis* (A06) and *Thouarella* sp. A (AC28B) than with any other *Thouarella* species included in the presented phylogeny (Fig. 2.2).

The sequences OPRIM-2201, OPRIM-2383, and OPRIM-2384 (from the east of the Weddell Sea, Southern Ocean) were included in a well-supported clade (PP>0.95), and in most (6/8) of SDA, they represent a single and potentially unnamed MOTU. Three sequences of *T. islai* plus one sequence attributed to *T. pendulina* form a well-supported clade (PP>0.95), which according to the 6/8 SDA likely represents a single MOTU. However, it must be noted that *T. islai* and the sequence regarded as *T. pendulina* are distinguishable by differences pairs bases in the *28S* locus as well as morphological features (Núñez-Flores *et al.* 2020). Seven sequences of a potentially unnamed *Thouarella* species

(OPRIMs 2091, 2105, 2113, 2202, 2241, 2254, 2255) plus one sequence of *T. chilensis* (N09) and *T. variabilis* (AR027) form a well-supported clade (PP>0.95), and in most of the SDA (6/8) they represent a single MOTU. However, it is possible to note that based on the 28S locus, *T. chilensis* (N09) and *T. variabilis* (AR027) could differ from those listed above.

In summary, our phylogenetic and species delimitation results reveal three distinct *Thouarella* lineages recovered in the Southern Ocean. After a detailed morphological comparison to previously named species, it was possible to recognize that they do not match any described nominal species in the genus. Consequently, in the next section, we provide formal descriptions of these new taxa.

2.3.2 Taxonomy

Order **Alcyonacea** Lamouroux, 1812

Suborder **Calcaxonia** Grasshoff, 1999

Family **Primnoidae** Milne-Edwards, 1857

Genus ***Thouarella*** Gray, 1870

Included species. *Thouarella antarctica* (Valenciennes, 1846) (type species), *T. hilgendorfi* (Studer, 1878), *T. variabilis* Wright & Studer, 1889, *T. brevispinosa* Wright & Studer, 1889, *T. affinis* Wright & Studer, 1889, *T. koellikeri* Wright & Studer, 1889, *T. moseleyi* Wright & Studer, 1889, *T. regularis* (Wright & Studer, 1889), *T. laxa* Versluys, 1906, *T. tydemani* Versluys, 1906, *T. brucei* Thomson & Richie, 1906, *T. striata* Kükenthal, 1907, *T. crenelata* Kükenthal, 1907, *T. clavata* Kükenthal, 1908, *T. pendulina* (Roule, 1908), *T. chilensis* Kükenthal, 1908, *T. coronata* Kinoshita, 1908, *T. parva* Kinoshita, 1908, *T. biserialis* (Nutting, 1908), *T. hicksoni* Thomson, 1911, *T. dispersa* Kükenthal, 1912, *T. grandiflora* Kükenthal, 1912, *T. bipinnata* Cairns, 2006, *T. grasshoffi* Cairns, 2006, *T. diadema* (Cairns, 2006), *T. viridis* Zapata-Guardiola & López-González, 2010a, *T. minuta* Zapata-Guardiola & López-González, 2010a, *T. andeep*

Zapata-Guardiola & López-González, 2010a, *T. undulata* (Zapata-Guardiola & López-González, 2010b), *T. cristata* Cairns, 2011, *T. trilineata* Cairns, 2011, *T. vitjaz* Zapata-Guardiola & López-González, 2012, *T. parachilensis* Taylor, Cairns, Agnew & Rogers, 2013, *T. taylorae* Cairns, Stone, Moon & Lee, 2018, *T. porcupinensis* Altuna & López-González, 2019, *T. islai* Nuñez-Flores, Gomez-Uchida & López-González, 2019, *T. weddellensis* Nuñez-Flores, Gomez-Uchida & López-González, 2019, *T. polarsterni* Nuñez-Flores, Gomez-Uchida & López-González, 2019, *Thouarella amundseni* sp. nov., *Thouarella dolichoespinosa* sp. nov., and *Thouarella pseudoislai* sp. nov.

Thouarella amundseni, sp. nov.

(Figs. 2.3–2.5)

***Holotype*.** MZB 2020-0643, **Antarctica**, Eastern Weddell Sea; 76° 19.33' S, 29° 8.44' W, collected 08.i.2014, *Polarstern* cruise ANT XXIX/9, stn. 053-1, 261 m depth.

***Paratypes*.** MZB 2020-0655 and MZB 2020-0656, **Antarctica**, with the same sampling data as the holotype. MZB 2020-0649, **Antarctica**, Eastern Weddell Sea; 76° 16.47' S, 29° 05.92' W, collected 21.i.2016, *Polarstern* cruise ANT XXXI/2, stn. 057-6, 293 m depth.

***Additional examined materials*.** MZB 2020-0650, **Antarctica**, Eastern Weddell SeaEastern Weddell Sea; 77° 0.93' S, 33° 41.71' W, collected 13.i.2014, *Polarstern* cruise ANT XXIX/9, stn. 084-1, 435 m depth. MZB 2020-0647, **Antarctica**, Eastern Weddell Sea; 77° 6.08' S, 36° 32.76' W, collected 10.i.2014, *Polarstern* cruise ANT XXIX/9, stn. 067-1, 1110 m depth. BECA-OPRIM-2091, **Antarctica**, Eastern Weddell Sea; 77° 0.28' S, 34° 9.34' W, collected 11.i. 2014, *Polarstern* cruise ANT XXIX/9, stn. 073-1, 570 m depth.

Diagnosis. Colony bottlebrush with flared, short (1–1.9 mm), isolated and moderately abundant (18–24 per cm) polyps on the branchlets but higher polyp density (up to 35 per cm) toward their apical section, with 3–4 scales in abaxial

rows, 3 scales in OL rows, and 2–3 scales in IL rows and 2 scales in the adaxial rows. Submarginal scales with a distal spine; marginal scales with a long spine which can reach up to 82% of the scale height; opercular scales mainly triangular in shape, some with a well-developed distal spine (spine longer than the proximal area) and other isosceles with a V-like keel over the distal area. Opercular scales around 50% smaller than the marginals. Accessory opercular scales present.

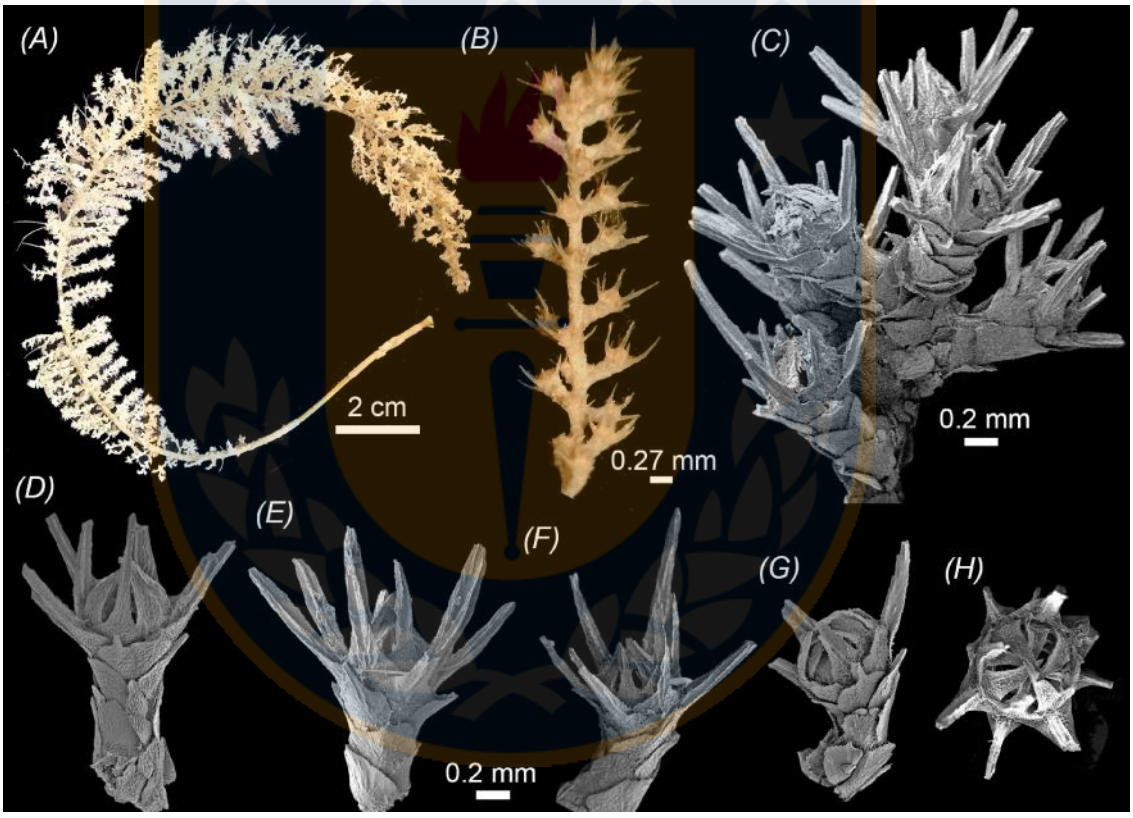

Figure 2.3. *Thouarella amundseni* sp. nov., holotype (MZB 2020-0643). (A), Whole colony; (B–C), details of the general polyp arrangement, including the densely packed polyps at the apical portion of some branches (C); polyps in adaxial (D), abaxial (E), lateral (F, G), and opercular (H) views. Note that D–H are on the same scale.

Description of the holotype. Colony bottlebrush, 26 cm height, and 3 cm width (Fig. 2.3A). Holdfast circular, 1.29 mm in diameter. Main stem simple, 1.22 mm

in diameter, flexible, golden in color. Branchlets originate in all directions from the main stem, with ramifications up to four- orders. First-order branchlets up to 1.4 cm in length. Polyps flared, isolated on branches and branchlets, moderately abundant, 18–24 per cm (mean 20 per cm). However, toward colony's apical region the of polyps density increases (up to 35 per cm) (Fig. 2.3B, C). Polyps short, 0.97–1.90 mm in length (mean 1.4 mm, including the long marginal scales), and curved inward, making an angle of ~57° with the main axis (Fig. 2.3B, C). Body scales arranged in five longitudinal rows with 3–4 scales in abaxial rows, 3 scales in OL rows, and 2–3 scales in IL rows and 2 scales in the adaxial rows (Fig. 2.3D, G).

Operculum relatively high (Fig. 2.3D–H), with eight scales. The opercular scales display two primary morphologies: triangle-shaped with rhomboidal proximal area, dented, irregular or arrow shape proximal edges, and very narrow distal edges with single to multikeels (Fig. 2.4A); and isosceles-shaped with laterally serrated distal edges with multikeels, and irregular to arrow shape proximal edges (Fig. 2.4B). In addition, smaller accessory opercular scales present (Fig. 2.4C), triangle-shaped to nearly tongue-shape scales with straight to irregular proximal edges and a laterally serrated wide spine with a keel in V-shape in their distal surface (Fig. 2.4C). Opercular scales ~45–50% smaller than marginal ones, 0.340–0.595 mm high (mean 0.440 mm), 0.130–0.315 mm wide (mean 0.205 mm), with a mean H:W of 2.15. Opercular accessory scales even smaller, 0.260–0.340 mm high (mean 0.300 mm), 0.080–0.170 mm wide (mean 0.130 mm), with a mean H:W of 2.4. Proximal 30–50% of opercular scales inner surface covered by small tubercles; outer surface longitudinally concave and smooth, with little and sparse tubercles arranged across proximal area (Fig. 2.4A–C).

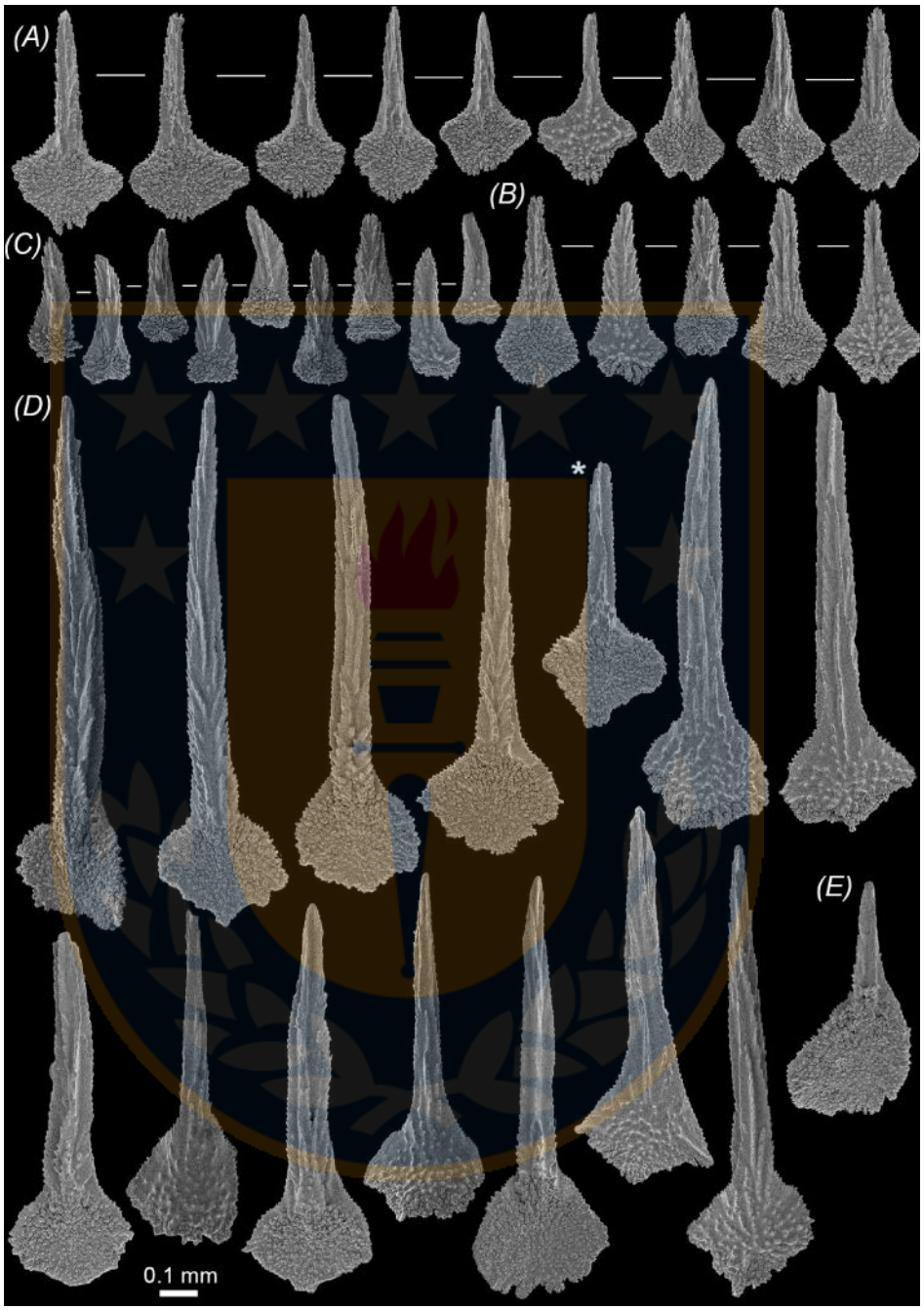

Figure 2.4. *Thouarella amundseni* sp. nov., holotype (MZB 2020-0643). (A), triangle-shaped opercular scales; (B), isosceles-shaped opercular scales; (C), accessory opercular scales; (D), marginal scales (asterisk in D denoted the adaxial marginal scale); (E), submarginal scales showing reduced spine.

Body scales differentiated in marginal, sub-marginal, and body-wall. Marginal scales (Fig. 2.4D), eight in number, predominantly with elongated distal spines and channeled keels in distal inner surface. Well-developed distal spine constitutes up to 75–82% of the scale height and has multikeels, especially serrated on their proximal inner section. Marginal scales size of 0.600–1.450 mm high (mean 0.950 mm), 0.250–0.385 mm wide (mean 0.315 mm), with a mean H:W of 3.1. Proximal area of marginal scales of variable shape, from rhomboid, with a “V” shaped proximal edges, to subcircular with irregular proximal edges (Fig. 2.4D). Lateral edge of marginal scales irregularly dentate to finely serrated. Adaxial marginal scales reduced in size, more diamond-shape in their proximal area, and with a shorter distal spine (Fig. 2.4D*). In proximal inner surface, 30–70% of the scale’s height (depending on the distal spine longitude) covered by tubercles. In medium to large size marginal scales, the proximal area of outer surface bears a radial-like granules arrangement (i.e., granules radiating from the center of the proximal area), but their proximal edge has small tubercles resembling those of the inner surface (Fig. 2.4D). Submarginal scales mainly subtriangular, with a wide proximal area and a distal spine much less developed than those of marginal scales (Fig. 2.4E), 0.250–0.600 mm high (mean 0.420 mm),- 0.220–0.340 mm wide (mean 0.290 mm), with a mean H:W of 1.6.

The body wall scales include various sub-circular, rectangular, and subtriangular shapes (Fig. 2.5A). Wider than high, 0.150–0.400 mm high (mean 0.290 µm), 0.200–0.500 mm wide (mean 0.345 mm), with a mean H:W of 0.9. Inner surface tuberculate, while outer surface bears sparse granules (Fig. 2.5A). Some portions of their lateral edges could display fine serrations. Coenenchymal scales irregular oval to elliptic in shape, slightly smaller than body wall scales, wider than high, 0.120–0.270 mm high (mean 0.230 mm), 0.300–0.500 mm wide (mean 0.400 mm), with a mean H:W of 0.6 (Fig. 2.5B). Inner surface covered with complex tubercles closely arranged and outer surface by abundant

granulates, which could radiate from the scale center (Fig. 2.5B). Some portions of their lateral edges could bear various degrees of fine serrations.

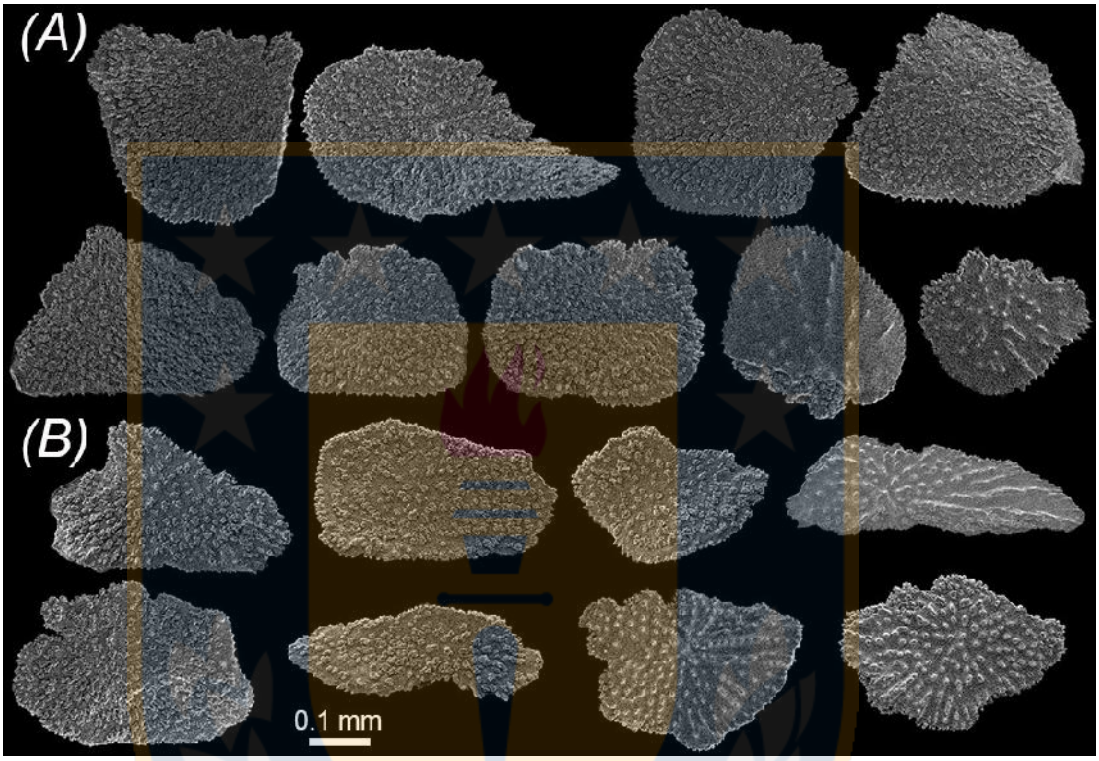

Figure 2.5. *Thouarella amundseni* sp. nov., holotype (MZB 2020-0643). (A), body-wall scales; (B), coenenchymal scales.

***Variability*.** The paratypes and the additional examined materials generally agree in the distribution, shape, and size of the scales from polyps and coenenchyme. However, the higher polyp density on the colony apical region appears to be variable, as several of the revised materials did not bear this feature. The larger examined colony reaches 29 cm in height.

Geographic and bathymetric distribution. Eastern Weddell Sea (near to Coats Land), Southern Ocean (Fig. 2.1), in depths between 261–1110 meters.

Nomenclatural statement. A LSID number was obtained for the new species: urn:lsid:zoobank.org:act:8B4BE5B9-B43F-42C1-ADE7-9B12A3C5507A

Etymology. This species is named after the Norwegian explorer Roald Amundsen, the first man to reach the South Pole in 1911.

Thouarella dolichoespinosa, sp. nov.

(Figs. 2.6–2.8)

***Holotype*.** MZB 2020-0642, **Antarctica**, Eastern Weddell Sea; 71° 11.30' S, 12° 15.40' W, collected 04.ii.2000, *Polarstern* cruise ANT XVII/3, stn. 085-1, 318 m depth.

***Paratype*.** MZB 2020-0652, **Antarctica**, Eastern Weddell Sea; 74° 14.65' S, 37° 42.35' W, collected 01.ii.2014, *Polarstern* cruise ANT XXIX/9, stn. 233-1, 833 m depth. MZB 2020-0654, **Antarctica**, Eastern Weddell Sea; 74° 42.19' S, 29° 48.59' W, collected 11.ii.2014, *Polarstern* cruise ANT XXIX/9, stn. 325-1, 428 m depth.

***Additional examined materials*.** BECA-OPRIM-2299, **Antarctica**, Eastern Weddell Sea; 76° 11.16' S, 30° 02.90' W, collected 21.i.2016, *Polarstern* cruise ANT XXXI/2, stn. 059-2, 392 m depth.

Diagnosis. Colony bottlebrush with flared and short (1.1–1.9 mm) polyps widely spaced on the branchlets in a roughly alternate arrangement; low polyp density (6–14 polyps/cm); with 3–4 scales in abaxial rows, 3 scales in OL rows, and 2–3 scales in IL rows and 2 adaxial rows; opercular scales of isosceles-triangle shape with pointed distal ends; marginal scales long, up to 2.3 mm, with a well-developed distal spinose projection which can represent up to 85% the scale height; adaxial marginal scales with significantly reduced spine and pointed end.

Description of the holotype. Colony bottlebrush, 24 cm height, and 5 cm width (Fig. 2.6A). Holdfast absent. Main stem simple, circular, 2.3 mm in diameter proximally, flexible, golden in color, with numerous closely spaced branchlets that originate on all sides of the main stem. Most of these branchlets (first-order) subdivided up to a third-order ramification. First-order branch simple with up to 2.5 cm in length (Fig. 2.6A). Polyps relatively scarce (8–12 polyps/cm), isolated

on branches and branchlets, widely spaced on branchlets in a roughly alternate arrangement in intervals of 0.3–1.4 mm (n=20), without polyps on the main stem (Fig. 2.6B–D). Polyps short, 1.1–1.9 mm long (mean 1.4 mm, including long marginal spines), and inclined 32–67° (mean 51°) with respect to the branches/branchlets. Body covered by 8 longitudinal rows of scales, decreasing in number to 5 at the polyp base, with 3–4 scales (excluding opercular scales) in abaxial rows, 3 scales in OL rows, 2–3 scales in IL rows, and 2 scales in adaxial rows (Fig. 2.6E–I).

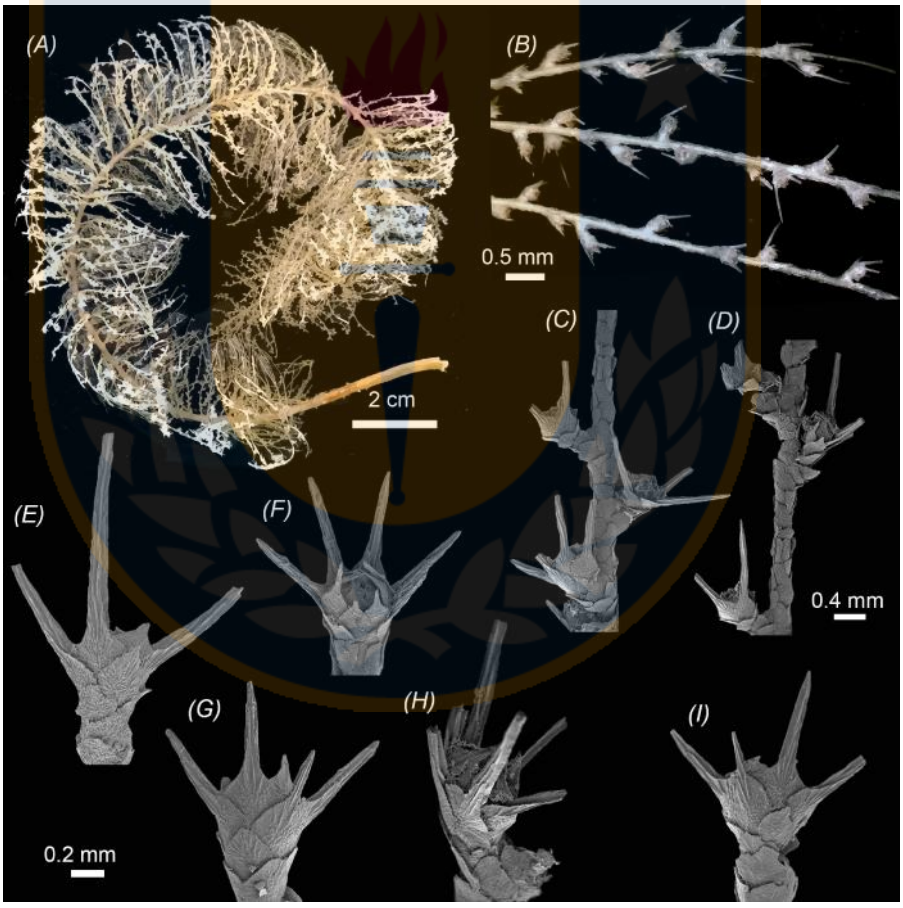

Figure 2.6. *Thouarella dolichoespinosa* sp. nov., holotype (MZB 2020-0642). (A), Whole colony; (B–D), details of the general polyp arrangement on branchets; polyps in adaxial (F), abaxial (E, G, I) and inner lateral (H) views. Note that C–D and E–I are on the same scale.

Opercular scales, mainly isosceles triangle shaped with pointed distal ends and broad proximal area (Fig. 2.7A, B). Opercular scales ~70% smaller than marginal ones, 0.210–0.440 mm high (mean 0.340 mm), 0.120–0.340 mm wide (mean 0.200 mm), with a mean H:W of 1.8 (Fig. 2.7A, B). Proximal edges irregular. Proximal outer surface with very few granules; inner surface tuberculate (Fig. 2.7A). Distal spine not keeled with lateral edges finely serrate.

Marginal scales predominantly diamond-shaped, with an elongated distal spine and channeled-keels along the distal inner surface, 0.300–1.750 mm high (mean 1.050 mm), 0.220–0.360 mm wide (mean 0.305 mm), with a mean H:W of 3.6 (Fig. 2.7C–E). The well-developed distal spine might represent 60–84 % of scale height, but spine length somewhat variable, OL scales with larger spines, reduced in IL scales (Figs. 2.7D and 2.6F), while adaxial scales with reduced spine (Fig. 2.7E). Basal part range 20–60% of scales height (depending on distal spine length). Proximal inner surface with complex tubercles; lateral edges mostly finely serrated (Fig. 2.7C–E); outer surface of the medium to large size scales with scarce tubercles on the proximal basal part, radial from the proximal area. Outer surface of adaxial scales with faint radial ridges (Fig. 2.7E).

Body wall scales in a variety of sub-circular to ovate shapes, slightly wider than high, 0.170–0.420 mm wide (mean 0.283 mm), 0.145–0.330 mm high (mean 0.255 mm), with a mean H:W of 0.9 (Fig. 2.8A). Scales with a moderately tuberculate inner surface and very scarce granules on the outer surface. Some portions of the lateral edges finely serrated. Coenenchymal scales irregularly oval to quadrangular in shape, wider than high and larger than the body wall scales, 0.250–0.580 mm wide (mean 0.41 mm), 0.250–0.310 mm high (mean 0.265 mm), with a mean H:W of 0.7 (Fig. 2.8B). All inner surfaces with complex tubercles; outer surface with scarce pointed granules. Lateral edges finely serrated.

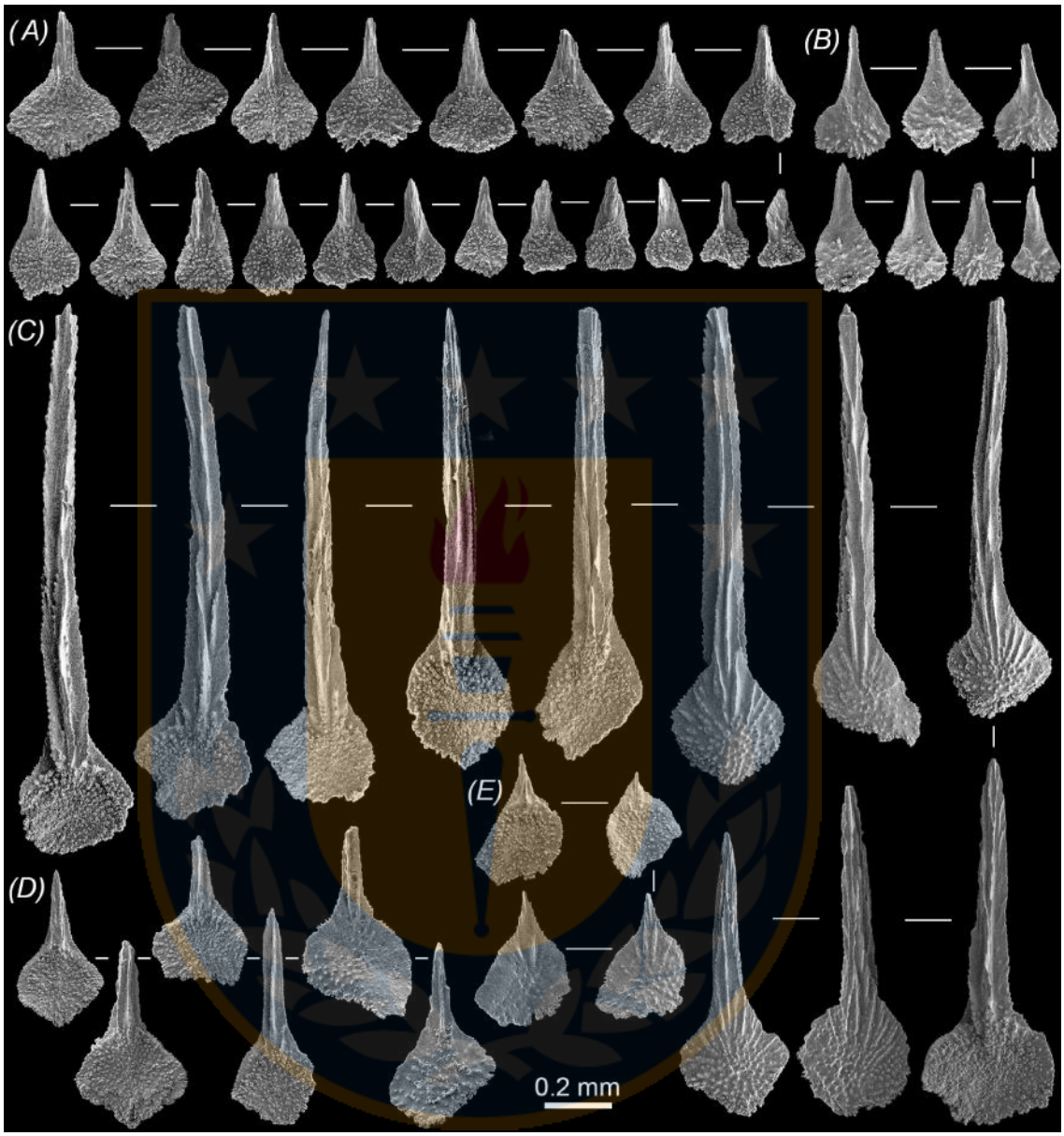

Figure 2.7. *Thouarella dolichoespinosa* sp. nov., holotype (MZB 2020-0642). Opercular scales in inner (A) and outer (B) surface view; (C), marginal scales; (D), inner lateral marginal scales showing reduced spine; (E), adaxial marginal scales.

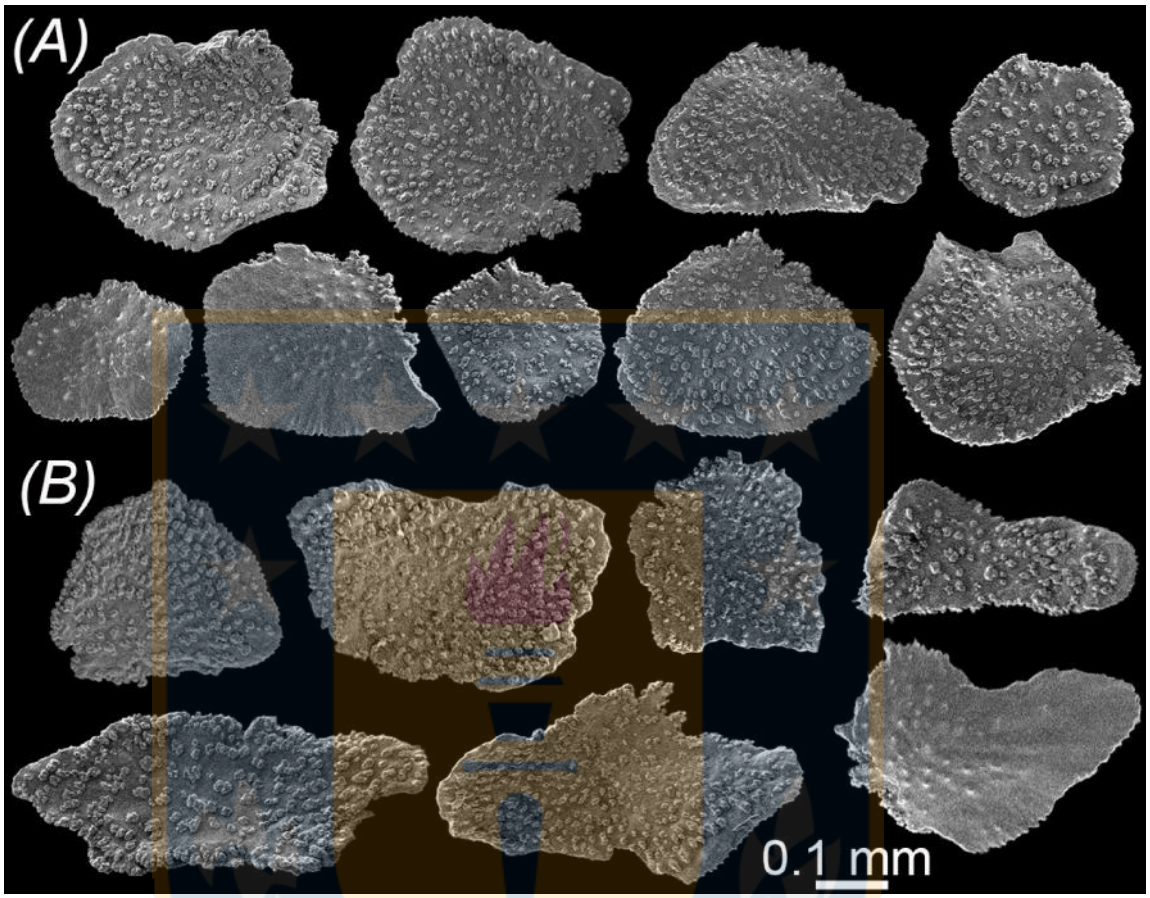

Figure 2.8. *Thouarella dolichoespinosa* sp. nov., holotype (MZB 2020-0642). (A), body-wall scales; (B), coenenchymal scales.

Variability. The paratypes and other examined materials, in general, agree in the distribution, shape, and size of the sclerites from polyps and coenenchyme. However, in the paratypes up to 6–14 polyps per cm have been observed, besides the marginal scales with elongated distal spine could reach up 2.3 to mm high.

Geographic and bathymetric distribution. Eastern Weddell Sea (Fig. 2.1), Antarctica, Southern Ocean, in depths between 318–833 meters.

Nomenclatural statement. A LSID number was obtained for the new species: urn:lsid:zoobank.org:act:AAA47564-5B5A-4DC5-AD06-6D5566B2F41B

Etymology. The words combination, *dolicho* (Greek), long, and *espinosa*, spine, refers to this taxon's long marginal spine.

Thouarella pseudoislai*,* sp. nov.

(Figs. 2.9–2.11)

***Holotype*.** MZB 2020-0641, **Antarctica**, north-eastern Weddell Sea; 70° 55.57' S, 10° 28.22' W, collected 16.ii.2014 aboard the *Polarstern* cruise ANT-XXIX/9 (PS82), stn. 349-1, 213 m depth.

Paratype. MZB 2020-0653, **Antarctica**, with the same sampling data as the holotype.

Additional examined material. BECA-OPRIM-2201, **Antarctica**, north-eastern Weddell Sea; 70° 53.45' S, 11° 08.20' W*,* collected 24.xii. 2015, aboard the *Polarstern* cruise ANT XXXI/2 (PS96), stn. 001-9, 314 m depth.

***Diagnosis*.** Colony bottlebrush-shaped with isolated, cylindrical and short polyps (<1.5 mm); polyp density 18–24 per cm; body scales arranged in eight longitudinal rows with 2–4 scales on abaxial rows, 2–3 scales in OL rows, 2–3 scales in IL rows, and 1–2 scales in adaxial rows. Marginal scales diamond-shaped with distally enlarged spines, representing up to 65% of their total length, with a mean H:W of 2.6. Submarginal scales with pointed distal ends.

Description of the holotype. Colony bottlebrush, without holdfast, of 22 cm height and 8.5 cm width (Fig. 2.9A). Main stem simple. Five first-order branches arise from the upper part of the main stem, up to 22 cm in length, disposed on a subparallel way. The branchlets (second-order branch) are usually subdivided, up to 13 cm in length, and the colony can reach a four-order ramification (Fig. 2.9A). Polyps slightly flared, predominantly isolated on branches and branchlets, but occasionally in pairs (Fig. 2.9B, C). Moderately abundant polyps, 19–23 polyps/cm (mean 21 polyps/cm). Polyps short, 0.64–1.68 mm in length (mean 1.2 mm, including the long marginal scales), and curved inward, making an angle of ~53° with the main axis (Fig. 2.9C). Body scales arranged in eight

longitudinal rows with 2–4 scales (excluding opercularars) on abaxial rows, 2–3 scales in OL rows, 2–3 scales in IL rows, and 1–2 scales in adaxial rows (Fig. 2.9D–I).

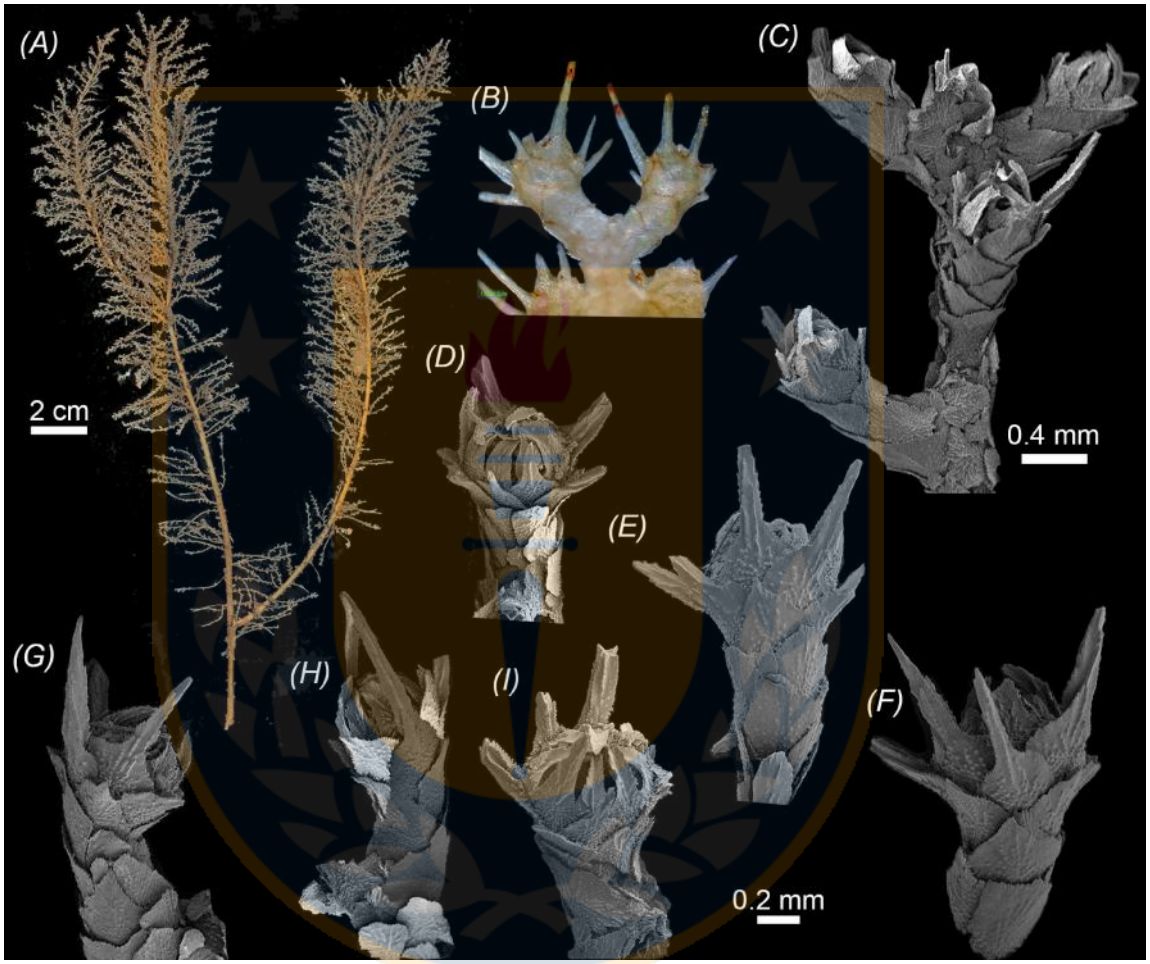

Figure 2.9. *Thouarella pseudoislai* sp. nov., holotype (MZB 2020-0641). (A), Whole colony; (B–C), details of the general polyp arrangement; polyps in adaxial (D), abaxial (E, F), outer lateral (G), and inner lateral (H, I) views. Note that D–I are on the same scale.

Operculum low (Fig. 2.9D, I), with eight scales, some triangle-shaped with rhomboidal to rounded proximal area and dented to rounded proximal edges, and narrow distal edges with single to multikeels (Fig. 2.10A); and others isosceles-shaped with wide distal edges (nearly tongue-shaped) without keels,

and serrate proximal edges (Fig. 2.10B). Opercular scales ~50% smaller than marginal ones, 0.190–0.535 mm high (mean 0.360 mm), 0.105–0.310 mm wide (mean 0.180 mm), with a mean H:W of 2 (Fig. 2.10A, B). Proximal 35–60% of the inner surface covered by small tubercles. Outer surface longitudinally concave and smooth distally, with tubercles sparsely radially arranged across proximal area (Fig. 2.10A, B).

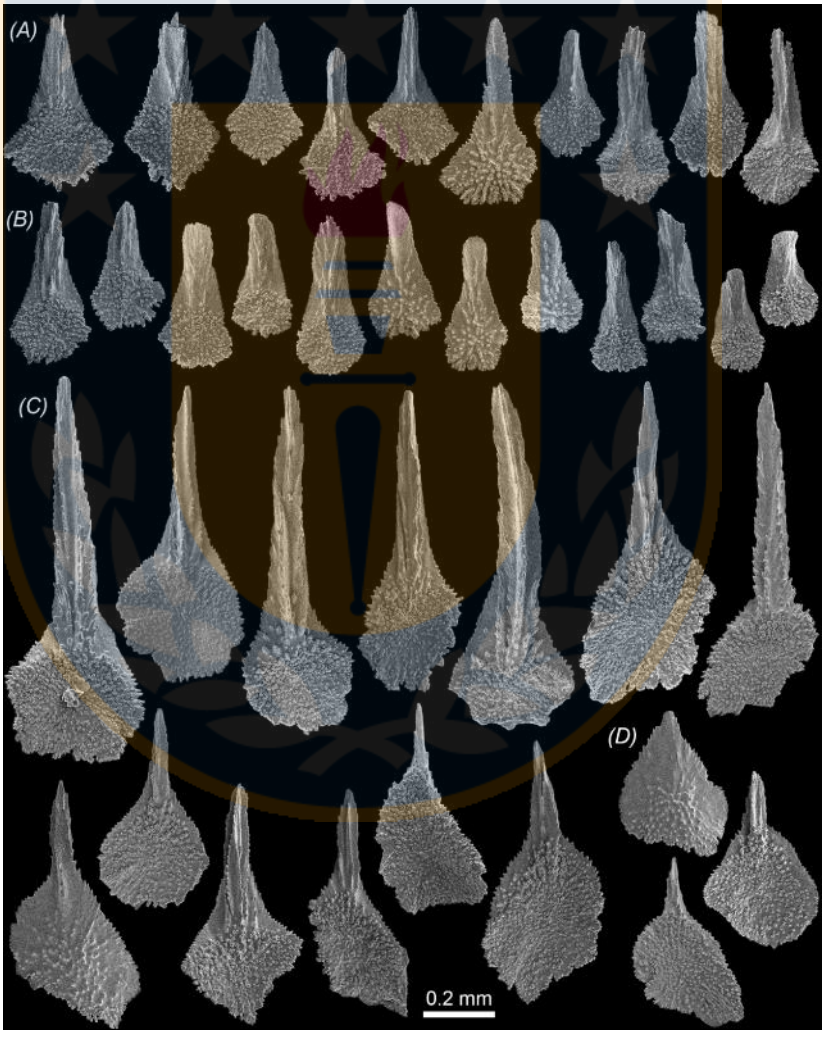

Figure 2.10. *Thouarella pseudoislai* sp. nov., holotype (MZB 2020-0641). (A), triangle-shaped opercular scales; (B), nearly tongue-shaped opercular scales; (C), marginal scales; (D), adaxial marginal scales with a reduced distal spine.

Body scales differentiated in marginal, sub-marginal, and body-wall. Eight marginal scales (Fig. 2.10C). The larger marginal scales have elongated distal spines and channeled keels in the distal inner surface, while the smaller have a reduced spine with channeled keels a reduced spine without keels, or pointed ends. Marginal scales of 0.275–1.160 mm high (mean 0.710 mm), 0.190–0.400 mm wide (mean 0.300 mm), with a mean H:W of 2.6. The well-developed distal spine constitutes up to 65% of the scale height, and serrated keels, especially on their proximal section. Proximal area of marginal scales variable in shape, from rhomboid with a “V” shaped proximal edges, to asymmetrically subtriangular (Fig. 2.10C). Distal edge of marginal scales irregularly dentate. Adaxial marginal scales reduced in size and more diamond-shape, with a pointed distal edge but with a shorter spine (Fig. 2.10D). Proximal inner surface completely covered by tubercles covering the 40–65% of scales height (depending on the distal spine longitude). Lateral edges, in general, finely serrate (Fig. 2.10C). Proximal area of the outer surface in medium to large-sized scales bears a radial-like granules arrangement (i.e., granules radiating from the center of the proximal area).

Submarginal scales variable in shape, mainly triangular, but diamond-like and pentagonal-like were observed (Fig. 2.11A). Despite their shape, conspicuously pointed in the distal edge, it could display between one to three points, 0.370–0.650 mm high (mean 0.475 mm), 0.240–0.650 mm wide (mean 0.375 mm), with a mean H:W of 1.3 (Fig. 2.11A). Some submarginal scales have simply to channeled keels on the inner surface. Lateral edges finely serrated. The body wall scales include a variety of sub-circular shapes, 0.190–0.600 mm high (mean 0.365 mm), 0.190–0.530 mm wide (mean 0.305 mm), with a mean H:W of 1.2 (Fig. 2.11B). Inner surface tuberculate, outer surface granular, while some portions of lateral edges could bear fine serrations.

The coenenchymal scales irregular oval to elliptic in shape and smaller than body wall scales, wider than high, 0.210–0.370 mm high (mean 0.285 mm),

0.330–0.626 mm wide (mean 0.440 mm), with a mean H:W of 0.7 (Fig. 2.11C). Inner surface with complex tubercles closely arranged and outer surface with granules which could irradiate from scale center. Some portions of their lateral edges could bear various degrees of coarse serrations.

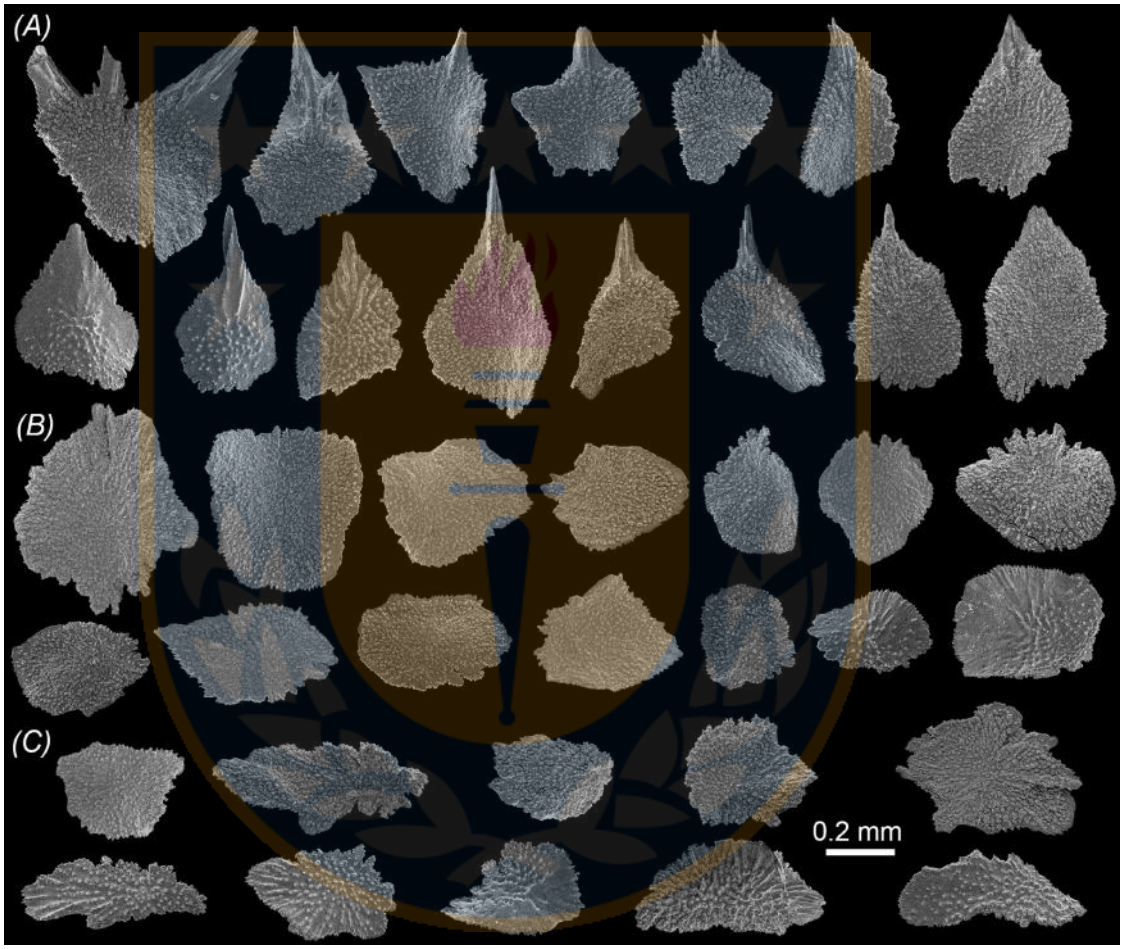

Figure 2.11. *Thouarella pseudoislai* sp. nov., holotype (MZB 2020-0641). (A), Submarginal scales; (B), body-wall scales; (C), coenenchymal scales.

***Variability*.** In the paratype and additional examined material, the colony shape is like that of the holotype. The polyp density varies from 18–24 polyps per cm. The shape, size, and arrangement of the opercular, marginal, body, and

coenenchymal scales also resemble the holotype. The submarginal scales have consistently pointed distal ends in all the examined colonies.

Geographic and bathymetric distribution. North-eastern Weddell Sea (Fig. 2.1), Antarctica, in depths between 213–314 meters.

Nomenclatural statement*.* A LSID number was obtained for the new species: urn:lsid:zoobank.org:act:77C0C18A-2B72-46A3-85D9-CD5D1F96D8CA

Etymology. The specific name, combining *pseudo* (Greek for false) and *islai*, refers to the new taxa's morphological similarity with other recently described, *T. islai*.

2.4 Discussion

2.4.1 Comparison of the new species with other congeners

Apart from the molecular differences mentioned above, the three new species here described can be differentiated from their closer congeners from a morphological perspective (Zapata-Guardiola and López-González 2010b; Taylor *et al.* 2013; Núñez-Flores *et al.* 2020). According to the species key in Taylor *et al.* (2013), the three new species previously described fall within "group one" by having isolated polyps. This same feature also allows us to include all the new described species in the subgenus *Thouarella* (*Thouarella*) (Cairns and Wirshing 2018). The three new species share several features as short polyp height (equal or less than 1.5 mm), fewer than five abaxial scales, and a prominent distal spine on the marginal scales. The presence of isolated polyps and a prominent distal spine on the marginal scales indicates close morphological similarities of the three new species (*T. pseudoislai*, *T. amundseni*, and *T. dolichoespinosa*), with *T. undulata*, *T. bayeri*, *T. diadema, T. islai* and *T. variabilis* (Cairns 2006; Zapata-Guardiola and López-González 2010b; Taylor *et al.* 2013; Núñez-Flores *et al.* 2020).

Unlike the previously mentioned species, *T. amundseni* (18–24 per cm), and *T. pseudoislai* (18–24 per cm) reach a higher density of polyps compared with *T. variabilis* (5–10 per cm), *T. bayeri* (9–12 per cm), *T. undulata* (10–11 per cm), and *T. dolichoespinosa* (6–14 per cm), being partially overlapping to *T. islai* (7–19 per cm) (Cairns 2006; Zapata-Guardiola and López-González 2010b; Taylor *et al.* 2013; Núñez-Flores *et al.* 2020). The three new species, *T. amundseni*, *T. pseudoislai* and *T. dolichoespinosa* have marginal scales with keels on their distal inner surfaces (keels absent in *T. diadema, T. bayeri* and *T. undulata*), and a narrow proximal area of marginal scales with variable forms from round to pentagonal shape (broad and rhomboidal in *T. undulata*, *T. bayeri*, *T. diadema, T. islai* and *T. variabilis* (Cairns 2006; Zapata-Guardiola and López-González 2010b; Taylor *et al.* 2013; Núñez-Flores *et al.* 2020)). Besides, the somewhat triangular opercular scales of *T. amundseni*, *T. pseduoislai,* and *T. dolichoespinosa* differs from the broad tongue-shape opercular scales of *T. diadema*, *T. undulata,* and *T. bayeri* (Cairns 2006; Zapata-Guardiola and López-González 2010b), and the narrow tongue-shape to triangular opercular scales of *T. islai* (Núñez-Flores *et al.* 2020). The new species are easily differentiated between them by the shape and relative size of their opercular and marginal scales and their polyp density and arrangement on branchlets (see details in Table 2.1).

Thouarella amundseni and *T. pseduoislai* have higher polyp density than *Thouarella dolichoespinosa*. Besides, the latter has polyps disposed of in a roughly alternate arrangement, unlike the formers (Table 2.1). *Thouarella amundseni* has broader marginal scales with larger distal spines and higher opercular scales with better developed distal spines than *T. pseduoislai* (Table 2.1). On the other hand, and as indicated by their name, *T. pseudoislai* indeed closely resembles *T. islai* (Núñez-Flores *et al.* 2020). The main difference between both is the consistently lacks of submarginal scales with pointed and spinose distal ends in the former (Núñez-Flores *et al.* 2020). Besides, *T.*

pseudoislai has longer marginal and submarginal scales and larger coenenchymal scales than *T. islai* (Núñez-Flores *et al.* 2020).

2.4.2 Species delimitation analyses

In the present work, we apply different species delimitation approaches (ABGD and bPTP) using three single loci (*MutS*, *Cox1,* and *28S*) to evaluate the existence of potentially undescribed primnoids within the speciose genus *Thouarella.* When only focus on the new set of molecular data obtained from broadly similar bottlebrush shaped colonies recovered from the Weddell, our species delimitation results consistently (and conservatively) support the existence of three previously unknown lineages (Fig. 2.2). At the same time, finer subdivisions among them were less sustained. The macro and microscopical morphological features found on the colonies of each of these lineages were consistent with the species delimitation results and allow us to formally describe three new species.

Moreover, regarding the results of the molecular species delimitation approaches, including all the available sequences of the genus *Thouarella*, we found a different number of putative species (Fig. 2.2). Depending on the method or loci chosen, different species delimitation hypotheses, recognizing from 17 to 30 putative species, can be proposed for the genus. Under both bPTP and ABGD approaches, a disparate number of putative species were recovered, with 19–30 and 17–28, respectively, depending on the loci chosen (Fig. 2.2). However, consistently using the concatenated loci allows us to detect a lower, and consequently more conservative, number of MOTUs. Yet, the findings of some incongruences among different methods and loci could suggest either a difference in the power to detect cryptic lineages across one or more of the approaches used here, but also that assumption of one or more of these methods could be violated (Carstens *et al.* 2013), or even the low number of informative phylogenetic characters in some loci. Despite this situation, it is clear

that inferences on species delimitation studies based on molecular data should be conservative and must be constructed upon the congruence between distinct approaches (Carstens *et al.* 2013).

To our knowledge, the only previous work using species delimitation methods on *Thouarella* and primnoids is those of Bogantes *et al.* (2020), who recognized at least 12 MOTUs (including some from the Ross Sea) within the genus using a single locus, the *MutS,* and the ABGD method. As these sequences were unidentified at the species level and only a single locus was available, we did not include it in our analyses. In any case, the actual number of *Thouarella* species is likely to be yet underestimated, especially in the Southern Ocean. For example, the polyphyletic arrangement of some taxa assigned to *T. antarctica*, *T. chilensis*, and *T. variabilis* (Cairns and Wirshing 2018; Núñez-Flores *et al.* 2020) may suggest the existence of cryptic species, sequences with undetected erroneous sequencer readings, or incorrect specimens' identifications due to closely or concordant morphological features (Núñez-Flores *et al.* 2020). Therefore, future studies combining molecular and morphological analyses will be necessary to elucidate the reasons behind these polyphyletic situations. Besides, even when our most conservative species delimitation results indicate at least 19 MOTUs in our dataset, only after the last issues will be resolved, the actual number of *Thouarella* species will be refined.

Given the unusually slow rates of mitochondrial gene evolution (Bilewitch and Degnan 2011), a combination of mitochondrial and nuclear loci have been considered informative and useful for octocoral taxonomy (McFadden *et al.* 2011). Our most conservative species delimitation results were obtained using three loci (*mtMutS*, *Cox1* and *28S*). Therefore, our findings complement previous ideas illustrating how combined mitochondrial and nuclear loci in species delimitation analysis may improve our ability to recover conservative boundaries in primnoids and likely other octocorals as well. Recent studies have identified multi-locus barcodes (including the *mtMutS*, *Cox*, and *28S*) capable of

distinguishing morphospecies of octocorals with a relatively high (70–83%) success (McFadden *et al.* 2011; Baco and Cairns 2012; McFadden *et al.* 2014a; McFadden *et al.* 2014b). In this sense, somewhat similar potential resolution limitations of combined mitochondrial and nuclear markers for octocorals species delimitation could be expected.

On the other hand, during the last decade, molecular tools for the taxonomic identification of organisms with conserved morphology have increased the recognized number of cryptic species in several invertebrate groups in the Southern Ocean (De Broyer *et al.* 2011; Halanych and Mahon 2018). Cryptic speciation appears to be a common and widespread feature in the Southern Ocean marine fauna (Halanych and Mahon 2018). Our species delimitation results might suggest, for the first time, the presence of the Antarctic and sub-Antarctic cryptic species of primnoids, based on the likely presence of sibling species within *T. undulata,* and *T. crenelata* (Fig. 2.2). While the last finding should not be surprising given the wide geographic distribution of these taxa (Taylor *et al.* 2013), as well as the fact that sibling species are ubiquitous in marine environments (Knowlton 1993), including in the Southern Ocean (Rogers 2007), a more intense molecular sampling effort (including use of NGS methods) is necessary to test to what extent this pattern is ubiquitous in Antarctic primnoids.

One of the new taxa here described, *Thouarella dolichoespinosa*, deserves a few additional comments. After a detailed morphological examination of the holotype, paratypes, and additional specimens regarded as this taxon, we could not find any significant variation between them. Likewise, the most conservative species delimitations results suggest all the analysed specimens belong to a single MOTUs (Fig. 2.2). However, the sample labeled as OPRIM 2299 differs from the other specimens in the same MOTUs in having a base change in the 692 position of the *mtMutS*, implying a more considerable intraspecific variability than those observed in newly described taxa within the

genus (Núñez-Flores *et al.* 2020). Given this situation, the specimen OPRIM 2299 is attributed to *T. dolichoespinosa*, but the future analysis on additional individuals will be necessary to quantify whether the sequenced specimens truly represent intraspecific variability or two sibling species.

2.4.3 Phylogenetic relationships within Thouarella

Our reconstructed phylogeny of the genus *Thouarella*, based on a concatenated dataset of mitochondrial and nuclear loci (Fig. 2.2), is likely the most complete so far, as they included at least 18 of the currently 41 named species within the genus. Although early works suggested that *Thouarella* is polyphyletic (Taylor and Rogers 2015), it has been recently shown that it is indeed a monophyletic genus (Cairns and Wirshing 2018). Among the monophyletic *Thouarella*, our reconstructed phylogeny based on three concatenated loci recovered two main clades (T_1 and T_2; Fig. 3.2), which appear to correspond to the two groups proposed (based only on morphological features, polyps isolated or arranged in whorls) by Taylor *et al.* (2013). In this sense, our finding supports previous ideas about the correspondence of these two morphological groupings (Taylor *et al.* 2013) with two different evolutionary lineages within the genus (Cairns and Wirshing 2018). According to Cairns and Wirshing (2018), the *Thouarella* species with isolated polyps must be included in the subgenus *Thouarella* (=clade T_2; Fig. 2.2), while the species with whorled polyps belongs to the subgenus *Euthouarella* (=clade T_1; Fig. 2.2). However, more recent molecular results, based on a single locus (*MutS*) and dozens of newly sequenced samples obtained from the Southern Ocean, indicate more than two main lineages within the genus (Bogantes *et al.* 2020). Therefore, the proposed correspondence between morphological and molecular classifications schemes (Cairns and Wirshing 2018) might not be so simple as expected, and a more comprehensive molecular sampling is necessary to clarify these issues.

Except for *T. antarctica*, *T. chilensis*, and *T. variabilis*, most of the species from which more than a single sequence was included in our phylogeny are monophyletic. These polyphetic scenarios agree with previous findings (Cairns and Wirshing 2018; Núñez-Flores *et al.* 2020). In these cases, we cannot support which of the different sequences identified as to given species is the closest one to the name-bearer of each species and then genuinely attributable to that species, hindering the opportunity to estimate a multi-locus species tree of the genus. The polyphyletic arrangement of these identified specimens could be associated with several, yet not mutually exclusive, reasons including cryptic speciation (i.e., taxa with unreliable or difficult morphological identification but recognizable as independent evolutionary lineages by molecular markers) (Bickford *et al.* 2007), sequences with undetected erroneous sequencer readings, or incorrect specimens' identifications (Núñez-Flores *et al.* 2020). While we cannot discard they represent cryptic species, it is more likely they were misidentified. In this sense, the taxonomic identification of the specimens associated with these sequences should be reassessed.

As mentioned above, the three new species here described broadly resemble one other more closely than other species in the genus. From a morphological perspective, it should be possible to think all these species have a shared ancestor. However, our phylogeny argued against this notion (Fig. 2.2). *Thouarella dolichoespinosa* are closely related to *T. polarsterni* and another lineage that deserves a re-revision (*Thouarella* cf. *variabilis* A06 plus *Thouarella* sp. AC28), while *T. amundseni*, *T. pseudoislai* and *T. islai* represents a single yet poorly resolved clade (Fig. 2.2). Interestingly, we found some incongruences in the mitochondrial and nuclear gene trees among the last three taxa (See Supplementary Figs. S1–S3). They have reached the reciprocal monophyly on the *Muts* and *Cox1* but did not in the *28S* locus. In fact, in the *28S* gene tree, the three taxa are included in a polytomy (Fig. S3). Aside from gene paralogy's potential complications, these discrepancies can be explained by two non-

exclusive evolutionary processes, introgressive hybridization and incomplete lineage sorting (ILS) (Maddison 1997; Nichols 2001). However, distinguishing between hybridization and ILS is challenging. Here, we argue that these incongruences fit better with a scenario where their speciation events occurred very rapidly and recently. Therefore, common ancestral alleles at the *28S* locus would remain in these species, hindering reach their reciprocal monophyly mainly due to incomplete lineage sorting. The rapid and recent speciation events inferred of these taxa, so far only known from the Southern Ocean, could have been enhanced by the impact of Pleistocene climatic oscillations in Antarctica and particularly the advance and retreat of the ice-sheets over the Southern Ocean continental shelf (Clarke and Crame 1992; Clarke and Crame 2010). However, the potential relevance of hybridization for explaining the pattern previously mentioned cannot be excluded entirely, as this process may have been present on some octocorals lineages (McFadden *et al.* 2010; Soler-Hurtado *et al.* 2017; Quattrini *et al.* 2019). In any case, additional molecular markers, as restriction-site associated DNA loci, and proper analyses for detecting introgression (Joly *et al.* 2009; Green *et al.* 2010; Pease and Hahn 2015) might be necessary to clarify the evolutionary process behind the origin of these *Thouarella* species.

2.4.4 Final remarks

The study of several bottlebrush colonies recovered in the Southern Ocean using an integrative taxonomic framework, enriched by the use of species delimitation approaches, has allowed us to recognize distinctive properties or lines of evidence supporting three new species within the speciose primnoid genus *Thouarella*. Therefore, our work highlights the usefulness of combining morphological and molecular evidence for supporting the proposal and even the delimitation of new octocoral taxa (Soler-Hurtado *et al.* 2017; Xu *et al.* 2020; Núñez-Flores *et al.* 2020). This framework is advised in this group of organisms,

as the distinction among some of the species based only on an examination of their macro and micro-morphological features could be difficult. The combined evidence here present indicate that these “minor” morphological differences between them cannot be considered just intraspecific variability or even morphological modifications due to associated organisms (e.g. scale worms) (Bogantes *et al.* 2020). In contrast, it can be used for characterizing different species in the genus *Thouarella*.

After describing the three new taxa here presented, the diversity of the genus increases to 41 species and reinforces *Thouarella* as the second-most species-rich genus within the family Primnoidae after *Narella* (Taylor and Rogers 2017). There are now 15 *Thouarella* species endemic to the Antarctic and sub-Antarctic waters, confirming previous assumptions about the genus’s hidden diversity in the Southern Ocean (Bogantes *et al.* 2020; Núñez-Flores *et al.* 2020). The Southern Ocean has been considered an evolutionary engine of marine fauna (Briggs 2003), and in the particular case of *Thouarella*, this ocean appears to be an authentic center for species radiation (Taylor *et al.* 2013; Núñez-Flores *et al.* 2020). However, given the geographic extension and the complicated and expensive both in time and funds to solve logistic difficulties in sampling their benthonic habitats, our knowledge about the Southern Ocean’s diversity is far from completely understood (Kaiser *et al.* 2013; Chown *et al.* 2015). In this sense, much more work is necessary to be done and mainly focused on studying the large number of primnoids materials collected in this remote area already deposited in several museums around the world due to many international and collaborative sampling efforts along the past decades.

Acknowledgments. The authors wish to acknowledge the valuable assistance of the officers and crew of the RV *Polarstern* and many colleagues on board during the ANT XVII/3 (2000), ANT XXIX/9 (2014), and ANT XXXI/2 (2016) cruises. We extend our thanks to the cruise leaders and steering committee of

the cruises especially Wolf E. Arntz and Julian Gutt (Alfred Wegener Institut, Bremerhaven), who kindly facilitated the work onboard, and for the opportunity to collaborate in these Antarctic programs. Special thanks to Josep Maria Gili, Enrique Isla Saavedra, Maria Isabel Alfonso, Rebeca Zapata-Guardiola, and Stefano Ambroso for helping in the collection of octocoral specimens during *Polarstern* cruises. We also acknowledge José Martín Garrido for his help with the DNA extraction and amplification, and the Norwegian Polar Institute for making the Quantarctica package available. Finally, we thank the two anonymous reviewers for their valuable comments and suggestions that improved the final version of this manuscript.

Declaration of funding. This research is supported by the project CTM2017–83920-P (DIVERSICORAL), Spanish Ministry of Economy, Industry, and Competitiveness (PLG). MNF acknowledges partial support from ANID-PCHA/Doctorado Nacional/2017–21170438, and Instituto Antártico Chileno (INACH) grant number DG_04_19.

Conflicts of interest. The authors declare that they have no conflicts of interest

Availability to data and materials. Supplemental data for this article can be accessed in the Supplementary File.

Table 3.1. Main characters used for the recognition and differentiation of the three new *Thouarella* species described in the present contribution and their closest relatives (see main text for details).

Taxa	Opercular scales		Marginal scales		Polyp height (mm)	Polyp density (polyps/cm)	Other relevant features
	H:W	Features	H:W	Features			
***Thouarella amundseni* sp. nov.**	2	Scales mainly triangular, some with a well-developed dist spine. Opercular scales are 45–50% smaller than margina scales.	3	Predominantly with elongated distal spines and channeled keels in the distal inner surface. The we developed distal spine constitutes up 75–82% of scale height and has multikeels, serrated on their proximal inner section. Scales up 1.45 mm high.	1–1.9 (mean 1.4)	18–24	Well-developed distal spine in opercular scales. Some opercular scales could be considered arrow-shape. Accessory opercular scales present. Submarginal scales with a distal spine. Polyps density toward the colony's apical region can reach up 35 per cm
***Thouarella dolichoespinosa* sp. nov.**	2	Isosceles triangular-shaped scales. Opercular scales siz around 65–75% those of marginal scales.	4	Predominantly diamond-shaped scales with a very long distal spine that could reach up 85% of scale height. Scale up 2.3 mm high.	1.1–1.9 (mean 1.4)	6–14	Polyps disposed of in a roughly alternate arrangement.
***Thouarella pseudoislai* sp. nov.**	2	Triangle-shaped with narrow distal edges and single to multikeels; isosceles-shaped with wide distal edges (near tongue-shaped) without keels, and serrate proximal edges Opercular scales are ~50% smaller than marginal ones.	3	Scales long (up 1.160 mm in height) and narrow, with a well-developed spine that can reach up to 65% of the scale height.	0.6–1.7 (mean 1.2)	18–24	Submarginal scales pointed, coenenchyma scales 50% larger than in *T. islai* .
T. islai	2	Isosceles-triangle shaped, and less commonly tongue-shaped (wide distally). Adaxial scales inner proximal surface with complex tubercles.	2	Diamond-shaped, with elongated distal spine and channelled-keels. Dista spine well-developed, up to 60% of the scale heigh	0.7–1.2 (mean 1)	7–14	—
T. variabilis	—	Isosceles triangle. Keel simple, flat-faced.	—	Tall, triangular-shaped, spinose. Keel channelled.	1.5–1.85	5–10	Spinose keeled marginal scales.
T. undulata	—	Two alternate cycles of four scales: inner cycle, with ova tips; outer cycle, bell-shape scales with convex inner dist surface.	—	Triangle-shaped with a high spinose projection. Spine 64-80% of total sclerite length. Spine with numerous longitudinal ridges on all sides.	1.7–2.4	10–11	Scales distinctly undulate medially, more pronounced in the outer cycle.
T. bayeri	—	Two alternate cycles of four scales: inner cycle with blun tips and squarish base; outer cycle with isosceles-shape scales.	—	Equilateral triangle-shaped with a long distal spine Spine than three-quarters of total sclerite length, wi numerous longitudinal ridges on all sides.	1.6–2.4	9–12	—
T. diadema	1.5–2.7	Isosceles triangles with somewhat blunt tips.	1.4–2.1	Prominent echinulate spine distally, which is round in cross-section. Spine length somewhat variable. Well-developed spines may constitute 75% of the length of a marginal scale.	4.2	Polyps closely spaced on the main stem and branchlets.	Lack of keels on the inner side of the opercular scales.

CHAPTER III. Diversification dynamics of a common deep-sea octocoral family linked to the Paleocene-Eocene thermal maximum[3]

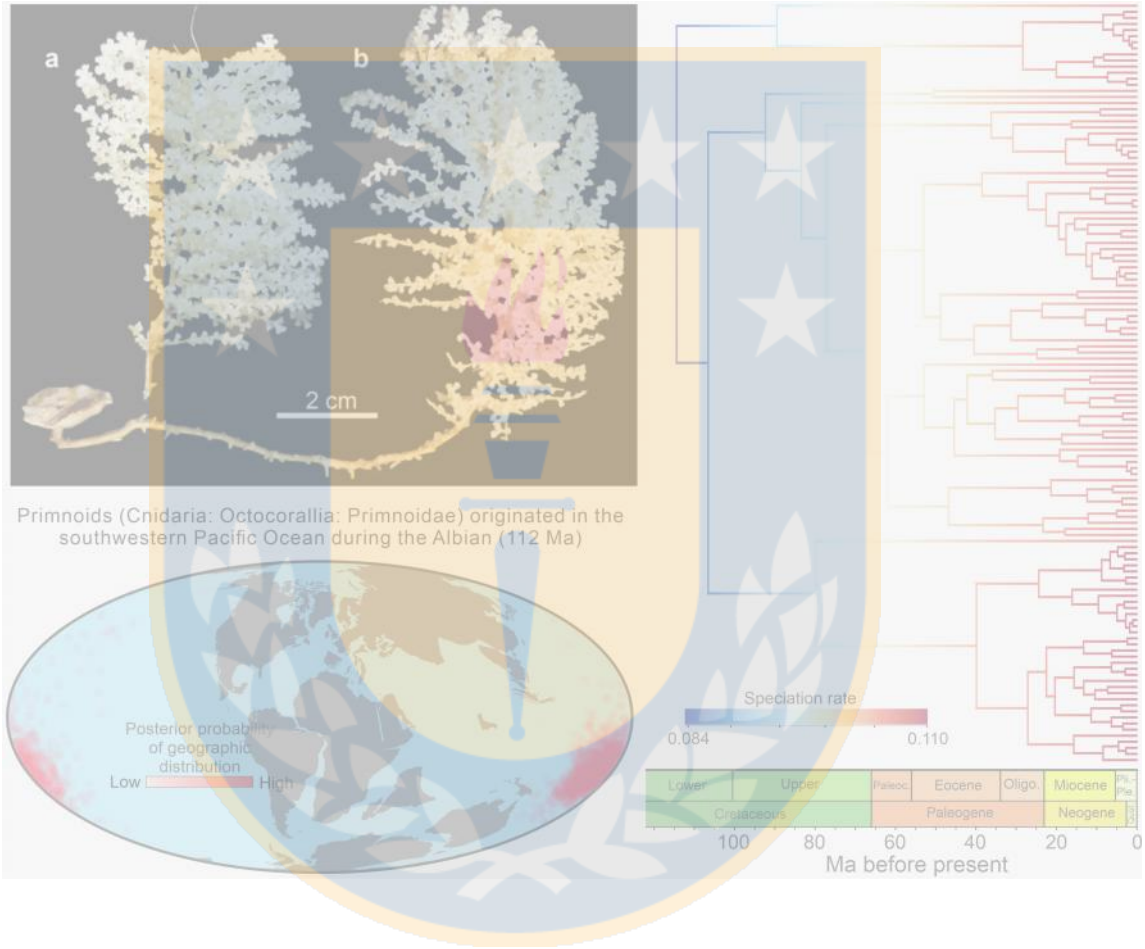

[3]**Artículo enviado**. Núñez-Flores M, Solórzano A, Avaria Llautureo J, Gómez Uchida D, López-González P (submitted). Diversification dynamics of a common deep-sea octocoral family linked to the Paleocene-Eocene thermal maximum. *Molecular Phylogenetics and Evolution.*

Diversification dynamics of a common deep-sea octocoral family linked to the Paleocene-Eocene thermal maximum

Mónica Núñez-Flores[1,2,3], Andrés Solórzano[4], Jorge Avaria-Llautureo[5], Daniel Gomez-Uchida[2], Pablo J. López-González[3]

[1]Programa Doctorado de Sistemática y Biodiversidad, Departamento de Zoología, Facultad de Ciencias Naturales y Oceanográficas, Universidad de Concepción, Barrio Universitario s/n, Casilla 160–C, Concepción, Chile

[2]Genomics in Ecology, Evolution, and Conservation Laboratory (GEECLAB), Department of Zoology, Facultad de Ciencias Naturales y Oceanográficas, Universidad de Concepción, Concepción, Chile

[3]Biodiversidad y Ecología Acuática. Departamento de Zoología, Facultad de Biología, Universidad de Sevilla, Reina Mercedes 6, 41012 Sevilla, Spain.

[4]Laboratorio de Mastozoología, Departamento de Zoología, Facultad de Ciencias Naturales y Oceanográficas, Universidad de Concepción, Concepción, Chile

[5]Centro de Estudios Avanzados en Zonas Áridas, CEAZA, Coquimbo, Chile

Corresponding author: Mónica Núñez-Flores, Email: nuez.monica@gmail.com, telf.: +56 946791586.

Abstract. The deep-sea has experienced dramatic changes in physical and chemical variables in the geological past, but little is known about how deep-sea species richness responds to such changes over time and space. Here, we studied the diversification dynamics of one of the most diverse octocorallian families that inhabit the deep-sea benthonic environments worldwide and sustain highly diverse ecosystems, Primnoidae or 'primnoids' (Cnidaria: Octocorallia: Anthozoa). For this, we built a new dated species-level phylogeny and inferred the historical biogeography (e.g., ancestral geographic locations and dispersal rates) of primnoid. Then, we tested whether their global and regional (the Southern Ocean, SO) diversification dynamics were mediated by biotic factors such as their rate of geographical dispersal (biotic driver) and/or time-continuous abiotic drivers such as changes in CO_2 or ocean geochemistry. Finally, we tested whether primnoids, at global and regional (SO) scales,

showed changes in speciation and extinction that occurred at discrete time points, affecting all lineages, as previously proposed for anthozoans. Our results suggested that primnoids likely originated in the southwestern Pacific Ocean during the Lower Cretaceous (~112 Ma; Albian) with further dispersal after the physical separation of continental landmasses along the late Mesozoic and Cenozoic. The only driver with a significant and positive effect on primnoid speciation rate was the ocean chemistry on a regional scale (SO). Finally, the Paleocene-Eocene thermal maximum, an abrupt planetary-scale climatic perturbation of extreme global warmth and ocean acidification, marked a significant increase in the diversification of primnoids at global and regional (SO) scales, likely by providing ecological opportunity and changing the deep-water ocean circulation transiently.

Keywords. Macroevolution, evolutionary dynamics, historical biogeography, climate change, deep-sea taxa, Southern Ocean.

3.1. Introduction

A feature of biological diversity on Earth is the extent to which species richness varies through space, time, or among taxa. Species richness is determined by historical variation in speciation (the rise of new species) and extinction (the complete demise of species) rates, which lead clades to wax and wane (Benton 2009; Wiens 2011; Morlon 2014). Furthermore, dispersal can also increase or decrease species richness at local and regional scales (Wiens 2011; Condamine *et al.* 2018b). Variation in diversification (speciation rate minus extinction rate) and dispersal rates contribute to notable species richness disparities. Thus, they are critical to understanding evolutionary histories and, ultimately, the origin of present biodiversity patterns (Morlon 2014).

Modeling diversification dynamics and its drivers have been primarily employed to unravel evolutionary histories for continental taxa (Gaston 2000), but with much less focus on marine taxa. This is intriguing, given that marine

environments cover nearly 70% of the Earth's surface (Tittensor *et al.* 2010), and marine and continental organisms have likely diversified throughout different pathways (Benton 1997). The deep sea, one of the largest regions of the sea comprising approximately 66% of the global seafloor area and more than half of the planet's surface (Rex *et al.* 1993; Woolley *et al.* 2016), has experienced dramatic changes in physical and chemical variables in the geological past (Zachos *et al.* 2001; Yasuhara *et al.* 2008; Sweetman *et al.* 2017). It is also the least-explored ecosystem on Earth, with many gaps about how marine species richness responds to such abiotic changes over extended temporal and spatial scales (Sweetman *et al.* 2017; Costello and Chaudhary 2017)

Here, we focused on one of the most diverse octocorallian families of the deep sea, Primnoidae ('primnoids'), ecologically important organisms that occur at high densities and sustain highly diverse ecosystems by providing substratum and shelter to other organisms (De Clippele *et al.* 2015; Buhl-Mortensen *et al.* 2016). Primnoids, characterized by a solid axis composed of calcium carbonate embedded in a gorgonin matrix, originated likely during the late Cretaceous, are considered the "quintessential deep-water octocorallian family". They comprise 43 genera and around 290 recognized species inhabiting the benthic environments, from the Arctic to Antarctica, at depths that extend below 200 m (but reach 6400 m depth) (Cairns and Bayer 2009; Taylor and Rogers 2015; Cairns 2016; Cairns and Wirshing 2018). Historical vicariance events and environmental gradients were deemed essential for the evolution of primnoids (Quattrini et al., 2013). However, our understanding of how, when, and where they have evolved is limited (Quattrini et al., 2020; Taylor & Rogers, 2017), and, specifically, both the timing and drivers of its diversification and historical biogeographical patterns remain to be determined.

Multiple studies have found that historical patterns of global temperature, ocean acidification, and continental fragmentation are the main abiotic drivers of the diversification of marine taxa (Tittensor *et al.* 2010; Kiessling and Simpson

2011; Zaffos *et al.* 2017). Among abiotic factors potentially driving primnoid diversification, it is possible to recognize factors related to geography with fragmentation and movements of landmasses (Zaffos *et al.* 2017), factors related to historical climate (e.g., temperature, CO_2 as a proxy of ocean acidification, and ocean chemical conditions) (Zachos *et al.* 2001; Royer *et al.* 2004; Prokoph *et al.* 2008; Hönisch *et al.* 2012), and factors likely related to the available area (e.g., sea levels) (Miller *et al.* 2005). Temperature is perhaps the most critical factor shaping the diversity of marine and deep-sea taxa (Tittensor *et al.* 2010; Yasuhara and Danovaro 2016), with diversification increasing at higher temperatures, driven by both faster generation of genetic variation and more substantial diversifying selection (Brown 2014). Rising atmospheric CO_2 will significantly increase seawater CO_2 partial pressure (pCO_2) and result in lower ocean pH or ocean acidification, which is predicted to impact the diversity of marine ecosystems at global scales profoundly and has been postulated to cause marine extinctions (Royer *et al.* 2004; Suggett *et al.* 2012). Ocean chemical conditions have cycled between aragonite and calcite seas, driven primarily by fluctuating Mg/Ca ratios through geologic time, where high Mg/Ca ratios favor the precipitation of aragonite and high-Mg calcite, and low Mg/Ca ratios favor the precipitation of low-Mg calcite (Ries 2010; Hönisch *et al.* 2012). Thus, octocorals with proteinaceous or calcitic skeletal types like primnoids should diversify more when Mg/Ca are low (Quattrini *et al.* 2020). On the other hand, one biotic factor, the dispersal capability, might also affect the diversification dynamics of primnoids because dispersal and speciation rates may be correlated (O'Donovan *et al.* 2018; Avaria-Llautureo *et al.* 2021), and highly dispersive lineages (i.e., broadcast spawner) are likely less prone to extinction or more able to speciate by facilitating geographical expansion across barriers (Dueñas *et al.* 2016). Recently, it has been suggested that the evolutionary diversification of anthozoans, a group including coral reef forming taxa and octocorals, is primarily coupled with mass extinction events and

significant reef crises triggered by ocean acidification and/or global warming (e.g., Paleocene-Eocene Thermal Maximum), while ocean geochemistry appears to be influential on the evolution of anthozoan skeletal types (Quattrini *et al.* 2020). Therefore, historical events of abrupt ocean acidification, global warming, and past ocean chemical conditions could be hypothesized, in advance, as the main abiotic factors potentially driving the long-term diversification of primnoids.

On the other hand, clades may show different temporal diversification dynamics across space (Skeels 2019). Consequently, it is also necessary to clarify the historical biogeography further to understand the diversification dynamics of the clade of interest. However, there is a limited understanding of large-scale historical biogeographical patterns for primnoids (Taylor and Rogers 2017). In fact, the ancestral location for primnoids origin is ambiguous, with two proposed regions, the Southern (Cairns and Bayer 2009) and Pacific (Taylor and Rogers 2015) oceans. Although globally distributed, primnoids show a high species richness and elevate endemism in the Southern Ocean (SO) at the genus level (López-González *et al.* 2002; Zapata-Guardiola and López-González 2010b; Núñez-Flores *et al.* 2021). Most of such endemic genera are included in a clade, recognized using molecular evidence, restricted to the Antarctic and sub-Antarctic waters that represent potential *in situ* species radiation that occurred during the early Eocene (~52 Ma; Taylor & Rogers, 2015).

The SO is a fascinating region given its complex geomorphology (unusually deep continental shelf) and unique tectonic and climatic history related to the establishment of the Antarctic Circumpolar Current (ACC) at the Eocene/Oligocene limit (34–28 Ma), the middle to late Miocene (14–12Ma) intensification of the ACC, and the Quaternary (2.5–0.01 Ma) glacial and interglacial periods (Clarke and Johnston 2003; Mackensen 2004; Torsvik *et al.* 2008). The establishment and intensification of the ACC could enhance

allopatric speciation mediated by the long-distance transport of species with low dispersal capacity to new habitats in the clockwise direction within the SO or through limited genetic connectivity at both sides of the ACC (Pearse *et al.* 2009; Chenuil *et al.* 2018). In addition, the Antarctic continental shelf was repeatedly fragmented during the Quaternary due to glacial advances and variations in the eustatic level, generating refugia and/or local extinctions and potentially triggering allopatric speciation (Clarke and Crame 2010; Chenuil *et al.* 2018). An early work proposed that fluctuations in the latitudinal positioning of the ACC during the middle Miocene perhaps contribute to the diversification of SO bottlebrush primnoids (Dueñas et al., 2016). Nevertheless, such a hypothesis remains to be examined with a broader sample of Antarctic and sub-Antarctic primnoids.

Elucidating the timing and drivers of diversification and historical biogeography for primnoids could be essential for better understanding long-term macroevolutionary patterns of deep benthic marine organisms, especially in regions with a long history of geographic isolation and complex geological and climatic history, like the SO. Moreover, it can also provide a framework for predicting their persistence under ongoing global warming and ocean acidification scenario (Pandolfi *et al.* 2011). Here, we inferred a four locus time-calibrated phylogeny for 124 primnoids species, using the novel fossilized birth-dead model (FBD) (Heath *et al.* 2014). Based on this phylogeny, we: 1) inferred their diversification dynamics and historical biogeography; 2) test whether primnoid global and regional (SO) diversification pattern was associated with ocean acidification, global temperature and/or past ocean chemical plus an additional selected sample of biotic and abiotic factors; and 3) test whether the middle Miocene ACC intensification (as well as other Cenozoic major abrupt oceanographic and climatic events in the SO) was the diversification driver of Antarctic and sub-Antarctic primnoids.

3.2. Materials and methods

3.2.1 Dataset

Four molecular markers, two nuclear and two mitochondrial, commonly used for octocoral systematics were selected; the mitochondrial cytochrome oxidase c subunit 1 (*Cox1*) and an apparent homolog of the bacterial mismatch repair gene *mut-S* unique in octocorals (*MtMutS*), plus two nuclear genes, *28S* and *18S* (McFadden *et al.* 2010; McFadden *et al.* 2011). These loci were chosen because they are among the most traditionally used for Octocorallia systematics, accumulating more information to date and having an equilibrium between nuclear and mitochondrial markers (McFadden *et al.* 2011). Such molecular markers were downloaded from the GenBank and complemented with one newly sequenced primnoid species (See Supplementary File 1). The protocol followed to obtain the new sequence is described in Núñez-Flores et al. (2020, 2021).

We included a sample of 215 extant Penatulaceans and Calcaxonia taxa (the latter including the Primnoidae family with 124 spp.) in our analyses, as such clades have a shared evolutionary history according to a recent molecular hypothesis based on hundreds of ultraconserved elements and exon loci (McFadden *et al.* 2021). A total of 215 sequences (Supplementary Table 1) were aligned separately for each gene using the online version of the multiple sequence alignment algorithm MAFFT (Katoh *et al.* 2009), with later manual editing. The alignment was 955 bp for *mtMutS*, 797 bp for *Cox1*, 887 bp for *28S*, 1814 for *18S*, and 4453 bp for the concatenated (*mtMutS* + *Cox1* + *28S* + *18S*) dataset. Individual genes were tested for substitution saturation using the DAMBE software (Xia and Xie 2001). After alignment, the best nucleotide substitution model was selected using the bModelTest package implemented in BEAST 2 software (Bouckaert *et al.* 2014; Bouckaert and Drummond 2017). The best-supported site model was GTR+G for *MutS* and *Cox1,* and TN93+G+I for *28S* and *18S*.

3.2.2 Time-calibrated phylogeny

Phylogenetic relationships and divergence times were inferred within a Bayesian framework in BEAST 2.6.6, employing the fossilized birth-dead model (FBD) with the Sampled Ancestors package (Gavryushkina *et al.* 2014; Heath *et al.* 2014). Despite primnoids lack fossil representatives, closely related octocorals do (Reich and Kutscher 2011; Taylor and Rogers 2015; Quattrini *et al.* 2020). Thus, six extinct taxa belonging to Ellisalidae, Isididae, Pennatulacea, and Heliaporacea clades were included as tips in our FBD analysis (see details in Supplementary File 2). We set an uncorrelated Relaxed Clock Log Normal model for each gene, assuming an exponential prior distribution for the lineage-specific substitution rate variation (parameters ucld.Mean with mean = 10, and ucldStdev with mean = 1). We used the FBD model (on the tree root) as the tree prior. The parameters of the FBD model are the follows: diversification rate d = λ – μ; turnover rate r = μ/λ; fossil sampling proportion s = ψ/ (μ + ψ). We assumed an exponential prior for diversification rate (d) with a mean of 1.0 (lineages per million years), a prior beta distribution for the sampling proportion (s) with Alpha and Beta of 2.0, and a 'uniform' (0,1) prior for the turnover (r) parameter. The Rho (ρ) parameter was given a value of 0.21 as 209 of around 1000 (Daly *et al.* 2007) extant species belonging to Ellisalidae, Isididae, Pennatulacea, Crysogorgidae, Heliaporacea, and Primnoidae were included in the analysis. Two independent Markov chain analyses were run for 500 million generations, sampling every 20,000 generations. Posterior trace plots, stationarity, convergence, and effective sample sizes (ESS) were inspected in Tracer 1.7 (Rambaut *et al.* 2018). The first 30% of each sampled chain was discarded as burn-in, and the remaining were combined in LogCombiner. Later, the FullToExtantTreeConverter tool implemented in BEAUti v.2.4.3 was used to prune the fossil lineages off the MCMC sample of combined trees. Then, we used TreeAnnotator to summarize the extant-only trees under a maximum clade

credibility tree (MCCT) with mean node heights. In addition, 250 trees were randomly sampled from the posterior distribution of the BEAST analysis (after a 70% burn-in with outgroups removed) to keep only primnoid representatives (124 spp.) for downstream analyses.

3.2.3 Historical biogeography

To assess where diversification occurred, we reconstructed the geographic locations of phylogenetic nodes in a continuous and three-dimensional space (O'Donovan, Meade, & Venditti, 2018; Pagel, Meade, & Barker, 2004), using the geographic locations of extant primnoids as input data. We use a sample of location data for every species, which accounts for each species' entire known geographic range. A total of 5,618 georeferenced occurrences (latitude, longitude, and depth) for primnoid taxa, included in our time-calibrated phylogeny, were obtained from specialized literature: the Global Biodiversity Information Facility (GBIF; https://doi.org/10.15468/dl.3zdfju; Downloaded on September 27, 2021) and the Ocean Biodiversity Information System (OBIS; https://obis.org/ Downloaded on September 27, 2021). Duplicate georeferenced occurrences from GBIF and OBIS were removed (Supplementary File 3).

Ancestral locations were estimated for each phylogenetic node using the Geographical model of BayesTraits 3.0 (O'Donovan et al., 2018; Pagel et al., 2004), which used continuous data (geographic coordinates), instead of discretely coded regions, to estimate dispersal trends in finer resolutions without the need to define geographic areas a priori (O'Donovan et al., 2018). This model estimates the posterior distribution of ancestral locations measured in longitude and latitude while sampling across all location data within species and explicitly considering the spherical nature of Earth (O'Donovan et al., 2018). We ran two MCMC chains for 700,000,000 iterations, sampling every 100,000 iterations and discarding 500,000,000 as burn-in. These procedures were conducted based on the Brownian motion (BM) and variable rates (VR) models.

The variable rates (VR) model detects shifts away from the background rate of evolution (or expectation under a Brownian motion (BM) model of evolution) in whole clades of the phylogeny or on individual branches (Venditti *et al.* 2011).

We selected the model (BM or VR) that fit our data better through Bayes factors (BF), using the marginal likelihoods estimated by steppingstone sampling (Raftery and Lewis 1996). We checked for chain convergence, ensuring outputs with ESS >> 200. To take advantage of the available primnoid occurrence data, we sample these multiple tip geographic locations in proportion to their probability. Along with tip and ancestral locations, we simultaneously estimated dispersal rates across the MCCT primnoid phylogeny under the VR model.

The rate of dispersal, i.e., the distance a species moves in an interval of 1 Myr, was considered the rate of species movement (O'Donovan *et al.* 2018; Avaria-Llautureo *et al.* 2021). Finally, we summarize: 1) the sample of the historical rate of movement estimations (=dispersal rate) for each branch in our phylogeny under a consensus tree which includes the uncertainty in ancestral location estimates, and 2) the mean dispersal rate along time, in bins of 1 Myr, taking into account the effects of shared ancestry following the method of Sakamoto & Venditti (2018). However, as such estimations along time could be biased as they represent averages by time bins, we smooth such biases and summarize it into a continuous dispersal rate by calculating a smoothing spline with the ss function of the R package NPREG (Helwig 2022), with default values. In addition, we sampled 2,000 posterior ancestral reconstructions from the converged portions of the MCMCs to summarize the centroid of locations (latitude and longitude) of each node in the phylogeny, allowing us to plot any the dispersal routes of any lineages along the tree.

3.2.4 Macroevolutionary drivers of global diversification of primnoids

To visualize broad patterns of lineage diversification through time, we generated a lineage-through time plot that tracks the number of species that have

descendants in the present through time using the package PHYTOOLS (Revell 2012) in the R environment after the MCCT of primnoids without outgroups. The 95% confidence interval based on the set of 250 random trees (only including primnoids) from the posterior distribution of the FBD analysis was also estimated with PHYTOOLS. Then, to automatically detect lineage-specific diversification rate shifts within primnoids without a priori specifying their locations on phylogeny, we employed the speciation-extinction model in the Bayesian Analysis of Macroevolutionary Mixtures program (BAMM v.2.5.0) (Rabosky 2014). This approach uses reversible-jump Markov chain Monte Carlo (MCMC) to average values over parameters and models (Rabosky 2014). We ran the BAMM analysis using the time-calibrated phylogeny (MCCT) of primnoids without outgroups. We used the 'setBAMMpriors' function in the R package BAMMtools (Rabosky *et al.* 2014) to select appropriate prior values. The analysis was conducted with a prior of one for the expected number of shifts and specified a global sampling fraction of 0.42 to account for missing primnoids taxa in our phylogeny (i.e., 124 of ~290 described primnoid species were sampled in our phylogeny), which we assumed to be missing at random. Two chains of 10,000,000 generations each were run using Metropolis-coupling, saving trees every 10,000 generations. The initial 25% of samples of the MCMC run were discarded as burn-in, and the remaining data were assessed for convergence using the R package CODA (Plummer M *et al.* 2006) to ensure that the ESS values were over 200.

To understand the relative contribution of biotic and abiotic factors that varies through time to the diversification dynamics of the primnoid family, we fitted a series of macroevolutionary models to our calibrated phylogeny on a Maximum Likelihood framework (Condamine *et al.* 2013; Morlon *et al.* 2016). We selected and compiled from literature five time-continuous abiotic factors that are expected to impact global primnoid diversification: global mean temperature based on $\delta^{18}O$ values of deep-sea benthic fauna (Prokoph *et al.*

2008), continental fragmentation (Zaffos *et al.* 2017), sea level (Miller *et al.* 2005), oceanic geochemistry changes (Ries 2010), and atmospheric CO_2 concentration (Royer *et al.* 2004). Except for deep-sea temperature proxy (data from the last 125 Ma (Prokoph *et al.* 2008)), all of the abiotic variables tested (CO_2 levels, continental fragmentation, sea level, and oceanic geochemistry) have data from the last 180 Ma. As abiotic factors were not necessarily the only ones that drove the clade's long-term diversification dynamics, we tested whether the temporal dynamics of smoothed dispersal rate (above estimated), as a biotic factor, influenced the diversification dynamics of primnoids. Additionally, we assessed variation in species diversification over time by performing constant and time-dependent diversification analyses (Morlon *et al.* 2016) using the RPANDA Maximum Likelihood framework.

For each abiotic factor, we tested four models: 1) speciation rate varies according to an abiotic factor without extinction; 2) speciation rate varies according to an environmental factor and extinction rate does not vary (constant extinction); 3) speciation rate is constant, and extinction rate varies according to an environmental factor; and 4) both speciation and extinction rates vary according to an environmental factor. A total of 30 diversification models were fitted, including models with constant diversification rates (2 models), time-varying (4 models), temperature-dependent (4 models), CO_2-dependent (4 models), continental fragmentation-dependent (4 models), sea level-dependent (4 models), oceanic geochemistry-dependent (4 models), and dispersal-dependent (4 models) (see Supplementary File 4, Table S1, for details of the fitted models). Speciation and extinction dependences were modeled as possible combinations of constant and exponential relationships considering birth-death and pure-birth models. Models were fitted by Maximum Likelihood using the fit_bd (for the time-constant and time-varying models) and fit_env (for the environment-dependent models) functions from the R package RPANDA 1.9 (Morlon *et al.* 2016). To consider the uncertainty in tree topology and divergence

time estimates, except for the dispersal-dependent models (fitted over the Primnoidae MCCT), we fit the above described macroevolutionary to a random sample of 250 trees from the posterior distribution of our time-calibration analysis. A sampling fraction of 0.42 was used for all analyses to consider unsampled taxa. The fitted models with biotic and abiotic factors were compared using the corrected Akaike information criterion (AICc) and Akaike weights (AICω). The model with the highest AICω was considered the best fitting model for the data.

Finally, we fitted additional models to detect possible changes in speciation and extinction that occurred at discrete time points and simultaneously affect all clades (episodic birth-death (Stadler 2011)) in the primnoid tree. Such episodic diversification changes, if any, could be potentially related to abrupt historical events that might have severe consequences for ancient marine ecosystems, like ocean acidification (Hönisch *et al.* 2012) or reef crises (Quattrini *et al.* 2020), using the R package TREEPAR (Stadler 2011). Changes in speciation and extinction rate were modeled to occur at discrete time points and simultaneously affect all clades in a tree, with the bd.shifts.optim function (Stadler 2011). TREEPAR analyses were run with the following settings: start = 0, end = crown age estimated by dating analyses, grid = 0.2 Ma (for a fine-scale estimation of rate shifts), sampling fraction = 0.42, and posdiv = FALSE to allow the diversification rate to be negative (i.e., allowing for periods of declining diversity). We estimated the 95% highest posterior density in magnitude and timing of rate shifts by using a wrapper for TREEPAR to include the random sample of 250 trees from the posterior distribution of the time-calibration analysis. The fitted models were compared using the corrected Akaike information criterion (AICc) and Akaike weights (AICω). The model with the highest AICω was considered the best fitting model for the data.

3.2.5 Macroevolutionary drivers of diversification of primnoids in the Southern Ocean

Clades may show different temporal diversification dynamics across space, and evolutionary patterns at global and regional scales are not necessarily the same. The SO has experienced dramatic and abrupt oceanographic and climatic perturbations during the last 50 Myr, and the global climate changes (e.g., global temperature), making it suitable to test whether primnoids diversification in regional (SO) scales differs from the global one. To this task, a series of macroevolutionary models were fitted, on a Maximum Likelihood framework (RPANDA), to assess the relative contribution of abiotic factors varying through time to SO primnoids diversification. In addition, we evaluate the contribution of the abrupt perturbations faced by the SO during the last 50 Myr over the diversification dynamics of the antarctic and sub-antarctic primnoids, using the R package TREEPAR (Stadler, 2011). For RPANDA and TREEPAR analyses, we consider the same potential abiotic factors and follow the specifications described above (except otherwise is indicated). Both analyses were performed on a random sample of 250 trees that only includes species reported in the Southern Ocean (52 spp.; Figure 1; Supplementary File 4, Table S2). A conservative sampling fraction of 0.35 was provided to account for the sampling probability of extant taxa within the sub-clade (but note that the actual primnoid diversity in the SO is probably underestimated (López-González 2006; Núñez-Flores *et al.* 2021)).

3.3. Results

3.3.1 Time-calibrated phylogeny

We inferred that primnoid was a monophyletic clade (posterior probability of 0.99), which the most recent common ancestor (TRMCA) dating backs to the Albian (Lower Cretaceous; mean of 111.8 Ma; 95% highest posterior densities (HPD) of 69.3–160.7 Ma). Moreover, the split of the early primnoid linage from

their sister group, some genera included in the Chrysogorgiidae family, occurred in the Upper Jurassic (mean 152.6 Ma; 95% HPD of 90.7–221.5 Ma) (Figure 3.1). In addition, our FBD analysis also recovered the called sub-Antarctic Primnoidae clade, which TRMCA had a Campanian estimated age (Upper Cretaceous; mean of 73.8 Ma; 95% HPD: 45.4–106 Ma). In addition, the two species-richer genera within primnoid, *Narella* (plus *Abyssoprimnoa gemina*), and *Thouarella*, have TRMCA that dated back to the Priabonian (upper Eocene; mean of 37.2 Ma; 95% HPD of 19.2–57.3 Ma) and Lutetian (lower Eocene; mean of 44.1 Ma; 95% HPD of 22.6–66.1 Ma), respectively (Figure 3.1). See Supplementary File 5 for more details on the complete time-calibrated tree of Calcaxonia plus Pennatulacea, including the position of the fossil tips.

We also estimated substitution rates for each gene partition within Calcaxonia plus Pennatulacean (mean in Myr^{-1}): 0.15% for *mtMuts*, 2.59% for *Cox1*, and 0.08% for the nuclear *28S* and *16S* genes (Supplementary File 6). All the examined genes evolved in a non-clocklike manner, as indicated by ucld.stdev values and the high coefficient of variation, which reflects the heterogeneity in substitution rates along tree branches, especially in the mitochondrial genes.

3.3.2 Historical biogeography: ancestral locations for primnoids and their dispersal through time

We found robust evidence to support the VR model over the BM model (BF>>10). Thus, the VR model was employed to estimate ancestral locations as well as dispersal rate and distance along the branches of the Primnoidae phylogeny (Figures 3.1–3.3). Our results indicate that the primnoid family's ancestral location was the southwestern Pacific Ocean (northeastern Australia landmass) during the Lower Cretaceous (Albian; Figure 3.1). Primnoids subsequently dispersed to other water masses following different routes along the late Mesozoic and Cenozoic (Figure 3.3). Moreover, the inferred ancestral

location of the MRCA of the sub-Antarctic primnoid clade and the genera *Narella* (plus *Abyssoprimnoa gemina*), and *Thouarella,* was constrained to the Southern Ocean (between the Antarctic Peninsula and southern South America), the north of the Pacific Ocean, and the Southern Ocean (between the Antarctic Peninsula and southern South America), respectively (Figure 3.1).

The estimated dispersal rate (=speed of geographical movement) was heterogeneous along time (Supplementary File 7) and clades (Figure 3.2). For instance, along the branches given rise to *Primnoa*, *Loboprimnoa*, *Candidella, Parastenella*, *Paracalyptrophora,* and *Calyptrophora,* we observed the highest rate of dispersal values; while along branches of the clade of sub-Antarctic primnoids the mean dispersal rate was generally low (Figure 3.2). Otherwise, the smoothed mean dispersal rate along time showed a broad wax and wane pattern (Supplementary File 7). In any case, the mean dispersal rate significantly increased since the middle Eocene (~45 Ma; Supplementary File 7). The distance of primnoids dispersal was predominantly low as 49% of the distance between pairs of ancestral and descendent nodes in the phylogeny was less than 10 km, and 32% of such distances were between 10–100 km (Figure 3.2). Dispersal events over 100 km were infrequent (11% is between 100–300 km and 6 % is between 300–600 km), while long-distance dispersal (>600 km; e.g., *Callozostron pinnatum*, *Primnoella insularis*) was rare (only 2%) (Figure 3.2). Considering all primnoids speciation events in our phylogeny, the estimated mean dispersal distance was 95.7 km.

3.3.3 Macroevolutionary drivers of primnoids global diversification

The slight change in the slope of the lineage-through time plot (denoted with a star in Figure 3.4a) suggested one change in the broad diversification dynamics at the end of the Paleocene (~58 Ma) after considering the MCCT of primnoids. BAMM analyses showed no significant discrete shifts in the rate of primnoids diversification along lineages (zero rate shifts; shift posterior distribution= 0.92)

irrespective of the initial value that governs the number of rate shifts (Figure 3.4c). However, the speciation rate estimated by BAMM increased continuously and slightly toward the present (Figure 3.4b).

After the analyses of a series of macroevolutionary models fitted to our data on ML framework, we also found that the constant-rate (constant speciation and constant extinction) was the best-fitted model to the global diversification of primnoids (AICω=0.13; AICω=0.06 and ΔAICc=1.53 for the second-best model that is the sea-level dependent model with variable speciation and constant extinction) (Table 3.1). However, the episodic diversification analyses rejected a constant rate diversification model for primnoids. The best-fitted model recovered one significant diversification rate shift at 56.5 ± 2.8 Ma (AICω=0.413) nearly the Eocene-Paleocene boundary (Table 3.2). The second-best model, with no shift time, had an AICω of 0.356 (ΔAICc=0.30).

3.3.4 Macroevolutionary drivers of diversification of primnoids in the Southern Ocean

Regarding macroevolutionary drivers of diversification of the Antarctic and sub-Antarctic primnoids, our RPANDA results suggested that the speciation variable with time and no extinction was the best-fitted model to their diversification (AICω=0.10; Supplementary File 4, Table S3). Furthermore, the second-best model was one in which speciation depends on the ocean chemistry with no extinction (AICω=0.10; Supplementary File 4, Table S3), and the fit of both models is nearly indistinguishable (AICc difference or ΔAICc = 0.07). However, much better than additional considered models. In addition, the best implemented episodic diversification model was those with one significant diversification rate shift identified at 58.1 ± 2 Ma (AICω=0.45) at the late Paleocene (near to the Eocene-Paleocene boundary; Supplementary File 4, Table S4). The second-best model, with no shift time, had an AICω of 0.43).

Thus, both models have a similar fit to our data (ΔAICc= 0.07) but were better than additional considered models.

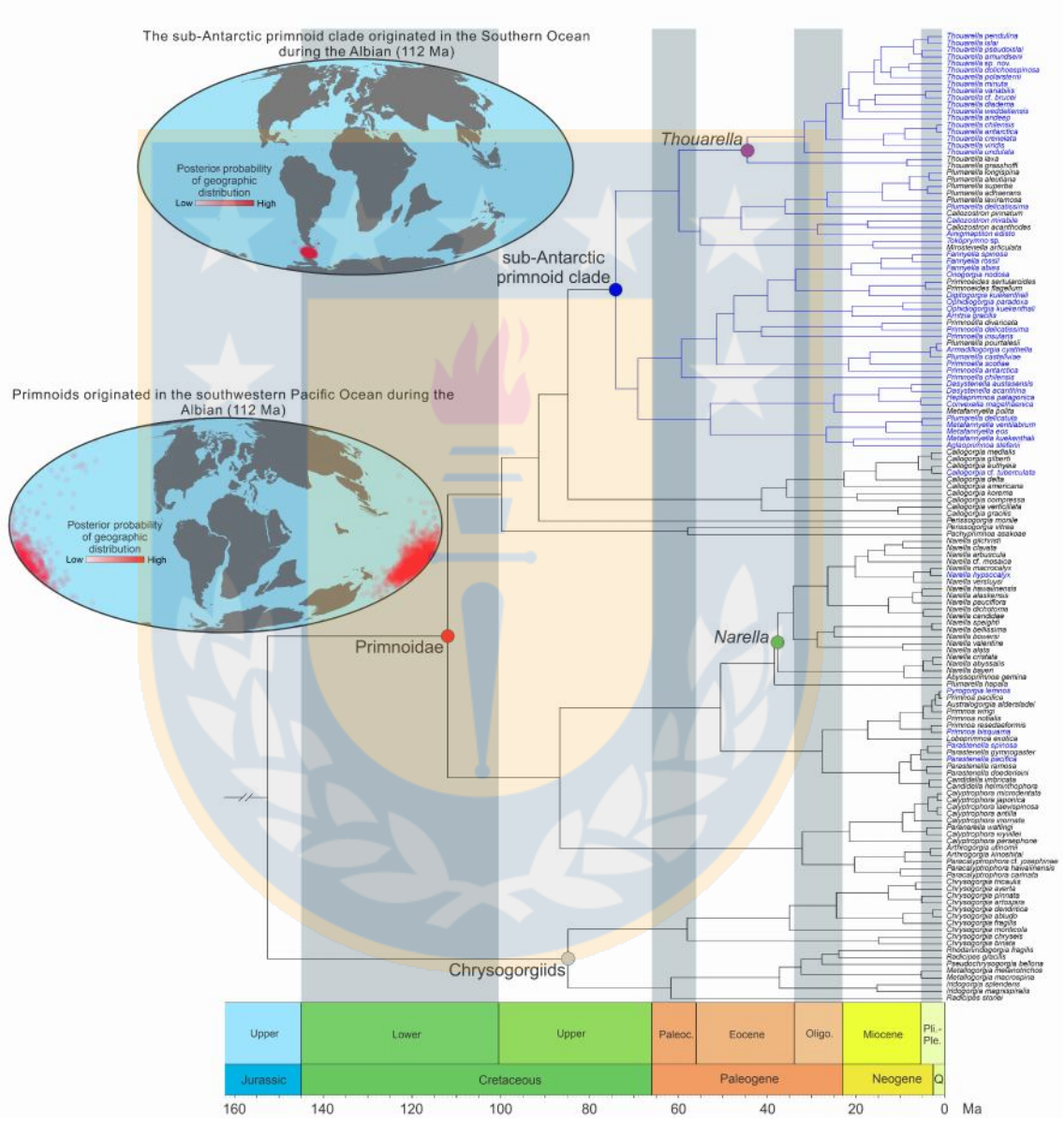

Figure 3.1. Time calibrated phylogeny of primnoids and closest outgroups and its historical biogeography. The red, blue, pink, green, and grey circles denote the TMRCA of Primnoidae (~112 Ma), the sub-Antarctic primnoid clade (~73.8Ma), Thourella genus (~44.1 Ma), Narella genus (~37.2 Ma), and Chrysogorgiids (as closer outgroup), respectively. Besides, species in blue are currently recognized (but not necessarily restricted to) in the Antarctic and sub-

Antarctic waters (= south of 55°S; 52 spp.). In addition, note that the ancestor of Primnoidae was distributed across the southwestern Pacific Ocean during the Albian (~112 Ma). In contrast, the ancestor of the clade of sub-Antarctic primnoids was distributed between the Antarctic Peninsula and southern South America (~63°S) during the Campanian (~74 Ma). Red dots in the maps denote the Bayesian posterior probability for the estimated geographic distribution of the phylogenetic nodes. The x-axis scale is in million years. Abbreviations: Paleoc.=Paleocene; Oligo.=Oligocene; Pli.-Ple= Pliocene/Pleistocene; Q= Quaternary.

3.4. Discussion

3.4.1 Time-calibrated phylogeny

In this study, we first took a novel approach (FBD model) to reconstruct the evolutionary history of primnoids, an ecologically important group of marine benthonic octocoral common on deep waters, integrating the fossil record of closely related clades and phylogenetic information of extant species.

Our tree topology (Figure 3.1) agrees well with previous molecular phylogenies inferred for the family (Taylor and Rogers 2015; Taylor and Rogers 2017; Cairns and Wirshing 2018; Núñez-Flores *et al.* 2020) recovering, among others, the monophyly of the family, a clade of sub-Antarctic primnoids (with a TMRCA at 73.8 Ma; Campanian; Upper Cretaceous) and a monophyletic *Thouarella* genus (with TMRCA at 44 Ma; Lutetian; early Eocene). Our calibrated MCCT (Figure 3.1) supported that the TMRCA of Primnoidae dates from the Lower Cretaceous (early Albian; ~111.8 Ma), nearly 30 Ma older than those recovered in an early work (Taylor and Rogers 2015).

The Cretaceous is well-known as a greenhouse period mainly caused by increased CO_2 from elevated global volcanic activity; it is also the last stage in the Gondwana break-up displaying high rates of seafloor spreading, high sea levels, and high ocean temperatures, as well as evidence for changes in global ocean circulation (Miller *et al.* 2005; Prokoph *et al.* 2008; Friedrich *et al.* 2012). The earliest Albian, in particular, has been interpreted as a warm and humid period with extensive freshwater flows into the ocean, which witnessed the

extinction of several marine organisms, as well as oceanic anoxic events (Föllmi 2012). Therefore, Cretaceous changes in sea temperature and anoxic events were likely critical for early primnoids evolution, as have been previously suggested for different octocorallian clades that appear to diversify in this epoch (Reich and Kutscher 2011; Taylor and Rogers 2015; García-Cárdenas *et al.* 2020; Goedert *et al.* 2022).

Significantly, our results pushed back the estimated time of divergence of Primnoidae from their closest relative (the polyphyletic Chrysogorgiidae family (Pante *et al.* 2012); Upper Jurassic; 152.6 Ma; Figure 3.1), as well as the TMRCA of the clade of sub-Antarctic primnoids and the speciose *Thouarella* genus in ~35, ~22 and ~31 Ma, respectively, in comparison with previous estimates based on node dating approaches (Taylor and Rogers 2015; Dueñas *et al.* 2016). Differences in calibration methods, molecular markers, and fossil taxa included in the analyses may account for differences from previous studies. Our time calibrate phylogeny include the most comprehensive taxon sampling at the species level (124 primnoid spp.) as well as six extinct taxa as tips, contrasting more limited sampling of extant species and calibrated nodes employed in early analyses dealing with primnoids and subordinate sub-clades (Taylor and Rogers 2015; Dueñas *et al.* 2016). The use of closely related fossil calibrations (as tips) to the clade of interest (McFadden *et al.* 2021) and the implementation of FBD model to calibrate the primnoids tree eliminates the need for ad hoc calibration priors. In addition, Bayesian inference under the FBD model appears to yield more accurate node age estimates while providing a coherent measure of the statistical uncertainty compared with typical calibration density (or node dating) approaches (Heath *et al.* 2014).

On the other hand, the mean substitution rate found for Calcaxonia and Pennatulacea mitochondrial *mtMutS* gene (mean of 0.15% Myr^{-1}; ranging between 0.09% and 0.21% Myr^{-1}), likely the most widely used locus for octocoral systematics, were highly congruent with previous authors' (ranging between

0.14% and 0.25% Myr^{-1}) based on a reduced sample of Holaxonia representatives (Thoma *et al.* 2009). The use of extrapolated substitution rates for one lineage to date another could be limited by the variation in the rate of molecular evolution among lineages (Bromham *et al.* 2000). However, despite this situation, we expected that our estimations, even when they reflect the broad rate heterogeneity present along tree branches of Calcaxonia and Pennatulacea, will provide valuable information for future time-calibrated phylogenies critical for addressing a wide range of questions in evolutionary biology.

3.4.2 Historical biogeography: Ancestral locations for primnoids and their dispersal through time

The Pacific Ocean was previously hypothesized as the ancestral geographic location of Primnoidae based on the geographic distribution of the species along the base of the molecular phylogeny of the family (Taylor and Rogers 2015). Our results support the Pacific Ocean hypothesis but provide a refined ancestral distribution for early primnoids to the southwestern of this ocean during the Albian (Figure 3.1). Further, our results shed light on several biogeographic patterns previously unrecognized. For example, we illustrated the diversity of routes taken for primnoids across the globe, even by taxa that ended up in nearly the same location (Figure 3.3).

Primnoids also showed a broad pattern whereby ancestral nodes primarily clustered together but with a descendant occasionally moving far away from its predecessors. Hence, their geographic expansion is mainly described by slow and short-distance movements between speciation events interspersed with a few events of relatively fast movements along with more considerable distances (Figures 3.2 and 3.3). Considering that gene flow within extant populations of primnoid species can reach up to 200 km (Yesson *et al.* 2018); our findings that nearly half of the evaluated speciation events in our primnoids

phylogeny were within relatively short distances (< 10 km), suggest that the sympatric mode of speciation could be widespread in this family of deep-sea organisms.

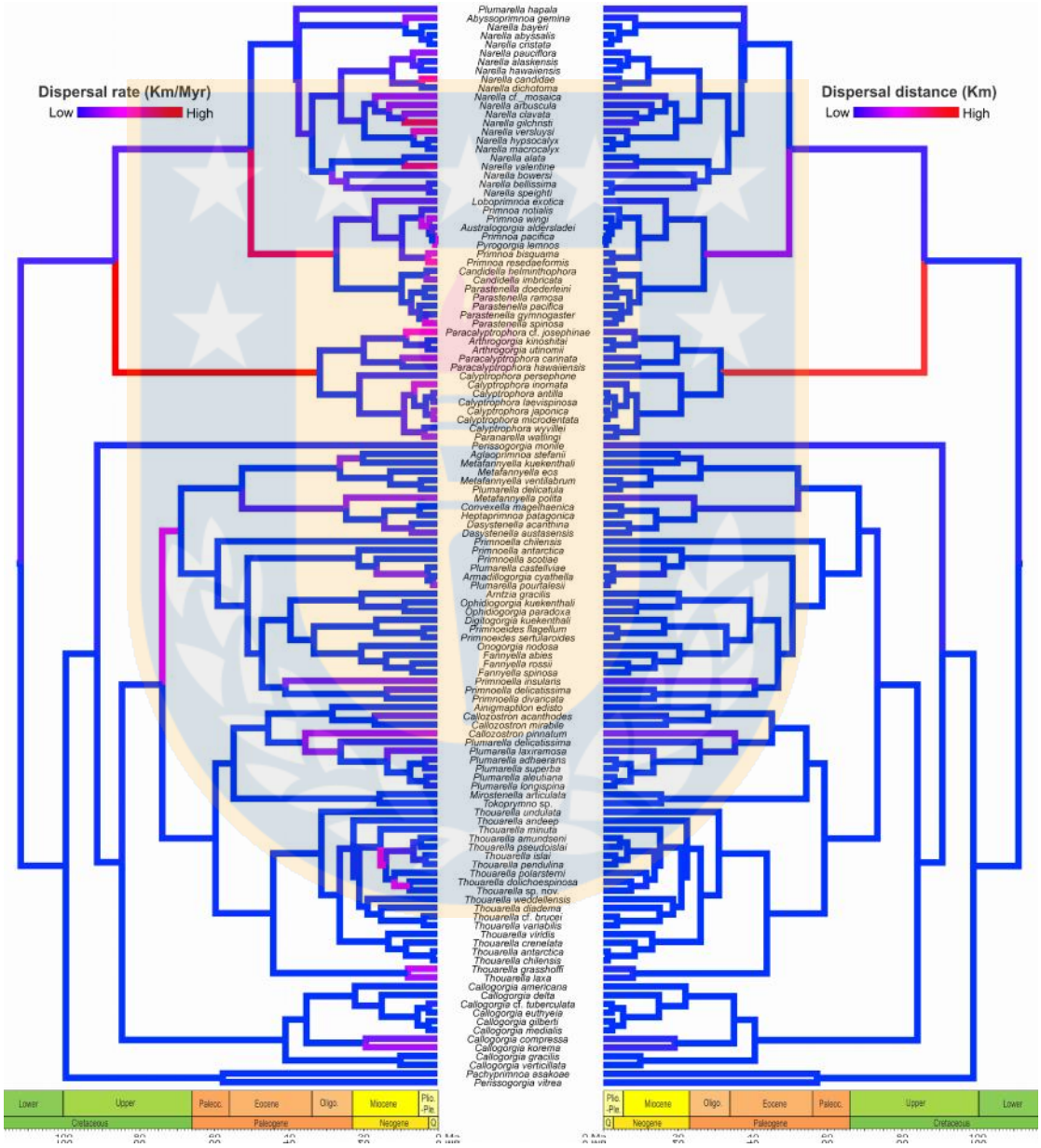

Figure 3.2. Phylogenetic tree (MMCT) of primnoids with branches colored to reflect the relative rate (left) and distance (right) of dispersal estimated along branches with the VR model. Note the

inferred predominance of low dispersal distances and the more variable dispersal rates. The abbreviation of geological times is the same as Figure 1.

Sympatric speciation on the sea has occurred in at least a few instances and is theoretically plausible; however, it is unclear whether it is common (Bolnick and Fitzpatrick 2007). Four criteria to infer sympatric speciation have been outlined: a sympatric distribution, a monophyletic sister species relationship, complete reproductive isolation, and an ecological setting where allopatric speciation is unlikely (e.g., isolated island habitat) (Coyne and Orr 2004). Such criteria are hard to discriminate with our primnoids data by the time and out the scope of the present contribution. Future efforts in this regard could provide novel examples on the breath of conditions under which sympatric speciation can occur in the sea.

On the other hand, speciation through long-distance dispersal, also termed 'founder-event' speciation, was inferred based on the few branches of our phylogeny that show high dispersal distances (Figure 3.2). Founder-event speciation is considered an essential process in oceanic islands (Matzke 2014), and for deep-sea octocorals seamounts could act as 'islands' promoting that a small number of individuals take part in the few and rare, long-distance colonization event that founds a population genetically isolated from the ancestral population (O'Hara 2007). However, as oceanic crust and seafloor are continually recycled under convergent margins into the mantle, this idea is hard to test. Long-distance dispersals could be predicted for broadcast spawner octocorals with a pelagic larval stage that can span from a few days to several months, but in much less intensity for brooding taxa that incubate their larvae and settle at short distances from their parents (Dueñas *et al.* 2016). The few studies dealing with sexual reproductive modes in primnoids indicate that they can be either broadcast spawners (e.g., *Primnoa, Primnoella*) or brooders (e.g.,

Thouarella spp. and *Fannyella* spp.) (Brito *et al.* 1997; Orejas *et al.* 2007; Waller *et al.* 2014; Rossin *et al.* 2017a).

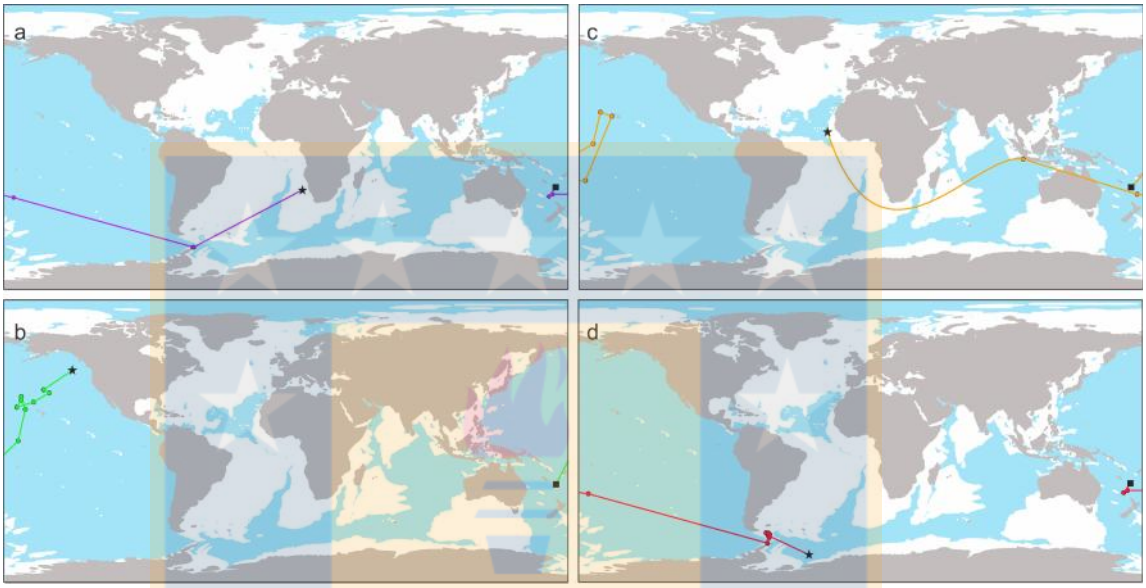

Figure 3.3. Reconstructed paths from the primnoid root node (black circle) to four extant species (black star): Fannyella spinosa (a), Narella alaskensis (b), Primnoa resedaeformis (c) and Thouarella weddellensis (d). The colored circles represent the centroids of the reconstructed ancestral locations. Paths were plotted onto modern continental maps (grey) with all preceding age level palaeomap layers plotted in white.

Although data of sexual reproductive strategies for the species included in our phylogeny is reduced and sparse, it is congruent with a scenario in which most of the speciation through long-distance dispersal events is exhibited primarily by broadcast spawners primnoids lineages. For instance, species within the genus *Primnoella* are broadcast spawning (Rossin *et al.* 2017a). Our findings indicate that *Primnoella insularis* shows an intermediate dispersal rate but very high (long-distance) dispersal distances (815 km) from its ancestral node. In contrast, species included within the genus *Thouarella*, especially those inhabiting the SO, have low dispersal rates and distance values (Figure 3.2). Therefore, we envisaged that primnoids long-distance dispersal was likely

facilitated by its reproductive modes (intrinsic species traits) and occurred mainly in broadcast spawning lineages. However, such a hypothesis remains to be tested after comprehensive reproductive studies of dozens of primnoids species are conducted.

Our results also highlighted specific patterns at regional (SO) scales. The SO marine fauna has been generated and maintained during progressive isolation and cooling suffered by the region during the last 40 Ma (Clarke and Crame 2010). However, the origin of its modern faunal communities is highly complex, as it consists of endemic elements diversifying *in situ* (even since the Mesozoic) and components that have immigrated from South America through the Scotia Arc and/or adjacent deep basins at different pulses during the Cenozoic (Crame 2018; Halanych and Mahon 2018). Our results pointed out that the SO colonization of primnoids begins as early as the Campanian (~74 Ma; Upper Cretaceous) by the TMRCA of the Antarctic and sub-Antarctic primnoids clade (hereafter sub-Antarctic clade), predating the middle Eocene onset of the ACC (Torsvik *et al.* 2008). Primnoids could be added to an increasing number of Antarctic marine invertebrates with a pre-ACC origin, such as isopods, ostracods, amphipods, and mollusks (Clarke 2008; Clarke and Crame 2010; Crame 2018), and supports that the family has a relatively long and prosperous *in situ* evolutionary history in the SO (Taylor and Rogers 2015).

Noteworthy, not all the species that can be ascribed to the sub-Antarctic primnoid clade are currently represented in the SO (e.g., *Thouarella laxa*), and some primnoids species (e.g., *Primnoa bisquama*) recognized within the SO cannot be included in the sub-Antarctic clade (Figure 3.1). This pattern denotes that the SO potentially acted as both a source (with in situ speciation and dispersal to other Oceans) and a sink (receiving immigrants from other Oceans) of primnoids diversity. Despite the incompletely sampled phylogeny, our results (Figure 3.1) suggests that, in fact, the SO acted primarily as a source of diversity, i.e., 15 spp. of the sub-Antarctic primnoid clade migrated or expanded

its distributional range to other oceans, and the clade has diversified primarily *in situ* at least since the Upper Cretaceous (Taylor and Rogers 2015). In contrast, only six primnoids species outside the sub-Antarctic primnoid clade immigrated or expanded its distributional range to the SO.

We found no co-occurrence of dispersal toward and outward the SO (Figures 3.1, 3.2). Immigrant primnoids reached the SO only recently (Pliocene/Pleistocene; the last 5.3 Ma), coinciding with glacial and interglacial periods (De Schepper *et al.* 2014). At the same time, emigrant primnoids from the sub-Antarctic primnoid clade disperse outside the SO in different moments along the Cenozoic, including dispersal events after the ACC onset and intensification (Torsvik *et al.* 2008). In this sense, our results strengthen the notion that the ACC could be considered a soft semi-permeable barrier to deep-sea octocorals capable of separating and structuring populations while allowing periods of gene flow and dispersal events (Dueñas *et al.* 2016). Considering that deep-waters move poleward and upward across the ACC (Rintoul 2018), and primnoids are mainly deep-water taxa, we hypothesize that their potential dispersal routes toward or outward the SO likely occur through deep-waters.

3.4.3 Macroevolutionary drivers of primnoids diversification at global and regional (SO) scales

Taking advantage of our novel time-calibrate phylogeny, we characterized the global primnoids diversification dynamics and assessed whether a selected sample of biotic (dispersal-dependent diversification) and abiotic (e.g., global climate) drivers had shaped it.

We found that variation in extant species richness within primnoids can be explained without invoking significative heterogeneous branch diversification (Figure 3.4c). Furthermore, we cannot find strong evidence favoring time-continuous abiotic (i.e., ocean geochemistry, temperature, CO_2) and biotic (i.e., dispersal rate) drivers on the diversification of primnoids globally (Table 3.1;

ΔAICc > 1.5). Indeed, the best model explaining their diversification was the one with constant speciation and extinction rate (Table 3.1). Consequently, our results suggest several scenarios: 1) global diversification rates could be primarily driven by additional time-continuous biotic or abiotic factors than those considered here; 2) diversification dynamics was governed by one of the considered factors, but this acted predominantly at regional rather than global scales; or 3) diversification dynamics responded to episodic changes rather than to time-continuous ones. Our results argued that the second and third scenarios are plausible.

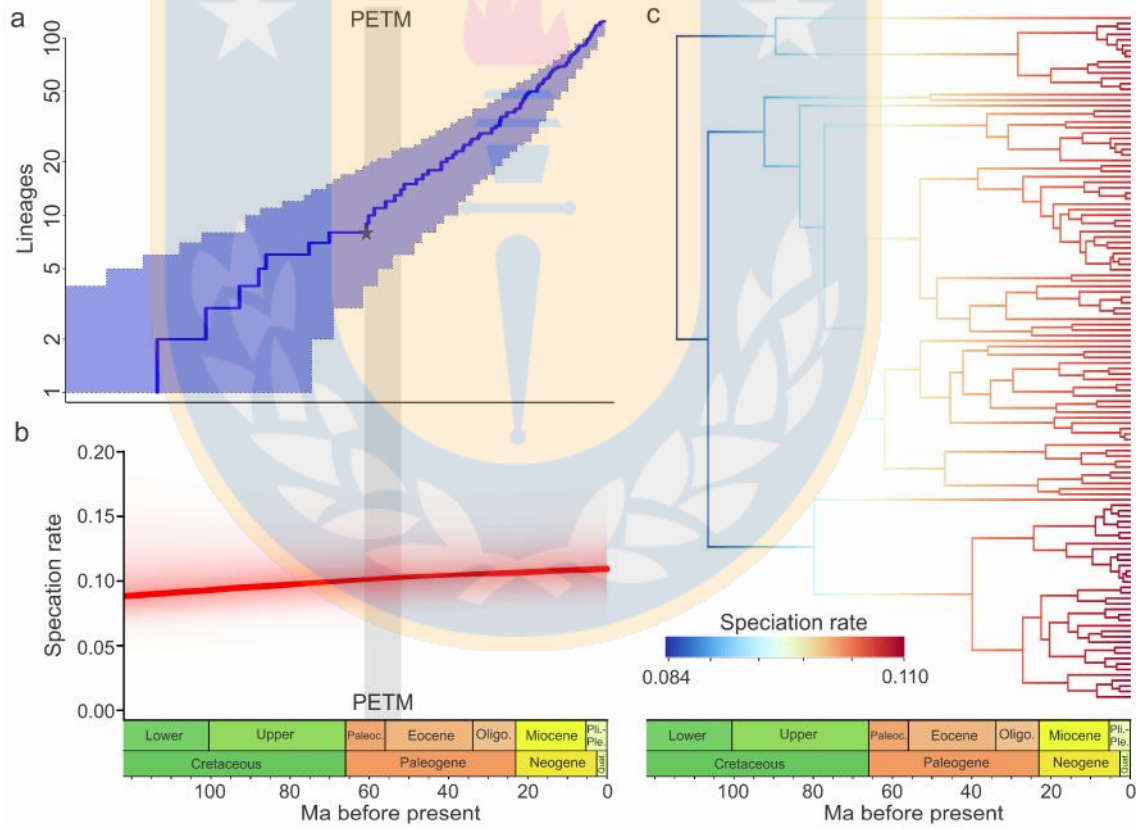

Figure 3.4. Lineages-through-time plot and speciation rates across Primnoidae. a, Lineages-through-time plot displaying the diversification pattern of primnoids (at global scale) based on the MCCT (red line) with the 95% confidence interval (pale blue) based on the set of 250 random trees from the posterior distribution of the FBD analysis. The grey star denotes the

apparent change in the LTT slope based on the MCCT. b, plot of speciation rate through time (red line) with confidence intervals (pale rose). c, branch-specific speciation rates across Primnoidae after BAMM results. The grey vertical band in a–b denotes the timing (with standard deviation) of the episodic shift in the diversification rate at the Paleocene-Eocene Thermal Maximum (PETM) detected with TREEPAR analysis for primnoids globally. The abbreviation of geological times is the same as Figure 1. The x-axis scale is in million years (Ma).

The episodic birth-dead models and likely the lineage-through time plot (Figure 3.4a) support one change in the global primnoid diversification dynamics at the Paleocene-Eocene boundary (~56 Ma), a period that corresponded with a key thermal maximum. The Paleocene-Eocene Thermal Maximum (PETM) was an abrupt planetary-scale climatic perturbation of extreme global warmth, superimposed on long-term greenhouse climate conditions, and coupled with a massive release of carbon into the ocean-atmosphere system (McInerney and Wing 2011; Dunkley Jones *et al.* 2013; Foster *et al.* 2018). Such abrupt climatic perturbation resulted in a rise of global sea temperatures by 4° to 8°C (deep-sea temperatures increased by 4°–6°C), severe ocean acidification often coupled with hypoxia (Tripati and Elderfield 2005; Zachos *et al.* 2008; McInerney and Wing 2011; Dunkley Jones *et al.* 2013), a critical upward of the calcium carbonate compensation depth in many parts of the oceans (Zachos *et al.* 2005), and transient changes in deep-ocean circulation patterns (Nunes and Norris 2006).

The biotic response to PETM on land and oceans was heterogeneous in nature and severity (Speijer *et al.* 2012). For instance, deep-sea benthic foraminifera suffered the extinction of 30%–50% of species during the PETM (Thomas 2007), and PETM coincides with one of the five most substantial metazoan reef crises (Kiessling and Simpson 2011). However, PETM was conceivably best characterized as a migration and origination event rather than an extinction one (Speijer *et al.* 2012) because oceanic plankton productivity seems to have increased spanning the PETM due to climatically enhanced

weathering (Stoll *et al.* 2007). Furthermore, our results indicated that primnoids had a positive net diversification rate (reflecting more significant speciation than extinction rates) after the PETM (Table 3.2). This pattern was similar to those reported in marine clades like tetraodontiform fishes (Arcila and Tyler 2017) and anthozoans (Quattrini *et al.* 2020).

Anthozoans, a group including primnoids, showed several pulses of diversification following mass extinctions and reef crises, including an episodic increase in diversification rate following the Paleocene-Eocene boundary (Quattrini *et al.* 2020). This is congruent with Quattrini et al. (2020) findings, who analyzed molecular from 250 anthozoan species, a reduced fraction of the standing diversity of modern anthozoans (>5000 spp.) (Daly *et al.* 2007). Episodic increases in anthozoans diversification rates recognized by Quattrini et al. (2020) were more noticeable in some clades than others. Such episodes were related to the expansion into new ecological niches following extinction events and reef crises (Quattrini *et al.* 2020). The last hypothesis seems plausible at first as scleractinians and octocorals compete for space and survival, especially in shallow-water environments in which anemones and octocorals can overgrow coral reefs following a reduction in live coral cover (Tkachenko *et al.* 2007), or because the scleractinian coral settlement could be inhibited by octocorals (Atrigenio *et al.* 2017). Nevertheless, this idea is hard to reconcile for the deep sea because the importance of ecological interactions in the deep sea (although present) remains to be characterized (Allcock and Johnson 2019).

The increase of primnoid diversification rate after the PETM was likely linked to ecological opportunity (i.e., the availability of potentially new, or empty, ecological niches) in the deep-sea following the extinction of competitors' taxa (Quattrini *et al.* 2020), which were not necessarily anthozoans. However, given the wide variability in modern drivers of deep-sea species distribution (e.g., habitat complexity imposed by topography, bottom currents, temperature, and

productivity (Costello & Chaudhary, 2017; Puerta et al., 2020)) it is hard to dismiss the role played by abiotic environmental factors in driving primnoids diversification patterns. In this sense, we suggest that the transient (~50 Kyr) interhemispheric switch in deep-water formation along the PETM (Nunes and Norris 2006) could also favor the detected diversification pattern of primnoids after increasing their geographic isolation (triggering allopatric speciation) and spurring novel ecological interactions (triggering sympatric speciation) than those faced under original (pre-PETM) oceanic circulation patterns. This hypothesis agrees well with recent studies proposing that climatically induced changes in ocean circulation could be considered a major stressor of marine ecosystems, mainly affecting propagule dispersal (van Gennip *et al.* 2017).

Conversely, clades do not radiate evenly across space and may show different temporal dynamics in different regions, and this could be expected in relatively isolated locations like the SO. Furthermore, primnoids are long-lived yet slow-growing organisms (Martinez-Dios *et al.* 2016), and therefore, their speciation rates may be slower (Thoma *et al.* 2009). Therefore, the generation of endemism through *in situ* diversification in relatively isolated locations likely should take longer. In this sense, sub-Antarctic primnoids are particularly interesting as they appear to radiate in the SO since the Upper Cretaceous (Campanian; 73.8 Ma; Figure 3.1) and consequently suffered unique Cenozoic abrupt climatic and oceanographic events along with their evolutionary history (Mackensen 2004; Torsvik *et al.* 2008). However, which of these discrete climatic/oceanographic episodes greatly impacted macroevolutionary processes in the SO remains discussed (e.g., Chenuil et al., 2018).

For sub-Antarctic primnoids, fluctuations in the latitudinal positioning of the ACC during the middle Miocene have been considered a factor contributing to their diversification (Dueñas *et al.* 2016). However, we found little support for the oceanographic (ACC) changes at the Eocene/Oligocene boundary and middle to late Miocene or the Quaternary glacial cycles as significant abiotic

events affecting the diversification dynamics (or even the biogeography) of sub-Antarctic primnoids. In contrast, sub-Antarctic primnoids showed a similar pattern exhibited by primnoids at a global scale, with only one abrupt change in their diversification dynamics occurring nearly the Paleocene/Eocene boundary (Supplementary File 4, Table S4). In this sense, the PETM perturbation significantly affected primnoids diversification at both global and regional scales, and similar global-scale climatic/oceanographic perturbations should be considered plausible macroevolutionary drivers of Antarctic biota, especially in clades with long *in situ* evolutionary histories in the SO.

On the other hand, the best RPANDA fitted model to sub-Antarctic primnoids was the one with speciation as a function of time and no extinction (Supplementary File 4, Table S3). However, the second-best model showed a correlation between the ocean geochemistry and the speciation rate without extinction. Both models have similar explanatory power as their AICc difference (ΔAICc) is 0.07 (Table S3). Models can usually be considered poor (relative to the best model) if they had ΔAICc >2 (Burnham and Anderson 2004). However, more recently has been argued that such inference can be better based on model likelihoods, probabilities, and evidence ratios and, in general, on all the examined models (Burnham *et al.* 2011). In this sense, we strengthen the significant effect of the ocean geochemistry in the diversification dynamics of the sub-Antarctic primnoids, i.e., primnoids diversification is positively (α=0.21) correlated with high Mg/Ca ratios in the seawater. Consequently, we support the previous hypothesis (Quattrini *et al.* 2020), highlighting ocean geochemistry's crucial role in octocorallian evolution and that global abiotic factors can profoundly impact specific regions of the Earth, particularly high-latitude ones.

It is necessary to highlight some potential methodological limitations of our analyses. For example, the reliability of birth-death models to assess the diversification dynamics from phylogenies of extant taxa has been questioned (Louca and Pennell 2020). Nevertheless, when combined with appropriate prior

hypotheses and regularization techniques (like those implemented here), extant phylogenies can provide relevant information about past diversification dynamics (Morlon *et al.* 2022). Furthermore, severely incomplete sampled phylogenies can lead to biased diversification rate estimates (Chang *et al.* 2020). In addition, TREEPAR results at a global and regional scale showed well yet not outstanding support (ΔAICc of between 0.3 and 0.07, respectively) for selecting one vs. no episodic changes in the diversification rates (Tables 3.2 and S4). Considering such methodological limitations, it is necessary to remain prudent with our estimates of diversification and the interpretation of the different models tested. It is also worth mentioning that TREEPAR and BAMM constitute distinctive methods that differ on how speciation and extinction rates are estimated, and both were used here to assess distinct patterns. TREEPAR was used to assess speciation and extinction rates and their respective variations through time, while BAMM was employed to automatically detect rate shifts within and among clades (Stadler 2011; Rabosky 2014). Thus, such diversification analyses should be complementary and not cross-validation procedures. Our finding of episodic changes and time-continuous correlates in the diversification dynamics of primnoids support this notion. In any case, our time-calibrated phylogeny of primnoids and its inferred diversification and biogeographical history should be considered a necessary first step in understanding the long-term evolution of the family. Furthermore, with the continuous and extensive increase in the taxonomic sampling of phylogenetic studies of primnoids (Taylor and Rogers 2015; Taylor and Rogers 2017; Cairns and Wirshing 2018; Núñez-Flores *et al.* 2020; Núñez-Flores *et al.* 2021), there will be novel opportunities to achieve more comprehensive insights into the macroevolutionary dynamics of this ecologically important clade of benthonic organisms that can form animal forests (Buhl-Mortensen *et al.* 2016).

3.5. Concluding remarks

Our genetic dataset of extant primnoids is the most comprehensive to date in terms of taxa included and gene sampling. Such a dataset and the novel FBD dating approach provide more confident interpretations regarding the evolutionary history of this common deep-sea octocoral family at global and regional scales. The ancestral location for primnoids origin, which dates from the Lower Cretaceous, was likely the southwestern Pacific Ocean. In addition, we recognized novel biogeographic patterns at a global scale: 1) primnoids dispersed along several routes across the globe, 2) it dispersal rate and distance was heterogeneous along with time and clades, with their geographic expansion mainly characterized by slow and short-distance movements interspersed with rate events of relatively fast movements along with more considerable distances, with sympatric speciation being likely more common than previously assumed in this group, 3) several long-distance dispersals were identified along with the evolutionary history of primnoids, likely facilitated by it sexual reproductive modes. Alternatively, the SO colonization of primnoids begins as early as the Campanian (~74 Ma; Upper Cretaceous) by the clade of sub-Antarctic primnoids. We suggest that the SO could act, from a macroevolutionary perspective, primarily as a source of primnoids diversity, with dispersals outward the SO occurring at different times along the Cenozoic.

From the selected sample abiotic and biotic factors, only one time-continuous abiotic factor, the ocean geochemistry, appears to drive the diversification of sub-Antarctic primnoids, encouraging previous hypotheses on the relevance of such a driver on anthozoan's evolution (Quattrini et al., 2020). In contrast, none of such biotic nor abiotic factors appear to be significant for primnoids diversification on a global scale, emphasizing that abiotic factors could act with more severity in some particular regions and taxa. Reinforcing previous findings (Quattrini et al., 2020), a significant and positive change in the global and regional (SO) primnoid diversification dynamics was detected at the

PETM, a time of abrupt climatic perturbations. The increase in the diversification rate after the PETM is probably related to the ecological opportunity following extinction events and reef crises, as previously proposed. Nevertheless, it is also plausible that the transient interhemispheric switch in deep-water formation along the PETM could increase the geographic isolation and spur novel ecological interactions than those faced by primnoids under pre-PETM oceanic circulation patterns. Finally, the PETM is perhaps the closest analog to present and future anthropogenic-induced climate change (Foster *et al.* 2018), affecting modern marine ecosystems and biodiversity in several ways at global and regional scales (Constable *et al.* 2014; Bryndum-Buchholz *et al.* 2019). However, considering how environmental conditions at the PETM appear to shape the diversification of primnoids, we remain optimistic that they will persist in the face of the Anthropocene changing oceans (Tyrrell 2011)

CRediT authorship contribution statement. Mónica Núñez-Flores: Conceptualization, Methodology, Validation, Formal analysis, Investigation, Data curation, Writing – original draft, Writing – review & editing, Funding acquisition. **Andrés Solórzano**: Methodology, Validation, Investigation, Data curation, Writing – review & editing. **Jorge Avaria-Llautureo**: Methodology, Validation, Resources, Investigation, Writing – review & editing, Supervision. **Daniel Gomez-Uchida**: Validation, Investigation, Writing – review & editing, Supervision. **Pablo López-González**: Validation, Investigation, Resources, Writing – review & editing, Supervision, Project administration, Funding acquisition.

Declaration of Competing Interest. The authors declare that they have no known competing financial interests or personal relationships that could have influenced the work reported in this paper.

Acknowledgements. We thank Chris Venditti for assistance in biogeographic analyses on BayesTraits, and José Garrido for help in lab work and protocols.

Funding. This research was partially funded by ANID–PCHA/Doctorado Nacional/2017–21170438 (to MNF), the Instituto Antártico Chileno (INACH; grant DG_04_19 to MNF), and the Spanish Ministry of Economy, Industry, and Competitiveness (grant CTM2017–83920-P DIVERSICORAL to PLG). JAL was supported by FONDECYT postdoctoral grant N° 3200654. AS was partially supported by FONDECYT postdoctoral grant N° 3220078.

Table 3.1. Results from RPANDA analyses of primnoids at global scale.

Models	Model acronym	NP	logL	AICc	AICω	ΔAICc	λ	α	μ	β
Constant	BCST	1	-507.85	1017.74	0.00	26.77	0.07	-	-	-
	BCSTDCST	**2**	**-493.44**	**990.97**	**0.13**	**0.00**	**0.16**	**-**	**0.13**	**-**
Time	BTimeVar	2	-496.5	997.1	0.01	6.13	0.1	-0.02	-	-
	BTimeVarDCST	3	-493.27	992.74	0.05	1.77	0.16	0	0.12	-
	BCSTDTimeVar	3	-493.25	992.71	0.05	1.74	0.16	-	0.13	0
	BTimeVarDTimeVar_EXPO	4	-493.1	994.53	0.02	3.56	0.17	-0.01	0.14	-0.02
Ocean Geochemestry	BGeoCheVar	2	-495.65	995.41	0.01	4.44	0.02	0.28	-	-
	BGeoCheVarDCST	3	-493.18	992.57	0.06	1.60	0.16	0.01	0.12	-
	BCSTDGeoCheVar	3	-493.22	992.64	0.06	1.67	0.16	-	0.13	-0.01
	BGeoCheVarDGeoCheVar	4	-492.94	994.22	0.03	3.25	0.42	-0.04	0.38	-0.04
Sea level	BSeaVar	2	-498.71	1001.52	0.00	10.55	0.07	-0.01	-	-
	BSeaVarDCST	3	-493.15	992.5	0.06	1.53	0.16	0	0.12	-
	BCSTDSeaVar	3	-493.2	992.61	0.06	1.64	0.16	-	0.13	0
	BSeaVarDSeaVar	4	-492.84	994.01	0.03	3.04	0.16	0	0.13	0
Temperature	BTempVar	2	-497.13	998.37	0.00	7.40	0.14	-0.09	-	-
	BTempVarDCST	3	-493.24	992.69	0.06	1.72	0.16	0	0.13	-
	BCSTDTempVar	3	-493.26	992.71	0.05	1.74	0.16	-	0.13	0
	BTempVarDTempVar	4	-492.84	994.03	0.03	3.06	0.16	0.01	0.14	0
Continental fragmentation	BFragVar	2	-495.92	995.95	0.01	4.98	0.08	-0.78	-	-

	BFragVarDCST	3	-493.19	992.58	0.06	1.61	0.17	-0.02	0.14	-
	BCSTDFragVar	3	-493.2	992.59	0.06	1.62	0.16	-	0.13	0.03
	BFragVarDFragVar	4	-492.84	994.02	0.03	3.05	0.18	0.12	0.15	0.16
CO_2	BCO2Var	2	-502.68	1009.46	0.00	18.49	0.12	0	-	-
	BCO2VarDCST	3	-493.24	992.69	0.06	1.72	0.16	0	0.13	-
	BCSTDCO2Var	3	-493.27	992.73	0.05	1.76	0.16	-	0.13	0
	BCO2VarDCO2Var	4	-493.23	994.79	0.02	3.82	0.15	0	0.13	0
Dispersal rate	BDrVar	2	-499.21	1002.52	0.00	11.55	0.06	0.35	-	-
	BDrVarDCST	3	-497.07	1000.36	0.00	9.39	0.13	0.04	0.09	-
	BCSTDDrVar	3	-496.89	999.99	0.00	9.02	0.13	-	0.09	-0.09
	BDrVarDDrVar	4	-496.82	1001.98	0.00	11.01	0.15	-0.09	0.11	-0.15

The table includes the model, the number of parameters in the model (NP), the estimated log-likelihood (logL), the corrected Akaike information criterion (AICc), the Akaike weight of the model (Akaike ω), the delta AIC (ΔAICc), and the corresponding parameter estimates (λ = speciation rate at present, α = parameter controlling the dependency of speciation rate on time or temperature, μ = extinction rate at present, and β = parameter controlling the dependency of extinction rate on time or temperature). The best-fitting model is highlighted in bold.

Table 3.2. Results from episodic diversification analyses in TREEPAR on a random sample of 250 time-calibrated trees of primnoids at a global scale.

Models	**BD with No Shift Time**	**BD with 1 Shift Time**	**BD with 2 Shift Times**	**BD with 3 Shift Times**	**BD with 4 Shift Times**
NP	2	**5**	8	11	14
logL	-493.440±1.476	**-490.088±1.472**	-487.555±1.467	-485.371±1.473	-483.442±1.476
AICc	990.980±2.953	**990.684±2.943**	992.362±2.934	995.100±2.945	998.737±2.952
AICω	0.356	**0.413**	0.178	0.045	0.007
r_1	0.032	**0.024±0.008**	0.019±0.008	0.015±0.010	0.006±0.014
ε_1	0.797±0.003	**0.802±0.035**	0.846±0.045	0.928±0.078	1.035±0.147
st_1	—	**56.527±2.768**	27.616±1.967	22.900±1.803	20.606±1.710
r_2	—	**-0.970±0.083**	-0.001±0.038	-0.005±0.032	-0.025±0.033
ε_2	—	**1.085±0.047**	0.899±0.058	0.936±0.061	0.941±0.063
st_2	—	—	70.606±2.522	40.687±2.092	37.393±2.084

r_3	—	—	-1.146±0.086	-0.005±0.050	0.057±0.065
ε_3	—	—	1.220±0.086	0.866±0.029	0.911±0.036
st_3	—	—	—	76.462±2.335	49.482±2.136
r_4	—	—	—	-1.238±0.087	-0.146±0.045
ε_4	—	—	—	1.356±0.121	1.427±0.386
st_4	—	—	—	—	81.463±2.239
r_5	—	—	—	—	-1.296±0.087
ε_5	—	—	—	—	1.409±0.121

Bold columns represent the best model. The best-supported model has a single rate-shift, as determined by the lowest AICc and highest AICω. r_1 denotes the diversification rate and ε_1 is the turnover, both inferred between the Present (0 Ma) and the shift time 1 (st_1). BD = birth-death; NP = number of parameters; logL = log-likelihood; AICc = corrected Akaike Information Criterion. Parameter estimates; AICω = Akaike Information Criterion weights. r = net diversification rate (speciation - extinction); ε= turnover (extinction/speciation); st = shift time on diversification rate.

DISCUSIÓN GENERAL

La presente tesis doctoral abordó tres líneas principales de investigación dentro de la biología evolutiva, incluyendo sistemática filogenética, biogeografía histórica y macroevolución, utilizando como modelo de estudio a la familia Primnoidae, un grupo de octocorales ecológicamente importante en aguas profundas, como modelo de estudio. Los principales resultados obtenidos durante el desarrollo de esta tesis doctoral son los siguientes: **1**) se describieron seis nuevas especies de formas *bottlebrush* del género *Thouarella* en el SO utilizando un enfoque integrativo (capítulos I–II); **2**) se estimó que el suroeste del Océano Pacífico es la probable área ancestral de la familia Primnoidae (capítulo III); y **3**) se infirió que el máximo térmico del Paleoceno-Eoceno y la química oceánica (proporción Mg/Ca) son los probables impulsores de la diversificación de la familia Primnoidae en el Océano Austral (capítulo III). Estos resultados se discuten con mayor detalle a continuación.

Seis nuevas especies del género *Thouarella* en el Océano Austral

La riqueza de especies en ambientes marinos esta infraestimada (Tittensor *et al.* 2010; Mora *et al.* 2011). Los octocorales de aguas profundos siguen estando poco explorados. La dificultad de muestrear en dichos ambientes, y en otros como por ejemplo el Océano Austral, aunado a la escasa financiación encaminada a la formación de nuevas generaciones de investigadores capaces de analizar caracteres de diferentes fuentes de información para delimitar taxones ocasiona la falta de especialistas para muchos grupos taxonómicos, y finalmente, al menos en parte, la presencia de déficit linneano y wallaceano en el grupo.

Para el estudio de la diversidad no descrita del género *Thouarella* del SO, se empleó una aproximación integrativa en la delimitación de especies (Dayrat 2005; De Queiroz 2005; De Queiroz 2007; Padial et al. 2010). En este

marco de trabajo, se utilizó el concepto “unificado” de especie, que se define como un linaje de metapoblación que evoluciona independientemente (De Queiroz 2007). Para ello entonces se utilizaron diferentes líneas de evidencia (i.e., divergencia morfológica y genética, monofilia), que son propiedades biológicas relevantes para la delimitación de especies (De Queiroz 2007). Cualquiera de estas caracteristicas, que antiguamente servían para definir conceptos de especies distintos, son ahora evidencias de la divergencia entre linajes, y cuantas más haya, más apoyo tendrá la hipótesis de la existencia de dos especies diferentes (Castroviejo-Fisher, 2009). Quizás una sola evidencia no sea suficiente para delimitar especies, pero tampoco ninguna de ellas debe erigirse como estrictamente necesaria, por lo que su ausencia no contradice la existencia de una separación entre los linajes (De Queiroz 2007).

Tal aproximación integrativa se utilizó por primera vez para la familia Primnoidae, e incluyó el estudio de marcadores mitocondriales (*MutS*, *Cox1*) y nucleares (*28S*) en conjunto con métodos de delimitación de especies y la revisión exhaustiva de los caracteres macro y microscópicos de las colonias y el escleroma, para abordar el estudio de la diversidad de *Thouarella* del SO (Núñez-Flores *et al.* 2020; Núñez-Flores *et al.* 2021). El uso de esta aproximación integrativa (cuando es posible) mitiga el impacto de utilizar sólo caracteres morfológicos como la única fuente de información para describir y delimitar especies. Nuestros resultados permitieron incrementar significativamente el entendimiento de la diversidad del género *Thouarella*, a partir de la descripción formal de seis nuevas especies: *T. islai, T. weddellensis, T.polarsterni, T. amundseni , T. dolichoespinosa* y *T. pseudoislai* (Núñez-Flores *et al.* 2020; Núñez-Flores *et al.* 2021).

Previo al presente trabajo, la diversidad global del género *Thouarella,* el segundo con más especies descritas dentro de la Familia Primnoidae alcanzaba las 35 especies, 21 de las cuales eran reconocidas en el Océano Austral y el Atlántico Sur, y nueve de ellas endémicas para las regiones Antártica y

subantártica (Zapata-Guardiola and López-González 2010a; Zapata-Guardiola y López-González 2010d; Zapata-Guardiola y López-González 2010b; Taylor *et al.* 2013). La alta endemicidad de este género en el Océano Austral es consistente con reconocidos altos niveles de endemismo para la fauna bentónica Antártica, que varía entre 50 y 97% según el grupo estudiado (Griffiths *et al.* 2009; Kaiser *et al.* 2013; Broyer *et al.* 2014). Con las seis nuevas especies formalmente descritas aquí, la diversidad del género aumentó a 41 especies (Taylor y Rogers 2017). De éstas 41 especies, 15 son endémicas de la Antártica y sub-Antártica, apoyando así la hipótesis de que la diversidad del género en el Océano Austral esta infraestimada (Bogantes *et al.* 2020; Núñez-Flores *et al.* 2020; Núñez-Flores *et al.* 2021).

El uso de una aproximación integrativa utilizando marcadores mitocondriales y nucleares en conjunto con datos morfológicos, nos permitió sugerir, por primera vez, la presencia de especies crípticas de primnoides Antárticos y sub-Antárticos, basándonos en la posible existencia de especies gemelas (*sibbling*) en *T. undulata y T. crenelata* (Núñez-Flores et al. 2021). De tal forma, los primnoides se unen al grupo de invertebrados marinos del Océano Austral que muestran evidencias de especiación críptica (Linse *et al.* 2007; De Broyer *et al.* 2011; Allcock *et al.* 2011; Halanych y Mahon 2018; González-Wevar *et al.* 2019). Adicionalmente se obtuvieron secuencias de los genes *Muts, Cox1* y *28S* para los holotipos de las especies de *Thouarella viridis* (Zapata-Guardiola y López-González 2010d), *Thouarella minuta* (Zapata-Guardiola y López-González 2010d), y *T. andeep* (Zapata-Guardiola y López-González 2010d), así como para otros ejemplares de primnoides pertenecientes a otros géneros que por el momento se encuentran en preparación para su descripción formal.

Finalmente, dada la gran extensión de los hábitats bentónicos del Océano Austral y su probable papel como centro de diversificación de diferentes géneros (Taylor y Rogers 2015; Núñez-Flores *et al.* 2021) es

esperable el descubrimiento de nuevas especies de primnoides a partir del estudio detallado de la gran cantidad de materiales depositados en varios museos y colecciones alrededor del mundo (e.g., USNM, BECA), como resultado de muchos esfuerzos de muestreo internacionales y de colaboración en la región. De hecho, trabajos en curso basados en especímenes de la colección BECA sugieren la existencia de 4–6 especies nuevas adicionales, solo dentro del género *Thouarella*, las cuales se encuentran en revisión y descripción actualmente.

Nuevos avances en nuestro entendimiento de la historia evolutiva de los primnoides a escalas regionales (SO) y globales

Sistemática molecular y tiempo de divergencia de la familia Primnoidae

La topología recuperada (capítulo III) concuerda bien con filogenias moleculares previas inferidas para la familia (Taylor y Rogers 2015, 2017; Cairns y Wirshing 2018; Núñez-Flores *et al.* 2020) recuperando, entre otros, la monofilia de la familia, la existencia del clado de primnoides subantárticos y la monofilia del género Thouarella. Adicionalmente, nuestra filogenia calibrada (capítulo III) sugiere que los primnoides tienen un ancestro común más reciente (TMRCA) que data del Albiense (Cretácico Inferior; 112 Ma). El tiempo de divergencia estimada de Primnoidae de su grupo hermano (miembros de la familia parafilética Chrysogorgiidae), así como el TMRCA del clado de sub-Antárctico, y los géneros con más especies descritas dentro de la familia, *Narella* y *Thouarella* es entre 20 y 30 Ma de años más antigua que la previamente sugerida (Taylor y Rogers 2015; Dueñas *et al.* 2016).

Parece plausible que las condiciones cambiantes y eventos anóxicos de los océanos Cretácicos (Prokoph *et al.* 2008; Friedrich *et al.* 2012; Föllmi 2012) fueran importantes en la evolución temprana de diferentes clados de

octocorales que parecen originarse y diversificarse durante este periodo (Reich y Kutscher 2011; Taylor y Rogers 2015; García-Cárdenas *et al.* 2020).

¿Cuál es el área de distribución ancestral de la familia Primnoidae?

Nuestros resultados respaldaron la hipótesis del Océano Pacífico como área ancestral de la familia Primnoidae, y brindan una distribución ancestral refinada para los primeros primnoides al suroeste de este océano durante el Albiense (112 Ma; Figura 3.1). Adicionalmente, nuestros resultados revelan varios patrones biogeográficos previamente desconocidos. Por ejemplo, ilustramos la diversidad de rutas tomadas por primnoides en todo el mundo, incluso por taxones que terminaron casi en el mismo lugar (Figura 3.3). Los primnoides también muestran un patrón general en el que los nodos ancestrales se agrupan generalmente, pero con un descendiente que ocasionalmente se aleja de sus predecesores. Por lo tanto, sus eventos de dispersión se describen principalmente por movimientos lentos y de corta distancia intercalados con algunos eventos de movimientos relativamente rápidos junto con distancias más considerables (Figura 3.2). Fue posible reconocer, además, que casi la mitad de los eventos de especiación evaluados en nuestra filogenia de primnoides ocurrieron dentro de distancias relativamente cortas (menores a 10 km). Considerando que puede existir flujo de genes dentro de poblaciones modernas de algunas especies de primnoides a lo largo de distancias de hasta 200 km (Yesson *et al.* 2018), es posible sugerir que el modo de especiación simpátrico podría ser relativamente común en esta familia de organismos de aguas profundas.

La velocidad de dispersión estimada para los primnoides fue heterogénea a lo largo del tiempo y entre clados, y se identificaron algunas instancias de especiación a través de la dispersión a larga distancia (Figura 3.2). La dispersión a larga distancia podría predecirse con mayor probabilidad para octocorales con una etapa larval pelágica (*broadcast spawners*) que puede

abarcar desde unos pocas semanas hasta varios meses, pero en menor probabilidad para octocorales que incuban sus larvas (*brooders*) y se asientan a distancias cortas de sus padres (Dueñas *et al.* 2016). Aunque existen pocos estudios sobre las estrategias reproductivas en primnoides, se han reconocido tanto taxones *broadcast spawners* (*Primnoa chilensis*) como *brooders* (*Thouarella* variabilis. *Fannyella spinora, F. rossi*) (Brito *et al.* 1997; Orejas *et al.* 2007; Waller *et al.* 2014; Rossin *et al.* 2017b). Aunque datos de las estrategias de reproducción sexual para las especies incluidas en nuestra filogenia son escasos, estos son congruentes con un escenario en el que la mayor parte de la especiación a través de eventos de dispersión a larga distancia se restringe principalmente a linajes primnoides tipo *broadcast spawners*. En este sentido, se propone que la distancia de dispersión de los primnoides probablemente fue mediada por características intrínsecas de la especie, como su modo de reproducción.

Nuestros resultados también subrayan patrones específicos para la fauna del Océano Austral. El origen de las comunidades faunísticas modernas del SO es complejo, ya que consiste en elementos endémicos que se diversifican in situ (incluso desde el Mesozoico) y componentes que han emigrado desde América del Sur a través del Arco de Escocia y/o cuencas profundas adyacentes en diferentes pulsos durante el Cenozoico (Crame 2018; Halanych y Mahon 2018). La colonización del SO (aguas al sur de los 55°S) por primnoides inició durante el Campaniense (~74 Ma; Cretácico superior) por el TMRCA del clado de primnoides antárticos y subantárticos (en adelante, clado Subantártico), decenas de millones de años antes del establecimiento de la ACC durante el Eoceno medio (Torsvik *et al.* 2008). Por lo tanto, los primnoides se unen a un número cada vez mayor de invertebrados marinos antárticos de origen pre-ACC, como isópodos, ostrácodos, anfípodos y moluscos (Clarke 2008; Clarke y Crame 2010; Crame 2018), y sugiere que el grupo tiene una larga y próspera historia evolutiva *in situ* en el SO (Taylor y Rogers 2015).

Nuestros resultados nos permiten reconocer, además, eventos de dispersión hacia y desde el SO, pero estos no ocurrieron simultáneamente o de forma simétrica (Figuras 3.1–3.3). Los primnoides inmigrantes llegaron al SO solo durante los últimos 5,3 Ma, coincidiendo con períodos glaciales e interglaciares (De Schepper *et al.* 2014), mientras que los primnoides emigrantes del clado de primnoides subantárticos se dispersan fuera del SO en diferentes momentos a lo largo del Cenozoico, incluidos eventos de dispersión después del inicio e intensificación de la ACC (Torsvik *et al.* 2008). En este sentido, nuestros resultados apoyan la noción de que la ACC podría considerarse una barrera semipermeable para los octocorales de aguas profundas incapaz de limitar los eventos de dispersión (Dueñas *et al.* 2016).

El SO pudo actuar como “fuente” (con especiación *in situ* y dispersión a otros océanos) y “sumidero” (recibiendo inmigrantes de otros océanos) de diversidad de primnoides, aunque con la primera predominando sobre la segunda. Finalmente, teniendo en cuenta que los primnoides son principalmente taxones de aguas profundas, es posible hipotetizar que sus posibles rutas de dispersión hacia o desde el SO probablemente fueran a lo largo de diferentes corrientes de aguas profundas (e.g., *Antarctic bottom water; Circumpolar Deep Water*; *North Atlantic Deep Water*). Por ejemplo, el movimiento hacia el norte de las aguas profundas de la Antártida (e.g., *Antarctic bottom water*) puede servir como conexión entre las aguas profundas del SO y otras cuencas profundas adyacentes (Saucède *et al.* 2014). Esta corriente ha sido invocada como principal mecanismo de dispersión de los Munnopsidae (Isopoda), originados en el Mar de Weddell, hacia aguas septentrionales del Atlántico (Malyutina y Brandt 2007). Por otra parte, en la sección atlántica por debajo de los 800-1000 m, una rama del agua profunda circumpolar (*Circumpolar Deep Water*) fluye hacia el norte dentro de la corriente de Malvinas; y debajo de esta existe una masa de agua más cálida (*North Atlantic Deep Water*) que fluye hacia la Antártica (Barboza *et al.* 2011; Saucède *et al.*

2014). Si las posibles rutas de dispersión hacia o desde el SO fueron las aguas profundas, entonces la presencia de primnoides en la plataforma continental del SO puede ser explicada a través de la emergencia polar, tal como se ha reportado en algunos linajes de pulpos (Strugnell *et al.* 2011). Sin embargo, estas hipótesis aún deben ser examinadas explícitamente.

Por otra parte, aun cuando el desarrollo de la presente tesis doctoral contribuyó a reducir el déficit linneano y wallaceano de los primnoides, es claro que nuestro conocimiento sobre la diversidad y distribución del grupo en el SO es aún incompleto. Por ejemplo, la mayoría de los especímenes revisados y secuenciados provienen de la Península Antártica y el Mar de Weddell. Por esta razón, no es posible reconocer patrones de distribución regional claros para los representantes de la familia, y menos compararlos con aquellos patrones reconocidos para otros grupos bentónicos en el SO (Knox 1960; Griffiths *et al.* 2009; Briggs y Bowen 2012; Broyer *et al.* 2014; González-Wevar *et al.* 2017). Tales estudios quedan supeditados a un esfuerzo de muestreo más completo, incluyendo áreas subantárticas (e.g., Islas Kerguelen).

¿Cuáles fueron los impulsores de la diversificación de la familia Primnoidae en el Océano Austral?

En el caso particular de los primnoides, previamente se propuso que las fluctuaciones en el posicionamiento latitudinal del ACC durante el Mioceno medio potencialmente contribuyeron a la diversificación de formas *bottlebrush* del SO (Dueñas *et al.* 2016). Sin embargo, tal hipótesis debería ser examinada, por ejemplo, utilizando el denominado “clado subantártico” ya que parece representar una radiación *in situ* que ocurrió previa al inicio del ACC durante finales del Eoceno (Taylor y Rogers 2015; Cairns y Wirshing 2018). Nuestros resultados (capítulo III) apoyan la existencia de un clado de primnoides subantártico (Figura 3.1), y sugieren, además, que su origen y colonización del SO se remonta a finales del Cretácico (~74 Ma). En consecuencia, la

antigüedad y distribución ancestral del grupo, permite evaluar explícitamente si los eventos climáticos/oceanográficos ocurridos durante los ultimo 40 Ma en el SO impactaron sobre sus dinámicas de diversificación en el SO.

En el capítulo III, el uso de modelos "*episodic birth-death*" (Stadler 2011) permitió detectar posibles cambios en la diversificación de los primnoides subantárticos los cuales pudieron haber ocurrido en cualquiera de los diferentes periodos temporales discretos ocurridos durante los últimos 40 Ma (e.g., 2.58–0.01 Ma, 34–28 Ma, 12–14 Ma) en el SO. Estos modelos fueron ajustados a una submuestra del árbol de primnoides que incluye únicamente taxones (52 spp.) cuya distribución geográfica se ha descrito en las regiones antárticas y subantárticas (>55°S). En contraposición a nuestra predicción, y con ideas de autores previos (Dueñas *et al.* 2016), los resultados indican que ninguno de los periodos temporales asociados al inicio e intensificación de la ACC, o a los ciclos glaciales del Plioceno y Pleistoceno afectaron de forma significativa la dinámica de diversificación de los primnoides del SO (capítulo III).

En contraste, el mejor modelo de diversificación episódica sugiere la existencia de un cambio significativo en la tasa de diversificación de los primnoides subantárticos durante el límite Paleoceno/Eoceno, cerca del Máximo Termal del Paleoceno-Eoceno (PETM, por sus siglas en inglés), una perturbación climática abrupta a escala planetaria de calor global extremo superpuesto a condiciones climáticas de efecto invernadero a largo plazo, junto con una liberación masiva de carbono en el sistema océano-atmósfera (McInerney y Wing 2011; Dunkley Jones *et al.* 2013; Foster *et al.* 2018). Durante el PETM, la temperatura de las profundidades oceánicas aumento entre 4° a 6°C, ocurrió una acidificación severa del océano a menudo acompañada de hipoxia, y se dieron cambios transitorios en los patrones de circulación profundidad en el océano (Zachos *et al.* 2005; Tripati y Elderfield 2005; Nunes y Norris 2006; Zachos *et al.* 2008; Dunkley Jones *et al.* 2013).

Nuestros resultados indican que los primnoides subantárticos muestran una diversificación neta positiva, lo que refleja una mayor tasa de especiación que de extinción, después del PETM. Este patrón es similar al reportado en otros grupos marinos como antozoos (Quattrini *et al.* 2020). Los antozoos, un grupo que incluye a los primnoides, muestra varios pulsos de diversificación luego de extinciones masivas y crisis de arrecifes, incluido un episodio de aumento de la tasa de diversificación cercano al límite Paleoceno-Eoceno (Quattrini *et al.* 2020). Estos autores plantearon la hipótesis de que tales aumentos en la diversificación pueden estar asociados a la expansión hacia nuevos nichos ecológicos luego de eventos de extinción y crisis de arrecifes (Quattrini *et al.* 2020). Tal explicación está relacionada al hecho que diferentes grupos de antozoos (e.g., escleractinios y octocorales) pueden competir por espacio y supervivencia especialmente en ambientes de aguas poco profundas (Tkachenko *et al.* 2007; Atrigenio *et al.* 2017). Sin embargo, en aguas profundas la importancia de las interacciones ecológicas, aunque presentes, aún debe caracterizarse más ampliamente (Allcock y Johnson 2019).

Es plausible que el incremento en la tasa de diversificación de los primnoides del SO posterior al PETM se relacione con la disponibilidad de nichos ecológicos en ambientes bentónicos profundos asociados a la extinción de taxones competidores (Quattrini *et al.* 2020), aunque éstos no fueran necesariamente otros antozoos. Sin embargo, dada la amplia variabilidad en los factores modernos regulando la distribución de especies de aguas profundas tales como la complejidad del hábitat, corrientes de fondo, temperatura, y productividad (Costello y Chaudhary 2017; Puerta *et al.* 2020), es difícil descartar el papel que juegan los factores abióticos (HCJ) en la conducción de los patrones de diversificación de los primnoides del SO. En este sentido, se sugiere que el cambio interhemisférico de corta duración (~50 Kyr) en la formación de aguas profundas a lo largo del PETM (Nunes y Norris 2006) también pudo favorecer el patrón de diversificación detectado de los primnoides

del SO, al aumentar su aislamiento geográfico (desencadenando la especiación alopátrica) y/o estimulando nuevas interacciones ecológicas (que desencadenan la especiación simpátrica) que a las que se enfrentaban bajo los patrones de circulación oceánica originales (pre-PETM).

Finalmente, los resultados del modelo de diversificación episódica son particularmente interesantes ya que la mayoría de los estudios enfocados en la historia evolutiva de la biota antártica no consideran eventos anteriores a los últimos 38 Ma (Halanych y Mahon 2018). En este sentido, futuros estudios deberían considerar evaluar el impacto de eventos geológicos/climáticos más antiguos que el establecimiento inicial de la ACC (e.g., PETM) sobre las dinámicas evolutivas de la fauna del SO, especialmente en grupos con una larga historia evolutiva *in situ*.

Por otra parte, los factores abióticos pueden modelar las tasas de diversificación de forma continua (Condamine *et al.* 2013; Morlon *et al.* 2016; Condamine *et al.* 2018b; Condamine y Kergoat 2021; Baird *et al.* 2021). Es por ello, que se evaluó si algunos factores abióticos continuos como la temperatura, el CO_2 (como proxy de acidificación de los océanos), el nivel del mar (como proxy de área), la fragmentación continental y las condiciones químicas oceanográficas afectaron las dinámicas de diversificación del clado de primnoides subantártico (ver detalles en el capítulo III). Por ejemplo, las fluctuaciones del radio Mg/Ca del agua de mar han fluctuado entre los llamados “mares de aragonito” y “mares de calcita” a través el tiempo geológico, donde proporciones altas de Mg/Ca favorecen la precipitación de aragonito y calcita alta en Mg, mientras que proporciones bajas de Mg/Ca promueven la precipitación de calcita baja en Mg (Ries 2010; Hönisch *et al.* 2012). Recientemente, se propuso que la química de los océanos ha sido importante en la evolución de los antozooa (Quattrini *et al.* 2020), donde los corales formadores de arrecifes aragoníticos (corales escleractinios) evolucionaron cuando las proporciones de Mg/Ca eran altas (mares de aragonito), mientras

que otros antozoos con diferentes tipos de esqueleto (e.g., proteináceo, calcítico) evolucionaron durante períodos no propicios para la precipitación de aragonito (mares de calcita) (Quattrini *et al.* 2020).

Utilizando modelos de diversificación dependientes de factores ambientales (y modelos nulos) (Condamine *et al.* 2013) en un marco de comparación de hipótesis basada en máxima verosimilitud (Morlon *et al.* 2016), se identificó que el modelo con mejor ajuste a los datos, es aquel, en el cual la especiación de los primnoides subantárticos varía en función del tiempo sin extinción (capítulo III). Sin embargo, el segundo mejor modelo apoya la correlación positiva entre la geoquímica del océano y la tasa de especiación de los primnoides subantárticos sin extinción. Ambos modelos tienen un poder explicativo similar, apoyando la idea que la geoquímica oceánica tuvo un papel relevante en la dinámica de diversificación de los primnoides subantárticos (i.e., su diversificación está correlacionada positivamente con altas relaciones Mg/Ca en el agua de mar). Estos resultados respaldan hipótesis previas (Quattrini *et al.* 2020), y son congruentes con la composición mineralógica de aragonito y calcita rica en magnesio del eje (*axis*) y base (*holdfast*) de las especies de primnoides reportadas en la literatura (Bayer and Macintyre 2001).

En resumen, nuestros novedosos resultados indican que los primnoides el SO exhiben una dinámica de diversificación acoplada a: 1) cambios abruptos en las condiciones ambientales durante el PETM, que pudieron desencadenar eventos de extinción y nichos ecológicos disponibles, así como cambios transitorios en las corrientes oceánicas profundas; y 2) cambios continuos de la química de los océanos, con una mayor diversificación en condiciones oceánicas con radios de Mg/Ca altos. Es entonces posible afirmar que la diversidad moderna de los primnoides antárticos fue generada por la acción de factores abióticos (HCJ) continuos (i.e., química oceánica) y abruptos (i.e., PETM), actuando sobre los procesos macroevolutivos a lo largo del tiempo geológico, y que estos factores actuaron posteriormente a la colonización

temprana del Océano Austral por pocos linajes de primnoides. De esta forma hemos encontrado soporte a la hipótesis planteada en esta tesis doctoral.

Finalmente, en conjunto, los resultados obtenidos durante el desarrollo de la presente tesis doctoral (Capítulos I-III) pueden ser enmarcados dentro de una las líneas de investigación del Programa Nacional de Ciencia Antártica (PROCIEN) enfocada en determinar el "Estado del ecosistema antártico" (Línea 1). Adicionalmente, contribuyen a responder una de las preguntas formuladas por el Comité Científico de Investigación Antártica (SCAR) en el 1st SCAR Antarctic and Southern Ocean Science Horizon Scan: "*How has life evolved in the SO in response to dramatic events in the Earth's history?*"(Kennicutt *et al.* 2015).

¿Cuáles fueron los impulsores de la diversificación de la familia Primnoidae a nivel global?

Finalmente, es importante considerar si las dinámicas de diversificación estimadas para la familia Primnoidae difieren a escalas geográficas. Especialmente porque las tasas diversificación pueden regionalmente heterogéneas incluso durante eventos que se manifestaron globalmente, destacando la necesidad de aproximaciones espacialmente explícitas de los procesos macroevolutivos a través del tiempo geológico (Flannery-Sutherland *et al.* 2022).

Los resultados de esta tesis revelan que la variación en la riqueza de especies dentro de los primnoides se puede explicar sin invocar dinámicas de diversificación de ramas heterogéneas (Figura 3.4b). El mejor modelo para explicar su diversificación fue el de tasa de especiación y extinción constante (Tabla 3.2). En este sentido, no se encontró evidencia del efecto significativo de los factores abióticos y bióticos (continuos en el tiempo) evaluados sobre la diversificación de los primnoides a nivel global, lo cual soporta la idea de que los clados no se diversifican uniformemente a través del espacio y que estos

pueden mostrar diferentes dinámicas temporales a diferentes escalas (Morlon 2014; Skeels 2019; Flannery-Sutherland *et al.* 2022), y es por ello que muchas veces los patrones globales de diversidad no reflejan las dinámicas que se dan a niveles regionales. Por otro lado nuestros resultados pueden sugerir varios escenarios, incluyendo que: 1) las tasas de diversificación global podrían ser impulsadas principalmente por factores bióticos o abióticos continuos en el tiempo adicionales a los considerados aquí, 2) su dinámica de diversificación estuvo desencadenada por uno de los factores considerados pero actuando predominantemente sobre escalas regionales en lugar de globales, o 3) su dinámica de diversificación responde a cambios episódicos en lugar de continuos en el tiempo. Nuestros resultados apuntan a que el segundo (ver sección anterior) y tercer escenario son plausibles.

Nuestros modelos de diversificación episódicos y gráfico LTT ilustran la existencia de un cambio significativo en la dinámica de diversificación global de primnoides durante el máximo termal del Paleoceno-Eoceno (~ 56 Ma; PETM), tal como ocurre cuando únicamente se evaluaron los primnoides subantárticos. En este sentido, el análisis a nivel global sugiere el PETM modificó las dinámicas de diversificación a escalas globales y regionales (SO), probablemente favoreciendo la disponibilidad de nichos ecológicos asociados a la extinción de taxones competidores, y/o al cambio interhemisférico de corta duración en la formación de aguas profundas. Finalmente, es posible sugerir que a nivel global y regional están actuando los mismos impulsores abruptos (PETM) sobre la diversificación, mientras que los factores abióticos continuos, específicamente la química de los océanos, parecen actuar diferencialmente en escalas regionales más que escalas globales.

CONCLUSIONES

- Reconocimos y describimos seis nuevas especies con formas bottlebrush del género *Thouarella* en el Océano Austral, *T. islai, T. weddellensis, T. polarsterni, T. amundseni, T. dolichoespinosa* y *T. pseudoislai*, utilizando un enfoque integrativo basado en una combinación de datos moleculares y morfológicos.
- Refinamos la sistemática molecular de la familia, y generamos la filogenia calibrada más completa que incluye 124 especies. Se encontró que el ancestro común más reciente de la familia monofilética Primnoidae data del Albiense (Cretácico Inferior; 112 Ma), mientras que el origen del clado de primnoides subantárticos se remonta al Campaniense (Cretácico Superior; 74 Ma).
- Se estimó el suroeste del Océano Pacífico, durante el Albiense, fue la localidad ancestral de la familia Primnoidae. Posteriormente, diferentes linajes de la familia se han dispersado alrededor del globo siguiendo numerosas rutas. Ademas, estos eventos de dispersión se describen predominantemente como lentos y de corta distancia, apoyando la hipótesis que la especiación simpátrica puede ser relativamente común en esta familia. La velocidad de dispersión estimada para los primnoides fue heterogénea a lo largo del tiempo, y se identificaron algunos eventos de dispersión a larga distancia. La distancia de dispersión de los primnoides probablemente fue mediada por su modo de reproducción, con eventos de dispersión a larga distancia restringidos principalmente a taxones *broadcast spawners*.
- La colonización del SO por primnoides inició durante el Campaniense (~74 Ma; Cretácico superior) decenas de millones de años antes del establecimiento de la ACC, lo que sugiere que el grupo tiene una larga y próspera historia evolutiva *in situ* en el SO. Se reconocieron diversos

eventos de dispersión hacia y desde el SO, pero éstos no ocurrieron simultáneamente o de forma simétrica. Los inmigrantes llegaron al SO solo durante los últimos 5,3 Ma, mientras que los emigrantes (del clado de primnoides subantárticos) se dispersan fuera del SO en diferentes momentos a lo largo del Cenozoico. En este sentido, la ACC podría considerarse una barrera semipermeable para los octocorales de aguas profundas incapaz de limitar eventos de dispersión.

- Nuestros resultados apoyan que la diversidad actual de los primnoides antárticos fue generada por la acción de diferentes factores abióticos actuando sobre los procesos macroevolutivos a lo largo del tiempo geológico. En particular, se reconoció que dos factores abióticos continuos (i.e., relaciones de Mg/Ca en el agua de mar) y abruptos (i.e., PETM) ejercieron una significativa influencia sobre la dinámica de diversificación de los primnoides antárticos.
- La diversificación de los primnoides antárticos está correlacionada positivamente con altas relaciones de Mg/Ca en el agua de mar, respaldando su relevancia en la evolución de los antozoos.
- Los primnoides exhibieron un cambio significativo (abrupto) en la tasa de diversificación cerca del límite Eoceno-Paleoceno (~58 Ma) a escala global y regional (SO), asociado al máximo termal del Paleoceno-Eoceno (PETM), un período de perturbación climática abrupta a escala planetaria de calor global extremo. Es plausible que el incremento en la tasa de diversificación de los primnoides posterior al PETM se relacione con la oportunidad ecológica, mediada por la disponibilidad de nichos ecológicos luego de la extinción de taxones competidores. Adicionalmente, el cambio interhemisférico de corta duración en la formación de aguas profundas a lo largo del PETM también pudo favorecer el patrón de diversificación detectado, al aumentar su aislamiento geográfico y/o estimulando nuevas interacciones ecológicas.

- El PETM es quizás el análogo más cercano al actual cambio climático global inducido de forma antropogénica, y considerando cómo este cambio abrupto en el clima afecto positivamente la diversificación de los primnoides, es posible hipotetizar que los primnoides tienen el potencial de persistir en los océanos cambiantes del Antropoceno.

BIBLIOGRAFÍA

Allcock, A. L., Barratt, I., Eléaume, M., Linse, K., Norman, M. D., Smith, P. J., Steinke, D., Stevens, D. W., and Strugnell, J. M. (2011). Cryptic speciation and the circumpolarity debate: A case study on endemic Southern Ocean octopuses using the COI barcode of life. *Deep-Sea Research Part II: Topical Studies in Oceanography* **58**, 242–249. doi:10.1016/j.dsr2.2010.05.016

Allcock, A. L., and Johnson, M. P. (2019). Interactions in the Deep Sea. In 'Interactions in the Marine Benthos'. pp. 474–487. (Cambridge University Press.) doi:10.1017/9781108235792.020

Alroy, J. (2010). Geographical, environmental and intrinsic biotic controls on Phanerozoic marine diversification. *Palaeontology* **53**, 1211–1235. doi:10.1111/j.1475-4983.2010.01011.x

Altuna, Á., and López-González, P. J. (2019). Description of two new species of bathyal Primnoidae (Octocorallia: Alcyonacea) from the Porcupine Bank (northeastern Atlantic). *Zootaxa* **4576**, 61–80. doi:10.11646/zootaxa.4576.1.3

Arcila, D., and Tyler, J. C. (2017). Mass extinction in tetraodontiform fishes linked to the Palaeocene-Eocene thermal maximum. *Proceedings of the Royal Society B: Biological Sciences* **284**. doi:10.1098/rspb.2017.1771

Atrigenio, M., Aliño, P., and Conaco, C. (2017). Influence of the blue coral Heliopora coerulea on scleractinian coral larval recruitment. *Journal of Marine Biology* **2017**. doi:10.1155/2017/6015143

Avaria-Llautureo, J., Venditti, C., Rivadeneira, M. M., Inostroza-Michael, O., Rivera, R. J., Hernández, C. E., and Canales-Aguirre, C. B. (2021). Historical warming consistently decreased size, dispersal and speciation rate of fish. *Nature Climate Change 2021 11:9* **11**, 787–793. doi:10.1038/s41558-021-01123-5

Baco, A. R., and Cairns, S. D. (2012). Comparing Molecular Variation to Morphological Species Designations in the Deep-Sea Coral *Narella* Reveals New Insights into Seamount Coral Ranges. *PLoS ONE* **7**, e45555. doi:10.1371/journal.pone.0045555

Baird, H. P., Miller, K. J., and Stark, J. S. (2011). Evidence of hidden biodiversity, ongoing speciation and diverse patterns of genetic structure in giant Antarctic amphipods. *Molecular Ecology* **20**, 3439–3454. doi:10.1111/j.1365-294X.2011.05173.x

Baird, H. P., Shin, S., Oberprieler, R. G., Hullé, M., Vernon, P., Moon, K. L., Adams, R. H., McKenna, D. D., and Chown, S. L. (2021). Fifty million years of beetle evolution along the Antarctic Polar Front. *Proceedings of the National Academy of Sciences of the United*

States of America **118**. doi:10.1073/pnas.2017384118

Barboza, C. A. de M., Moura, R. B., Lanna, A. M., Oackes, T., and Campos, L. S. (2011). ECHINODERMS AS CLUES TO ANTARCTIC ~ SOUTH AMERICAN CONNECTIVITY. *Oecologia Australis* **15**, 86–110. doi:10.4257/oeco.2011.1501.08

Barnosky, A. D. (2001). Distinguishing the effects of the Red queen and Court Jester on Miocene mammal evolution in the northern Rocky Mountains. *Journal of Vertebrate Paleontology* **21**, 172–185. doi:10.1671/0272-4634(2001)021[0172:DTEOTR]2.0.CO;2

Bayer, F. M., Grasshoff, M., and Verseveldt, J. (1983). Illustrated Trilingual Glossary of Morphological and Anatomical Terms Applied to Octocorallia. *Book*, 75.

Bayer, F. M., and Macintyre, I. G. (2001). The mineral component of the axis and holdfast of some gorgonacean octocorals (Coelenteratea: Anthozoa), with specieal reference to the family Gorgoniidae. *Proceedings of the Biological Society of Washington* **114**, 309–345. Available at: https://repository.si.edu/handle/10088/8300 [accessed 13 June 2022]

Bayer, F. M., and Stefani, J. (1988). Primnoidae (Gorgonacea) de Nouvelle-Calédonie. *Bulletin du Muséum National D'Histoire Naturelle* **4**, 449–518.

Benton, M. J. (1997). Models for the diversification of life. *Trends in ecology & evolution* **12**, 490–495. doi:10.1016/S0169-5347(97)84410-2

Benton, M. J. (2009). The Red Queen and the Court Jester: Species diversity and the role of biotic and abiotic factors through time. *Science* **323**, 728–732. doi:10.1126/science.1157719

Bickford, D., Lohman, D. J., Sodhi, N. S., Ng, P. K. L., Meier, R., Winker, K., Ingram, K. K., and Das, I. (2007). Cryptic species as a window on diversity and conservation. *Trends in Ecology & Evolution* **22**, 148–155. doi:10.1016/J.TREE.2006.11.004

Bilewitch, J. P., and Degnan, S. M. (2011). A unique horizontal gene transfer event has provided the octocoral mitochondrial genome with an active mismatch repair gene that has potential for an unusual self-contained function. *BMC Evolutionary Biology* **11**, 1–14. doi:10.1186/1471-2148-11-228

Bogantes, V. E., Whelan, N. V., Webster, K., Mahon, A. R., and Halanych, K. M. (2020). Unrecognized diversity of a scale worm, *Polyeunoa laevis* (Annelida: Polynoidae), that feeds on soft coral. *Zoologica Scripta* **49**, 236–249. doi:10.1111/zsc.12400

Bolnick, D. I., and Fitzpatrick, B. M. (2007). Sympatric speciation: Models and empirical evidence. *Annual Review of Ecology, Evolution, and Systematics* **38**, 459–487. doi:10.1146/annurev.ecolsys.38.091206.095804

Bouchet, P. (2006). 'The magnitude of marine biodiversity. In: Duarte C. M, editor. The exploration of marine biodiversity: scientific and technological challenges'.

Bouckaert, R. R., and Drummond, A. J. (2017). bModelTest: Bayesian phylogenetic site model averaging and model comparison. *BMC Evolutionary Biology* **17**, 1–11. doi:10.1186/s12862-017-0890-6

Bouckaert, R. R., Heled, J., Kühnert, D., Vaughan, T., Wu, C. H., Xie, D., Suchard, M. A., Rambaut, A., and Drummond, A. J. (2014). BEAST 2: A Software Platform for Bayesian Evolutionary Analysis Ed A. Prlic. *PLoS Computational Biology* **10**, e1003537. doi:10.1371/journal.pcbi.1003537

Brandt, A., De Broyer, C., Gooday, A. J., Hilbig, B., and Thomson, M. R. A. (2004). Introduction to ANDEEP (ANtarctic benthic DEEP-sea biodiversity: Colonization history and recent community patterns) - A tribute to Howard L. Sanders. *Deep-Sea Research Part II: Topical Studies in Oceanography* **51**, 1457–1465. doi:10.1016/j.dsr2.2004.08.006

Brandt, A., De Broyer, C., De Mesel, I., Ellingsen, K. E., Gooday, A. J., Hilbig, B., Linse, K., Thomson, M. R. A., and Tyler, P. A. (2007a). The biodiversity of the deep Southern Ocean benthos. *Philosophical Transactions of the Royal Society B: Biological Sciences* **362**, 39–66. doi:10.1098/rstb.2006.1952

Brandt, A., Gooday, A. J., Brandão, S. N., Brix, S., Brökeland, W., Cedhagen, T., Choudhury, M., Cornelius, N., Danis, B., De Mesel, I., Diaz, R. J., Gillan, D. C., Ebbe, B., Howe, J. A., Janussen, D., Kaiser, S., Linse, K., Malyutina, M., Pawlowski, J., Raupach, M., and Vanreusel, A. (2007b). First insights into the biodiversity and biogeography of the Southern Ocean deep sea. *Nature* **447**, 307–311. doi:10.1038/nature05827

Briggs, J. C. (2003). Marine centres of origin as evolutionary engines. *Journal of Biogeography* **30**, 1–18. doi:10.1046/j.1365-2699.2003.00810.x

Briggs, J. C., and Bowen, B. W. (2012). A realignment of marine biogeographic provinces with particular reference to fish distributions. *Journal of Biogeography* **39**, 12–30. doi:10.1111/J.1365-2699.2011.02613.X

Brito, T. A. S., Tyler, P. A., and Clarke, A. (1997). Reproductive biology of the Antarctic octocoral Thouarella variabilis Wright & Studer, 1889 - British Antarctic Survey. In 'Proceedings of the 6th International Conference on Coelenterate Biology'. (Ed J. C. den Hartog.) pp. 63–69. (National Museum of Natural History: Leiden.) Available at: https://www.bas.ac.uk/data/our-data/publication/reproductive-biology-of-the-antarctic-octocoral-thouarella-variabilis-wright/ [accessed 25 January 2022]

Bromham, L., Penny, D., Rambaut, A., and Hendy, M. D. (2000). The power of relative rates tests depends on the data. *Journal of Molecular Evolution* **50**, 296–301. doi:10.1007/s002399910034

Brown, J. H. (2014). Why are there so many species in the tropics? Ed J.-C. Svenning. *Journal*

of Biogeography **41**, 8–22. doi:10.1111/jbi.12228

Brown, J. H., and Lomolino, M. V. (1998). 'Biogeography'. (Sinauer Associates.)

De Broyer, C., Danis, B., Louise, A., Martin, A., Claudia, A., Tom, A., David, B., Marthan, B., Kasia, B. S., Magda, B., Jens, B., Nunes, B. S., Angelika, B., Bruno, D., Bruno, D., De Claude, B., de Miguel, S., Marc, E., Christian, E., Daphne, F., Kai-Horst, G., David, G., Andrew, G., Russ, H., Michel, J., Dorte, J., Philippe, K., Juliana, K., Piotr, K., Ryszard, L., Dhugal, L., Katrin, L., Matt, L., Pablo, L. G., Patrick, M., Tomas, M., Ute, M. S., Birger, N., Jon, N., Catherine, O. C., Evgeny, P., William, P., Victor, P., Álvaro, P. C., Uwe, P., Annelies, P. B., Anna, R., José, S. S., Luitfried, S. P., Victor, S., Stefano, S., Michael, S., Enrico, S., Fiona, S., Jacek, S., Volker, S., Igor, S., Sven, T., Andrei, U., Ann, V., Christian, W., Eric, W., Krzysztof, Z., and Wolfgang, Z. (2011). How many species in the Southern Ocean? Towards a dynamic inventory of the Antarctic marine species. *Deep-Sea Research Part II: Topical Studies in Oceanography* **58**, 5–17. doi:10.1016/j.dsr2.2010.10.007

Broyer, C., Koubbi, P., Griffiths, H. J., Raymond, B., Udekem d'Acoz, C., Van de Putte, A. P., Danis, B., David, B., Grant, S., Gutt, J., Held, C., Hosie, G., Huettmann, F., Post, A., and Ropert-Coudert, Y. (2014). 'Biogeographic atlas of the Southern Ocean'. (Cambridge, SCAR.: Cambridge.) Available at: https://www.scar.org/library/scar-publications/occasional-publications/3501-biogeographic-atlas-of-the-southern-ocean-selected-chapters/ [accessed 29 January 2019]

Bryndum-Buchholz, A., Tittensor, D. P., Blanchard, J. L., Cheung, W. W. L., Coll, M., Galbraith, E. D., Jennings, S., Maury, O., and Lotze, H. K. (2019). Twenty-first-century climate change impacts on marine animal biomass and ecosystem structure across ocean basins. *Global Change Biology* **25**, 459–472. doi:10.1111/GCB.14512

Buhl-Mortensen, L., and Buhl-Mortensen, P. (2006). Distribution and diversity of species associated with deep-sea gorgonian corals off Atlantic Canada. In 'Cold-Water Corals and Ecosystems'. pp. 849–879. (Springer-Verlag: Berlin/Heidelberg.) doi:10.1007/3-540-27673-4_44

Buhl-Mortensen, P., Buhl-Mortensen, L., and Purser, A. (2016). Trophic Ecology and Habitat Provision in Cold-Water Coral Ecosystems. In 'Marine Animal Forests'. pp. 1–26. (Springer, Cham.) doi:10.1007/978-3-319-17001-5_20-1

Burnham, K. P., and Anderson, D. R. (2004). 'Model Selection and Multimodel Inference'. (Springer New York.) doi:10.1007/b97636

Burnham, K. P., Anderson, D. R., and Huyvaert, K. P. (2011). AIC model selection and multimodel inference in behavioral ecology: Some background, observations, and comparisons. *Behavioral Ecology and Sociobiology* **65**, 23–35. doi:10.1007/S00265-010-

1029-6/FIGURES/3

Cairns, S. D. (2011). A Revision of the Primnoidae (Octocorallia: Alcyonacea) from the Aleutian Islands and Bering Sea. *Smithsonian Contributions to Zoology*, 1–55. doi:10.5479/si.00810282.634

Cairns, S. D. (2016). New abyssal Primnoidae (Anthozoa: Octocorallia) from the Clarion-Clipperton Fracture Zone, equatorial northeastern Pacific. *Marine Biodiversity* **46**, 141–150. doi:10.1007/s12526-015-0340-x

Cairns, S. D. (2006). Studies on western Atlantic Octocorallia (Coelenterata: Anthozoa). Part 6: The genera *Primnoella* Gray, 1858; *Thouarella* Gray, 1870; *Dasystenella* Versluys, 1906. *Proceedings of the Biological Society of Washington* **119**, 161–194. doi:10.2988/0006-324X(2006)119[161:SOWAOC]2.0.CO;2

Cairns, S. D., and Baco, A. (2007). Review and five new Alaskan species of the deep-water octocoral *Narella* (Octocorallia: Primnoidae). *Systematics and Biodiversity* **5**, 391–407. doi:10.1017/S1477200007002472

Cairns, S. D., and Bayer, F. M. (2009). A generic revision and phylogenetic analysis of the Primnoidae (Cnidaria: Octocorallia). *Smithsonian Contributions to Zoology*, 1–79. doi:10.5479/si.00810282.629

Cairns, S. D., Stone, R. P., Moon, H.-W., and Lee, J. H. (2018). Primnoidae (Octocorallia: Calcaxonia) from the Emperor Seamounts, with notes on *Callogorgia elegans* (Gray, 1870). *Pacific Science* **72**, 125–142. doi:10.2984/72.1.8

Cairns, S. D., and Wirshing, H. H. (2018). A phylogenetic analysis of the Primnoidae (Anthozoa: Octocorallia: Calcaxonia) with analyses of character evolution and a key to the genera and subgenera. *BMC Evolutionary Biology* **18**, 66. doi:10.1186/s12862-018-1182-5

Carstens, B. C., Pelletier, T. A., Reid, N. M., and Satler, J. D. (2013). How to fail at species delimitation. *Molecular Ecology* **22**, 4369–4383. doi:10.1111/mec.12413

Chang, J., Rabosky, D. L., and Alfaro, M. E. (2020). Estimating Diversification Rates on Incompletely Sampled Phylogenies: Theoretical Concerns and Practical Solutions. *Systematic Biology* **69**, 602–611. doi:10.1093/sysbio/syz081

Chenuil, A., Saucède, T., Hemery, L. G., Eléaume, M., Féral, J.-P., Améziane, N., David, B., Lecointre, G., and Havermans, C. (2018). Understanding processes at the origin of species flocks with a focus on the marine Antarctic fauna. *Biological Reviews* **93**, 481–504. doi:10.1111/brv.12354

Chown, S. L., Clarke, A., Fraser, C. I., Cary, S. C., Moon, K. L., and McGeoch, M. A. (2015). The changing form of Antarctic biodiversity. *Nature* **522**, 431–438. doi:10.1038/nature14505

Clarke, A. (2008). Antarctic marine benthic diversity: patterns and processes. *Journal of*

Experimental Marine Biology and Ecology **366**, 48–55. doi:10.1016/j.jembe.2008.07.008

Clarke, A., and Arntz, W. E. (2006). An introduction to EASIZ (Ecology of the Antarctic Sea Ice Zone): An integrated programme of water column, benthos and bentho-pelagic coupling in the coastal environment of Antarctica. *Deep Sea Research Part II: Topical Studies in Oceanography* **53**, 803–814. doi:10.1016/J.DSR2.2006.05.001

Clarke, A., and Crame, J. A. (2010). Evolutionary dynamics at high latitudes: Speciation and extinction in polar marine faunas. *Philosophical Transactions of the Royal Society B: Biological Sciences* **365**, 3655–3666. doi:10.1098/rstb.2010.0270

Clarke, A., and Crame, J. A. (1992). The Southern Ocean Benthic Fauna and Climate Change: A Historical Perspective. *Philosophical Transactions of the Royal Society B: Biological Sciences* **338**, 299–309. doi:10.1098/rstb.1992.0150

Clarke, A., and Johnston, N. M. (2003). Antarctic marine benthic diversity. In 'Oceanography and Marine Biology, An Annual Review, Volume 41'. pp. 55–57. (CRC Press.) doi:10.1201/9780203180570-8

De Clippele, L. H., Buhl-Mortensen, P., and Buhl-Mortensen, L. (2015). Fauna associated with cold water gorgonians and sea pens. *Continental Shelf Research* **105**, 67–78. doi:10.1016/J.CSR.2015.06.007

Colombo, M., Damerau, M., Hanel, R., Salzburger, W., and Matschiner, M. (2015). Diversity and disparity through time in the adaptive radiation of Antarctic notothenioid fishes. *Journal of Evolutionary Biology* **28**, 376–394. doi:10.1111/jeb.12570

Condamine, F. L., Antonelli, A., Lagomarsino, L. P., Hoorn, C., and Liow, L. H. (2018a). Teasing Apart Mountain Uplift, Climate Change and Biotic Drivers of Species Diversification. In 'Mountains, Climate and Biodiversity'. (Eds C. Hoorn and A. Antonelli.) pp. 257–272. (Wiley Blackwell: New York.)

Condamine, F. L., and Kergoat, G. J. (2021). Antarctica as an evolutionary arena during the Cenozoic global cooling. *Proceedings of the National Academy of Sciences* **118**. doi:10.1073/PNAS.2108886118

Condamine, F. L., Rolland, J., Höhna, S., Sperling, F. A. H., and Sanmartín, I. (2018b). Testing the Role of the Red Queen and Court Jester as Drivers of the Macroevolution of Apollo Butterflies Ed B. Wiegmann. *Systematic Biology* **67**, 940–964. doi:10.1093/sysbio/syy009

Condamine, F. L., Rolland, J., and Morlon, H. (2013). Macroevolutionary perspectives to environmental change Ed H. Maherali. *Ecology Letters* **16**, 72–85. doi:10.1111/ele.12062

Constable, A. J., Melbourne-Thomas, J., Corney, S. P., Arrigo, K. R., Barbraud, C., Barnes, D. K. A., Bindoff, N. L., Boyd, P. W., Brandt, A., Costa, D. P., Davidson, A. T., Ducklow, H. W., Emmerson, L., Fukuchi, M., Gutt, J., Hindell, M. A., Hofmann, E. E., Hosie, G. W., Iida, T.,

Jacob, S., Johnston, N. M., Kawaguchi, S., Kokubun, N., Koubbi, P., Lea, M. A., Makhado, A., Massom, R. A., Meiners, K., Meredith, M. P., Murphy, E. J., Nicol, S., Reid, K., Richerson, K., Riddle, M. J., Rintoul, S. R., Smith, W. O., Southwell, C., Stark, J. S., Sumner, M., Swadling, K. M., Takahashi, K. T., Trathan, P. N., Welsford, D. C., Weimerskirch, H., Westwood, K. J., Wienecke, B. C., Wolf-Gladrow, D., Wright, S. W., Xavier, J. C., and Ziegler, P. (2014). Climate change and Southern Ocean ecosystems I: how changes in physical habitats directly affect marine biota. *Global Change Biology* **20**, 3004–3025. doi:10.1111/GCB.12623

Convey, P., Chown, S. L., Clarke, A., Barnes, D. K. A., Bokhorst, S., Cummings, V., Ducklow, H. W., Frati, F., Green, T. G. A., Gordon, S., Griffiths, H. J., Howard-Williams, C., Huiskes, A. H. L., Laybourn-Parry, J., Lyons, W. B., McMinn, A., Morley, S. A., Peck, L. S., Quesada, A., Robinson, S. A., Schiaparelli, S., and Wall, D. H. (2014). The spatial structure of antarctic biodiversity. *Ecological Monographs* **84**, 203–244. doi:10.1890/12-2216.1

Cordeiro, R. ., van Ofwegen, L. ., and Williams, G. (2018). World List of Octocorallia. Narella Gray, 1870. Accessed through:

Costello, M. J., and Chaudhary, C. (2017). Marine Biodiversity, Biogeography, Deep-Sea Gradients, and Conservation. *Current Biology* **27**, R511–R527. doi:10.1016/J.CUB.2017.04.060

Costello, M. J., Coll, M., Danovaro, R., Halpin, P., Ojaveer, H., and Miloslavich, P. (2010). A Census of Marine Biodiversity Knowledge, Resources, and Future Challenges Ed S. Humphries. *PLoS ONE* **5**, e12110. doi:10.1371/journal.pone.0012110

Coyne, J. A., and Orr, H. A. (2004). 'Speciation'. (Sinauer Associates, Inc: Sunderland, MA.)

Crame, J. A. (2018). Key stages in the evolution of the Antarctic marine fauna. *Journal of Biogeography* **45**, 986–994. doi:10.1111/jbi.13208

Cristini, L., Grosfeld, K., Butzin, M., and Lohmann, G. (2012). Influence of the opening of the Drake Passage on the Cenozoic Antarctic Ice Sheet: A modeling approach. *Palaeogeography, Palaeoclimatology, Palaeoecology* **339**, 66–73. doi:10.1016/J.PALAEO.2012.04.023

Daly, M., Brugler, M. R., Cartwright, P., Collins, A. G., Dawson, M. N., Fautin, D. G., France, S. C., McFadden, C. S., Opresko, D. M., Rodriguez, E., Romano, S. L., and Stake, J. L. (2007). The phylum Cnidaria: A review of phylogenetic patterns and diversity 300 years after Linnaeus. In: Zhang, Z.-Q. & Shear, W.A. (Eds) Linnaeus Tercentenary: Progress in Invertebrate Taxonomy. *Zootaxa* **1668**, 127–182. doi:10.1016/j.biopsych.2005.09.016

Darriba, D., Taboada, G. L., Doallo, R., and Posada, D. (2012). JModelTest 2: More models, new heuristics and parallel computing. *Nature Methods* **9**, 772. doi:10.1038/nmeth.2109

Davies, B. J., Hambrey, M. J., Smellie, J. L., Carrivick, J. L., and Glasser, N. F. (2012). Antarctic Peninsula Ice Sheet evolution during the Cenozoic Era. *Quaternary Science Reviews* **31**, 30–66. doi:10.1016/J.QUASCIREV.2011.10.012

Dayrat, B. (2005). Towards integrative taxonomy. *Biological Journal of the Linnean Society* **85**, 407–415. doi:10.1111/j.1095-8312.2005.00503.x

Dueñas, L. F., Alderslade, P., and Sánchez, J. A. (2014). Molecular systematics of the deep-sea bamboo corals (Octocorallia: Isididae: Keratoisidinae) from New Zealand with descriptions of two new species of *Keratoisis*. *Molecular Phylogenetics and Evolution* **74**, 15–28. doi:10.1016/j.ympev.2014.01.031

Dueñas, L. F., and Sánchez, J. A. (2009). Character lability in deep-sea bamboo corals (Octocorallia, Isididae, Keratoisidinae). *Marine Ecology Progress Series* **397**, 11–23. doi:10.3354/meps08307

Dueñas, L. F., Tracey, D. M., Crawford, A. J., Wilke, T., Alderslade, P., and Sánchez, J. A. (2016). The Antarctic Circumpolar Current as a diversification trigger for deep-sea octocorals. *BMC Evolutionary Biology* **16**, 2. doi:10.1186/s12862-015-0574-z

Dunkley Jones, T., Lunt, D. J., Schmidt, D. N., Ridgwell, A., Sluijs, A., Valdes, P. J., and Maslin, M. (2013). Climate model and proxy data constraints on ocean warming across the Paleocene–Eocene Thermal Maximum. *Earth-Science Reviews* **125**, 123–145. doi:10.1016/J.EARSCIREV.2013.07.004

Eguchi, M. (1948). Fossil Helioporidae from Japan and the South Sea islands. *Journal of Paleontology* **22**, 362–364.

Erwin, D. H. (2009). Climate as a Driver of Evolutionary Change. *Current Biology* **19**, R575–R583. doi:10.1016/J.CUB.2009.05.047

FitzJohn, R. G., Maddison, W. P., and Otto, S. P. (2009). Estimating Trait-Dependent Speciation and Extinction Rates from Incompletely Resolved Phylogenies. *Systematic Biology* **58**, 595–611. doi:10.1093/sysbio/syp067

Flannery-Sutherland, J. T., Silvestro, D., and Benton, M. J. (2022). Global diversity dynamics in the fossil record are regionally heterogeneous. *Nature Communications 2022 13:1* **13**, 1–17. doi:10.1038/s41467-022-30507-0

Föllmi, K. B. (2012). Early Cretaceous life, climate and anoxia. *Cretaceous Research* **35**, 230–257. doi:10.1016/J.CRETRES.2011.12.005

Foster, G. L., Hull, P., Lunt, D. J., and Zachos, J. C. (2018). Placing our current hyperthermal in the context of rapid climate change in our geological past. *Philosophical Transactions of the Royal Society A: Mathematical, Physical and Engineering Sciences* **376**. doi:10.1098/RSTA.2017.0086

France, S. C., and Hoover, L. L. (2001). Analysis of variation in mitochondrial DNA sequences (ND3, ND4L, MSH) among Octocorallia (=Alcyonaria) (Cnidaria: Anthozoa). *Bulletin of the Biological Society of Washington* **10**, 110–118.

Friedrich, O., Norris, R. D., and Erbacher, J. (2012). Evolution of middle to Late Cretaceous oceans—A 55 m.y. record of Earth's temperature and carbon cycle. *Geology* **40**, 107–110. doi:10.1130/G32701.1

Futuyma, D. J. (2005). 'Evolution' Sinauer As. (Massachusetts.)

García-Cárdenas, F. J., Núñez-Flores, M., and López-González, P. J. (2020). Molecular phylogeny and divergence time estimates in pennatulaceans (Cnidaria: Octocorallia: Pennatulacea). *Scientia Marina* **84**, 317–330. doi:10.3989/SCIMAR.05067.28A

Gaston, K. J. (2000). Global patterns in biodiversity. *Nature* **405**, 220–227. doi:10.1038/35012228

Gavryushkina, A., Welch, D., Stadler, T., and Drummond, A. J. (2014). Bayesian Inference of Sampled Ancestor Trees for Epidemiology and Fossil Calibration. *PLOS Computational Biology* **10**, e1003919. doi:10.1371/JOURNAL.PCBI.1003919

van Gennip, S. J., Popova, E. E., Yool, A., Pecl, G. T., Hobday, A. J., and Sorte, C. J. B. (2017). Going with the flow: the role of ocean circulation in global marine ecosystems under a changing climate. *Global Change Biology* **23**, 2602–2617. doi:10.1111/GCB.13586

Goedert, J. L., Guthrie, L. S., and Kiel, S. (2022). Octocorals (Alcyonacea and Pennatulacea) from Paleogene deep-water strata in western Washington State, USA. *Journal of Paleontology*, 1–13. doi:10.1017/JPA.2022.5

González-Wevar, C. A., Gérard, K., Rosenfeld, S., Saucède, T., Naretto, J., Díaz, A., Morley, S. A., Brickle, P., and Poulin, E. (2019). Cryptic speciation in Southern Ocean Aequiyoldia eightsii (Jay, 1839): Mio-Pliocene trans-Drake Passage separation and diversification. *Progress in Oceanography* **174**, 44–54. doi:10.1016/j.pocean.2018.09.004

González-Wevar, C. A., Hüne, M., Segovia, N. I., Nakano, T., Spencer, H. G., Chown, S. L., Saucède, T., Johnstone, G., Mansilla, A., and Poulin, E. (2017). Following the Antarctic Circumpolar Current: patterns and processes in the biogeography of the limpet Nacella (Mollusca: Patellogastropoda) across the Southern Ocean. *Journal of Biogeography* **44**, 861–874. doi:10.1111/JBI.12908

González-Wevar, C. A., Nakano, T., Cañete, J. I., and Poulin, E. (2010). Molecular phylogeny and historical biogeography of *Nacella* (Patellogastropoda: Nacellidae) in the Southern Ocean. *Molecular Phylogenetics and Evolution* **56**, 115–124. doi:10.1016/J.YMPEV.2010.02.001

González-Wevar, C. A., Saucède, T., Morley, S. A., Chown, S. L., and Poulin, E. (2013).

Extinction and recolonization of maritime Antarctica in the limpet Nacella concinna (Strebel, 1908) during the last glacial cycle: toward a model of Quaternary biogeography in shallow Antarctic invertebrates. *Molecular Ecology* **22**, 5221–5236. doi:10.1111/MEC.12465

Grant, R. B. (1976). The marine fauna of New Zealand: Isididae (Octocorallia: Gorgonacea) from New Zealand and the Antarctic. *Memoirs of the New Zealand Oceanographic Institute, Wellington.* **66**, 1–56.

Grasshoff, M. (1999). The shallow water Gorgonians of New Caledonia and adjacent islands (Coelenterata: Octocorallia). *Senckenbergiana Biologica* **78**, 1–245.

Grassle, J. F. (1989). Species diversity in deep-sea communities. *Trends in Ecology & Evolution* **4**, 12–15. doi:10.1016/0169-5347(89)90007-4

Gray, J. E. (1870). 'Catalogue of the Lithophytes or Stony Corals in the Collection of the British Museum' Ed L. British Museum. (London.)

Green, R. E., Krause, J., Briggs, A. W., Maricic, T., Stenzel, U., Kircher, M., Patterson, N., Li, H., Zhai, W., Fritz, M. H. Y., Hansen, N. F., Durand, E. Y., Malaspinas, A. S., Jensen, J. D., Marques-Bonet, T., Alkan, C., Prüfer, K., Meyer, M., Burbano, H. A., Good, J. M., Schultz, R., Aximu-Petri, A., Butthof, A., Höber, B., Höffner, B., Siegemund, M., Weihmann, A., Nusbaum, C., Lander, E. S., Russ, C., Novod, N., Affourtit, J., Egholm, M., Verna, C., Rudan, P., Brajkovic, D., Kucan, Ž., Gušic, I., Doronichev, V. B., Golovanova, L. V., Lalueza-Fox, C., De La Rasilla, M., Fortea, J., Rosas, A., Schmitz, R. W., Johnson, P. L. F., Eichler, E. E., Falush, D., Birney, E., Mullikin, J. C., Slatkin, M., Nielsen, R., Kelso, J., Lachmann, M., Reich, D., and Pääbo, S. (2010). A draft sequence of the neandertal genome. *Science* **328**, 710–722. doi:10.1126/science.1188021

Griffiths, H. J., Barnes, D. K. A., and Linse, K. (2009). Towards a generalized biogeography of the Southern Ocean benthos. *Journal of Biogeography* **36**, 162–177. doi:10.1111/j.1365-2699.2008.01979.x

Gutt, J., Sirenko, B. I., Smirnov, I. S., and Arntz, W. E. (2004). How many macrozoobenthic species might inhabit the Antarctic shelf? In 'Antarctic Science'. pp. 11–16. (Cambridge University Press.) doi:10.1017/S0954102004001750

Gutt, J., and Starmans, A. (1998). Structure and biodiversity of megabenthos in the Weddell and Lazarev Seas (Antarctica): ecological role of physical parameters and biological interactions. *Polar Biology* **20**, 229–247. doi:10.1007/s003000050300

Halanych, K. M., and Mahon, A. R. (2018). Challenging Dogma Concerning Biogeographic Patterns of Antarctica and the Southern Ocean. *Annual Review of Ecology, Evolution, and Systematics* **49**, 355–378. doi:10.1146/annurev-ecolsys-121415-032139

Hauptvogel, D. W., and Passchier, S. (2012). Early–Middle Miocene (17–14 Ma) Antarctic ice

dynamics reconstructed from the heavy mineral provenance in the AND-2A drill core, Ross Sea, Antarctica. *Global and Planetary Change* **82**–**83**, 38–50. doi:10.1016/J.GLOPLACHA.2011.11.003

Heath, T. A., Huelsenbeck, J. P., and Stadler, T. (2014). The fossilized birth–death process for coherent calibration of divergence-time estimates. *Proceedings of the National Academy of Sciences* **111**, E2957–E2966. doi:10.1073/PNAS.1319091111

Held, C. (2003). Molecular evidence for cryptic speciation within the widespread Antarctic crustacean Ceratoserolis trilobitoides (Crustacea, Isopoda) Eds A. H. L. Huiskes, W. W. C. Gieskes, J. Rozema, R. M. L. Schorno, S. M. VanDerVies, and W. J. Wolff. *Antarctic Biology in a Global Context, Proceedings* **3**, 135--139 338.

Helwig, N. E. (2022). npreg: Nonparametric Regression via Smoothing Splines. Available at: https://cran.r-project.org/package=npreg

Hillebrand, H. (2004). On the generality of the latitudinal diversity gradient. *The American naturalist* **163**, 192–211. doi:10.1086/381004

Hodel, F., Grespan, R., de Rafélis, M., Dera, G., Lezin, C., Nardin, E., Rouby, D., Aretz, M., Steinnman, M., Buatier, M., Lacan, F., Jeandel, C., and Chavagnac, V. (2021). Drake Passage gateway opening and Antarctic Circumpolar Current onset 31 Ma ago: The message of foraminifera and reconsideration of the Neodymium isotope record. *Chemical Geology* **570**, 120171. doi:10.1016/J.CHEMGEO.2021.120171

Hönisch, B., Ridgwell, A., Schmidt, D. N., Thomas, E., Gibbs, S. J., Sluijs, A., Zeebe, R., Kump, L., Martindale, R. C., Greene, S. E., Kiessling, W., Ries, J., Zachos, J. C., Royer, D. L., Barker, S., Marchitto, T. M., Moyer, R., Pelejero, C., Ziveri, P., Foster, G. L., and Williams, B. (2012). The geological record of ocean acidification. *Science* **335**, 1058–1063. doi:10.1126/science.1208277

Hoorn, C., Wesselingh, F. P., ter Steege, H., Bermudez, M. A., Mora, A., Sevink, J., Sanmartín, I., Sanchez-Meseguer, A., Anderson, C. L., Figueiredo, J. P., Jaramillo, C., Riff, D., Negri, F. R., Hooghiemstra, H., Lundberg, J., Stadler, T., Särkinen, T., and Antonelli, A. (2010). Amazonia through time: Andean uplift, climate change, landscape evolution, and biodiversity. *Science (New York, N.Y.)* **330**, 927–31. doi:10.1126/science.1194585

Hourigan, T. F., Etnoyer, P. J., and Cairns, S. D. (2017). The State of Deep-Sea Coral and Sponge Ecosystems of the United States.

Jablonski, D., Roy, K., and Valentine, J. W. (2006). Out of the tropics: evolutionary dynamics of the latitudinal diversity gradient. *Science (New York, N.Y.)* **314**, 102–6. doi:10.1126/science.1130880

Joly, S., McLenachan, P. A., and Lockhart, P. J. (2009). A Statistical Approach for Distinguishing

Hybridization and Incomplete Lineage Sorting. *The American Naturalist* **174**, E54–E70. doi:10.1086/600082

Kaiser, S., Brandão, S. N., Brix, S., Barnes, D. K. A., Bowden, D. A., Ingels, J., Leese, F., Schiaparelli, S., Arango, C. P., Badhe, R., Bax, N., Blazewicz-Paszkowycz, M., Brandt, A., Brenke, N., Catarino, A. I., David, B., De Ridder, C., Dubois, P., Ellingsen, K. E., Glover, A. G., Griffiths, H. J., Gutt, J., Halanych, K. M., Havermans, C., Held, C., Janussen, D., Lörz, A.-N., Pearce, D. A., Pierrat, B., Riehl, T., Rose, A., Sands, C. J., Soler-Membrives, A., Schüller, M., Strugnell, J. M., Vanreusel, A., Veit-Köhler, G., Wilson, N. G., and Yasuhara, M. (2013). Patterns, processes and vulnerability of Southern Ocean benthos: a decadal leap in knowledge and understanding. *Marine Biology* **160**, 2295–2317. doi:10.1007/s00227-013-2232-6

Kapli, P., Lutteropp, S., Zhang, J., Kobert, K., Pavlidis, P., Stamatakis, A., and Flouri, T. (2017). Multi-rate Poisson tree processes for single-locus species delimitation under maximum likelihood and Markov chain Monte Carlo. *Bioinformatics* **33**, 1630–1638. doi:10.1093/bioinformatics/btx025

Katoh, K., Asimenos, G., and Toh, H. (2009). Multiple Alignment of DNA Sequences with MAFFT. *Methods in Molecular Biology* **537**, 39–64. doi:10.1007/978-1-59745-251-9_3

Kennicutt, M. C., Chown, S. L., Cassano, J. J., Liggett, D., Peck, L. S., Massom, R., Rintoul, S. R., Storey, J., Vaughan, D. G., Wilson, T. J., Allison, I., Ayton, J., Badhe, R., Baeseman, J., Barrett, P. J., Bell, R. E., Bertler, N., Bo, S., Brandt, A., Bromwich, D., Cary, S. C., Clark, M. S., Convey, P., Costa, E. S., Cowan, D., Deconto, R., Dunbar, R., Elfring, C., Escutia, C., Francis, J., Fricker, H. A., Fukuchi, M., Gilbert, N., Gutt, J., Havermans, C., Hik, D., Hosie, G., Jones, C., Kim, Y. D., Le Maho, Y., Lee, S. H., Leppe, M., Leitchenkov, G., Li, X., Lipenkov, V., Lochte, K., López-Martínez, J., Lüdecke, C., Lyons, W., Marenssi, S., Miller, H., Morozova, P., Naish, T., Nayak, S., Ravindra, R., Retamales, J., Ricci, C. A., Rogan-Finnemore, M., Ropert-Coudert, Y., Samah, A. A., Sanson, L., Scambos, T., Schloss, I. R., Shiraishi, K., Siegert, M. J., SimÃes, J. C., Storey, B., Sparrow, M. D., Wall, D. H., Walsh, J. C., Wilson, G., Winther, J. G., Xavier, J. C., Yang, H., and Sutherland, W. J. (2015). A roadmap for Antarctic and Southern Ocean science for the next two decades and beyond. *Antarctic Science* **27**, 3–18. doi:10.1017/S0954102014000674

Kiessling, W., and Simpson, C. (2011). On the potential for ocean acidification to be a general cause of ancient reef crises. *Global Change Biology* **17**, 56–67. doi:10.1111/J.1365-2486.2010.02204.X

Kinoshita, K. (1908). Gorgonacea no ikka Primnoidae ni tsuite. *Dobutsugaku zasshi* **20**, 517–528.

Kisel, Y., and Timothy, T. G. (2010). Speciation has a spatial scale that depends on levels of gene flow. *The American naturalist* **175**, 316–334. doi:10.1086/650369

Knowlton, N. (1993). Sibling species in the sea. *Annual Review of Ecology and Systematics* **24**, 189–216. doi:10.1146/annurev.es.24.110193.001201

Knox, G. A. (1960). Littoral ecology and biogeography of the southern oceans. *Proceedings of the Royal Society of London. Series B. Biological Sciences* **152**, 577–624. doi:10.1098/rspb.1960.0068

Krug, A. Z., Jablonski, D., Roy, K., and Beu, A. G. (2010). Differential Extinction and the Contrasting Structure of Polar Marine Faunas. *PLOS ONE* **5**, e15362. doi:10.1371/JOURNAL.PONE.0015362

Kükenthal, W. (1908). Diagnosen neuer Gorgoniden (4. Mitteilung). *Zoologischer Anzeiger* **33**, 9–20.

Kükenthal, W. (1912). Die Alcyonaria der Deutschen Südpolar, Expedition 1901–1903. *Deutsche Südpolar Expedition 1901–1903, Zoologie* **5**, 289–349.

Kükenthal, W. (1907). Gorgoniden der Deutschen Tiefsee–Expedition. *Zoologischer Anzeiger* **31**, 202–212.

Kumar, S., Stecher, G., and Tamura, K. (2016). MEGA7: Molecular Evolutionary Genetics Analysis Version 7.0 for Bigger Datasets. *Molecular biology and evolution* **33**, 1870–1874. doi:10.1093/molbev/msw054

Kuzmicheva, E. I. (1987). Verkhnemelovye i Paleogenovye Korally SSSR [Upper Cretaceous and Paleogene Corals of the USSR]. *Moskva: Nauka.*

Lagabrielle, Y., Goddéris, Y., Donnadieu, Y., Malavieille, J., and Suarez, M. (2009). The tectonic history of Drake Passage and its possible impacts on global climate. *Earth and Planetary Science Letters* **279**, 197–211. doi:10.1016/j.epsl.2008.12.037

Lamouroux, J. V. F. (1812). Extrait d'un mémoire sur la classification des polypiers coralligènes non entierement pierreux. *Nouveau Bulletin des Sciences par la Société Philomatique de Paris* **3**, 181–188.

Lawver, L. A., and Gahagan, L. M. (2003). Evolution of Cenozoic seaways in the circum-Antarctic region. *Palaeogeography, Palaeoclimatology, Palaeoecology* **198**, 11–37. doi:10.1016/S0031-0182(03)00392-4

Lehtonen, S., Silvestro, D., Karger, D. N., Scotese, C., Tuomisto, H., Kessler, M., Peña, C., Wahlberg, N., and Antonelli, A. (2017). Environmentally driven extinction and opportunistic origination explain fern diversification patterns. *Scientific Reports* **7**, 4831. doi:10.1038/s41598-017-05263-7

Leprieur, F., Descombes, P., Gaboriau, T., Cowman, P. F., Parravicini, V., Kulbicki, M., Melián,

C. J., de Santana, C. N., Heine, C., Mouillot, D., Bellwood, D. R., and Pellissier, L. (2016). Plate tectonics drive tropical reef biodiversity dynamics. *Nature Communications* **7**, 11461. doi:10.1038/ncomms11461

Leray, M., Knowlton, N., Ho, S.-L., Nguyen, B. N., and Machida, R. J. (2019). GenBank is a reliable resource for 21st century biodiversity research. *Proceedings of the National Academy of Sciences*, 201911714. doi:10.1073/pnas.1911714116

Liebrand, D., De Bakker, A. T. M., Beddow, H. M., Wilson, P. A., Bohaty, S. M., Ruessink, G., Pälike, H., Batenburg, S. J., Hilgen, F. J., Hodell, D. A., Huck, C. E., Kroon, D., Raffi, I., Saes, M. J. M., Van Dijk, A. E., and Lourens, L. J. (2017). Evolution of the early Antarctic ice ages. doi:10.1073/pnas.1615440114

Linse, K., Cope, T., Lörz, A.-N., and Sands, C. (2007). Is the Scotia Sea a centre of Antarctic marine diversification? Some evidence of cryptic speciation in the circum-Antarctic bivalve Lissarca notorcadensis (Arcoidea: Philobryidae). *Polar Biology* **30**, 1059–1068. doi:10.1007/s00300-007-0265-3

Lomolino, M. V., Riddle, B. R., Brown, J. H., and Brown, J. H. (2006). 'Biogeography.' (Sinauer Associates.)

López-González, P. J. (2006). A new gorgonian genus from deep-sea Antarctic waters (Octocorallia, Alcyonacea, Plexauridae). *Helgoland Marine Research* **60**, 1–6. doi:10.1007/s10152-005-0008-1

López-González, P. J., Gili, J. M., and Orejas, C. (2002). A new primnoid genus (Anthozoa: Octocorallia) from the Southern Ocean. *Scientia Marina* **66**, 383–397. doi:10.3989/scimar.2002.66n4383

Louca, S., and Pennell, M. W. (2020). Extant timetrees are consistent with a myriad of diversification histories. *Nature* **580**, 502–505. doi:10.1038/s41586-020-2176-1

Mackensen, A. (2004). Changing Southern Ocean palaeocirculation and effects on global climate. *Antarctic Science* **16**, 369–386. doi:10.1017/S0954102004002202

Maddison, W. P. (1997). Gene trees in species trees Ed J. J. Wiens. *Systematic Biology* **46**, 523–536. doi:10.1093/sysbio/46.3.523

Malyutina, M., and Brandt, A. (2007). Diversity and zoogeography of Antarctic deep-sea Munnopsidae (Crustacea, Isopoda, Asellota). *Deep Sea Research Part II: Topical Studies in Oceanography* **54**, 1790–1805. doi:10.1016/J.DSR2.2007.07.017

Martinez-Dios, A., Dominguez-Carrió, C., Zapata-Guardiola, R., and Gili, J.-M. (2016). New insights on Antarctic gorgonians' age, growth and their potential as paleorecords. *Deep Sea Research Part I: Oceanographic Research Papers* **112**, 57–67. doi:10.1016/J.DSR.2016.03.007

Matsuoka, K., Skoglund, A., and Roth, G. (2018). Quantarctica [Dataset]. *Norwegian Polar Institute*. doi:10.21334/npolar.2018.8516e961

Matzke, N. J. (2014). Model selection in historical biogeography reveals that founder-event speciation is a crucial process in island clades. *Systematic Biology* **63**, 951–970. doi:10.1093/sysbio/syu056

McFadden, C. S., Benayahu, Y., Pante, E., Thoma, J. N., Nevarez, P. A., and France, S. C. (2011). Limitations of mitochondrial gene barcoding in Octocorallia. *Molecular Ecology Resources* **11**, 19–31. doi:10.1111/j.1755-0998.2010.02875.x

McFadden, C. S., Brown, A. S., Brayton, C., Hunt, C. B., and van Ofwegen, L. P. (2014a). Application of DNA barcoding in biodiversity studies of shallow-water octocorals: Molecular proxies agree with morphological estimates of species richness in Palau. *Coral Reefs* **33**, 275–286. doi:10.1007/s00338-013-1123-0

McFadden, C. S., France, S. C., Sánchez, J. A., and Alderslade, P. (2006). A molecular phylogenetic analysis of the Octocorallia (Cnidaria: Anthozoa) based on mitochondrial protein-coding sequences. *Molecular Phylogenetics and Evolution* **41**, 513–527. doi:10.1016/j.ympev.2006.06.010

McFadden, C. S., and van Ofwegen, L. P. (2013a). A second, cryptic species of the soft coral genus Incrustatus (Anthozoa: Octocorallia: Clavulariidae) from Tierra del Fuego, Argentina, revealed by DNA barcoding. *Helgoland Marine Research* **67**, 137–147. doi:10.1007/s10152-012-0310-7

McFadden, C. S., and van Ofwegen, L. P. (2013b). Molecular phylogenetic evidence supports a new family of octocorals and a new genus of Alcyoniidae (Octocorallia, Alcyonacea). *ZooKeys*, 59–83. doi:10.3897/zookeys.346.6270

McFadden, C. S., Quattrini, A. M., Brugler, M. R., Cowman, P. F., Dueñas, L. F., Kitahara, M. V, Paz-García, D. A., Reimer, J. D., and Rodríguez, E. (2021). Phylogenomics, Origin, and Diversification of Anthozoans (Phylum Cnidaria). *Systematic Biology* **70**, 635–647. doi:10.1093/SYSBIO/SYAA103

McFadden, C. S., Reynolds, A. M., and Janes, M. P. (2014b). DNA barcoding of xeniid soft corals (Octocorallia: Alcyonacea: Xeniidae) from Indonesia: Species richness and phylogenetic relationships. *Systematics and Biodiversity* **12**, 247–257. doi:10.1080/14772000.2014.902866

McFadden, C. S., Sanchez, J. A., and France, S. C. (2010). Molecular Phylogenetic Insights into the Evolution of Octocorallia: A Review. *Integrative and Comparative Biology* **50**, 389–410. doi:10.1093/icb/icq056

McInerney, F. A., and Wing, S. L. (2011). The paleocene-eocene thermal maximum: A

perturbation of carbon cycle, climate, and biosphere with implications for the future. *Annual Review of Earth and Planetary Sciences* **39**, 489–516. doi:10.1146/annurev-earth-040610-133431

Miller, K. G., Kominz, M. A., Browning, J. V., Wright, J. D., Mountain, G. S., Katz, M. E., Sugarman, P. J., Cramer, B. S., Christie-Blick, N., and Pekar, S. F. (2005). The phanerozoic record of global sea-level change. *Science* **310**, 1293–1298. doi:10.1126/science.1116412

Miller, M. A., Pfeiffer, W., and Schwartz, T. (2010). Creating the CIPRES Science Gateway for inference of large phylogenetic trees. In 'Gateway Computing Environments Workshop, GCE 2010'. pp. 1–8. (New Orleans.) doi:10.1109/GCE.2010.5676129

Milne-Edward, H. (1857). 'Histoire naturelle des coralliaires ou polypes proprement dits (Vol. 2)' Ed Roret. (Paris.)

Mittelbach, G. G., Schemske, D. W., Cornell, H. V., Allen, A. P., Brown, J. M., Bush, M. B., Harrison, S. P., Hurlbert, A. H., Knowlton, N., Lessios, H. A., McCain, C. M., McCune, A. R., McDade, L. A., McPeek, M. A., Near, T. J., Price, T. D., Ricklefs, R. E., Roy, K., Sax, D. F., Schluter, D., Sobel, J. M., and Turelli, M. (2007). Evolution and the latitudinal diversity gradient: speciation, extinction and biogeography. *Ecology Letters* **10**, 315–331. doi:10.1111/j.1461-0248.2007.01020.x

Mora, C., Tittensor, D. P., Adl, S., Simpson, A. G. B., and Worm, B. (2011). How Many Species Are There on Earth and in the Ocean? Ed G. M. Mace. *PLoS Biology* **9**, e1001127. doi:10.1371/journal.pbio.1001127

Moreau, C., Saucède, T., Jossart, Q., Agüera, A., Brayard, A., and Danis, B. (2017). Reproductive strategy as a piece of the biogeographic puzzle: a case study using Antarctic sea stars (Echinodermata, Asteroidea). *Journal of Biogeography* **44**, 848–860. doi:10.1111/JBI.12965

Morlon, H. (2014). Phylogenetic approaches for studying diversification Ed A. Mooers. *Ecology Letters* **17**, 508–525. doi:10.1111/ele.12251

Morlon, H., Lewitus, E., Condamine, F. L., Manceau, M., Clavel, J., and Drury, J. (2016). RPANDA: an R package for macroevolutionary analyses on phylogenetic trees Ed R. Fitzjohn. *Methods in Ecology and Evolution* **7**, 589–597. doi:10.1111/2041-210X.12526

Morlon, H., Robin, S., Hartig, F., and Morlon, H. (2022). Studying speciation and extinction dynamics from phylogenies: addressing identifiability issues. *Trends in Ecology & Evolution* **2022**. doi:10.1016/j.tree.2022.02.004

Near, T. J., Dornburg, A., Kuhn, K. L., Eastman, J. T., Pennington, J. N., Patarnello, T., Zane, L., Fernandez, D. A., and Jones, C. D. (2012). Ancient climate change, antifreeze, and the

evolutionary diversification of Antarctic fishes. *Proceedings of the National Academy of Sciences* **109**, 3434–3439. doi:10.1073/pnas.1115169109

Ng, J., and Smith, S. D. (2014). How traits shape trees: new approaches for detecting character state-dependent lineage diversification. *Journal of Evolutionary Biology* **27**, 2035–2045. doi:10.1111/jeb.12460

Nichols, R. (2001). Gene trees and species trees are not the same. *Trends in Ecology & Evolution* **16**, 358–364.

Norris, R. D., Turner, S. K., Hull, P. M., and Ridgwell, A. (2013). Marine ecosystem responses to Cenozoic global change. *Science (New York, N.Y.)* **341**, 492–8. doi:10.1126/science.1240543

Nunes, F., and Norris, R. D. (2006). Abrupt reversal in ocean overturning during the Palaeocene/Eocene warm period. *Nature* **439**, 60–63. doi:10.1038/nature04386

Núñez-Flores, M., Gomez-Uchida, D., and López-González, P. J. (2020). Molecular and morphological data reveal three new species of *Thouarella* (Anthozoa: Octocorallia: Primnoidae) from the Southern Ocean. *Marine Biodiversity* **50**, 1–21. doi:10.1007%2Fs12526-020-01053-z

Núñez-Flores, M., Gomez-Uchida, D., and López-González, P. J. (2021). Molecular systematics of *Thouarella* (Octocorallia : Primnoidae) with the description of three new species from the Southern Ocean based on combined molecular and morphological evidence. *Invertebrate Systematics* **35**, 655–674. doi:10.1071/IS20078

Nutting, C. C. (1908). Descriptions of the Alcyonaria collected by the U.S. Bureau of Fisheries steamer Albatross in the vicinity of the Hawaiian Islands in 1902. *Proceedings of the United States National Museum* **34**, 543–601. doi:10.5479/ si.00963801.34-1624.543

O'Donovan, C., Meade, A., and Venditti, C. (2018). Dinosaurs reveal the geographical signature of an evolutionary radiation. *Nature Ecology and Evolution* **2**, 452–458. doi:10.1038/s41559-017-0454-6

O'Hara, T. D. (2007). Seamounts: centres of endemism or species richness for ophiuroids? *Global Ecology and Biogeography* **16**, 720–732. doi:10.1111/J.1466-8238.2007.00329.X

Orejas, C., Gili, J. M., López-González, P. J., Hasemann, C., and Arntz, W. E. (2007). Reproduction patterns of four Antarctic octocorals in the Weddell Sea: An inter-specific, shape, and latitudinal comparison. *Marine Biology* **150**, 551–563. doi:10.1007/S00227-006-0370-9/FIGURES/6

Padial, J. M., Miralles, A., De la Riva, I., and Vences, M. (2010). The integrative future of taxonomy. *Frontiers in Zoology* **7**. doi:10.1186/1742-9994-7-16

Pagel, M., and Meade, A. (2004). A phylogenetic mixture model for detecting pattern-

heterogeneity in gene sequence or character-state data. *Systematic Biology* **53**, 571–581. doi:10.1080/10635150490468675

Pagel, M., and Meade, A. (2008). Modelling heterotachy in phylogenetic inference by reversible-jump Markov chain Monte Carlo. *Philosophical Transactions of the Royal Society B: Biological Sciences* **363**, 3955–3964. doi:10.1098/rstb.2008.0178

Pagel, M., Meade, A., and Barker, D. (2004). Bayesian Estimation of Ancestral Character States on Phylogenies. *Systematic Biology* **53**, 673–684. doi:10.1080/10635150490522232

Pandolfi, J. M., Connolly, S. R., Marshall, D. J., and Cohen, A. L. (2011). Projecting coral reef futures under global warming and ocean acidification. *Science* **333**, 418–422. doi:10.1126/science.1204794

Pante, E., France, S. C., Couloux, A., Cruaud, C., McFadden, C. S., Samadi, S., and Watling, L. (2012). Deep-sea origin and in-situ diversification of chrysogorgiid octocorals. *PLoS ONE* **7**. doi:10.1371/journal.pone.0038357

Pante, E., Schoelinck, C., and Puillandre, N. (2015). From integrative taxonomy to species description: One step beyond. *Systematic Biology* **64**, 152–160. doi:10.1093/sysbio/syu083

Pearse, J. S., Mooi, R., Lockhart, S. J., and Brandt, A. (2009). Brooding and Species Diversity in the Southern Ocean: Selection for Brooders or Speciation within Brooding Clades? In 'Smithsonian at the poles : contributions to International Polar Year science'. pp. 181–196. (Smithsonian Institution Scholarly Press.) doi:10.5479/si.097884601X.13

Pease, J. B., and Hahn, M. W. (2015). Detection and Polarization of Introgression in a Five-Taxon Phylogeny. *Systematic Biology* **64**, 651–662. doi:10.1093/sysbio/syv023

Pekar, S. F., and DeConto, R. M. (2006). High-resolution ice-volume estimates for the early Miocene: Evidence for a dynamic ice sheet in Antarctica. *Palaeogeography, Palaeoclimatology, Palaeoecology* **231**, 101–109. doi:10.1016/J.PALAEO.2005.07.027

Pérez, C. D., Neves, B. de M., Cordeiro, R. T., Williams, G. C., and Cairns, S. D. (2016). Diversity and Distribution of Octocorallia. In 'The Cnidaria, Past, Present and Future'. pp. 109–123. (Springer International Publishing: Cham.) doi:10.1007/978-3-319-31305-4

Plummer M, Best N, Cowles K, and Vines K (2006). CODA: Convergence Diagnosis and Output Analysis for MCMC. *R News* **6**, 7–11. Available at: https://cran.r-project.org/web/packages/coda/citation.html [accessed 9 October 2021]

Poulin, E., González-Wevar, C., Díaz, A., Gérard, K., and Hüne, M. (2014). Divergence between Antarctic and South American marine invertebrates: What molecular biology tells us about Scotia Arc geodynamics and the intensification of the Antarctic Circumpolar Current. *Global and Planetary Change* **123**, 392–399. doi:10.1016/j.gloplacha.2014.07.017

Prada, C., Schizas, N. V., and Yoshioka, P. M. (2008). Phenotypic plasticity or speciation? A

case from a clonal marine organism. *BMC Evolutionary Biology* **8**, 47. doi:10.1186/1471-2148-8-47

Prokoph, A., Shields, G. A., and Veizer, J. (2008). Compilation and time-series analysis of a marine carbonate δ18O, δ13C, 87Sr/86Sr and δ34S database through Earth history. *Earth-Science Reviews* **87**, 113–133. doi:10.1016/J.EARSCIREV.2007.12.003

Puerta, P., Johnson, C., Carreiro-Silva, M., Henry, L. A., Kenchington, E., Morato, T., Kazanidis, G., Rueda, J. L., Urra, J., Ross, S., Wei, C. L., González-Irusta, J. M., Arnaud-Haond, S., and Orejas, C. (2020). Influence of Water Masses on the Biodiversity and Biogeography of Deep-Sea Benthic Ecosystems in the North Atlantic. *Frontiers in Marine Science* **7**, 239. doi:10.3389/FMARS.2020.00239/BIBTEX

Puillandre, N., Lambert, A., Brouillet, S., and Achaz, G. (2012). ABGD, Automatic Barcode Gap Discovery for primary species delimitation. *Molecular Ecology* **21**, 1864–1877. doi:10.1111/j.1365-294X.2011.05239.x

Quattrini, A. M., Georgian, S. E., Byrnes, L., Stevens, A., Falco, R., and Cordes, E. E. (2013). Niche divergence by deep-sea octocorals in the genus Callogorgia across the continental slope of the Gulf of Mexico. *Molecular Ecology* **22**, 4123–4140. doi:10.1111/mec.12370

Quattrini, A. M., Rodríguez, E., Faircloth, B. C., Cowman, P. F., Brugler, M. R., Farfan, G. A., Hellberg, M. E., Kitahara, M. V., Morrison, C. L., Paz-García, D. A., Reimer, J. D., and McFadden, C. S. (2020). Palaeoclimate ocean conditions shaped the evolution of corals and their skeletons through deep time. *Nature Ecology and Evolution* **4**, 1531–1538. doi:10.1038/s41559-020-01291-1

Quattrini, A. M., Wu, T., Soong, K., Jeng, M. S., Benayahu, Y., and McFadden, C. S. (2019). A next generation approach to species delimitation reveals the role of hybridization in a cryptic species complex of corals. *BMC Evolutionary Biology* **19**, 1–19. doi:10.1186/s12862-019-1427-y

De Queiroz, K. (2005). A Unified Concept of Species and Its Consequences for the Future of Taxonomy. *Proceedings of the California Academy of Sciences* **56**, 196–215.

De Queiroz, K. (2007). Species Concepts and Species Delimitation. *Systematic Biology* **56**, 879–886. doi:10.1080/10635150701701083

Rabosky, D. L. (2014). Automatic Detection of Key Innovations, Rate Shifts, and Diversity-Dependence on Phylogenetic Trees Ed S.-O. Kolokotronis. *PLoS ONE* **9**, e89543. doi:10.1371/journal.pone.0089543

Rabosky, D. L., Grundler, M., Anderson, C., Title, P., Shi, J. J., Brown, J. W., Huang, H., and Larson, J. G. (2014). BAMMtools: an R package for the analysis of evolutionary dynamics on phylogenetic trees Ed S. Kembel. *Methods in Ecology and Evolution* **5**, 701–707.

doi:10.1111/2041-210X.12199

Raftery, A. E., and Lewis, S. M. (1996). Implementing MCMC. In 'Markov Chain Monte Carlo in Practice'. (Eds W. R. Gilks, D. J. Spiegelhalter, and S. Richardson.) pp. 115–130. (Chapman and Hall: London.)

Rambaut, A., and Drummond, A. (2010). TreeAnnotator version 1.6.1.

Rambaut, A., Drummond, A. J., Xie, D., Baele, G., and Suchard, M. A. (2018). Posterior Summarization in Bayesian Phylogenetics Using Tracer 1.7 Ed E. Susko. *Systematic biology* **67**, 901–904. doi:10.1093/sysbio/syy032

Reich, M., and Kutscher, M. (2011). Sea pens (Octocorallia: Pennatulacea) from the Late Cretaceous of northern Germany. *Journal of Paleontology* **85**, 1042–1051. doi:10.1666/10-109.1

Revell, L. J. (2012). phytools: An R package for phylogenetic comparative biology (and other things). *Methods in Ecology and Evolution* **3**, 217–223. doi:10.1111/j.2041-210X.2011.00169.x

Rex, M. A., Stuart, C. T., Hessler, R. R., Allen, J. A., Sanders, H. L., and Wilson, G. D. F. (1993). Global-scale latitudinal patterns of species diversity in the deep-sea benthos. *Nature* **365**, 636–639. doi:10.1038/365636a0

Reznick, D. N., and Ricklefs, R. E. (2009). Darwin's bridge between microevolution and macroevolution. *Nature* **457**, 837–842. doi:10.1038/nature07894

Ricklefs, R. E. (2007). Estimating diversification rates from phylogenetic information. *Trends in Ecology and Evolution* **22**, 601–610. doi:10.1016/j.tree.2007.06.013

Ries, J. B. (2010). Review: Geological and experimental evidence for secular variation in seawater Mg/Ca (calcite-aragonite seas) and its effects on marine biological calcification. *Biogeosciences* **7**, 2795–2849. doi:10.5194/BG-7-2795-2010

Rintoul, S. R. (2018). The global influence of localized dynamics in the Southern Ocean. *Nature 2018 558:7709* **558**, 209–218. doi:10.1038/s41586-018-0182-3

Roberts, A. P., Wilson, G. S., Harwood, D. M., and Verosub, K. L. (2003). Glaciation across the Oligocene–Miocene boundary in southern McMurdo Sound, Antarctica: new chronology from the CIROS-1 drill hole. *Palaeogeography, Palaeoclimatology, Palaeoecology* **198**, 113–130. doi:10.1016/S0031-0182(03)00399-7

Rogers, A. D. (2007). Evolution and biodiversity of Antarctic organisms: A molecular perspective. *Philosophical Transactions of the Royal Society B: Biological Sciences* **362**, 2191–2214. doi:10.1098/rstb.2006.1948

Ronquist, F., and Huelsenbeck, J. P. (2003). MrBayes 3: Bayesian phylogenetic inference under mixed models. *Bioinformatics* **19**, 1572–1574. doi:10.1093/bioinformatics/btg180

Rossin, A. M., Waller, R. G., and Försterra, G. (2017a). Reproduction of the cold-water coral <i>Primnoella chilensis<i/> (Philippi, 1894). *Continental Shelf Research* **144**, 31–37. doi:10.1016/J.CSR.2017.06.010

Rossin, A. M., Waller, R. G., and Försterra, G. (2017b). Reproduction of the cold-water coral Primnoella chilensis (Philippi, 1894). *Continental Shelf Research* **144**, 31–37. doi:10.1016/J.CSR.2017.06.010

Roule, L. (1908). Alcyonaires. *Expedition Antarctique Francaise (1903–1905), Sciences Naturelles: Documents Scientifiques* **15**, 1–6.

Roy, K., and Goldberg, E. E. (2007). Origination, extinction, and dispersal: integrative models for understanding present-day diversity gradients. *The American naturalist* **170 Suppl 2**, S71-85. doi:10.1086/519403

Royer, D. L., Berner, R. A., Montanez, I. P., Tabor, N. J., and Beerling, D. J. (2004). CO2 as a primary driver of Phanerozoic climate. *GSA Today* **14**, 4–10. doi:10.1130/1052-5173(2004)014<4:CAAPDO>2.0.CO;2

Sakamoto, M., and Venditti, C. (2018). Phylogenetic non-independence in rates of trait evolution. *Biology Letters* **14**, 20180502. doi:10.1098/RSBL.2018.0502

Saucède, T., Pierrat, B., Danis, B., David, B., and others (2014). Biogeographic processes in the Southern Ocean. In 'Biogeographic Atlas of the Southern Ocean'. (Ed U. d'Acoz C. d' De Broyer C., Koubbi P., Griffiths H.J., Raymond B.) pp. 456–463. (Scientific Committee on Antarctic Research: Cambridge.)

De Schepper, S., Gibbard, P. L., Salzmann, U., and Ehlers, J. (2014). A global synthesis of the marine and terrestrial evidence for glaciation during the Pliocene Epoch. *Earth-Science Reviews* **135**, 83–102. doi:10.1016/J.EARSCIREV.2014.04.003

Skeels, A. (2019). Lineages through space and time plots: Visualising spatial and temporal changes in diversity. *Frontiers of Biogeography* **11**. doi:10.21425/f5fbg42954

Soler-Hurtado, M. M., López-González, P. J., and Machordom, A. (2017). Molecular phylogenetic relationships reveal contrasting evolutionary patterns in Gorgoniidae (Octocorallia) in the Eastern Pacific. *Molecular Phylogenetics and Evolution* **111**, 219–230. doi:10.1016/j.ympev.2017.03.019

Solórzano, A., Núñez-Flores, M., Inostroza-Michael, O., and Hernández, C. E. (2020). Biotic and abiotic factors driving the diversification dynamics of Crocodylia. *Palaeontology* **63**, 415–429. doi:10.1111/pala.12459

Speijer, R. P., Scheibner, C., Stassen, P., and Morsi, A.-M. M. (2012). Response of marine ecosystems to deep-time global warming: a synthesis of biotic patterns across the Paleocene-Eocene thermal maximum (PETM). *Austrian Journal of Earth Sciences* **105**, 6–

16. doi:10.4103/fjs.fjs_120_18

Stadler, T. (2011). Mammalian phylogeny reveals recent diversification rate shifts. *Proceedings of the National Academy of Sciences of the United States of America* **108**, 6187–92. doi:10.1073/pnas.1016876108

Starmans, A., Gutt, J., and Arntz, W. E. (1999). Mega-epibenthic communities in Arctic and Antarctic shelf areas. *Marine Biology* **135**, 269–280. doi:10.1007/s002270050624

Stoll, H. M., Shimizu, N., Archer, D., and Ziveri, P. (2007). Coccolithophore productivity response to greenhouse event of the Paleocene–Eocene Thermal Maximum. *Earth and Planetary Science Letters* **258**, 192–206. doi:10.1016/J.EPSL.2007.03.037

Strugnell, J. M., Cherel, Y., Cooke, I. R., Gleadall, I. G., Hochberg, F. G., Ibáñez, C. M., Jorgensen, E., Laptikhovsky, V. V., Linse, K., Norman, M., Vecchione, M., Voight, J. R., and Allcock, A. L. (2011). The Southern Ocean: Source and sink? *Deep Sea Research Part II: Topical Studies in Oceanography* **58**, 196–204. doi:10.1016/J.DSR2.2010.05.015

Strugnell, J. M., Rogers, A. D., Prodöhl, P. A., Collins, M. A., and Allcock, A. L. (2008). The thermohaline expressway: The Southern Ocean as a centre of origin for deep-sea octopuses. *Cladistics* **24**, 853–860. doi:10.1111/j.1096-0031.2008.00234.x

Studer, T. (1878). Übersicht der Anthozoa Alcyonaria, welche während der Reise S.M.S Gazelle um die Erde gesammelt wurden. *Monatsbericht der Königlic Preussischen Akademie der Wissenschaften zu Berlin*, 632–688.

Suggett, D. J., Hall-Spencer, J. M., Rodolfo-Metalpa, R., Boatman, T. G., Payton, R., Tye Pettay, D., Johnson, V. R., Warner, M. E., and Lawson, T. (2012). Sea anemones may thrive in a high CO2 world. *Global Change Biology* **18**, 3015–3025. doi:10.1111/J.1365-2486.2012.02767.X

Sweetman, A. K., Thurber, A. R., Smith, C. R., Levin, L. A., Mora, C., Wei, C. L., Gooday, A. J., Jones, D. O. B., Rex, M., Yasuhara, M., Ingels, J., Ruhl, H. A., Frieder, C. A., Danovaro, R., Würzberg, L., Baco, A., Grupe, B. M., Pasulka, A., Meyer, K. S., Dunlop, K. M., Henry, L. A., and Roberts, J. M. (2017). Major impacts of climate change on deep-sea benthic ecosystems. *Elementa* **5**. doi:10.1525/ELEMENTA.203/112418

Taylor, M. L., Cairns, S. D., Agnew, D. J., and Rogers, A. D. (2013). A revision of the genus *Thouarella* Gray, 1870 (Octocorallia: Primnoidae), including an illustrated dichotomous key, a new species description, and comments on *Plumarella* Gray, 1870 and *Dasystenella*, Versluys, 1906. *Zootaxa* **3602**, 1–105.

Taylor, M. L., and Rogers, A. D. (2015). Evolutionary dynamics of a common sub-Antarctic octocoral family. *Molecular Phylogenetics and Evolution* **84**, 185–204. doi:10.1016/j.ympev.2014.11.008

Taylor, M. L., and Rogers, A. D. (2017). Primnoidae (Cnidaria: Octocorallia) of the SW Indian Ocean: new species, genus revisions and systematics. *Zoological Journal of the Linnean Society* **181**, 70–97. doi:10.1093/zoolinnean/zlx003

Thatje, S., Hillenbrand, C.-D., and Larter, R. (2005). On the origin of Antarctic marine benthic community structure. *Trends in Ecology & Evolution* **20**, 534–540. doi:10.1016/J.TREE.2005.07.010

Thoma, J. N., Pante, E., Brugler, M. R., and France, S. C. (2009). Deep-sea octocorals and antipatharians show no evidence of seamount-scale endemism in the NW Atlantic. *Marine Ecology Progress Series* **397**, 25–35. doi:10.3354/MEPS08318

Thomas, E. (2007). Cenozoic mass extinctions in the deep sea: What perturbs the largest habitat on Earth? *Special Paper of the Geological Society of America* **424**, 1–23. doi:10.1130/2007.2424(01)

Thomson, J. A. (1911). Zoological studies chiefly on alcyonarians (fifth and sixth series). *Aberdeen University studies* **48**, 1–177. doi:10.5962/bhl.title.27083

Thomson, J. A., and Richie, J. (1906). The Alcyonarians of the Scottish National Antarctic Expedition. *Transactions of the Royal Society of Edinburgh* **41**, 851–860.

Tittensor, D. P., Mora, C., Jetz, W., Lotze, H. K., Ricard, D., Berghe, E. Vanden, and Worm, B. (2010). Global patterns and predictors of marine biodiversity across taxa. *Nature* **466**, 1098–1101. doi:10.1038/nature09329

Tkachenko, K. S., Wu, B. J., Fang, L. S., and Fan, T. Y. (2007). Dynamics of a coral reef community after mass mortality of branching Acropora corals and an outbreak of anemones. *Marine Biology* **151**, 185–194. doi:10.1007/S00227-006-0467-1/FIGURES/5

Torsvik, T. H., Gaina, C., and Redfield, T. F. (2007). Antarctica and global paleogeography: from Rodinia, rhrough Gondwanaland and Pangea, to the birth of the Southern Ocean and the opening of gateways. doi:10.3133/OFR20071047KP11

Torsvik, T. H., Gaina, C., and Redfield, T. F. (2008). Antarctica and Global Paleogeography: From Rodinia, Through Gondwanaland and Pangea, to the Birth of the Southern Ocean and the Opening of Gateways. In 'Antarctica: A Keystone in a Changing World - Online Proceedings for the 10th International Symposium on Antarctic Earth Sciences'. (Eds A. K. Cooper, P. J. Barrett, H. Stagg, B. Storey, E. Stump, and W. Wise.) pp. 125–140. (The National Academies Press: Washington, DC.) doi:10.3133/OFR20071047KP11

Tripati, A., Backman, J., Elderfield, H., and Ferretti, P. (2005). Eocene bipolar glaciation associated with global carbon cycle changes. *Nature* **436**, 341–346. doi:10.1038/nature03874

Tripati, A., and Elderfield, H. (2005). Paleoclimate: Deep-sea temperature and circulation

changes at the Paleocene-Eocene Thermal Maximum. *Science* **308**, 1894–1898. doi:10.1126/SCIENCE.1109202/SUPPL_FILE/TRIPATI-SOM.PDF

Tu, T. H., Dai, C. F., and Jeng, M. S. (2015). Phylogeny and systematics of deep-sea precious corals (Anthozoa: Octocorallia: Coralliidae). *Molecular Phylogenetics and Evolution* **84**, 173. doi:10.1016/j.ympev.2014.09.031

Turelli, M., Barton, N. H., and Coyne, J. A. (2001). Theory and speciation. *Trends in Ecology and Evolution* **16**, 330–343. doi:10.1016/S0169-5347(01)02177-2

Tyler, P. A. (2003). 'Ecosystems of the deep oceans'. (Elsevier.)

Tyrrell, T. (2011). Anthropogenic modification of the oceans. *Philosophical Transactions of the Royal Society A: Mathematical, Physical and Engineering Sciences* **369**, 887–908. doi:10.1098/RSTA.2010.0334

Van Valen, L. (1973). A new evolutionary law. *Evol Theory* **1**, 1–30.

Valenciennes, A. (1846). Atlas of Zoophytes. In 'Voyage autour du monde sur la frégate la Vénus, pendant les annees 1836-1839'. (Ed Dupetit-Thouars.) (Atlas de Zoologie Gide et Cie: Paris.)

Vargas, S., Guzman, H. M., Breedy, O., and Wörheide, G. (2014). Molecular phylogeny and DNA barcoding of tropical eastern Pacific shallow-water gorgonian octocorals. *Marine Biology* **161**, 1027–1038. doi:10.1007/s00227-014-2396-8

Venditti, C., Meade, A., and Pagel, M. (2011). Multiple routes to mammalian diversity. *Nature* **479**, 393–396. doi:10.1038/nature10516

Venditti, C., Meade, A., and Pagel, M. (2010). Phylogenies reveal new interpretation of speciation and the Red Queen. *Nature* **463**, 349–352. doi:10.1038/nature08630

Versluys, J. (1906). Die Gorgoniden der Siboga-Expedition. *Siboga-Expeditie* **13a**, 1–187.

Vrba, E. S. (1993). Turnover-pulses, the Red Queen, and related topics. *American Journal of Science* **293 A**, 418–452. doi:10.2475/ajs.293.A.418

Waller, R. G., Stone, R. P., Johnstone, J., and Mondragon, J. (2014). Sexual Reproduction and Seasonality of the Alaskan Red Tree Coral, Primnoa pacifica. *PLOS ONE* **9**, e90893. doi:10.1371/JOURNAL.PONE.0090893

Wiens, J. J. (2011). The Causes Of Species Richness Patterns Across Space, Time, And Clades And The Role Of "Ecological Limits". *The Quarterly Review of Biology* **86**, 75–96. doi:10.1086/659883

Willig, M. R., Kaufman, D. M., and Stevens, R. D. (2003). Latitudinal Gradients of Biodiversity: Pattern, Process, Scale, and Synthesis. *Annual Review of Ecology, Evolution, and Systematics* **34**, 273–309. doi:10.1146/annurev.ecolsys.34.012103.144032

Woolley, S. N. C., Tittensor, D. P., Dunstan, P. K., Guillera-Arroita, G., Lahoz-Monfort, J. J.,

Wintle, B. A., Worm, B., and O'Hara, T. D. (2016). Deep-sea diversity patterns are shaped by energy availability. *Nature* **533**, 393–396. doi:10.1038/nature17937

Wright, E. P., and Studer, T. (1889). Report on the Alcyonaria Collected by H.M.S. Challenger during the Years 1873–76. *Report on the Scientifi c Results of the Voyage of H.M.S. Challenger during the Years 1873–76, Zoology* **31**, 1– 314.

Xia, X., and Xie, Z. (2001). DAMBE: Software package for data analysis in molecular biology and evolution. *Journal of Heredity* **92**, 371–373. doi:10.1093/jhered/92.4.371

Xia, X., Xie, Z., Salemi, M., Chen, L., and Wang, Y. (2002). An index of sustitution saturation and its application. *Mol. Phylogenet. Evol.* **26**, 1–7.

Xu, Y., Zhan, Z., and Xu, K. (2020). Morphology and molecular phylogeny of three new deep-sea species of *Chrysogorgia* (Cnidaria, Octocorallia) from seamounts in the tropical Western Pacific Ocean. *PeerJ* **2020**, e8832. doi:10.7717/peerj.8832

Yasuhara, M., Cronin, T. M., Demenocal, P. B., Okahashi, H., and Linsley, B. K. (2008). Abrupt climate change and collapse of deep-sea ecosystems. *Proceedings of the National Academy of Sciences* **105**, 1556–1560. doi:10.1073/PNAS.0705486105

Yasuhara, M., and Danovaro, R. (2016). Temperature impacts on deep-sea biodiversity. *Biological Reviews* **91**, 275–287. doi:10.1111/BRV.12169

Yesson, C., Wright, E., and Braga-Henriques, A. (2018). Population genetics of Narella versluysi (Octocorallia: Alcyonacea, Primnoidae) in the Bay of Biscay (NE Atlantic). *Marine Biology* **165**, 1–12. doi:10.1007/S00227-018-3394-Z/TABLES/4

Zachos, J. C., Dickens, G. R., and Zeebe, R. E. (2008). An early Cenozoic perspective on greenhouse warming and carbon-cycle dynamics. *Nature* **451**, 279–283. doi:10.1038/nature06588

Zachos, J. C., Pagani, H., Sloan, L., Thomas, E., and Billups, K. (2001). Trends, rhythms, and aberrations in global climate 65 Ma to present. *Science* **292**, 686–693. doi:10.1126/science.1059412

Zachos, J. C., Röhl, U., Schellenberg, S. A., Sluijs, A., Hodell, D. A., Kelly, D. C., Thomas, E., Nicolo, M., Raffi, I., Lourens, L. J., McCarren, H., and Kroon, D. (2005). Rapid acidification of the ocean during the paleocene-eocene thermal maximum. *Science* **308**, 1611–1615. doi:10.1126/science.1109004

Zaffos, A., Finnegan, S., and Peters, S. E. (2017). Plate tectonic regulation of global marine animal diversity. *Proceedings of the National Academy of Sciences of the United States of America* **114**, 5653–5658. doi:10.1073/pnas.1702297114

Zapata-Guardiola, R., and López-González, P. J. (2010a). Designation of Thouarella abies Broch, 1965 as the type species of the subgenus *Fannyella* (*Scyphogorgia*) Cairns and

Bayer, 2009, and description of a new genus for *Stenella* (*Dasystenella*) *liouvillei* Gravier, 1913 (Octoco. *Journal of Natural History* **44**, 1995–2013. doi:10.1080/00222933.2010.485739

Zapata-Guardiola, R., and López-González, P. J. (2010b). Four new species of *Thouarella* (Anthozoa: Octocorallia: Primnoidae) from Antarctic waters. *Scientia Marina* **74**, 131–146. doi:10.3989/scimar.2010.74n1131

Zapata-Guardiola, R., and López-González, P. J. (2010c). Redescription of *Thouarella brucei* Thomson and Ritchie, 1906 (Cnidaria: Octocorallia: Primnoidae) and description of two new Antarctic primnoid species.

Zapata-Guardiola, R., and López-González, P. J. (2012). Revision and redescription of the species previously included in the genus *Amphilaphis* Studer and Wright in Studer, 1887 (Octocorallia: Primnoidae). *Scientia Marina* **76**, 357–380. doi:10.3989/scimar.03278.18B

Zapata-Guardiola, R., and López-González, P. J. (2010d). Two new gorgonian genera (Octocorallia: Primnoidae) from Southern Ocean waters. *Polar Biology* **33**, 313–320. doi:10.1007/s00300-009-0707-1

Zapata-Guardiola, R., and López-González, P. J. (2010e). Two new species of Antarctic gorgonians (Octocorallia: Primnoidae) with a redescription of *Thouarella laxa* Versluys, 1906. *Helgoland Marine Research* **64**, 169–180. doi:10.1007/s10152-009-0176-5

Zapata-Guardiola, R., López-González, P. J., and Gili, J.-M. (2013). A review of the genus *Mirostenella* Bayer, 1988 (Octocorallia: Primnoidae) with a description of a new subgenus and species. *Helgoland Marine Research* **67**, 229–240. doi:10.1007/s10152-012-0318-z

Zhang, J., Kapli, P., Pavlidis, P., and Stamatakis, A. (2013). A general species delimitation method with applications to phylogenetic placements. *Bioinformatics* **29**, 2869–2876. doi:https://doi.org/10.1093/bioinformatics/btt499

APÉNDICES

Apéndice 1. Material electrónico suplementario para "*Molecular and morphological data reveal three new species of Thouarella (Anthozoa: Octocorallia: Primnoidae) from the Southern Ocean*".

Supplementary file 1. Primers used to amplify the regions of *Cox1*, *MutS* and *28S*.

Primer name (gene)	Sequence	(Initial Temp:Time) (Annealing Temp:Time) (Extension Temp:Time)	No. of cycles/(Final Extension Temp:Time)	
	Cox1			
COII8068F COIOCTR	CCA TAA CAG GAC TAG CAG CATC ATC ATA GCA TAG ACC ATA CC	95°C:15sg 58°C:15sg 72°C:15sg	35/(72°C:300sg	(1) (4)
	MutS			
ND4L2475F ND42625F MUT3458R	TAG TTT TAC TGG CCT CTA C TAC GTG GYA CAA TTG CTG TSG AGC AAA AGC CAC TCC	95°C:15sg 51°C:15sg 72°C:15sg	35/(72°C:300) sg	(1) (2) (5)
	28S			
28S-Far 28S-Rar	CACGAGACCGATAGCGAACAAGTA TCATTTCGACCCTAAGACCTC	95°C:15sg 50°C:15sg 72°C:15sg	35/(72°C:300) sg	(3)

References: (1) McFadden et al. 2004; (2) McFadden et al. 2006b; (3) McFadden and van Ofwegen (2012); (4) France and Hoover 2002; (5) Sánchez et al. 2003. F= forward primer, R= reverse primer.

Supplementary File 2. GenBank accession numbers of the primnoids specimens used for the molecular analysis. Materials in bold are the newly sequenced for this study.

Specimen code and species name	Collection code (Reference)	*Cox1*	*MutS*	28S
		Genbank number	Genbank number	Genbank number
Armadillogorgia sp.	FD11	KP677971	KP324353	KP324582

Armadillogorgia sp.	FD67	KP677973	KP324355	KP324584
Arntzia gracilis	AR002	KP677919	KP324300	-
Arntzia gracilis	AR058	KP677926	KP324306	-
Callogorgia sp.	AR119	KP677935	KP324315	KP324551
Callogorgia sp.	AR201	KP677952	KP324333	KP324565
Callogorgia sp.	AR223	KP677958	KP324340	KP324569
Callozostron mirabile	N77603	MG986927	MG986976	MG980146
Callozostron acanthodes	AR185	KP677947	KP324329	KP324561
Chrysogorgia averta	LII10-609	KC788235	KC788265	KC788258
Calyptrophora inornata	N11159	MG986936	MG986985	MG980154
Calyptrophora microdentata	USNM1120699	MG986914	MG986963	MG980136
Calyptrophora wyvillei	USNM1170789	MG986937	MG986986	MG980155
Convexella magelhaenica	USNM1113007	MG986931	MG986980	MG980149
Convexella magelhaenica	USNM1232168	MG986932	MG986981	MG980150
Convexella sp.	FP65	KP677974	KP324356	KP324585
Dasystenella austasensis	AE021	KP677909	KP324290	KP324529
Dasystenella acanthina	AR054	KP677925	KP324305	KP324543
Dasystenella acanthina	N33	KP677989	KP324371	KP324598
Fanellia euthyeia	AR213	KP677956	KP324338	KP324567
Fanellia medialis	AR210	KP677955	KP324337	KP324566
Fanellia cf. *tuberculata/granulosa*	AR220	KP677957	KP324339	KP324568
Fannyella (*Cyathogorgia*) *spinosa*	AR085	KP677927	KP324307	KP324545
Fannyella (*Cyathogorgia*) *spinosa*	AR123	KP677937	KP324317	KP324553
Fannyella (*Fannyella*) *rossi*	AR019	KP677922	KP324302	KP324540
Fannyella (*Fannyella*) *rossi*	AR095	KP677930	KP324310	KP324548
Fannyella (*Fannyella*) *rossi*	AR167	KP677943	KP324324	KP324558
Metafannyella kuekenthali	D3	KP677968	KP324350	KP324579
Metafannyella ventilabrum	N73567	MG986924	MG986973	MG980144
Metafannyella kuekenthali	R23	KP677999	KP324380	KP324604
Mirostenella articulata	AC35	KP677905	KP324286	KP324525
Mirostenella articulata	AE002	KP677906	KP324287	KP324526
Mirostenella articulata	AE093	KP677916	KP324297	KP324535
Narella macrocalyx	USNM1149566	MG986938	MG986987	MG980156

Narella clavata	AR236	KP677961	KP324343	KP324572
Narella speighti	SW3719	KP678015	KP324399	KP324622
Narella valentine	SW3807	KP678017	KP324401	KP324624
Onogorgia nodosa	N28	KP677986	KP324368	KP324595
Onogorgia nodosa	N30	KP677988	KP324370	KP324597
Ophidogorgia kuekenthali	AR099	KP677932	KP324312	KP324549
Ophidogorgia cf. *kuekenthali*	AR131	KP677938	KP324318	KP324554
Ophidogorgia cf. *kuekenthali*	AR133	KP677939	KP324319	KP324555
Parastenella pacifica	N94401	MG986920	MG986969	MG980141
Parastenella spinosa	G60	KP677975	KP324357	KP324586
Parastenella spinosa	T147	KP678022	KP324405	KP324628
Perissogorgia vitrea	N9882	MG986915	MG986964	MG980137
Plumarella (Plumarella) pourtalesii	USNM79782	MG986933	MG986982	MG980151
Plumarella delicatissima	O24	KP677992	KP324374	-
Plumarella cf. *delicatissima*	N05	KP677982	KP324364	KP324591
Thouarella diadema	AE068	KP677915	KP324296	KP324534
Thouarella diadema	B34	KP677965	KP324347	KP324576
Thouarella diadema	S060	KP678001	KP324382	KP324606
Thouarella diadema	Z051	KP678026	KP324408	KP324632
Thouarella undulata	B48	KP677966	KP324348	KP324577
Thouarella undulata	S093	KP678002	KP324383	KP324607
Thouarella undulata	Z046	KP678025	KP324407	KP324631
Primnoa bisquama	SW3518	KP678013	KP324397	KP324620
Primnoeides sp.	SW3291	KP678011	KP324395	KP324618
Primnoeides flagellum	SW3564	KP678014	KP324398	KP324621
Primnoeides sertularoides	SW3149	KP678006	KP324389	KP324612
Primnoeides sertularoides	SW3165	KP678007	KP324391	KP324614
Primnoella antarctica	N25	KP677984	KP324366	KP324593
Primnoella antarctica	N26	KP677985	KP324367	KP324594
Primnoella chilensis	H39	KP677977	KP324359	KP324588
Primnoella chilensis	T124	KP678020	KP324403	KP324627
Primnoella delicatissima	PRIM02	KP677994	KP324377	KP324602
Primnoella scotiae	B32	KP677964	KP324346	KP324575
Primnoella scotiae	I25	KP677979	KP324361	KP324589

Primnoella scotiae	L25	KP677980	KP324362	KP324590
Thouarella antarctica	AE064	KP677914	KP324295	KP324533
Thouarella antarctica	AR018	KP677921	KP324301	KP324539
Thouarella cf. *antarctica*	AR175	KP677946	KP324328	KP324560
Thouarella cf. *brucei*	T125	KP678021	KP324404	-
Thouarella chilensis	AE026	KP677910	KP324291	KP324530
Thouarella chilensis	N09	KP677983	KP324365	KP324592
Thouarella chilensis	R54	KP678000	KP324381	KP324605
Thouarella crenelata	AR091	KP677928	KP324308	KP324546
Thouarella crenelata	W54	KP678024	KP324406	KP324630
Thouarella laxa	AR194	KP677950	KP324331	KP324563
Thouarella laxa	AR200	KP677951	KP324332	KP324564
Thouarella cf. *laxa*	AR232	KP677960	KP324342	KP324571
Thouarella pendulina	AR135	KP677941	KP324321	KP324556
Thouarella variabilis	AE059	KP677913	KP324294	KP324532
Thouarella variabilis	AR027	KP677923	KP324303	KP324541
Thouarella cf. *variabilis*	A06	KP677902	KP324283	KP324524
Thouarella viridis	AE019	KP677908	KP324289	KP324528
Thouarella viridis	H13	KP677976	KP324358	KP324587
Tokoprymno sp.	PRIM09	KP677996	KP324379	-
Tokoprymno sp.	PRIM10	KP677997	-	-
Thouarella weddellensis sp. nov.	MZB 2019-1967	MN914149	MN916716	MN921246
Thouarella weddellensis sp. nov.	MZB 2019-1970	MN914150	MN916717	MN921247
Thouarella weddellensis sp. nov.	MZB 2019-1969	MN914151	MN916718	MN921248
Thouarella polarsterni sp. nov.	MZB 2019-1984	MN914145	MN916712	-
Thouarella polarsterni sp. nov.	MZB 2019-1983	MN914146	MN916713	-
Thouarella polarsterni sp. nov.	MZB 2019-1986	MN914147	MN916714	MN921245
Thouarella polarsterni sp. nov.	MZB 2019-1981	MN914148	MN916715	-
Thouarella islai sp. nov.	MZB 2019-1966	MN914144	MN916709	-
Thouarella islai sp. nov.	MZB 2019-1965	MN914143	MN916710	-
Thouarella islai sp. nov.	MZB 2019-1964	MN914142	MN916711	MN921244

Apéndice 2. Material electrónico suplementario para "*Molecular systematics of Thouarella (Octocorallia: Primnoidae) with the description of three new species from the Southern Ocean based on combined molecular and morphological evidence*".

Table S1. GenBank accession numbers of the primnoids specimens used for the molecular analysis. Materials in bold are the newly sequenced for this study.

Specimen code and species name	**GenBank ID (Collection number)**	***MutS***	***COX1***	***28S***
Callozostron acanthodes	AR185	KP677947	KP324329	KP324561
Thouarella diadema	AE068	KP677915	KP324296	KP324534
Thouarella diadema	B34	KP677965	KP324347	KP324576
Thouarella diadema	S060	KP678001	KP324382	KP324606
Thouarella diadema	Z051	KP678026	KP324408	KP324632
Thouarella undulata	B48	KP677966	KP324348	KP324577
Thouarella undulata	S093	KP678002	KP324383	KP324607
Thouarella undulata	Z046	KP678025	KP324407	KP324631
Thouarella antarctica	AE064	KP677914	KP324295	KP324533
Thouarella antarctica	AR018	KP677921	KP324301	KP324539
Thouarella cf. *antarctica*	AR175	KP677946	KP324328	KP324560
Thouarella cf. *brucei*	T125	KP678021	KP324404	---
Thouarella chilensis	AE026	KP677910	KP324291	KP324530
Thouarella chilensis	N09	KP677983	KP324365	KP324592
Thouarella chilensis	R54	KP678000	KP324381	KP324605
Thouarella crenelata	AR091	KP677928	KP324308	KP324546
Thouarella crenelata	W54	KP678024	KP324406	KP324630
Thouarella laxa	AR194	KP677950	KP324331	KP324563
Thouarella laxa	AR200	KP677951	KP324332	KP324564
Thouarella cf. *laxa*	AR232	KP677960	KP324342	KP324571
Thouarella pendulina	AR135	KP677941	KP324321	KP324556
Thouarella variabilis	AE059	KP677913	KP324294	KP324532
Thouarella variabilis	AR027	KP677923	KP324303	KP324541
Thouarella cf. *variabilis*	A06	KP677902	KP324283	KP324524
Thouarella viridis	AE019	KP677908	KP324289	KP324528
Thouarella viridis	H13	KP677976	KP324358	KP324587

Thouarella weddellensis	OPRIM-1922 (MZB 2019-1967)	MN914149	MN916716	MN921246
Thouarella weddellensis	OPRIM-2081 (MZB 2019-1970)	MN914150	MN916717	MN921247
Thouarella weddellensis	OPRIM-307 (MZB 2019-1969)	MN914151	MN916718	MN921248
Thouarella polarsterni	OPRIM-2111 (MZB 2019-1984)	MN914145	MN916712	---
Thouarella polarsterni	OPRIM-2112 (MZB 2019-1983)	MN914146	MN916713	---
Thouarella polarsterni	OPRIM-2209 (MZB 2019-1986)	MN914147	MN916714	MN921245
Thouarella polarsterni	OPRIM-2282 (MZB 2019-1981)	MN914148	MN916715	---
Thouarella islai	OPRIM- 2168 (MZB 2019-1966)	MN914144	MN916709	---
Thouarella islai	OPRIM- 2169 (MZB 2019-1965)	MN914143	MN916710	---
Thouarella islai	OPRIM- 2194 (MZB 2019-1964)	MN914142	MN916711	MN921244
***Thouarella dolichoespinosa* sp. nov.**	**OPRIM 1253 (MZB 2020-0642)**	**MT894198**	**MT892693**	**MT892733**
***Thouarella dolichoespinosa* sp. nov.**	**OPRIM-2268 (MZB 2020-0652)**	**MT894196**	**MT892691**	**---**
***Thouarella dolichoespinosa* sp. nov.**	**OPRIM-2386 (MZB 2020-0654)**	**MT894197**	**MT892692**	**---**
***Thouarella dolichoespinosa* sp. nov.**	**BECA-OPRIM-2299**	**MT894195**	**MT892690**	**---**
***Thouarella pseudoislai* sp. nov.**	**OPRIM-2384 (MZB 2020-0641)**	**MT894219**	**MT892714**	**MT892730**
***Thouarella pseudoislai* sp. nov.**	**OPRIM-2383 (MZB 2020-0653)**	**MT894218**	**MT892713**	**MT892729**
***Thouarella pseudoislai* sp. nov.**	**BECA-OPRIM-2201**	**MT894217**	**MT892712**	**---**
***Thouarella amundseni* sp. nov.**	**OPRIM 2105 (MZB 2020-0643)**	**MT894200**	**MT892703**	**MT892720**
***Thouarella amundseni* sp. nov.**	**BECA-OPRIM-2091**	**MT894199**	**MT892702**	**MT892719**
***Thouarella amundseni* sp. nov.**	**OPRIM-2113 (MZB 2020-0647)**	**MT894201**	**MT892704**	**MT892721**
***Thouarella amundseni* sp. nov.**	**OPRIM-2202 (MZB 2020-0649)**	**MT894202**	**MT892706**	**---**
***Thouarella amundseni* sp. nov.**	**OPRIM-2241 (MZB 2020-0650)**	**MT894203**	**MT892707**	**MT892723**
***Thouarella amundseni* sp. nov.**	**OPRIM-2454 (MZB 2020-0655)**	**MT894205**	**MT892708**	**---**
***Thouarella amundseni* sp. nov.**	**OPRIM-2455 (MZB 2020-0656)**	**MT894206**	**MT892709**	**---**
Thouarella viridis	**BECA-OPRIM-1933**	**MT894191**	**MT892683**	**MT892715**

Thouarella viridis	**BECA-OPRIM-1934**	**MT894192**	**MT892684**	**---**
Thouarella andeep	**OPRIM 2000 (ZIZMH-C11745a)**	**MT894190**	**MT892685**	**MT892716**
Thouarella andeep	**OPRIM 6262 (ZIZMH-C11745b)**	**MT894188**	**MT892686**	**MT892717**
Thouarella andeep	**OPRIM 6260 (BECA-OPRIM-2609)**	**MT894189**	**MT892687**	**MT892718**

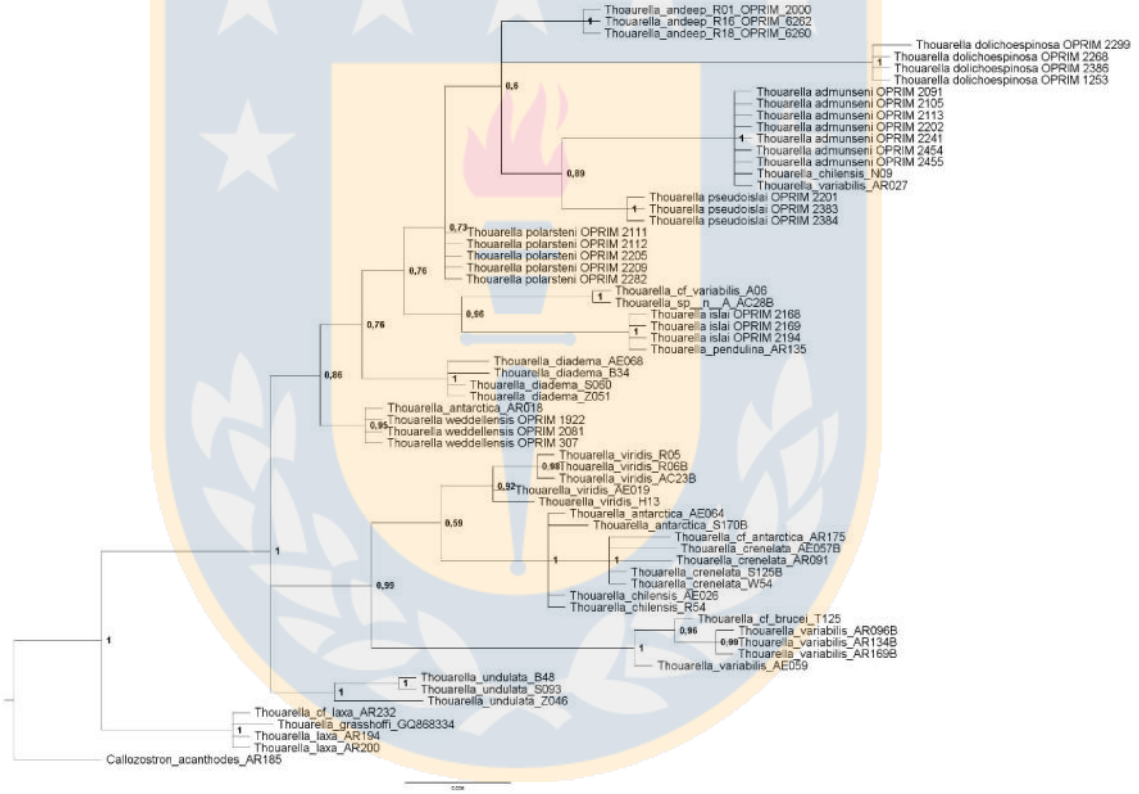

Figure S1. Bayesian phylogeny based on the *mtMutS* locus. The number near nodes represent the posterior probabilities support.

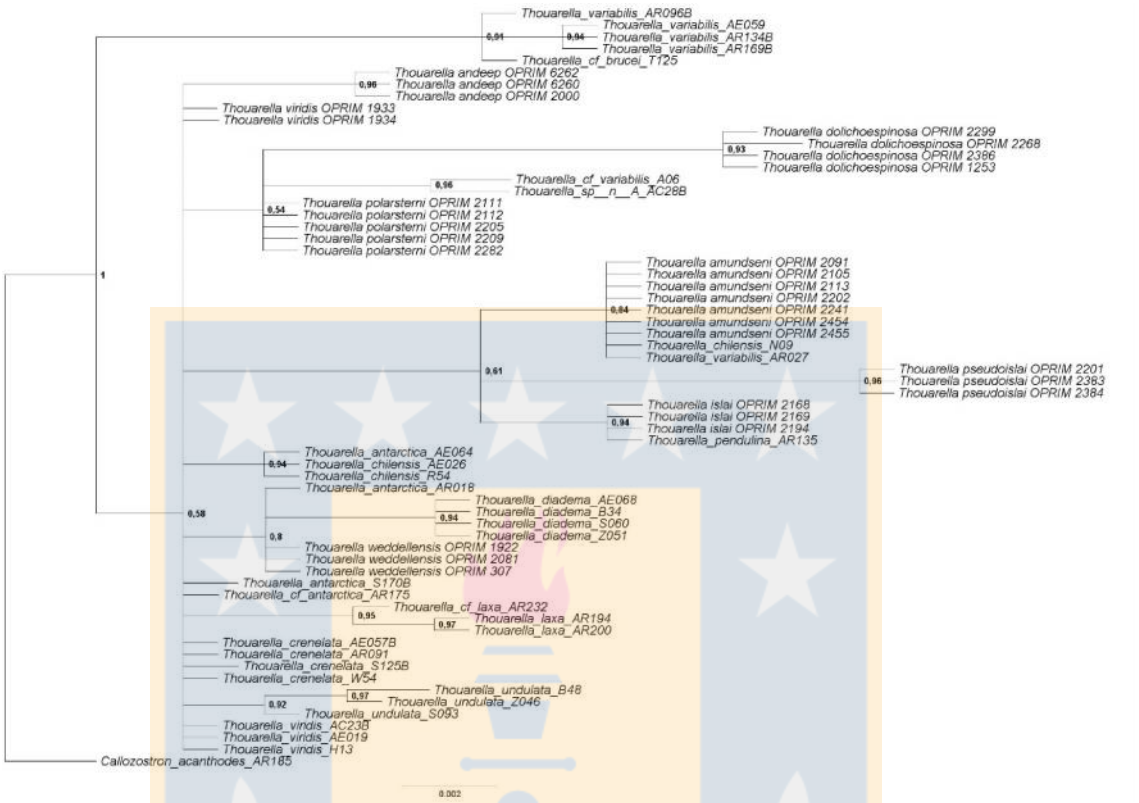

Figure S2. Bayesian phylogeny based on the *Cox1* locus. The number near nodes represent the posterior probabilities support.

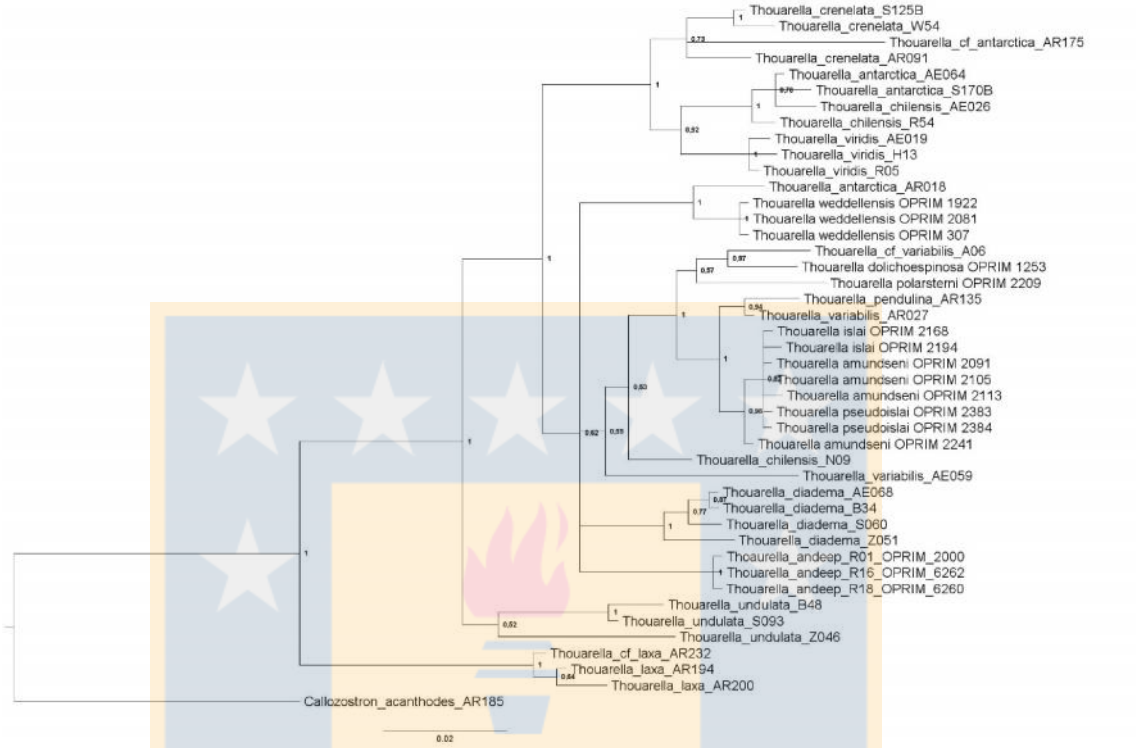

Figure S3. Bayesian phylogeny based on the *28S* locus. The number near nodes represent the posterior probabilities support.

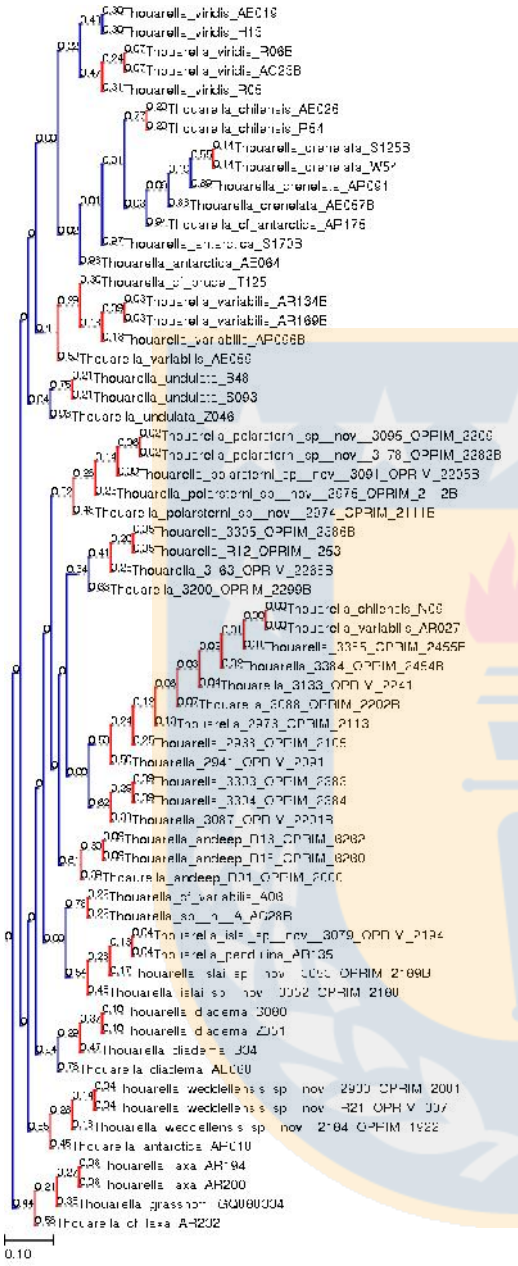

 # Most supported partition found by simple heuristic search
Species 1 (support = 0.439): Thouarella_cf_laxa_AR232, Thouarella_grasshoffi_GQ868334, Thouarella_laxa_AR194, Thouarella_laxa_AR200
Species 2 (support = 0.612): Thoaurella_andeep_R01_OPRIM_2000, Thouarella_andeep_R16_OPRIM_6262, Thouarella_andeep_R18_OPRIM_6260
Species 3 (support = 0.517): Thouarella_polarsterni_OPRIM_2111B, Thouarella_polarsterni_OPRIM_2112B, Thouarella_polarsterni_OPRIM_2205B, Thouarella_polarsterni_OPRIM_2209, Thouarella_polarsterni_OPRIM_2282B
Species 4 (support = 0.555): Thouarella_antarctica_AR018, Thouarella_weddellensis_OPRIM_1922, Thouarella_weddellensis_OPRIM_2081, Thouarella_weddellensis_OPRIM_307
Species 5 (support = 0.409): Thouarella_cf_brucei_T125, Thouarella_variabilis_AR096B, Thouarella_variabilis_AR134B, Thouarella_variabilis_AR169B, Thouarella_variabilis_AE059
Species 6 (support = 0.502): Thouarella_OPRIM_2091, Thouarella_OPRIM_2105, Thouarella_OPRIM_2113, Thouarella_OPRIM_2202B, Thouarella_OPRIM_2241, Thouarella_OPRIM_2454B, Thouarella_OPRIM_2455B, Thouarella_chilensis_N09, Thouarella_variabilis_AR027
Species 7 (support = 0.618): Thouarella_OPRIM_2201B, Thouarella_OPRIM_2383, Thouarella_OPRIM_2384
Species 8 (support = 0.981): Thouarella_antarctica_AE064
Species 9 (support = 0.975): Thouarella_antarctica_S170B
Species 10 (support = 0.765): Thouarella_chilensis_AE026, Thouarella_chilensis_R54
Species 11 (support = 0.780): Thouarella_cf_variabilis_A06, Thouarella_sp__n__A_AC28B
Species 12 (support = 0.545): Thouarella_islai_OPRIM_2168, Thouarella_islai_OPRIM_2169B, Thouarella_islai_OPRIM_2194, Thouarella_pendulina_AR135
Species 13 (support = 0.939): Thouarella_cf_antarctica_AR175
Species 14 (support = 0.876): Thouarella_crenelata_AE057B
Species 15 (support = 0.752): Thouarella_undulata_B48, Thouarella_undulata_S093
Species 16 (support = 0.957): Thouarella_undulata_Z046
Species 17 (support = 0.292): Thouarella_diadema_B34, Thouarella_diadema_S060, Thouarella_diadema_Z051
Species 18 (support = 0.765): Thouarella_diadema_AE068
Species 19 (support = 0.472): Thouarella_viridis_R05, Thouarella_viridis_R06B, Thouarella_viridis_AC23B
Species 20 (support = 0.304): Thouarella_viridis_AE019
Species 21 (support = 0.304): Thouarella_viridis_H13
Species 22 (support = 0.545): Thouarella_crenelata_S125B, Thouarella_crenelata_W54
Species 23 (support = 0.687): Thouarella_crenelata_AR091
Species 24 (support = 0.410): Thouarella_OPRIM_2268B, Thouarella_OPRIM_2386B, Thouarella_OPRIM_1253
Species 25 (support = 0.661): Thouarella_3200_OPRIM_2299B

Figure S4. Highest Bayesian supported solution based on the single locus *mtMuts* and the bPTP approach. On the left are details of the 25 putative species provided by the bPTP analysis.

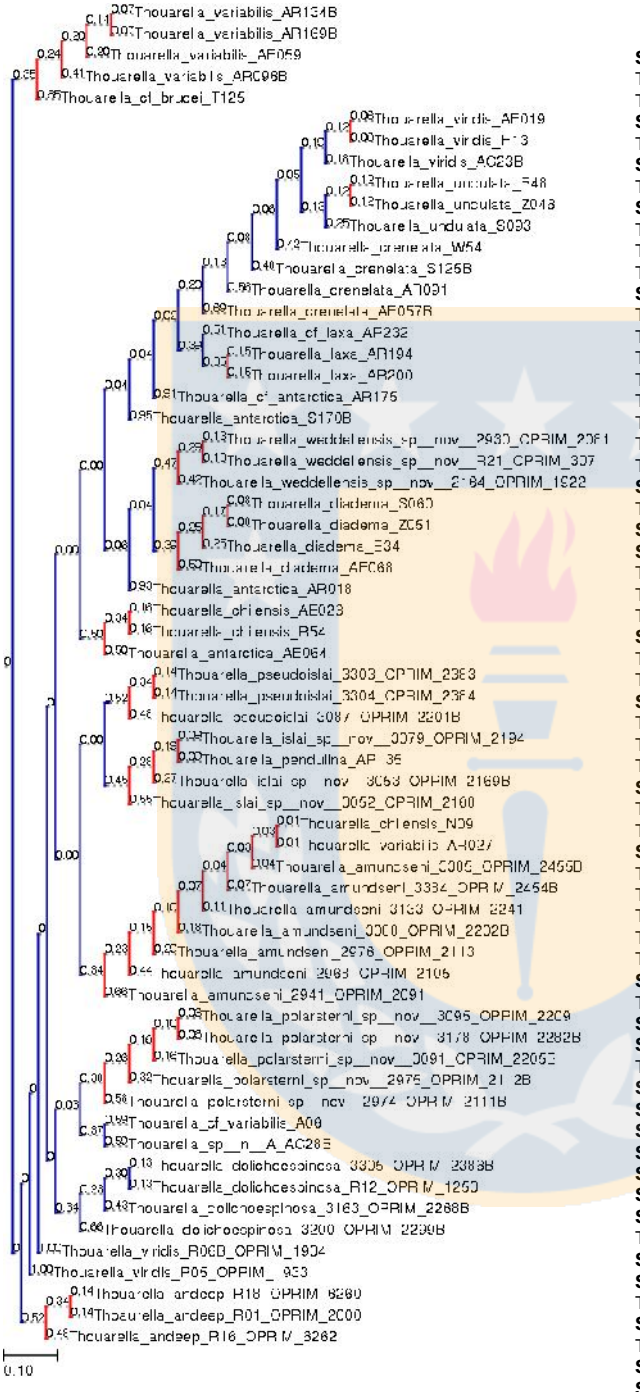

 # Most supported partition found by simple heuristic search

Species 1 (support = 0.352): Thouarella_cf_brucei_T125, Thouarella_variabilis_AE059, Thouarella_variabilis_AR134B, Thouarella_variabilis_AR169B, Thouarella_variabilis_AR096B
Species 2 (support = 1.000): Thouarella_viridis_R06B_OPRIM_1934
Species 3 (support = 1.000): Thouarella_viridis_R05_OPRIM_1933
Species 4 (support = 0.523): Thouarella_andeep_OPRIM_6262, Thouarella_andeep_OPRIM_6260, Thoaurella_andeep_OPRIM_2000
Species 5 (support = 0.337): Thouarella_amundseni_OPRIM_2091, Thouarella_amundseni_OPRIM_2105, Thouarella_amundseni_OPRIM_2113, Thouarella_amundseni_OPRIM_2202B, Thouarella_amundseni_OPRIM_2241, Thouarella_amundseni_OPRIM_2454B, Thouarella_amundseni_OPRIM_2455B, Thouarella_chilensis_N09, Thouarella_variabilis_AR027
Species 6 (support = 0.499): Thouarella_antarctica_AE064, Thouarella_chilensis_AE026, Thouarella_chilensis_R54
Species 7 (support = 0.931): Thouarella_antarctica_AR018
Species 8 (support = 0.467): Thouarella_weddellensis_OPRIM_1922, Thouarella_weddellensis_OPRIM_2081, Thouarella_weddellensis_OPRIM_307
Species 9 (support = 0.391): Thouarella_diadema_AE068, Thouarella_diadema_B34, Thouarella_diadema_S060, Thouarella_diadema_Z051
Species 10 (support = 0.516): Thouarella_pseudoislai_OPRIM_2201B, Thouarella_pseudoislai_OPRIM_2383, Thouarella_pseudoislai_OPRIM_2384
Species 11 (support = 0.447): Thouarella_islai_OPRIM_2168, Thouarella_islai_OPRIM_2169B, Thouarella_islai_OPRIM_2194, Thouarella_pendulina_AR135
Species 12 (support = 0.383): Thouarella_polarsterni_OPRIM_2111B, Thouarella_polarsterni_OPRIM_2112B, Thouarella_polarsterni_OPRIM_2205B, Thouarella_polarsterni_OPRIM_2209, Thouarella_polarsterni_OPRIM_2282B
Species 13 (support = 0.659): Thouarella_dolichoespinosa_3200_OPRIM_2299B
Species 14 (support = 0.951): Thouarella_antarctica_S170B
Species 15 (support = 0.914): Thouarella_cf_antarctica_AR175
Species 16 (support = 0.692): Thouarella_crenelata_AE057B
Species 17 (support = 0.559): Thouarella_crenelata_AR091
Species 18 (support = 0.482): Thouarella_crenelata_S125B
Species 19 (support = 0.422): Thouarella_crenelata_W54
Species 20 (support = 0.595): Thouarella_cf_variabilis_A06
Species 21 (support = 0.595): Thouarella_sp__n__A_AC28B
Species 22 (support = 0.125): Thouarella_undulata_B48, Thouarella_undulata_Z046
Species 23 (support = 0.246): Thouarella_undulata_S093
Species 24 (support = 0.431): Thouarella_dolichoespinosa_OPRIM_2268B
Species 25 (support = 0.122): Thouarella_viridis_AE019, Thouarella_viridis_H13
Species 26 (support = 0.180): Thouarella_viridis_AC23B
Species 27 (support = 0.508): Thouarella_cf_laxa_AR232
Species 28 (support = 0.354): Thouarella_laxa_AR194, Thouarella_laxa_AR200
Species 29 (support = 0.131): Thouarella_dolichoespinosa_OPRIM_2386B
Species 30 (support = 0.131): Thouarella_dolichoespinosa_OPRIM_1253

Figure S5. Highest Bayesian supported solution based on the single locus *Cox1* and the bPTP approach. On the left are details of the 30 putative species provided by the bPTP analysis.

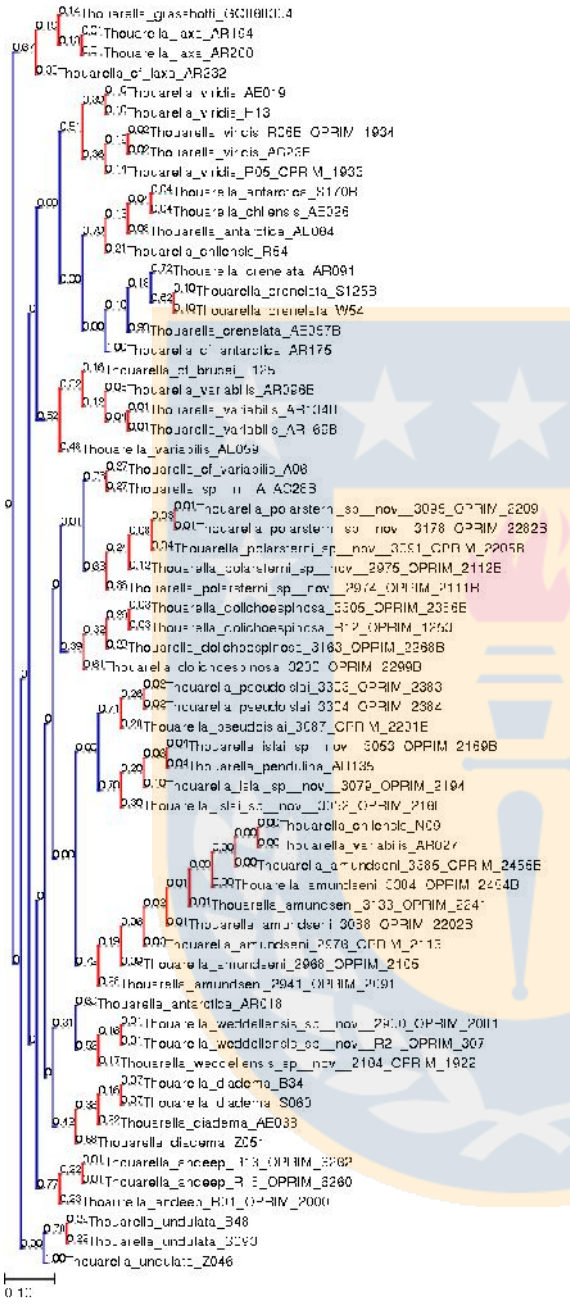

 # Most supported partition found by simple heuristic search

Species 1 (support = 0.652): Thouarella_cf_laxa_AR232, Thouarella_laxa_AR194, Thouarella_laxa_AR200

Species 2 (support = 1.000): Thouarella_variabilis_AE059

Species 3 (support = 0.998): Thouarella_chilensis_N09

Species 4 (support = 0.526): Thouarella_undulata_B48, Thouarella_undulata_S093

Species 5 (support = 0.999): Thouarella_undulata_Z046

Species 6 (support = 0.433): Thouarella_pendulina_AR135, Thouarella_variabilis_AR027, Thouarella_islai_OPRIM_2168, Thouarella_islai_OPRIM_2194, Thouarella_OPRIM_2091, Thouarella_OPRIM_2105, Thouarella_OPRIM_2113, Thouarella_OPRIM_2383, Thouarella_OPRIM_2384, Thouarella_OPRIM_2241

Species 7 (support = 0.640): Thouarella_crenelata_S125B, Thouarella_crenelata_W54

Species 8 (support = 0.991): Thouarella_cf_antarctica_AR175

Species 9 (support = 0.991): Thouarella_crenelata_AR091

Species 10 (support = 0.700): Thoaurella_andeep_OPRIM_2000, Thouarella_andeep_OPRIM_6262, Thouarella_andeep_OPRIM_6260

Species 11 (support = 0.987): Thouarella_polarsterni_OPRIM_2209

Species 12 (support = 0.510): Thouarella_antarctica_AE064, Thouarella_antarctica_S170B, Thouarella_chilensis_AE026, Thouarella_chilensis_R54

Species 13 (support = 0.559): Thouarella_viridis_AE019, Thouarella_viridis_H13, Thouarella_viridis_R05

Species 14 (support = 0.925): Thouarella_cf_variabilis_A06

Species 15 (support = 0.925): Thouarella_R12_OPRIM_1253

Species 16 (support = 0.465): Thouarella_diadema_AE068, Thouarella_diadema_B34, Thouarella_diadema_S060

Species 17 (support = 0.799): Thouarella_diadema_Z051

Species 18 (support = 0.884): Thouarella_antarctica_AR018

Species 19 (support = 0.617): Thouarella_weddellensis_OPRIM_1922, Thouarella_weddellensis_OPRIM_2081, Thouarella_weddellensis_OPRIM_307

Figure S6. Highest Bayesian supported solution based on the single locus *28S* and the bPTP approach. On the left are details of the 19 putative species provided by the bPTP analysis.

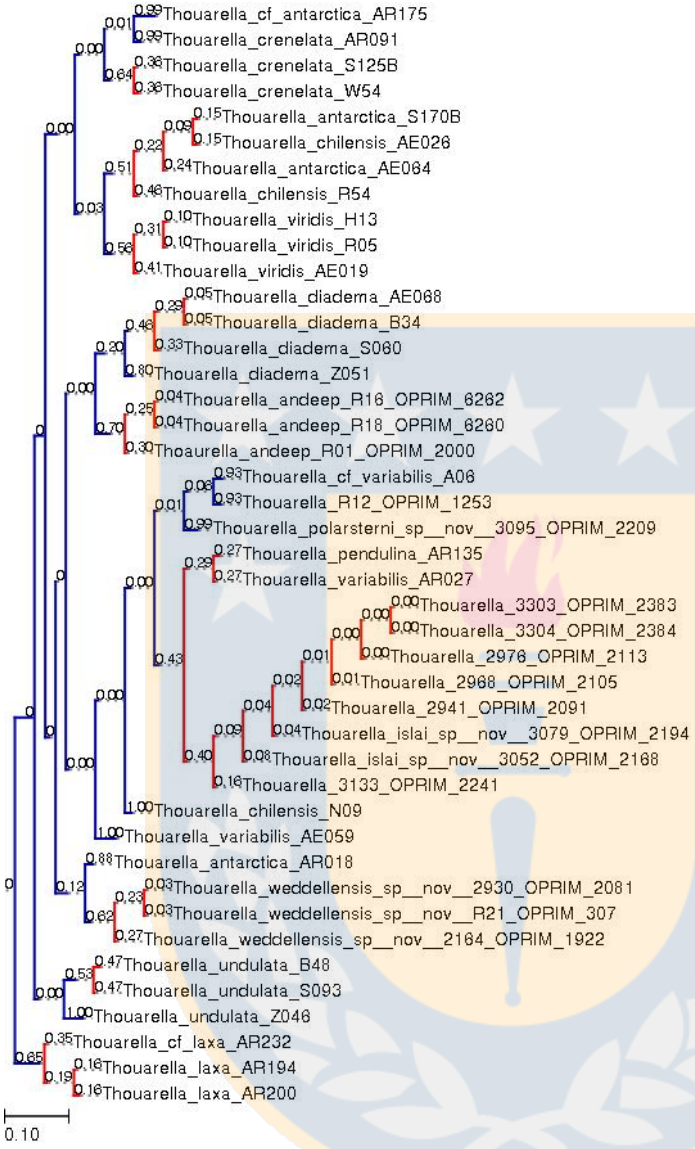

 # Most supported partition found by simple heuristic search
Species 1 (support = 0.669):
Thouarella_cf_laxa_AR232,
Thouarella_grasshoffi_GQ868334,
Thouarella_laxa_AR194, Thouarella_laxa_AR200
Species 2 (support = 0.515):
Thouarella_cf_brucei_T125,
Thouarella_variabilis_AR096B,
Thouarella_variabilis_AR134B,
Thouarella_variabilis_AR169B,
Thouarella_variabilis_AE059
Species 3 (support = 0.394):
Thouarella_dolichoespinosa_OPRIM_2299B,
Thouarella_dolichoespinosa_OPRIM_2268B,
Thouarella_dolichoespinosa_OPRIM_2386B,
Thouarella_dolichoespinosa_OPRIM_1253
Species 4 (support = 0.766):
Thoaurella_andeep_OPRIM_2000,
Thouarella_andeep_OPRIM_6262,
Thouarella_andeep_OPRIM_6260
Species 5 (support = 0.508):
Thouarella_viridis_OPRIM_1933,
Thouarella_viridis_OPRIM_1934,
Thouarella_viridis_AC23B,
Thouarella_viridis_AE019, Thouarella_viridis_H13
Species 6 (support = 0.418):
Thouarella_diadema_AE068,
Thouarella_diadema_B34,
Thouarella_diadema_S060,
Thouarella_diadema_Z051
Species 7 (support = 0.781):
Thouarella_undulata_B48,
Thouarella_undulata_S093
Species 8 (support = 1.000):
Thouarella_undulata_Z046
Species 9 (support = 0.785):
Thouarella_antarctica_AE064,
Thouarella_antarctica_S170B,
Thouarella_chilensis_AE026,
Thouarella_chilensis_R54
Species 10 (support = 0.999):
Thouarella_cf_antarctica_AR175
Species 11 (support = 0.722):
Thouarella_amundseni_OPRIM_2091,
Thouarella_amundseni_OPRIM_2105,
Thouarella_amundseni_OPRIM_2113,
Thouarella_amundseni_OPRIM_2202B,
Thouarella_amundseni_OPRIM_2241,
Thouarella_amundseni_OPRIM_2454B,
Thouarella_amundseni_OPRIM_2455B,
Thouarella_chilensis_N09,
Thouarella_variabilis_AR027
Species 12 (support = 0.713):
Thouarella_pseudoislai_OPRIM_2201B,
Thouarella_pseudoislai_OPRIM_2383, Thouarella_pseudoislai_OPRIM_2384
Species 13 (support = 0.697): Thouarella_islai_OPRIM_2168, Thouarella_islai_OPRIM_2169B, Thouarella_pendulina_AR135, Thouarella_islai_OPRIM_2194
Species 14 (support = 0.727): Thouarella_cf_variabilis_A06, Thouarella_sp__n__A_AC28B
Species 15 (support = 0.631): Thouarella_polarsterni_OPRIM_2111B, Thouarella_polarsterni_OPRIM_2112B, Thouarella_polarsterni_OPRIM_2205B, Thouarella_polarsterni_OPRIM_2209, Thouarella_polarsterni_OPRIM_2282B
Species 16 (support = 0.688): Thouarella_antarctica_AR018
Species 17 (support = 0.522): Thouarella_weddellensis_OPRIM_1922, Thouarella_weddellensis_OPRIM_2081, Thouarella_weddellensis_OPRIM_307
Species 18 (support = 0.899): Thouarella_crenelata_AE057B
Species 19 (support = 0.718): Thouarella_crenelata_AR091
Species 20 (support = 0.615): Thouarella_crenelata_S125B, Thouarella_crenelata_W54

Figure S7. Highest Bayesian supported solution based on the concatenated multilocus dataset and the bPTP approach. On the left are details of the 20 putative species provided by the bPTP analysis.

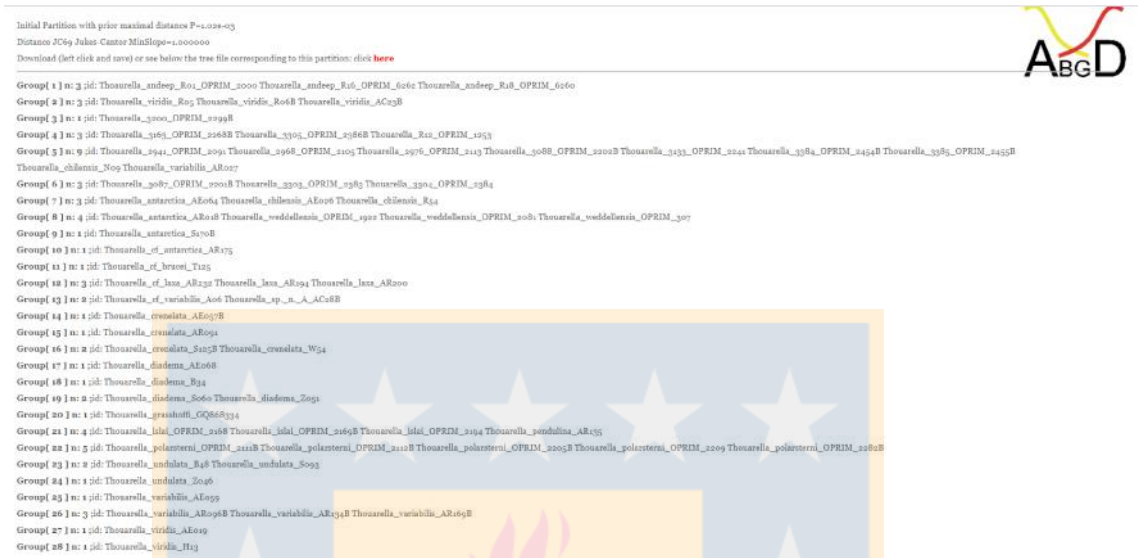

Figure S8. Results from the ABGD approach based on the *mtMuts* locus. Note the presence of 28 putative species or MOTUs.

Figure S9. Results from the ABGD approach based on the *Cox1* locus. Note the presence of 21 putative species or MOTUs.

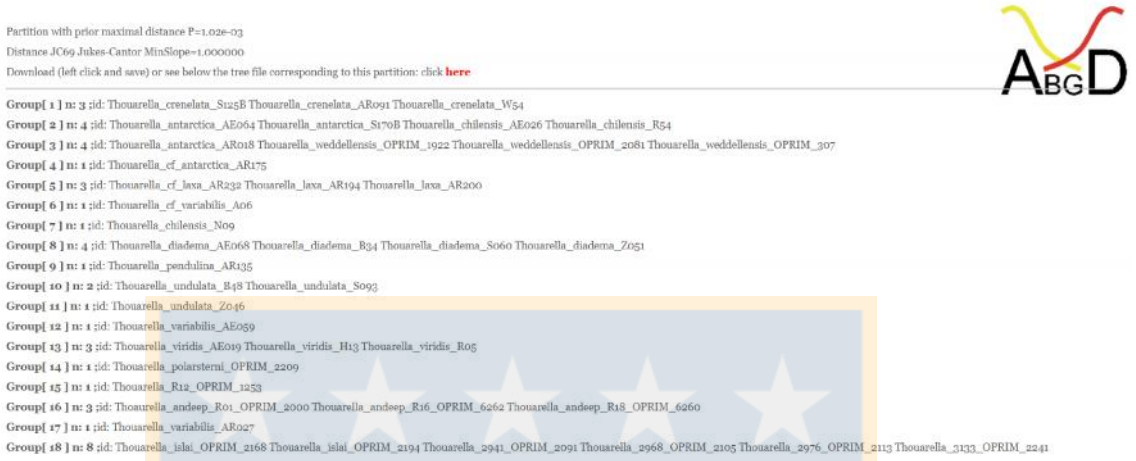

Figure S10. Results from the ABGD approach based on the *28S* locus. Note the presence of 18 putative species or MOTUs.

Figure S11. Results from the ABGD approach based on the concatenated dataset (three loci). Note the presence of 17 putative species or MOTUs.

Apéndice 3. Material electrónico suplementario para "*Diversification dynamics of a common deep-sea octocoral family linked to the Paleocene-Eocene thermal maximum*".

Supplementary File 1. GenBank accession numbers of the specimens used for the molecular analysis. Materials in bold are the newly sequenced for this study.

Family	**Taxa**	***MutS***	***COX1***	***28S***	***18S***
Primnoidae	*Abyssoprimnoa gemina*	MG986922	MG986971	MG980143	MG980108
Primnoidae	*Aglaoprimnoa stefanii*	MG986940	-	MG980158	MG980124
Primnoidae	*Ainigmaptilon edisto*	KP324314	KP677934	-	-
Primnoidae	*Armadillogorgia cyathella*	MG986930	MG986979	MG980148	MG980114
Primnoidae	*Arntzia gracilis*	MG986934	MG986983	MG980152	MG980118
Primnoidae	*Arthrogorgia kinoshitai*	EU268063.1	-	-	-
Primnoidae	*Arthrogorgia utinomii*	MF319931.1	-	-	-
Primnoidae	*Australogorgia aldersladei*	MG986919	MG986968	MG980140	MG980105
Chrysogorgiidae	*Chrysogorgia abludo*	GQ180138.1	GQ868324.1	-	-
Chrysogorgiidae	*Chrysogorgia artospira*	GQ180135.1	GQ868315.1	-	-
Chrysogorgiidae	*Chrysogorgia averta*	KC788265.1	KC788235.1	KC788258.1	-
Chrysogorgiidae	*Chrysogorgia binata*	MK431862.1	-	-	-
Chrysogorgiidae	*Chrysogorgia chryseis*	DQ297421.1	GQ868308.1	-	AF052913.1
Chrysogorgiidae	*Chrysogorgia dendritica*	MT269888.1	-	-	-
Chrysogorgiidae	*Chrysogorgia fragilis*	MN510471.1	-	-	-
Chrysogorgiidae	*Chrysogorgia monticola*	JN227989.1	JN227955.1	-	JN227961.1
Chrysogorgiidae	*Chrysogorgia pinnata*	JN227988.1	JN227956.1	-	JN227960.1
Chrysogorgiidae	*Chrysogorgia tricaulis*	GQ180126.1	GQ868314.1	-	-
Chrysogorgiidae	*Helicogorgia flagellata*	JN227929.1	JN227953.1	-	JN227971.1
Chrysogorgiidae	*Helicogorgia spiralis*	JN227930.1	-	-	-
Chrysogorgiidae	*Iridogorgia magnispiralis*	KC788263.1	KC788237.1	-	FJ526216.1
Chrysogorgiidae	*Iridogorgia splendens*	KC788271.	KC788229.	KX890215.	JN227968.

		1	1	1	1
Chrysogorgiidae	*Isidoides armata*	JN227946.1	JN227951.1	-	JN227972.1
Chrysogorgiidae	*Metallogorgia macrospina*	MT050468.1	JN227952.1	-	JN227966.1
Chrysogorgiidae	*Metallogorgia melanotrichos*	GQ868340.1	GQ868320.1	-	FJ526215.1
Chrysogorgiidae	*Pseudochrysogorgia bellona*	GQ868332.1	ADJ53877.1	-	HM590865.1
Chrysogorgiidae	*Radicipes gracilis*	DQ297424.1	AEI73134.1	-	HM590864.1
Chrysogorgiidae	*Radicipes stonei*	MG986912.1	MG986961.1	-	-
Chrysogorgiidae	*Rhodaniridogorgia fragilis*	AFM97575.1	AFM97515.1	-	JN247405.1
Chrysogorgiidae	*Stephanogorgia faulkneri*	GQ342485.1	GQ342406.1	JX203718.1	JN227967.1
Primnoidae	*Callogorgia americana*	KC771869	KC771712	KC771880	-
Primnoidae	*Callogorgia cf. tuberculata*	KP324339	KP677957	KP324568	KP324677
Primnoidae	*Callogorgia compressa*	EU268065.1	-	-	-
Primnoidae	*Callogorgia delta*	MT795620.1	-	-	-
Primnoidae	*Callogorgia euthyeia*	KP324338	KP677956	KP324567	KP324676
Primnoidae	*Callogorgia formosa*	GQ342525.1	GQ342453.1	JX203749.1	-
Primnoidae	*Callogorgia gilberti*	MG986950	MG986997	-	-
Primnoidae	*Callogorgia gracilis*	KC771844	KC771689	KC771878	-
Primnoidae	*Callogorgia korema*	KP324341	KP677959	KP324570	KP324679
Primnoidae	*Callogorgia medialis*	KP324337	KP677955	KP324566	KP324675
Primnoidae	*Callogorgia verticillata*	KC771847	KC771681	KC771879	-
Primnoidae	*Callozostron acanthodes*	KP324329	KP677947	KP324561	-
Primnoidae	*Callozostron mirabile*	MG986927	MG986976	MG980146	-
Primnoidae	*Callozostron pinnatum*	MG986928	MG986977	MG980147	MG980112
Primnoidae	*Calyptrophora antilla*	MW514669.1	-	-	-
Primnoidae	*Calyptrophora inornata*	MG986936	MG986985	MG980154	MG980120
Primnoidae	*Calyptrophora japonica*	DQ234756.1	-	-	-
Primnoidae	*Calyptrophora laevispinosa*	JX561177	JX561162	-	-
Primnoidae	*Calyptrophora microdentata*	MG986914	MG986963	MG980136	MG980100
Primnoidae	*Calyptrophora persephone*	-	-	-	KX384619.1
Primnoidae	*Calyptrophora wyvillei*	MG986937	MG986986	MG980155	MG980121
Primnoidae	*Candidella helminthophora*	MG986921	MG986970	MG980142	MG980107
Primnoidae	*Candidella imbricata*	EU268058.1	-	-	-

Cornulariidae	*Cervera atlantica*	JN620804.1	JN620805.1	-	-
Cornulariidae	*Cornularia cornucopiae*	-	JX203848.1	JX203760.1	-
Cornulariidae	*Cornularia pabloi*	JX203792.1	JX203847.1	JX203699.1	-
Primnoidae	*Convexella magelhaenica*	KP324352	KP677970	KP324581	KP324690
Primnoidae	*Dasystenella acanthina*	KP324305	KP677925	KP324543	KP324649
Primnoidae	*Dasystenella austasensis*	KP324290	KP677909	KP324529	KP324638
Primnoidae	*Digitogorgia kuekenthali*	KP324372	KP677990	KP324599	KP324707
Ellisellidae	*Dichotella gemmacea*	GQ342492.1	GQ342415.1	JX203701.1	-
Ellisellidae	*Ellisella schmitti*	JN227995	MK153473.1	-	FJ526217.1
Ellisellidae	*Huziogorgia utinomii*	MT312234.1	MT312237.1	-	-
Ellisellidae	*Ifalukella yanii*	GQ342501.1	GQ342427.1	JX203717.1	JN874924.1
Ellisellidae	*Nicella carinata*	KF803721.1	-	-	-
Primnoidae	*Fannyella abies*	MG986952	MG986999	-	-
Primnoidae	*Fannyella rossi*	MG986925	MG986974	MG980145	MG980110
Primnoidae	*Fannyella spinosa*	KP324307	KP677927	KP324545	KP324651
Helioporacea	*Heliopora coerulea*	DQ302872.1	GQ342426.1	-	AF052923.1
Helioporacea	*Nanipora kamurai*	KP195280.1	KP195281.1	-	-
Primnoidae	*Heptaprimnoa patagonica*	-	KP678023	KP324629	KP324738
Isididae	*Acanella eburnea*	EF060014.1	EF672731.2	-	GU206549.1
Isididae	*Chelidonisis aurantiaca*	KC788274.1	KC788226.1	KX890211.1	-
Isididae	*Isidella elongata*	AGU93482	-	-	KX362260.1
Isididae	*Isidella tentaculum*	ACG69787	-	-	KX362270.1
Isididae	*Isis hippuris*	AEM37866	-	-	-
Isididae	*Jasminisis zebra*	EU268048.1	-	-	-
Isididae	*Jasonisis thresheri*	JN620806.1	JN620807.1	-	KX362282.1
Isididae	*Keratoisis flexibilis*	KC660878.1	-	-	-
Isididae	*Keratoisis glaesa*	KC660848.1	-	-	-
Isididae	*Keratoisis grayi*	KX362308.1	KX530101.1	-	KX362305.1
Isididae	*Keratoisis hikurangiensis*	AGU93306	-	-	-
Isididae	*Keratoisis magnifica*	KX362330.	-	-	KX362295.

		1			1
Isididae	*Keratoisis peara*	AGU93366	-	-	-
Isididae	*Keratoisis projecta*	AGU93308	-	-	-
Isididae	*Lepidisis olapa*	DQ297426.1	AY351662.1	-	-
Isididae	*Primnoisis chatham*	KT070948.1	KT152012.1	-	-
Isididae	*Primnoisis delicatula*	KT070945.1	KT152009.1	-	-
Isididae	*Primnoisis erymna*	KT070944.1	KT152008.1	-	-
Isididae	*Primnoisis formosa*	KT070942.1	KT152006.1	-	-
Isididae	*Primnoisis fragilis*	KT070934.1	KT151998.1	-	-
Isididae	*Primnoisis gracilis*	KT070913.1	KT151978.1	-	-
Isididae	*Primnoisis millerae*	KT070908.1	KT151973.1	-	-
Isididae	*Primnoisis niwa*	KT070905.1	KT151971.1	-	-
Isididae	*Primnoisis tasmani*	KT070900.1	KT151967.1	-	-
Primnoidae	*Loboprimnoa exotica*	MG986916	MG986965	-	MG980102
Primnoidae	*Metafannyella eos*	MG986953	MG987000	-	-
Primnoidae	*Metafannyella kuekenthali*	KP324380	KP677999	KP324604	KP324716
Primnoidae	*Metafannyella polita*	-	-	MG980166	MG980132
Primnoidae	*Metafannyella ventilabrum*	MG986924	MG986973	MG980144	MG980109
Primnoidae	*Mirostenella articulata*	KP324287	KP677906	KP324526	KP324635
Primnoidae	*Narella abyssalis*	JX561169	JX561167	-	-
Primnoidae	*Narella alaskensis*	JX561172	JX561153	-	-
Primnoidae	*Narella alata*	JX561168	JX561147	-	-
Primnoidae	*Narella arbuscula*	MG986923	MG986972	-	-
Primnoidae	*Narella bayeri*	JX561170	JX561145	-	-
Primnoidae	*Narella bellissima*	MH660500.1	MH660479.1	-	-
Primnoidae	*Narella bowersi*	-	AF385315.1	-	AF052905.1
Primnoidae	*Narella candidae*	KP324400	KP678016	KP324623	-
Primnoidae	*Narella cf. mosaica*	KP324316	KP677936	KP324552	KP324657
Primnoidae	*Narella clavata*	KP324343	KP677961	KP324572	KP324681
Primnoidae	*Narella cristata*	JX561171	JX561166	-	-
Primnoidae	*Narella dichotoma*	EU293800	GQ868316	-	HM590862
Primnoidae	*Narella gilchristi*	KP324402	KP678019	KP324626	-
Primnoidae	*Narella hawaiinensis*	JX561184	JX561148	-	-

Primnoidae	*Narella hypsocalyx*	MG986954	MG987001	-	-
Primnoidae	*Narella macrocalyx*	MG986938	MG986987	MG980156	MG980122
Primnoidae	*Narella pauciflora*	KC788272	KC788228	-	-
Primnoidae	*Narella speighti*	KP324399	KP678015	KP324622	KP324733
Primnoidae	*Narella valentine*	KP324401	KP678017	KP324624	KP324734
Primnoidae	*Narella versluysi*	GQ868337	FJ268637	-	FJ358841
Primnoidae	*Onogorgia nodosa*	KP324368	KP677986	KP324595	KP324703
Primnoidae	*Ophidiogorgia paradoxa*	-	MN263856.1	-	-
Primnoidae	*Ophidogorgia kuekenthali*	KP324312	KP677932	KP324549	KP324655
Stolonifera	*Coelogorgia palmosa*	DQ302805.1	GQ342413.1	JX203698.1	AF052932.1
Pennatulacea	*Acanthoptilum gracile*	JN866529	KF874188	-	-
Pennatulacea	*Actinoptilum molle*	GQ342491	GQ342414	JX203738	-
Pennatulacea	*Anthoptilum grandiflorum*	MK919655	MK919655	-	-
Pennatulacea	*Calibelemnon hinoenma*	MW168258	-	-	-
Pennatulacea	*Cavernularia pusilla*	MT968957	MT952706	MT951908	-
Pennatulacea	*Distichoptilum gracile*	MK919657	MK919657	-	-
Pennatulacea	*Echinoptilum macintoshi*	MK133373	-	-	-
Pennatulacea	*Funiculina sp.A OPEN-466 (G-86)*	MT968959	MT952708	MT951910	-
Pennatulacea	*Funiculina sp.B2*	MT968960	MT952709	MT951911	-
Pennatulacea	*Gilibelemnon octodentatum*	MK603841	MK603855	MK603851	-
Pennatulacea	*Gyrophyllum hirondellei*	MT968964	MT952713	MT951915	-
Pennatulacea	*Gyrophyllum sibogae*	-	JX203865	JX203740	-
Pennatulacea	*Halipteris californica*	JN866541	KF874202	-	-
Pennatulacea	*Halipteris finmarchica*	DQ302868	GQ342425	JX203741	-
Pennatulacea	*Halipteris willemoesi*	JN866543	KF874204.1	-	-
Pennatulacea	*Kophobelemnon macrospinum*	DQ302865	GQ342429	JX203742	-
Pennatulacea	*Kophobelemnon pauciflorum*	KF313836	-	-	-
Pennatulacea	*Pennatula aculeata*	MK919663	MK919663	-	-
Pennatulacea	*Pennatula antarctica*	MK603849	MK603859	MK882493	-
Pennatulacea	*Pennatula cf. Inflata*	MK919666	MK919666	-	-
Pennatulacea	*Pennatula grandis NMS.Z.2019.25.9*	MK919665	MK919665	-	-
Pennatulacea	*Pennatula phosphorea*	MK603848	MK603858	MK882492	-
Pennatulacea	*Pennatula rubra*	MK603845	MK603857	MK603852	-
Pennatulacea	*Protoptilum carpenteri*	MK919667	MK919667	-	-
Pennatulacea	*Pteroeides griseum*	MT968965	MT952714	MT951916	-

Pennatulacea	*Ptilella grandis*	MK603844	MK603860	MK603854	-
Pennatulacea	*Ptilella grayi*	MK603846	MK603856	MK603853	-
Pennatulacea	*Ptilosarcus gurneyi*	JN866540	KF874201	-	-
Pennatulacea	*Renilla muelleri*	JX023273	JX023273	-	U19552.1
Pennatulacea	*Stylatula elongata*	JX023275	JX023275	-	-
Pennatulacea	*Umbellula huxleyi*	MT968966	MT952715	MT951917	-
Pennatulacea	*Umbellula sp.*	MK919670	MK919670	-	-
Pennatulacea	*Veretillum cynomorium*	MT968958	MT952707	MT951909	-
Pennatulacea	*Viminella sp.*	JX203794	JX203852	JX203703	-
Pennatulacea	*Virgularia mirabilis*	MT968969	MT952718	MT951919	-
Pennatulacea	*Virgularia schultzei*	GQ342527	GQ342459	JX203743	-
Primnoidae	*Pachyprimnoa asakoae*	MG986939	MG986988	MG980157	MG980123
Primnoidae	*Paracalyptrophora carinata*	KC788273	KC788227	-	-
Primnoidae	*Paracalyptrophora cf. josephinae*	-	KP677948	KP324562	KP324668
Primnoidae	*Paracalyptrophora hawaiinensis*	JX561189	JX561161	-	-
Primnoidae	*Paranarella watlingi*	-	-	MG980167	MG980133
Primnoidae	*Parastenella doederleini*	MW514670.1	-	-	-
Primnoidae	*Parastenella gymnogaster*	JX561188	JX561157	-	-
Primnoidae	*Parastenella pacifica*	MG986920	MG986969	MG980141	MG980106
Primnoidae	*Parastenella ramosa*	JX561185	JX561156	-	-
Primnoidae	*Parastenella spinosa*	KP324405	KP678022	KP324628	KP324737
Primnoidae	*Perissogorgia monile*	KP324344	KP677962	KP324573	KP324682
Primnoidae	*Perissogorgia vitrea*	MG986915	MG986964	MG980137	MG980101
Primnoidae	*Plumarella adhaerans*	NC_046480.1	NC_046480.1	-	-
Primnoidae	*Plumarella aleutiana*	MG986957	MG987004	-	-
Primnoidae	*Plumarella castellviae*	MG986913	MG986962	MG980135	MG980099
Primnoidae	*Plumarella delicatissima*	KP324374	KP677992	-	KP324709
Primnoidae	*Plumarella delicatula*	MG986958	MG987005	-	-
Primnoidae	*Plumarella hapala*	MF319950.1	-	-	-
Primnoidae	*Plumarella laxiramosa*	MG986942	-	MG980160	MG980127
Primnoidae	*Plumarella longispina*	MG986929	MG986978	-	MG980113
Primnoidae	*Plumarella pourtalesii*	MG986933	MG986982	MG980151	MG980117
Primnoidae	*Plumarella superba*	MF319954.1	-	-	-
Primnoidae	*Primnoa_bisquama*	KP324397	KP678013	KP324620	KP324731
Primnoidae	*Primnoa notialis*	MG986917	MG986966	MG980138	MG980103

Primnoidae	*Primnoa pacifica*	MG986944	-	MG980162	MG980129
Primnoidae	*Primnoa resedaeformis*	MG986945	MG986992	-	-
Primnoidae	*Primnoa wingi*	MG986948	MG986995	-	-
Primnoidae	*Primnoeides flagellum*	KP324398	KP678014	KP324621	KP324732
Primnoidae	*Primnoeides sertularoides*	KP324389	KP678006	KP324612	KP324724
Primnoidae	*Primnoella antarctica*	KP324367	KP677985	KP324594	KP324702
Primnoidae	*Primnoella chilensis*	KP324359	KP677977	KP324588	KP324697
Primnoidae	*Primnoella delicatissima*	KP324377	KP677994	KP324602	KP324711
Primnoidae	*Primnoella divaricata*	-	KP677998	KP324603	KP324715
Primnoidae	*Primnoella insularis*	MG986935	MG986984	MG980153	MG980119
Primnoidae	*Primnoella scotiae*	KP324361	KP677979	KP324589	KP324698
Primnoidae	*Pyrogorgia lemnos*	-	MG986991	MG980165	MG980131
Primnoidae	*Thouarella amundseni*	MT894200	MT892703	MT892720	-
Primnoidae	*Thouarella andeep*	MT894190	MT892685	MT892716	-
Primnoidae	*Thouarella antarctica*	KP324295	KP677914	KP324533	KP324640
Primnoidae	*Thouarella cf. brucei*	KP324404	KP678021	-	-
Primnoidae	*Thouarella chilensis*	KP324381	KP678000	KP324605	KP324717
Primnoidae	*Thouarella crenelata*	KP324406	KP678024	KP324630	KP324739
Primnoidae	*Thouarella diadema*	KP324296	KP677915	KP324534	KP324641
Primnoidae	*Thouarella dolichoespinosa*	MT894198	MT892693	MT892733	-
Primnoidae	*Thouarella grasshoffi*	GQ868334	-	-	-
Primnoidae	*Thouarella islai*	MN914142	MN916711	MN921244	-
Primnoidae	*Thouarella laxa*	KP324332	KP677951	KP324564	KP324671
Primnoidae	*Thouarella minuta*	ON010024	-	-	-
Primnoidae	*Thouarella pendulina*	KP324321	KP677941	KP324556.1	KP324661
Primnoidae	*Thouarella polarsterni*	MN914147	MN916714	MN921245	-
Primnoidae	*Thouarella pseudoislai*	MT894219	MT892714	MT892730	-
Primnoidae	*Thouarella* sp. nov.	MT892688	MT894193	MT892731	-
Primnoidae	*Thouarella undulata*	KP324348	KP677966	KP324577	KP324686
Primnoidae	*Thouarella variabilis*	KP324294	KP677913	KP324532	KP324639
Primnoidae	*Thouarella viridis*	MT894191	MT892683	MT892715	-
Primnoidae	*Thouarella weddellensis*	MN914149	MN916716	MN921246	-
Primnoidae	*Tokoprymno maia*	-	-	KT259944.1	-
Primnoidae	*Tokoprymno sp.*	KP324379	KP677996	-	KP324713

Supplementary File 2. Calibration information (from fossils) used in the FBD dating analysis.

Fossil species	Affinities	Age Range (Ma)	Approach	Citation
Keratoisis tangentis	Keratoisidinae	16-23	Tips	(Grant 1976)
Graphularia quadrata	Pennatulacea	66-72.1	Tips	(Reich and Kutscher 2011)
Graphularia rugia	Pennatulacea	69-72.1	Tips	(Reich and Kutscher 2011)
Glyptosceptron zitteli	Pennatulacea	69-72.1	Tips	(Reich and Kutscher 2011)
Heliopora japonica	Heliaporacea	113-125	Tips	(Eguchi 1948)
Nicella bursini	*Nicella* (Ellisellidae)	69-72.1	Tips	(Kuzmicheva 1987)
Calcaxonia+Pennatulacea	basal node	327 (267-392)	node	(Quattrini *et al.* 2020)

Supplementary File 4. Details of episodic and environmental-driven diversification analyses over the primnoids from the SO.

Table S1. Descriptions of the 30 different birth-death models fitted to the primnoid pylogeny, including speciation and extinction equations, the number of free parameters to optimize by maximum likelihood, and the acronym as used in Tables 1 and S3.

Type of model	Model description	Model equation	Number of parameters	Model acronym
Constant-rate models	Constant speciation and no extinction	λ(t)=λ0; μ(t)=0	1	BCST
	Constant speciation and constant extinction	λ(t)=λ0 and μ(t)=μ0	2	BCSTDCST
Time-dependent models	Speciation variable and no extinction	λ(t)=λ0eαt nd μ(t)=0	2	BTimeVar
	Speciation variable and constant extinction	λ(t)=λ0eαt and μ(t)=μ0	3	BTimeVarDCST
	Constant speciation and extinction variable	λ(t)=λ0 and μ(t)=μ0eβt	3	BCSTDTimeVar
	Both speciation and extinction variable	λ(t)=λ0eαt and μ(t)=μ0eβt	4	BTimeVarDTimeVar
Temperature-dependent models	Speciation variable and no extinction	λ(t)=λ0eαT(t) and μ(t)=0	2	BTempVar
	Speciation variable and constant extinction	λ(t)=λ0eαT(t) and μ(t)=μ0	3	BTempVarDCST
	Constant speciation and extinction variable	λ(t)=λ0 and μ(t)=μ0eβT(t)	3	BCSTDTempVar

	Both speciation and extinction variable	λ(t)=λ0eαS(t) and μ(t)=μ0eβS(t)	4	BTempVarDTempVar
Sea level-dependent models	Speciation variable and no extinction	λ(t)=λ0eαS(t) and μ(t)=0	2	BSeaVar
	Speciation variable and constant extinction	λ(t)=λ0eαS(t) and μ(t)=μ0	3	BSeaVarDCST
	Constant speciation and extinction variable	λ(t)=λ0 and μ(t)=μ0eβS(t)	3	BCSTDSeaVar
	Both speciation and extinction variable	λ(t)=λ0eαS(t) and μ(t)=μ0eβS(t)	4	BSeaVarDSeaVar
CO2-dependent models	Speciation variable and no extinction	λ(t)=λ0eαC(t) and μ(t)=0	2	BCO2Var
	Speciation variable and constant extinction	λ(t)=λ0eαC(t) and μ(t)=μ0	3	BCO2VarDCST
	Constant speciation and extinction variable	λ(t)=λ0 and μ(t)=μ0eβC(t)	3	BCSTDCO2Var
	Both speciation and extinction variable	λ(t)=λ0eαC(t) and μ(t)=μ0eβC(t)	4	BCO2VarDCO2Var
Fragmentation-dependent models	Speciation variable and no extinction	λ(t)=λ0eαF(t) and μ(t)=0	2	BFragVar
	Speciation variable and constant extinction	λ(t)=λ0eαF(t) and μ(t)=μ0	3	BFragVarDCST
	Constant speciation and extinction variable	λ(t)=λ0 and μ(t)=μ0eβF(t)	3	BCSTDFragVar
	Both speciation and extinction variable	λ(t)=λ0eαF(t) and μ(t)=μ0eβF(t)	4	BFragVarDFragVar
Geochemistry-dependent models	Speciation variable and no extinction	λ(t)=λ0eαG(t) and μ(t)=0	2	BGeoCheVar
	Speciation variable and constant extinction	λ(t)=λ0eαG(t) and μ(t)=μ0	3	BGeoCheVarDCST
	Constant speciation and extinction variable	λ(t)=λ0 and μ(t)=μ0eβG(t)	3	BCSTDGeoCheVar
	Both speciation and extinction variable	λ(t)=λ0eαG(t) and μ(t)=μ0eβG(t)	4	BGeoCheVarDGeoCheVar
Dispersal rate	Speciation variable and no extinction	λ(t)=λ0eαDr(t) and μ(t)=0	2	BDrVar
	Speciation variable and constant extinction	λ(t)=λ0eαDr(t) and μ(t)=μ0	3	BDrVarDCST
	Constant speciation and extinction variable	λ(t)=λ0 and μ(t)=μ0eβDr(t)	3	BCSTDDrVar
	Both speciation and extinction variable	λ(t)=λ0eαDr(t) and μ(t)=μ0eβDr(t)	4	BDrVarDDrVar

Table S3. Results from RPANDA analyses of sub-Antarctic primnoids.

Models	means.Models	means.NP	means.logL	means.AICc	AICw	DeltaAICc	means.Lambda	means.AlphaTime	means.Mu	means.BetaTime
Constant	BCST	1	-225.076	452.231	0.01	4.832	0.056	NA	NA	NA
	BCSTDCST	2	-221.976	448.191	0.07	0.792	0.106	NA	0.072	NA

Time	BTimeVar	**2**	**-221.579**	**447.399**	**0.10**	**0.000**	**0.081**	**-0.015**	**NA**	**NA**
	BTimeVarDCST	3	-221.396	449.282	0.04	1.884	0.093	-0.008	0.031	NA
	BCSTDTimeVar	3	-221.158	448.805	0.05	1.406	0.089	NA	0.037	0.018
	BTimeVarDTimeVar	4	-220.851	450.536	0.02	3.137	0.094	0.025	0.075	0.033
CO2	BCO2Var	2	-222.084	448.409	0.06	1.010	0.114	-0.001	NA	NA
	BCO2VarDCST	3	-221.108	448.706	0.05	1.308	0.120	-0.001	0.045	NA
	BCSTDCO2Var	3	-220.986	448.462	0.06	1.063	0.092	NA	0.034	0.001
	BCO2VarDCO2Var	4	-220.591	450.014	0.03	2.616	0.116	0.000	0.150	-0.001
Temperature	BTempVar	2	-222.618	449.476	0.03	2.077	0.094	-0.058	NA	NA
	BTempVarDCST	3	-221.679	449.847	0.03	2.449	0.107	-0.017	0.053	NA
	BCSTDTempVar	3	-221.201	448.893	0.05	1.494	0.091	NA	0.036	0.066
	BTempVarDTempVar	4	-220.284	449.401	0.04	2.002	0.072	0.085	0.048	0.119
Sea Level	BSeaVar	2	-223.870	451.980	0.01	4.582	0.058	-0.007	NA	NA
	BSeaVarDCST	3	-221.703	449.896	0.03	2.498	0.115	0.001	0.086	NA
	BCSTDSeaVar	3	-221.742	449.974	0.03	2.575	0.105	NA	0.070	0.003
	BSeaVarDSeaVar	4	-221.099	451.030	0.02	3.632	0.125	0.006	0.099	0.008
OceanChemestry	BGeoCheVar	**2**	**-221.615**	**447.470**	**0.10**	**0.071**	**0.026**	**0.210**	**NA**	**NA**
	BGeoCheVarDCST	3	-221.516	449.522	0.03	2.123	0.050	0.136	0.025	NA
	BCSTDGeoCheVar	3	-221.383	449.256	0.04	1.857	0.090	NA	28.883	-0.621
	BGeoCheVarDGeoCheVar	4	-221.201	451.235	0.01	3.836	0.080	0.098	0.286	-0.645
Continental Fragment	BFragVar	2	-223.447	451.135	0.02	3.736	0.066	-0.439	NA	NA
	BFragVarDCST	3	-221.623	449.735	0.03	2.337	0.118	0.128	0.097	NA
	BCSTDFragVar	3	-221.531	449.552	0.03	2.154	0.096	NA	0.051	0.888
	BFragVarDFragVar	4	-220.484	449.801	0.03	2.402	0.128	0.751	0.117	1.008

The table includes the model, the number of parameters in the model (NP), the estimated log-likelihood (logL), the corrected Akaike information criterion (AICc), the Akaike weight of the model (Akaike ω), the delta AIC (ΔAICc), and the corresponding parameter estimates (λ = speciation rate at present, α = parameter controlling the dependency of speciation rate on time or temperature, μ = extinction rate at present, and β = parameter controlling the dependency of extinction rate on time or temperature). The best-fitting model is highlighted in bold.

Table S4. Results from episodic diversification analyses in TreePar on a random sample of 250 time-calibrated trees of sub-Antarctic primnoids.

means.Model	NoShiftTime	1ShiftTime	2ShiftTimes	3ShiftTimes	4ShiftTimes
means.NP	2	**5**	8	11	14
means.logL	-221.976	**-218.424**	-215.899	-214.159	-212.682
means.AICc	448.191	**448.124**	451.071	456.758	464.416

AICw	0.438	**0.453**	0.104	0.006	0.000
DeltaAICc	0.07	**0.00**	2.95	8.63	16.29
means.DivRate1	0.034	**0.023**	0.025	0.021	0.020
means.Turnover1	0.670	**0.723**	0.639	0.656	0.646
means.ShiftTime1	NA	**58.142**	34.372	30.800	28.816
means.DivRate2	NA	**-0.503**	-0.106	-0.088	-0.103
means.Turnover2	NA	**1.554**	0.910	0.939	0.961
means.ShiftTime2	NA	NA	69.576	47.116	43.672
means.DivRate3	NA	NA	-0.661	-0.094	-0.084
means.Turnover3	NA	NA	1.834	1.892	1.963
means.ShiftTime3	NA	NA	NA	74.202	58.090
means.DivRate4	NA	NA	NA	-0.681	-0.191
means.Turnover4	NA	NA	NA	1.968	1.626
means.ShiftTime4	NA	NA	NA	NA	79.230
means.DivRate5	NA	NA	NA	NA	-0.699
means.Turnover5	NA	NA	NA	NA	2.146

Bold columns represent the best model. The best-supported model has a single rate-shift, as determined by the lowest AICc and highest AICω. r_1 denotes the diversification rate and ε_1 is the turnover, both inferred between the Present (0 Ma) and the shift time 1 (st_1). BD = birth-death; NP = number of parameters; logL = log-likelihood; AICc = corrected Akaike Information Criterion. Parameter estimates; AICω = Akaike Information Criterion weights. r = net diversification rate (speciation - extinction); ε= turnover (extinction/speciation); st = shift time on diversification rate.

Supplementary File 5. Complete time-calibrated tree of Calcaxonia plus Pennatulacea, including the position of the fossil tips.

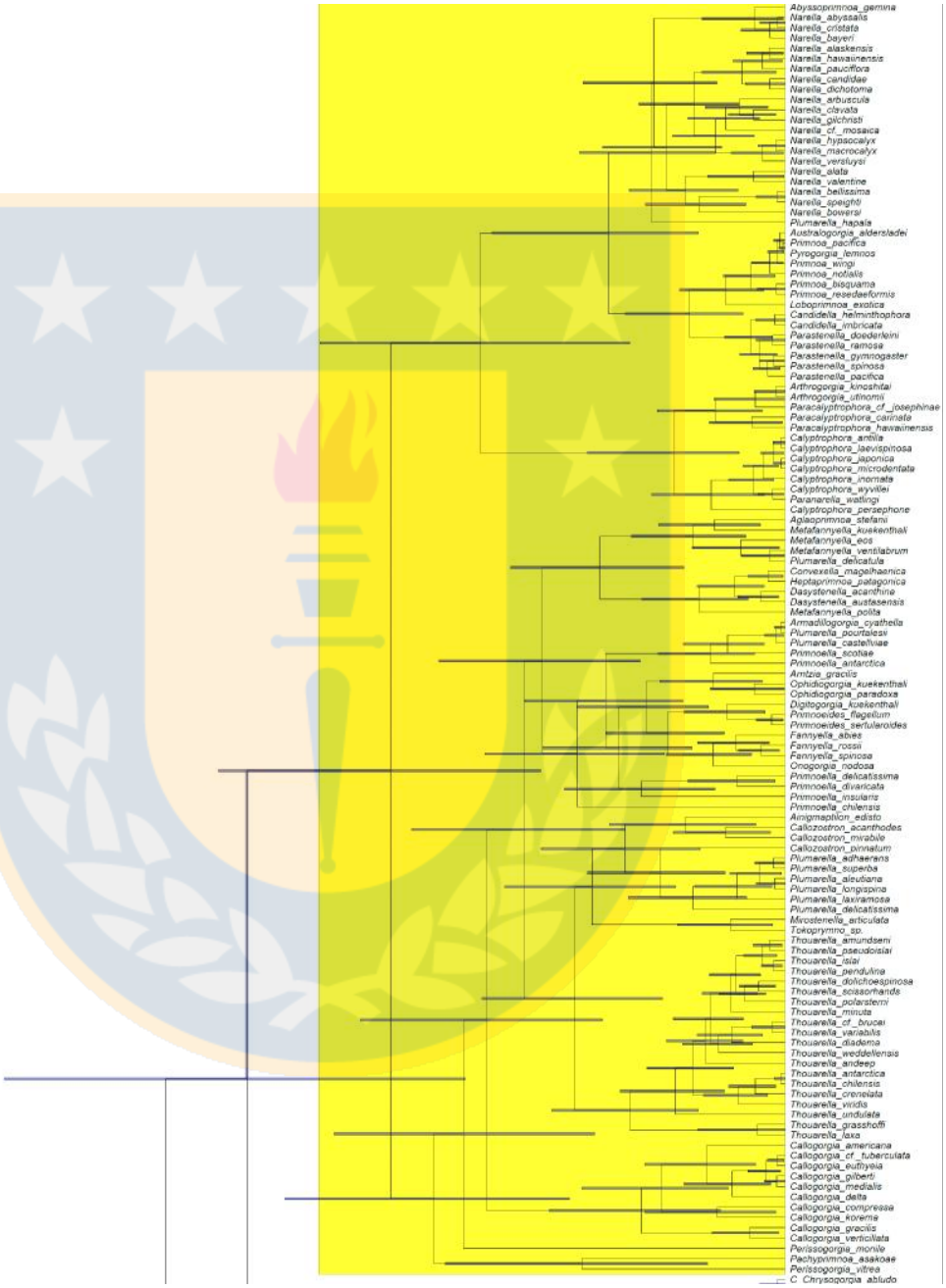

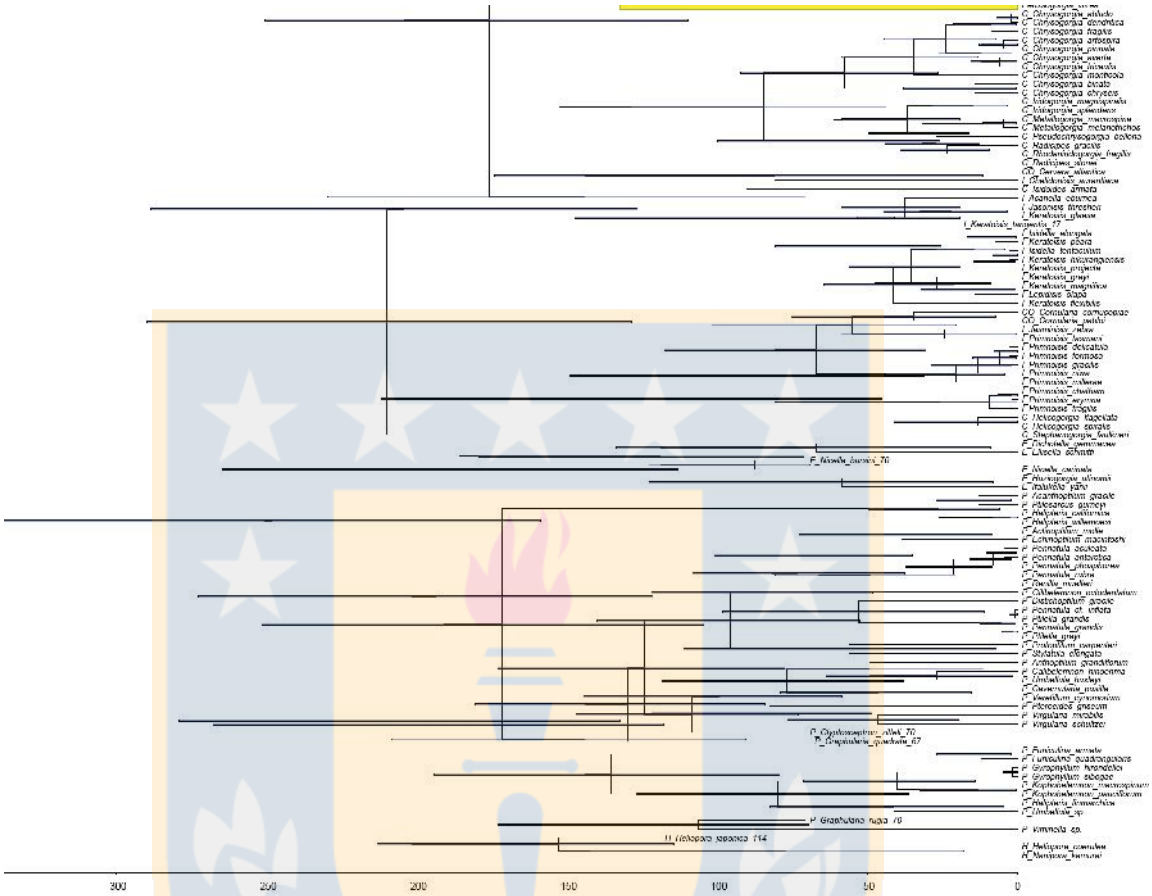

Suplementary File 6. Estimated substitution rates per gene for Calcaxonia plus Pennatulacea (Anthozoa: Octocorallia) obtained with the fossilized birth-dead model (FBD) implemented in BEAST based on fossil calibrations.

loci	Mean rate	ucld.mean	ucld.stdev	Coefficient of variance
mtMuts	0.0015 (0.0009–0.0021)	0.0012 (0.0007–0.0017)	1.6786 (1.5186–1.8354)	3.9763 (3.0639–4.9455)
Cox1	0.0259 (0.0087–0.0486)	0.0299 (0.0046–0.0690)	3.2751 (2.8947–3.6904)	12.6457 (9.994–15.5378)
28S* and *16S	0.0008 (0.0005–0.0011)	0.0009 (0.0005–0.0012)	0.7752 (0.6502–0.9044)	0.9078 (0.7282–1.0972)

Ucld.mean = mean rate under the uncorrelated log-normal relaxed molecular clock (in real space); ucld.stdev = standard deviation (σ) of the uncorrelated log-normal relaxed clock (in log-space). In parenthesis (below the mean) are the 95% HPD interval for each parameter.

Supplementary File 7. Summary of the smoothed dispersal rate of primnoids through time.